Helsinki University of Technology Department of Communications and Networking
Teknillinen korkeakoulu Tietoliikenne- ja tietoverkkotekniikan laitos
Espoo 2009 Report 4/2009

RADAR SPURIOUS EMISSION: MEASUREMENT AND IMPACT ON RADIO COMMUNICATION SYSTEM PERFORMANCE

Tuure Ikäheimonen

Helsinki University of Technology
Faculty of Electronics, Communications and Automation
Department of Communications and Networking

Teknillinen korkeakoulu
Elektroniikan, tietoliikenteen ja automaation tiedekunta
Tietoliikenne- ja tietoverkkotekniikan laitos

Helsinki University of Technology Department of Communications and Networking
Teknillinen korkeakoulu Tietoliikenne- ja tietoverkkotekniikan laitos
Espoo 2009 Report 4/2009

RADAR SPURIOUS EMISSION: MEASUREMENT AND IMPACT ON RADIO COMMUNICATION SYSTEM PERFORMANCE

Tuure Ikäheimonen

Dissertation for the degree of Doctor of Science in Technology to be presented with due permission of the Faculty of Electronics, Communication and Automation, for public examination and debate in Auditorium S4 at Helsinki University of Technology (Espoo, Finland) on 11th of December, at 12 o'clock noon.

Helsinki University of Technology
Faculty of Electronics, Communications and Automation
Department of Communications and Networking

Teknillinen korkeakoulu
Elektroniikan, tietoliikenteen ja automaation tiedekunta
Tietoliikenne- ja tietoverkkotekniikan laitos

Distribution:
Helsinki University of Technology
Department of Communications and Networking
P.O. Box 3000
FIN-02015 TKK
Tel. +358-9-451 5300
Fax +358-9-451 2474

© Tuure Ikäheimonen 2009. Verbatim copying and distribution of this entire document are permitted worldwide, without royalty, in any medium, provided this notice is preserved.
Articles included in print version: © as specified therein.

ISBN 978-952-248-155-9
ISBN 978-952-248-156-6 (pdf)
ISSN 1797-478X
ISSN 1797-4798 (pdf)

Multiprint Oy
Espoo 2009

HELSINKI UNIVERSITY OF TECHNOLOGY P.O.BOX 1000, FI-02015 TKK http://www.tkk.fi	ABSTRACT OF DOCTORAL DISSERTATION
Author Tuure Olavi Ikäheimonen	
Name of dissertation RADAR SPURIOUS EMISSION: MEASUREMENT AND IMPACT ON RADIO COMMUNICATION SYSTEM PERFORMANCE	
Date of manuscript 28.5.2008	Date of the dissertation 11.12.2009
Form of dissertation Article dissertation (monogram)	
Faculty	Faculty of Electronics, Communication and Automation
Department	Department of Communications and Networking
Field of Research	Telecommunications technique
Opponent	Doctor Erkki Salonen and Doctor Antti Tuohimaa
Supervisor	Prof. Sven-Gustav Häggman

ABSTRACT

In this thesis is presented a useful and economic measuring principle with which radar spurious emissions can be investigated under field conditions without disturbing the function of the radar in any way. The method presented here consists of two parts: In the time-domain parameter study is presented, how the radar antenna rotation produces radar pulses to the measuring receiver. Also is presented, how receiver parameters are defined by availability and use of radar pulses in the measurement. In the frequency spectrum measurement part a new sweep measurement system is presented. In this measurement the YIG filter presented by ITU [1] is replaced by a similar multistage tunable band-stop filter, which meets similar filtering characteristics, this is more easy to use and a less expensive filter. It is explained how the needed measurement dynamics are achieved and how the measurement time is determined and optimized in different situations. A two part measuring approach like this has not been reported before.

ITU recommendations for attenuation of radar spurious emissions are updated to 100 dB below the radar nominal frequency (*NF*) signal level. The fulfillment of these spurious level requirements sets a hard challenge for measuring dynamics: dynamics must be more than 110 dB. The author provides in this work a solution to this requirement.

This measuring method produces results, with which one can conclude the relative power level of radar spurious emissions and its effect on other radio services. In this work the spectrum produced by a 5 GHz weather radar has been studied and the results have been applied to study radar impact to terrestrial digital radio relay systems (TDRRS). The achieved result is both very important and current, and it can be utilized in the planning of new radar systems as also in the planning of new radio networks operating in the frequency ranges adjacent to radar frequencies. Possible radio networks in addition to TDRRSs that can be interfered from radar spurious emissions are Wireless Local Area Networks (WLAN), Worldwide Interoperability for Microwave Area (WiMAX) and Ultra Wide Band (UWB) systems. These systems also can interfere with radar frequencies.

Keywords: Radar Pulse Measurement, Measurement System, Measurement Dynamic Range, Radar Spurious Emissions, Weather Radar, Terrestrial Digital Radio Relay Systems, Radar Interference to Radio Communications Systems

ISBN (printed)	978-952-248-155-9	ISBN (pdf)	978-952-248-156-6
ISSN	1797-478X	ISSN (pdf)	1797-4798
Language	English	Number of pages	162
Publisher	Helsinki University of Technology, Dept. of Communication and Networking		
The dissertation can be read at http://lib.tkk.fi/Diss/2009/isbn9789522481566			

TEKNILLINEN KORKEAKOULU PL 1000, 02015 TKK http://www.tkk.fi	VÄITÖSKIRJAN TIIVISTELMÄ
Tekijä Tuure Olavi Ikäheimonen	
Väitöskirjan nimi TUTKAN HARHASÄTEILY: MITTAAMINEN JA VAIKUTUS MUIDEN RADIOJÄRJESTELMIEN SUORITUSKYKYYN	
Käsikirjoituksen jättämispäivä 28.5.2008	Väitöstilaisuuden ajankohta 11.12.2009
Väitöskirjan muoto (monogrammi)	

Tiedekunta	Elektroniikan, tietoliikenteen ja automaation tiedekunta
Laitos	Tietoliikenne- ja tietoverkkotekniikan laitos
Tutkimusala	Tietoliikennetekniikka
Vastaväittäjät	TkT Erkki Salonen ja TkT Antti Tuohimaa
Työn valvoja	Prof. Sven-Gustav Häggman

TIIVISTELMÄ

Tässä työssä esitellään uusi käyttökelpoinen ja edullinen mittausmenetelmä jolla kyetään mittaamalla kartoittamaan tutkan harhasäteilyä kenttäolosuhteissa, häiritsemättä mitenkään tutkan toimintaa. Kirjoittajan esittämä menetelmä sisältää kaksi osaa: aika-alueen parametritutkimuksen ja taajuusaluemittauksen. Aika-alueen parametritutkimuksessa analysoidaan ja selvitetään kuinka mitattava tutka tuottaa antennin pyöriessä tutkapulsseja mittausvastaanottimelle. Samoin selvitetään kuinka vastaanottimen parametrit määräytyvät tutkapulssien saatavuudesta ja käytöstä. Taajuusaluemittauksessa esitellään uusi pyyhkäisevä mittausmenetelmä. Siinä ITU:n [1] esittämän mittauskytkennän YIG-suodin on korvattu vastaavalla suodatusominaisuuden täyttävällä, halvemmalla ja helpompikäyttöisellä moniasteisella viritettävällä kaistanestosuotimella (BS-filter). Mittauskytkennällä näytetään kuinka saavutetaan vaadittava mittausdynamiikka ja kuinka mittausaika määritellään, sekä optimoidaan eri tapauksissa. Tällaista kaksiosaista mittausongelman lähestymistapaa ei ole aiemmin missään esitetty.

ITU:n suositus tutkan harhasäteilyn vaimennusvaatimukselle on suurimmillaan 100 dB alle tutkan nimellistaajuisen (*NF*) signaalin tehon. Tämä vaimennusvaatimuksen täyttäminen asettaa mittausdynamiikalle kovan vaatimuksen: dynamiikan täytyy olla suurempi kuin 110 dB. Tähän vaatimukseen kirjoittaja on tässä työssä vastannut.

Mittausmenetelmä tuottaa tuloksia joiden perusteella voidaan päätellä tutkan häiriösäteilyn suhteellinen tehotaso ja sen mahdolliset vaikutukset muihin radioverkkoihin. Tässä työssä on tutkittu 5 GHz:n säätutkan tuottamaa spektriä ja siitä saatuja tuloksia on sovellettu digitaalisen radiolinkin Terrestial Digital Radio Relay Systems:in (TDRRS) häiriintyvyyden tutkimiseen. Saatu tulos on erittäin tärkeä ja ajankohtainen, ja sitä voidaan hyödyntää niin tutkajärjestelmien suunnittelussa, kuin tutkataajuuksien kanssa samoille taajuusalueille tulevien radiojärjestelmien suunnittelussa ja käytössä. Mahdollisia muita tutkan harhasignaalista häiriintyviä radiojärjestelmiä voivat olla esim., Wireless Local Area Network (WLAN), Worldwide Interoperability for Microwave Area (WiMAX) ja Ultra Wide Band (UWB) järjestelmät. Yllä mainitun kaltaiset radiojärjestelmät, kuten WLAN, voivat myös aiheuttaa häiriöitä tutkan käyttötaajuuksille, joista on jo kansainvälisestikin raportoitu.

Avainsanat: tutkapulssin mittaus, mittausjärjestelmä, mittausdynamiikka, tutkan harhalähetteet, säätutka, maanpäälliset radiolinkkijärjestelmät, tutkahäiriöt radiotietoliikennelaitteissa

ISBN (painettu)	978-952-248-155-9	ISBN (pdf)	978-952-248-156-6
ISSN	1797-478X	ISSN (pdf)	1797-4798
Kieli	Englanti	Sivumäärä	162
Julkaisija	Teknillinen korkeakoulu, Tietoliikenne- ja tietoverkkotekniikan laitos		
Väitöskirja luettavissa verkossa http://lib.tkk.fi/Diss/2009/isbn9789522481566			

PREFACE

This work has been made during the years 2002 - 2008 in the Communications Laboratory (since 2008 part of the Department of Communications and Networking) at Helsinki University of Technology under the guidance of Professor Sven-Gustav Häggman. I thank him for the guidance of my work, the many useful conversations and discussions about general academic views, about this work and matters concerning its content.

I have been working at the Finnish Communications Regulatory Authority - FICORA (former Telecommunication Administration Center (TAC) and Post and Telecomm Administration (PTH)) since 1975. I would like to thank my employer for this long period and possibility to work with radar measurement. The content of this work in holds many matters and ideas collected through experiences made in the various measurements in this period of time.

Especially I would like to thank my colleges with whom I have made many of my measurement trips, had many debates, plenty of moments of thought and contemplations in testing measurement techniques leading partly or as whole ideas to the results presented in this work. MSc. Erkki Saarinen has been my college for the longest time. From him I have got valuable pieces of advice and hints for which I would like to especially thank him. My other college has been Mr. Kalle Pikkarainen. With him I have considered, tested and realized measurements needed in this work. Thank you for this valuable cooperation. Both these colleges of mine are specialists in the fields of terrestrial radio relay systems and radar techniques and other close matters to these.

My special thanks I would like to present to the translator of this work, my college and technical planner Mr. Norbert Kelzenberg, who without prejudice and not knowing how much work this kind translation generates boldly accepted this challenge.

I would like to thank all the radar and terrestrial radio relay system specialists with whom I have been straightening out radio relay interferences caused by radar. Every one of them can with pride say that they have taken part in fulfilling and processing this work into this written output.

Hausjärvi, November 2009

Tuure Ikäheimonen

INDEX

Symbols

α	Spctrum roll-off parametric identifying the total bandwidth
β_0	Main lobe of the antenna
β_1	Main lobe of the antenna, positive angle (*f*)
β_2	Main lobe of the antenna, negative angle (*f*)
$\delta\left(f-\frac{n}{\tau}\right)$	Dirac impulse function at the frequency $f = n/\tau$
ΔT	Time variation of the FB
$\boldsymbol{\Phi}$	Auxiliary variable in diffraction loss calculation
φ	Carrier phase
$\varphi_{ant.lobe}$	Width of the antenna lobe
Γ	Signal to noise ratio
Γ_{64QAM}	Signal to noise ratio in 64QAM
λ	Wavelength
θ	Direction of the radar with respect of the TDRRS receiver l.o.s direction
θ_m	Horizontal angle compared to pattern in degrees
τ	Radar pulse duration
τ_p	Pulse duration
A	Attenuation
$A_{calib,\ 1\ldots n\ (f)}$	Calibration curve
A_{dup}	Attenuation of duplexer
$A_{splitter}$	TX branch attenuation in dB of the duplex filters
$\boldsymbol{a}$	Wanted signal vector
B_c	Deviation of carrier
B_{IF}	Intermediate frequency filter bandwidth
B_{meas}	Measurement bandwidth
$B_{meas.\ 1\ldots n\ (f)}$	Measured spectrum bandwidth
B_{ref}	Reference bandwidth of radar pulse
B_{VIDEO}	Bandwidth of video filter of the equipment
B_{20dB}	20 dB bandwidth of a filter
BER	Bit error rate
$\boldsymbol{b}$	Interference signal vector
C	Symbol energy
C/I	Carrier to Interference Ratio
C/N	Carrier to Noise Ratio
$C/N(10^{-3})$	Carrier to Noise Ratio for BER=10^{-3}
$C/(N+I)$	Interference Tolerance Level
$C_{calc.\ 1\ldots n\ (f)}$	Relative power curve of the spectrum
$\boldsymbol{c}$	Interfered signal vector
c	Height of dominating obstacle above virtual line-of-sight
D	Antenna diameter
DR_{max}	Maximum measurement dynamics
DR_{sig}	Dynamic range of the measurement signal
$\boldsymbol{d}$	Decision-making distance vector
d	Distance (between transmitter antenna and receiver antenna).
d_{hor}	Sum of the distances to the radio horizon
$d_{1,2}$	Distance from transmitter antenna to obstacle and from to receiver antenna
$E_{average}$	Average energy of the pulse
E_{echo}	Energy of the echo pulse

E_{pulse}	Energy of the pulse
E_1	Electrical voltage level of link pulses in input of TDRRS with interference
E_2	Electrical voltage level of radar pulses in input of digital TDRRS with interference
E_3	Electrical voltage level of radar pulses in input of digital TDRRS without interference
F	Noise factor
FB	Fly back time
F_{BF}	Noise of the Band-Pass filter
F_n	Noise factor of different receiver stages
F_r	Reduced noise factor
F_{tot}	Total noise factor
F_{YIG}	Noise of the YIG-filter
F_1	Noise factor of the LNA
F_2	Noise factor of the SA
$F_{3,4}$	Total noise factor of the two BS filters
f	Frequency
f_C	Carrier frequency
f_{NF}	Nominal frequency
f_{PRF}	Pulse repetition frequency
f_{SF}	Spurious frequency
f_{s1}	Spurious frequency lower than nominal frequency
f_{s2}	Spurious frequency higher than nominal frequency
$f_{1,2}$	Lowest and highest value for measurement frequency
G	Gain
G_θ	TDRRS antenna gain as function of horizontal angle to bore-sight
G_{ant}	Gain of antenna
$G_{ant.radar}$	Gain of radar antenna
$G_{link\ ant}$	Gain of radio relay system antenna
$G_{link\ ant(\theta)}$	Gain of radio relay system antenna as function of angle
G_{max}	Maximum gain of antenna
$G_{meas.ant}$	Gain of measurement antenna
G_n	Gain of different receiver stages
G_1	Corresponds to the maximum gain of the first side lobe
G_1	Absolute value of gain of the LNA
G_2	Gain of the LNA
$G_{3,4}$	Total gain of the two BS filters
h	Antenna height
h_r	Radar antenna height
h_t	Link antenna height
I	Radar interference power
K_{filter}	Form factor of a filter
k	Coefficient of earth radius
L	Attenuation
L_A	Attenuation of adjustable attenuator
L_{BP1}	Pass-band loss of band stop-filter 1
L_{BP2}	Pass-band loss of band stop-filter 2
L_{BPY}	Pass band loss of YIG-filter
L_{BS1}	Stop-band loss of band-stop filter 1
L_{BS2}	Stop-band loss of band-stop filter 2

L_{BSY}	Stop band loss of YIG-filter
L_c	Free-space attenuation
L_{diff}	Diffraction attenuation
L_{fs}	Free-space attenuation
L_{mc}	Attenuation of measurement cable
L_{path}	Attenuation of signal path
$L_{rx\text{-}filter}$	Attenuation of RX filter of TDRRS receiver
M	Flat fade margin
M_{64QAM}	Flat fade margin of 64QAM system
N	Noise power level
$N_{bit,4PSK}$	Number of bits in 4PSK system
$N_{bit,64QAM}$	Number of bits in 64QAM system
N_P	Amount of radar pulses received
N_{Pulse}	Number of pulses
N_S	Constellation size of TDRRS modulation
NF	Nominal Frequency
n	Order of antenna revolution
P	Power
$P_{av,rect}$	Average power of the rectangular pulse
$P_{av,trap}$	Average power of the trapezoidal pulse
P_d	Power on equipment display
P_{in}	Power in input of first filter
$P_{in,SA}$	Power in input of SA
$P_{lin,in}$	Power in input of a digital TRRS
$P_{N,lin,max}$	Maximum spurious power level at the digital TRRS input
$P_{lin,out}$	Power in output of a digital TRRS
$P_{lin,ref}$	Reference power of a digital TRRS
$P_{max,rect}$	Maximum power of the rectangular pulse
$P_{max,trap}$	The maximum power of the trapezoidal pulse
P_{meas}	Measured power
P_N	Noise power
$P_{N,in,SA}$	SA's noise power + incoming noise power in a 1 MHz measurement bandwidth
$P_{N,LNA}$	Total noise power at the LNA input
$P_{N,rx}$	Reduced total noise power sum at the Rx input
$P_{N,spektr}$	Noise power in input of SA
$P_{N,sys}$	Average level of the measurement noise level
$P_{N,4PSK}$	Noise power in 4PSK
$P_{N,64QAM}$	Noise power in 64QAM
P_{NF}	Power of a nominal frequency signal
$P_{NF,in\ A}$	*NF* peak power level at point A
$P_{NF,in\ BS1}$	Power of a nominal frequency signal at BS1 input
$P_{NF,max}$	Maximum *NF* level at the TDRRS input
$P_{NFin,SA,max}$	Maximum *NF* power level requirement at the SA mixer diode (input)
P_{peak}	Pulse peak power
$P_{peak,max}$	Maximum pulse peak power
P_{pulse}	Pulse power
P_{radar}	Power of radar transmitter
$P_{radar.ref}$	Reference power of radar transmitter
P_{ref}	Reference power level

P_{rx}	Power level at RX input
$P_{SA,in}$	Power in input of SA
P_{SF}	Actual spurious power level
$P_{SF,in\ A}$	*SF* peak power level at in A
$P_{SF,max}$	Maximum *SF* peak power level
P_t	Output power of a digital TRRS
P_{tot}	Total power
P_1	Received power in digital TRRS input, where the *C/I* ratio approaches 3 dB
P_2	Received power in digital TRRS input, where the *C/I* ratio is 3 dB
P_3	Turning point of bit error ratio curve (in Figure 58)
R_{eq}	Earth equivalent radius
R_{F1}	Radius of the first Fresnel-zone
R_s	Symbol rate
RSP	Radar signal peak
r	Radius (distance of induction field)
S	Power density
$S_{rect}\ (t)$	Expression for the power spectrum of a periodic rectangular pulse sequence
$S_{trap}\ (t)$	Expression for the power spectrum of a periodic trapezoidal pulse sequence
SF	Spurious Frequency
SNR	Signal to noise ratio
SNR_{min}	Minimum signal to noise ratio
ST	Sweep Time
ST_s	Single sweep time
ST_{tot}	Total sweep time
s (t)	Signal in the time domain
T	Pulse interval
T_φ	Time necessary for sweeping angle
T_a	Remaining measurement bandwidth to achieve
T_b	Total sum of sweep times needed for the remaining undisplayed portion of the spectrum after *n* antenna revolutions
T_c	Time corresponding the unswept portion of the measurement bandwidth $f_1 \ldots f_2$ after an illumination
T_{chirp}	Chirp duration of phase coded modulation
T_{ill}	Illumination time
T_L	Long time period for digital error determination
T_{once}	Duration of one sweep
T_{pi}	Radar pulse time interval
$T_{st.tot}$	Total sweep time
T_{sweep}	Sweep time
T_0	Time cycle for digital error
$T_{1\ldots2}$	Sweep time for frequency from f_1 to f_2
T_{360°	Time of one antenna revolution
t_k	Defines the time shift of k's radar pulses
W_{meas}	Bandwidth to bee measured range
X	Distance between *NF* and *SF* signal levels
$X_{rect}\ (t)$	Expression for the power spectrum of a periodic rectangular pulse seq
$X_{trap}\ (t)$	Expression for the power spectrum of a periodic trapezoidal pulse seq
$x_k(t\text{-}t_k)$	Pulse shape of the kth transmitted radar pulse

ABBREVIATIONS

0-128	
0-span	Spectrum Analyzer Work on spot frequency
3G	Third Generation Cellular Systems
4G	Fourth Generation Cellular Systems
2PSK	2-level Phase Shift Keying
4PSK	4-level Phase Shift Keying
8QAM	8-level Quadrature Amplitude Modulation
16QAM	16-level Quadrature Amplitude Modulation
32QAM	32-level Quadrature Amplitude Modulation
64QAM	64-level Quadrature Amplitude Modulation
128QAM	128-level Quadrature Amplitude Modulation
A	
AGC	Automatic Gain Control
B	
BPF	Band-pass filter
BSF	Band-stop filter
C	
CEPT	European Conference of Postal and Telecommunications Administration (CEPT)
CW	Carrier Wave
C-band	Frequency Band 4...8 GHz (for Radar)
D	
dBc	Variation from carrier level in decibel
DTIC	Defense Technical Information Center
DR	Dynamic range
E	
EIRP	Effective Radiation Power of isotropic antenna
ERP	Effective Radiation Power
ES	Errored second
F	
FB	Fly Back Sweep
FICORA	Finnish Communications Regulatory Authority
FM	Frequency Modulation
FM-CW	Frequency Modulated Carrier Wave Radar
FMTV 8000	TV program distribution link
FW	Frequency Window
G	
GSM	Global System for Mobile Communications
H	
HF	High frequency
HPF	High-pass filter
I	
IEEE	The Institute of Electrical and Electronics Engineers
IMT 2000	International Mobile Telecommunications 2000
ITU	International Telecommunication Union
K	
K_u, K, K_a	Radar frequency letter designations according to waveguide size

L	
LNA	Low Noise Amplifier
LPF	Low-pass filter
M	
Max-hold	Hold of maximum level on display of the spectrum analyzer
MMFR	Maximum measured frequency range
MRK	Mark generator shows frequency and power level at SA display
N	
NF	Nominal Frequency
NTIA	National Telecommunications and Information Administration
P	
PCM	Pulse Code Modulation
PDH	Plesiochronous Digital Hierarchy
PMP	Point to multipoint
PRF	Pulse Repetition Frequency
PRR	Pulse Repetition Rate
R	
RX	Receiver
S	
SA	Spectrum Analyzer
SDH	Synchronous Digital Hierarchy
SES	Severe Errored Seconds
SFS	Suomen Standardisoimisliitto SFS ry (Standardization Organization of Finland)
SHF	Super High Frequency
SPAN	Frequency Span
SPEED	Speed of sweep of the spectrum analyzer
SWR	Standing Wave Ratio
T	
TRRS	Terrestrial Radio Relay System
TARRS	Terrestrial Analogue Radio Relay System
TDRRS	Terrestrial Digital Radio Relay System
TR-switch	Transmitter-Receiver Switch
TX	Transmitter
U	
UHF	Ultra High Frequency
ULA	Analogical audio broadcasting network (frequency band 87.5 – 108 MHz)
UWB	Ultra Wide Band
V	
VHF	Very High Frequency
VIEW	Viewing state for display of equipment
VR	Valtion rautatiet (State Railways)
W	
WLAN	Wireless Local Area Network
WiMAX	Worldwide Interoperability for Microwave Access
Y	
YIG-filter	Yttrium-Iron-Garnet Filter
YLE	OY Yleisradio AB, (Finnish Broadcasting Company)

1 INTRODUCTION

1.1 General background

The rising demand of useful frequencies for radio communications has lead to more effective use of the spectrum. The more efficient use of spectrum has lead to the utilization of channels neighboring radar frequencies. Also use of frequencies interfered by radar, both harmonic and non-harmonic interference, has increased. Therefore, the demands for even cleaner nominal frequency (*NF*) spectrum and less disturbing spurious frequency (*SF*) signals have increased. In the increasing amount of radar systems all the time this causes more and more interference situations between radar systems and other radio communication systems.

When the telephone trunk network was automatized in Finland in the 1970's many connections between telephone exchanges (PBX) were built using terrestrial radio relay systems (TRRS). The total or partial outages of digital TRRSs lead to extensive interference investigations and measurement campaigns especially in eastern parts of Finland, where the interference situation was most severe. Based on these investigations it was found that many of the interferences were caused by radar signals whose origin was located east of the eastern Finnish borderline. Radar signals were observed either directly on frequencies allocated for TRRS use or their *SF* signals spread to these frequencies causing interference. When the Finnish aeronautical regulator (FINAVIA), formerly Civil Aviation Administration, and the Finnish meteorological institute started building their radar systems also the amount of high power radar stations in Finland begun to increase. In addition also the Finnish defense force built their own radar system. This lead to systematic inspection of high power radar stations in civilian use in Finland.

It is known, that radar signals always in addition to their *NF* signal also contain small amounts of spurious signals. These spurious signals are harmonic and non-harmonic spurious frequency signals. Therefore other radio communication systems than radars operating on same or neighboring frequency bands have to deal with the received interfering radar *SF* signals. One typical type of interference created by radar is a pulse signal burst observed every 5…20 seconds. This interference is present always when the antenna main lobes of the interfered radio system and the radar overlap once on every radar antenna revolution (for example 6.66 revolutions per minute = 9 s/full circle). This event will be called “illumination” in the sequel. When taking into account the gain of the radar antenna the peak burst power can be as high as in the Gigawatt range. While rotating the radar antenna distributes pulse bursts uniformly in all directions. If the pulse burst interval is shorter than 10 second this may prevent digital radio systems, for example TDRRSs, to return to availability state. If the interfering *SF* comes from a weather radar operating in the 5 GHz (C-band), the interfered system can be a wireless local area network (WLAN), a worldwide interoperability for microwave access (WiMAX), an ultra wide band system (UWB), a TDRRS, a satellite telecommunications or radio astronomy system or another radar operating in the same frequency band.

General knowledge of both wanted and unwanted components in the radar spectrum are needed increasingly. The International Telecommunication Union (ITU) recommendation ITU-R M.1177-3 [1] presents a measurement system for measuring the unwanted spectrum components inside the radar spectrum (Appendix I). Due to the lack of frequencies and in using neighboring channels to radar systems this need is emphasized.

Even though the amount of spurious signals (*SF*) around radar frequencies has been decreasing due to development of radar the problem is still present. The number of radar systems is ever increasing and due to economical reasons crossed-field type radio frequency power generators are used and these produce large amounts of *SF* signals.

1.2 Related work

The returning radar echo pulse has been studied and written about extensively in contrast to minor documentation on the subject of interference and measurement of interferences caused by radar. The ITU has stated the subject of the significance of radar *SF* signals and has presented recommendations on measurement of *SF* ITU-R RECOMMENDATION M.1177-3 [1] and measurement results ITU-R RECOMMENDATION M.1314 [2] and other technical qualities concerning radar use (Appendix II Table and III). In literature there can also be found e.g. a National Telecommunications and Information Administration (NTIA) report on radar interference measurement NTIA Report 94-313 [3] and NTIA Report TR 05-420 [4] that are based on the same principles as in the ITU recommendation. Other recommendations and reports on this subject are found as follows: ITU-R SM.329-10 [5], ITU-R SM.1541 [6], RCG-27 [7], RRS-138 [8], Defense Technical Information Center (DTIC) [9] and Science Links Japan [10].

Information on the study of interference to digital TRRS caused by radar and their measurement and the effects on availability or non-availability of TDRRSs as presented in this work is found in some data bases. Information in this direction can be found in the following documents: CCIR, Geneva; March 1991, Volume XV-4, Addendum No1, Question 159/9: "Effects of unwanted emissions, from Radar systems in the radio determination service on systems in the fixed service" [11], H.U. Eichhorn, "Radio interference into high capacity digital radio", Apr 1989 Proc. 2.BCRR, p.187 [12], ITU-R F.1190 [13], IEEE Explore [14], GFI 0501 report [15], Bradley J. Ramsey, "Investigations of Radar Interference to Satellite Earth Stations and Terrestrial Microwave Communication Sites.", Institute for Telecommunication Sciences, Boulder, Colorado 80303 USA, IEEE 1998. [16] and NTIA Technical Memorandum TM-05-431 [17].

During these studies the Finnish telecommunication authority had decided to use a measurement technique based on the same principles, but did carry out the measurement in a different way. The ITU recommendation is based on spot frequency measurement done step by step using the 0-SPAN function of the measurement equipment, computer control, computer controlled YIG filter and an adjustable attenuator. The new measuring system is based on frequency sweep and the use of max-hold function.

1.3 Research problem

1.3.1 ITU recommendation

In the ITU recommendation [1] the *SF* signal measurement is based on suppressing the high power *NF* signal with an optional filter. A band-stop filter (BSF) can be applied here. Measurement of harmonic components can be done either with a BSF or with low-pass filters (LPF) and high-pass filters (HPF), that attenuate the *NF* signal sufficiently enough. The measurement proceeds step by step while a computer is controlling the measuring equipment, a spectrum analyzer (SA), the adjustable attenuator and the YIG filter. A suitable low noise amplifier can improve the sensitivity. The signal power levels are matched with the attenuator. This kind of measurement procedure, however, can not be used above the

radar *NF*, because the YIG filter in this procedure is a band-pass filter (BPF) when a BSF is required. Finding a suitable YIG-filter that can be computer controlled in the 5 GHz frequency band has made it difficult to apply the measurement system advised in the ITU recommendation. The measuring method described above has proven to be unreasonably difficult especially in field measurement. Due to this reason a different measuring method is described in this work. The YIG-filter is substituted by a BSF tuned to the *NF*. In doing so one does not have to take into account the high power *NF* during measurement and system components need not to be tuned after basic setup tuning.

A frequency sweep is used in this method created by the author and used at the Finnish Communications Regulatory Authority (FICORA). Here the outcome or the partial results are available immediately after the sweep or sweeps. Also the outcome can be recalled from the memory of measurement equipment at a later time. The measurement control in the ITU method requires computer control. Ending up with the measuring method, requiring no computer, presented in this work was quite natural since mobile computer units (i.e. laptops) were not common at the time the ITU method was created. At FICORA this method is still used with or without computer controlling. The speed of the manual measurement method is not depending on the measurement method itself but on the rotation speed of the radar antenna and the technical characteristics of the analyzer.

1.3.2 Study problem 1

In radar measurement (while antenna is rotating) synchronization of the rotation speed of the antenna and the SA sweep time (*ST*) causes a problem. The SA measuring time is difficult to lock on the antenna rotation speed when one has to find an optimal solution between measuring time and probability of completeness of spectrum measurement. After successful synchronization one talks about a synchronized measuring method. However, if synchronization is not achieved one talks about non-synchronized measuring method.

The high noise level of the SA (here the noise figure is 27 dB) and a modest measuring dynamics (40...60 dB) are also problems. To reduce noise level one can use a low noise preamplifier (LNA). However, this leads to the risk of SA overloading which therefore results in the need of a BSF to attenuate the *NF*. The measuring dynamics can be raised with both procedures described before (requirement over 110 dB). The key factor for measuring dynamics is a correctly dimensioned BSF. The availability of a BSF can lead to problems in the measurement. Recalibration of the system after modifying connections must always be done when using described components where the BSF is a frequency depending component.

One must be able to determine the balance of spectrum (how much spectrum can be measured in different situations) because it depends directly on the measurement time used. The measuring time and its optimization are key factors for the staff doing the measurement. The use and determination of measurement parameters before this work have varied and lead to varying measurement time and this leads to that the outcome of the measurement being doubtful due to varying measurement times. In the eyes of radar users and TRRS operators one should be able to determine the minimum protection distance between radar transmitters and TRRS receivers to avoid interference between these radio systems. Both the solution to these measurement problems and their functionality are described with help of example cases.

1.3.3 Study problem 2

Applying results of radar measurement to an interfered digital radio system and the impact on the system involves several problems. One has to know the modulation method of the

radio system. Also one has to know the impact of a single radar pulse to the instantaneous behavior of the decision process of the radio system and on the recovery from a possible loss of synchronization. On larger scale one must study the state of the radio system and compare its signal levels with the radar signal levels using link budgets. This is one possibility to find possible violations of the interference criteria. Both in radio system planning and radar *SF* signal filtering the effect of the other system must be considered. In this work the system states are compared with respect is characteristics interference with an example (radar vs. TDRRS).

1.4 Scope and goals

Inspections prior to taking into use radio stations (also radar stations) and solving of radio traffic interference cases are one task of the Finnish radio frequency management authority. This includes the necessary measurements. The most important goals in this work are:

a) To present a measurement system that can be used for the radar station inspections described above and for interference measurement under field conditions with sufficiently simple and economical measurement equipment.
b) The goal of the measurement system is to obtain a sufficient measuring dynamics (>100 dB) to be able to conduct the required measurements,
c) to measure relative spurious signal levels and frequencies and
d) based on the measurement results to estimate the interference risk of surrounding radio communication systems and to set possible restrictions to the use of the interfering radar.

- Additionally, one goal is to determine and optimize the time needed for measurement.

These goals have been realized as an application in studying a radar signal containing spurious frequencies. Furthermore, by studying disturbances caused to digital radio systems by an interfering spurious frequency of radar signal in the time and frequency domain and its effect to the system status (has been investigated).

1.5 Contributions

A common problem is how to measure a signal neighboring another far higher powered signal adequately reliable. This kind of signal can be for example a radar *SF* signal 100 dB lower than the *NF* signal of the radar. The author has in this work developed a measurement method for the determination of the spurious signals of high power radars. The author has also implemented a measurement system with easily available measuring equipment ending up with a field capable, economically implemented, and sufficiently reliable system. The study made for this work focuses on solving this problem and presenting a new useful measurement system based on practical knowledge and differing from earlier measurement systems. The novelty value of this measurement system is based on a simple, field qualified and economical procedure that for the first time analyzes availability of radar pulses and utilization in the measurement. This study on the time domain parameters gives the qualification to make measurements in frequency domain in which a full picture of the radar signal spectrum and its signal components can be presented with the sufficient 110 dB measurement dynamics.

The author has clearly shown in this work that low power signals neighboring high-powered signals can be measured with the new measuring method even though the

difference in level is over 100 dB. The measurement method has been applied to determine characteristics of radar interference signals while the radar antenna is rotating. This has been done by extending the measurement dynamics and by optimizing measurement time. Also this work presents how to choose the different measurement parameter values to succeed in the measurement and to be able to optimize the measurement time. Radar interference into terrestrial radio relay systems (TRRS) has been studied because of the fact that radar most commonly produces interference to frequencies used by TRRSs.

By applying well-known radio link budget principles a novel method for estimation of the protection distance between a radar and a digital radio communication link is developed. The use of beyond-the-horizon propagation models seems to not have been applied in this context earlier. A new contribution to the work of e.g. a frequency regulatory authority is the proposal to use a modified version of the new measurement system to check the sufficiency of the protection distance by measuring the radar interference in the real situation.

Most severely radar interference influences digital radio systems (TDRRS). Therefore interference mechanisms impacting TDRRSs have been studied and applied to interference measurement results obtained from the new measurement system. The approach could as well be used to study interference impact to WLAN, WiMAX, UWB or any other digital radio systems. Then the method must be adapted according to the performance requirements of each system.

1.6 Outline of the thesis

Chapter 2 of this work presents a few high power radio signal sources. Near an antenna radiating radio frequency signals the possibility of interference signals is not dependent on whether the signal power comes from a "low power" mobile cellular base station or a "high power" broadcasting station. The attenuation of a radio signal propagating in free space is proportional to the squared distance and frequency. So the signal source power, the distance between study point and object to study and the used frequency all play a major role when evaluating the impact of the radar transmitter on the disturbed communication receiver.

Radar, its basic operation and frequency bands are described in **Chapter 2**. A radar pulse in the time domain and the corresponding power spectrum in the frequency domain are also presented. The simulated ideal and the measured power spectrum created by a radar pulse have been compared. Radar power, radar use and parts of the mechanical construction have been presented. Also inspection of radars, measurement problems and interference created by radar have been dealt with in this chapter. The possible operating range in view of health questions is presented.

Chapter 3 deepens knowledge about routine measurement of radar spectrum. It is also explained how to map unknown radar frequencies for measurement. Also the aspects that must and how these must be taken into account when preparing measurements and how the measurement equipment should be set up are presented. In this chapter it is described with what measuring equipment and accessories the measurements in this work have been done. The received radar echo, which usually is the most interesting factor in radar operation has no significance at all in this work. The highest interest is focused on the transmitted radar pulse and its measurable spectrum before the pulse hits its target and is reflected back. At the end of **Chapter 3** a flowchart how to map an unknown target (part 1) is presented.

The most important chapter in this work is **Chapter 4**. In this chapter the developed radar measurement technique is presented in detail with help of block diagrams and radar budgets. The measurement technique has been implemented in two different parts. The first part is the time domain parameter measurement. In this the pulses sent by radar are analyzed

and processed in different situations (rotating speed of radar antenna, width of the antenna lobe, the repetition frequency of the radar and length of pulse). This part gives the parameters used in the later frequency domain measurement. This is the second part of the measuring technique being presented here. It gives measurement results about radar *SF* relative signal levels. The frequency domain measurement can be made alone but the time domain parameter study on its own does not give results of the different spectrum components powers and frequencies. However, it helps understanding the whole measurement technique and is therefore important.

One of the most important decisions influencing the measurement results for this measuring method is the selection of measuring bandwidth. How this is done is presented in **Section 4.1**.

Various sweep measurement methods and optimization of the frequency domain measurements are presented in the time domain parameter study. These have been applied in this work. At the end of **Section 4.2** the progress of the time domain parameter study is presented in a flow diagram (part 2).

Radar measurement in the frequency domain gives results about power and frequency of the spectrum components. In **Section 4.3** is shown how the systems (two different versions of measuring system) have been set up and also the signal flow from transmitter to measurement equipment input is shown. Dynamics and need of its extension are shown mathematically in **Sections 4.3.1 and 4.3.2**.

In **Section 4.4** radar antenna features and their influence on the measurement results and interpretation of these are discussed. Examples are presented both as measured in practice and as calculated results. At the end of **Chapter 4** the frequency and antenna impact on the measurement are presented in a flow diagram (Part 3). In **Appendix V** the complete flow diagram is presented (Parts 1, 2 and 3).

In **Chapter 5** a TDRRS is presented in the extent necessary for examining its interfered state. A brief arch of development into the present time for national TRRSs is also presented. Locations of link hops in Finland in a certain radio band together with locations of weather radar stations of the Finnish meteorological institute are presented in this chapter. In **Section 5.4** the quality requirements for digital connections are presented and mirrored against interference produced by radar. The interference mechanisms are also described both theoretically in time and frequency domains. The measurement of interference to TDRRS is presented using the same principles as were used for radar measurement.

In **Chapter 6** it is shown how radar interferes the TDRRS, how it can be observed and how the interference can be presented in time and frequency domains. A method for estimation of the protection distance between an interfering radar and a TDRRS receiver is given and results for several MQAM radio links are shown. Finally, the application of a modified measurement system for the checking of the sufficiency of the estimated and implemented radar distance is outlined.

Chapter 7 summarizes the work and points out the main results and their importance for radar measurements from the point of view of the regulator. Conclusions are drawn. Advantages and limitations of the new measurement systems and the applications based on the results are shortly evaluated. Proposals for further research are given.

2 HIGH POWER RADIO FREQUENCY SOURCES

What is a high power radio frequency source? This question can not be answered unambiguously. The answer is depending on to what source the radiating power is compared to, in what situation the comparison is made and where the comparing is made. The biggest radio frequency source, mankind is continuously confronted with, is the Sun. The total radiation flux of the Sun has been estimated being $3.99 \cdot 10^{26}$ W [18] or equivalently 296 dBm. A part of this radiation is radiation in the radio frequency spectrum. Even though the distance between Sun and Earth is 150 000 000 km, a radiation flux density of about 1370 W/m^2 [19] at the Earth surface is measured. The biggest part of this flux is visible and infrared light. Only less than 1% [19] of the power is radio frequency radiation. This radiation is spread over the whole radio frequency spectrum. The frequency spectrum between 3 kHz and 3 000 GHz is defined as radio frequency spectrum. In the universe there can be found even bigger electromagnetic radiation sources, for example quasars (quasi-stellar radio source). The radiation flux of quasars is typically between 10^{39} and 10^{41} W [19]. The distance between quasars and the Earth compared to the distance between the Sun and Earth is enormous. Therefore the radiation amount of these quasars at Earth surface is insignificant.

Without the radiation of the Sun life on Earth would be completely impossible. If utilization of electromagnetic radiation of the Sun is examined, its use focuses mainly on visible light. Use of radio frequency radiation is minimal. If then interference of radiation from the Sun is examined, it is found that radio frequency electromagnetic radiation power is disturbingly high. Magnetic storms in the Sun for example cause big problems to electronic devices at the Earth's surface and to orbiting satellites in space. Even under normal circumstances there are problems in satellite reception, when the Sun and a satellite are seen from Earth at the same direction.

High power radio frequency radiation sources constructed by man are for example broadcast transmitters. The power radiated from the UHF TV transmitter antenna in an analogue network was at the highest 1000 kW (ERP) [20]. Equivalently radiated power in analogue sound broadcast networks (FM) is at its highest 60 kW (ERP) [20]. Powers of broadcasting transmitters are concentrated to narrow parts of the radio frequency spectrum and are usually directed towards the horizon (FM and TV networks). This radiated power can depending on propagation and terrestrial circumstances be utilized in reception at distances up to 100 km. At the reception point the power density is attenuated significantly if compared to the transmitting antenna radiating power density. Other high power radio frequency emissions can be found between antenna electrodes in plastic welders and glue dryers in wood processing. In these processes the radio frequency power is focused on very small physical areas (high power density). This causes heating of the processed materials and to welding of plastic or drying of glue in wood processing. Power density in these focused radio frequency radiation points can be up to 100 kW/m^2. When correctly sealed off, radio frequency interference is not found outside this equipment.

What about microwave ovens or mobile telephone equipment (GSM)? Inside a microwave oven there is a high frequency field conducted usually from a power source less than 1 kW. However this power is big enough to get the water molecules inside the object to be heated into motion so creating heat to get the object heated in a reasonable time. Outside a microwave oven, when examining from this studies view, there are usually found very low power levels. This, however, can cause problems to for example a WLAN connection in the same room.

Radiating power from a GSM phone is usually maximally 2 W (ERP) for vehicle stations and 0.2 W for portable phones and up to 600 W for the base station [21]. If an omni-directional antenna with 12 dB gain in the horizontal plane is presumed for the base station, the radiation power density at a distance of about 1 km (free space loss) is 757 $\mu W/m^2$. While using a mobile phone, at a distance of 5 cm of the mobile phones isotropic antenna, peak power density levels up to 6.366 W/m^2 can occur. In time-division multiplex (first generation GSM) the peak power density occurs during 1/8 part of the time. Average power density that could be absorbed to tissue and cause tissue warming is 1/8 part of the peak power density. Mobile phone antennas are constructed so, that a minimal amount of radiated power is directed towards the users head. The body of the user reflects about half of the impacting power back. When using a mobile phone the power density influencing the users head stays clearly under the recommended safety maximum value of 0.397 W/m^2 [22]. Under present knowledge the radio frequency emission levels of mobile phones are not hazardous to health.

One big radio frequency source are radars. Radar sends power as short pulses. In these pulses the peak power measured including antenna gain is in the Gigawatt range. When the pulse length is 1 microsecond, the pulse peak power is 1 GW and pulse repetition frequency is for example 1000 Hz the average radiated EIRP is up to 1 MW.

High power radio frequency is used in many practical applications. In broadcasting and TV networks transmitter power is one of the key factors when one is at the same time trying to gain maximum coverage at an economically reasonable cost. Selected operating frequency and technical solutions are also significant.

Heating and melting of materials need immense amounts of power. The object to be heated or melted absorbs this power. Radio frequency radiation can be chosen as the power source. Radar is used in air and sea surveillance. In addition to the selected frequency the amount of electromagnetic radiating power of radar is a key factor, when aiming for maximum range of the surveillance area. The power of mobile telephone network base stations and mobile devices is relatively low. Since the aim of mobile telephone networks is not to gain maximum coverage with one base station, lower power levels are adequate. Maximum coverage is achieved by placing base stations as tight as needed and by taking into account user needs with accurately directed or adaptable base station antenna solutions.

To sum up the above shortly, a high amount of electromagnetic radiation power is not always a primary target in technical applications. In some applications maximizing power is the primary target. In others it is not a key factor, as long as there is a high enough power level. Also there are situations, when power levels have to be very small but satisfactory high to make it possible to obtain the appropriate performance. A radio technical function of this kind can be the measurement of a high power radiation source. The use of this kind of source can increase the risk of interference to the source apparatus itself or in other electrical applications in the immediate surroundings. In some cases the risk of interference applies even to electrical applications very far from the source.


KAISERLICHES PATENTAMT.

AUSGEGEBEN DEN 21. NOVEMBER 1904.

PATENTSCHRIFT

– № 165546 –

KLASSE 74 d.

CHR. HÜLSMEYER IN DÜSSELDORF.

Verfahren, um entfernte metallische Gegenstände mittels elektrischer Wellen einem Beobachter zu melden.

Patentiert im Deutschen Reiche vom 30. April 1904 ab.

Fig. 1.

Figure 1. Radar patent from 1904.

2.1 Radar transmission

In nature there are several animals, which use radar like sonar when moving or hunting. To list up some of these animals using sonar, there are bats, dolphins, whales, certain birds and even shrew mice. These animals send sonic or ultrasonic sound pulses and receive echoes from these pulses. With help of these echoes they can recognize their surroundings or navigate or prey. Bats for example use sound frequencies in the range of 20…100 kHz. Bats recognize their own echo that means that their sound bursts must be unique (coded). The principle of technical radar (copied from nature by humans) was invented 1904. At this time C. Hülsmeyer patented his own innovation [23]. The patent is shown in Figure 1. Both the British and the Germans started developing radar before World War II. First after inventing the cavity and vane magnetrons the real development of radar began. During World War II the Americans were capable of producing magnetrons needed in radars at a rate of 2600 units per day. Radar proved itself very quickly useful in war actions. Later it also became useful in civil use.

The principle of radar is very simple. First a short radio or audio pulse is sent. Then, with an accurate clock, the time between pulse transmission and echo reception is measured. When the speed of the used wave in a certain medium is known, the distance to the target can be calculated and presented visually. Some question arises on how animal radars work. Are bats using the same method? How accurate clocks do they have? Do bats know the speed of sound waves in air and in water and how temperature and moisture affect this speed?

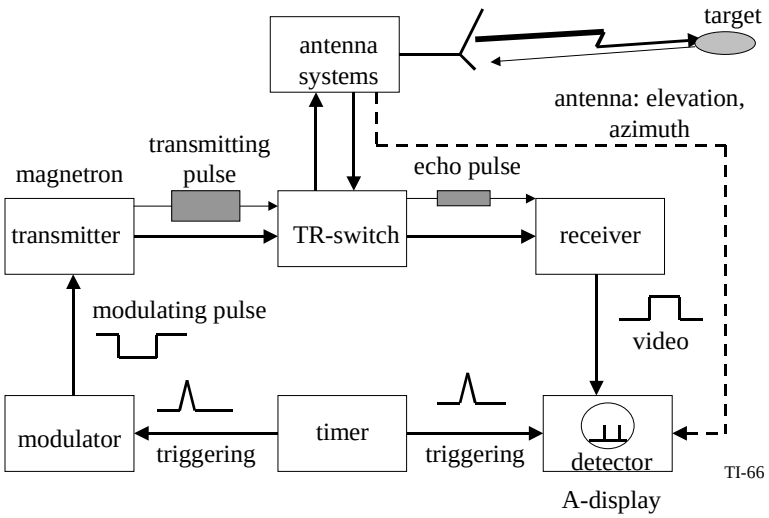

Figure 2. Simplified schematic diagram of a pulse radar

A simplified schematic diagram of a pulse radar is presented in Figure 2. The modulator modulates the radar transmitter carrier (in high power radars typically a klystron or magnetron). In this case the transmitter consists of a magnetron. Also other techniques (i.e. klystron, solid state transistor) can be used. The high frequency (MHz or GHz) and high power (MW or GW) pulses are fed to the antenna. This is done via the transmit / receive switch (T/R-switch). The returning echo is forwarded through the T/R-switch to the receiver and demodulator. For displaying a cathode ray tube can be used. It also is possible to store the received data into a digital database for further processing with a computer. The timer controls both the modulator and the demodulator to run synchronously.

2.1.1 Use of radar and frequency bands

The selection of frequency band is affected by the intended use of the radar. The realization of the technical construction is the simpler the lower the used frequency. Sufficient power is also easier to create at lower frequencies. The lobe width and of the antenna in the measuring direction (H=horizontal or V=vertical polarization) affects the accuracy of the radar. The narrower the lobe the more accurate the radar (this does not apply for SAR systems). The impact of rain on the path attenuation of radio waves in dB in the frequency range 6…40 GHz is approximately a quadratic function of frequency. The higher the frequency is, the shorter is the measuring distance. Radar cross-sectional surface of raindrops and small particles in the air is proportional to the power four of the used frequency. The impact of the ionosphere is the inverse of the used frequency and may be significant up to 3 GHz. Use of frequencies has been agreed on an international basis and is documented in the Radio Regulations by the ITU [24]. In Finland the regulator has directed use of radio frequencies in a national frequency allocation table [25].

Use (in Finland) of radio frequencies for radars is categorized based on the intended use of the radar systems:

High frequency band (HF-band) 3…30 MHz

- Measurement beyond the horizon
- Long-range
- Low resolution and measurement accuracy

There is no allocated frequency slot for radar system use in Finland in this frequency band. However, a few exceptions have been allowed. Sodankylä Geophysical Observatory of the University of Oulu may use ionosphere sounding radar in the frequency range from 500 kHz to 30 MHz in Sodankylä, Enontekiö and Muonio. Also the Finnish Meteorological Institute is allowed to operate a radar system in the frequency range from 9040 kHz to 19990 kHz at Hankasalmi.

Very high and ultra high frequency bands (VHF, UHF bands) 30 MHz…3000 MHz

- Long range.
- Surveillance of air space above the horizon.
- Medium resolution and measurement accuracy.
- No significant impact by weather.

In Finland the frequency range from 960 MHz to 1350 MHz is allocated for radio navigation / radar and secondary radar use. Secondary radar is used to receive flight information data from an approaching airplane at the airport. The airplane sends its feedback with a transponder. The frequency pair of secondary radars is 1030 MHz/1090 MHz.

The following radar operating frequencies are usually named according to the US nomenclature for microwave frequencies.

L-band, 1…2 GHz

- Long range
- Medium resolution
- Some influence of weather

S-band, 2…4 GHz

- Short range surveillance radar
- Long range tracking radar
- Medium resolution
- Significant weather impact by heavy rain and snow fall

In Finland the frequency range from 2700 MHz to 3400 MHz is allocated for radio navigation / radar.

C-band, 4...8 GHz (contain 3.90…6.20 GHz)

- Short range surveillance
- Long range tracking
- High resolution
- Significant weather impact by rain and snow fall

In Finland the frequency range from 5250 MHz to 5850 MHz is allocated for radio navigation / radar / weather radar.

X-band, 8…12 GHz

- Short range surveillance
- Long range tracking with high resolution in clear weather

In Finland the frequency range from 8500 MHz to 10000 MHz is allocated for radio navigation / radar / ship-, boat-, controlling-, surveillance- and alarm radar systems and radar transponders.

Also in the frequency range from 10.450 GHz to 10.500 GHz allocations are made for radio navigation / radar / controlling-, surveillance- and alarm radar systems.

K_U – K – K_A-band, 12...40 GHz

- Small size antennas
- Capable of operation in any weather

In Finland there are several frequency bands allocated for radio navigation / radar / controlling-, surveillance- and alarm radar systems. The bands are: 15.700...17.300 GHz; 24.000...24.250 GHz and 30.400...36.000 GHz.

Millimeter band, 30...300 GHz

- Short-range tracking

In Finland there are two frequency ranges allocated for radio navigation / radar. The frequency ranges are 33.400...36.000 GHz and 76.000...81.000 GHz.

To improve, extend or alter certain characteristics of the before mentioned radars it is possible to have exceptions from the given frequency bands.

One has to consider the intended use of a radar system when planning and constructing radar. There is a difference between displaying the structure of cloud layers, weather fronts or wind speeds and displaying moving objects from behind clouds. The first radar system described is a weather radar mapping different components (clouds, weather fronts, e.g. and their intensity below 10 km altitude) of the atmosphere. The clouds, weather fronts and their echoes are in this case primary targets. The second radar system could be a military radar, where impact from weather can be harmful to the system and must be avoided. Also the aim can be in getting information about targets and their speed. In this case fixed targets are harmful and must be eliminated. Remote sensing radar determines topography and crust of the ground. The echoes from different types of solid ground shapes are the most important observations. With this kind of radar it is also possible to for example determine the thickness of ice or different ground layers. Also surfaces of the planets in our

solar system and their satellites and comets in space can be remotely sensed by this radar type.

2.1.2 Modeling of a radar pulse train

The output of the radar transmitter is a sequence of short pulses. A general representation of this signal *s(t)* in the time domain is given by Equation 2.1

$$s(t) = \sum_{k=-\infty}^{\infty} x_k(t - t_k)\cos(2\pi f_c(t - t_k) + \varphi_k) \tag{2.1}$$

In Equation 2.1

- *x(t)* is the infinitely long transmitted radar pulse sequence,
- φ is the carrier phase,
- *t* defines the time shift of the radar pulses,
- *k* is the order of a transmitted radar pulse and
- f_c is the modulated carrier frequency

This representation allows each pulse $x_k(t)$ to be of different shape and the interval between the different pulses may vary.

In this context, however, it will be assumed that the pulse shape will not vary and that the time interval between the pulses is constant. This results in a periodic radar signal given in Equation 2.2 .

$$s(t) = \sum_{k=-\infty}^{\infty} x(t - kT - t_0)\cos(2\pi\ f_c\ t + \varphi) \tag{2.2}$$

additionally in Equation 2.2

- *T* is the pulse interval (*T=1/PRR*),
- t_0 defines the time shift of the radar pulses,

An ideal radar pulse would be of rectangular shape as shown in Figure 3a. The practical radar pulse, however, will have a finite rise time and decay time and the exact shape of the rise and decay will depend on the actual transmitter implementation. A simple approximation of the practical shape, also considering finite rise time and decay time, is the trapezoidal pulse shape shown in Figure 3b.

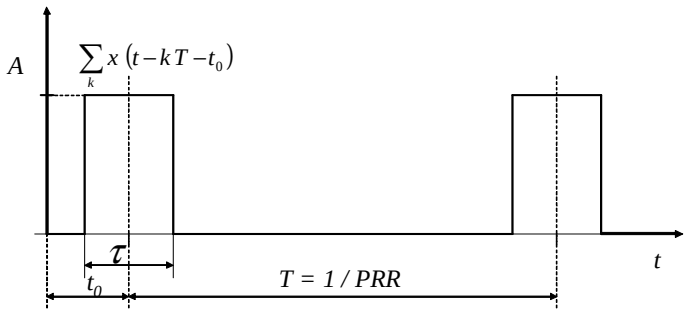

Figure 3a.

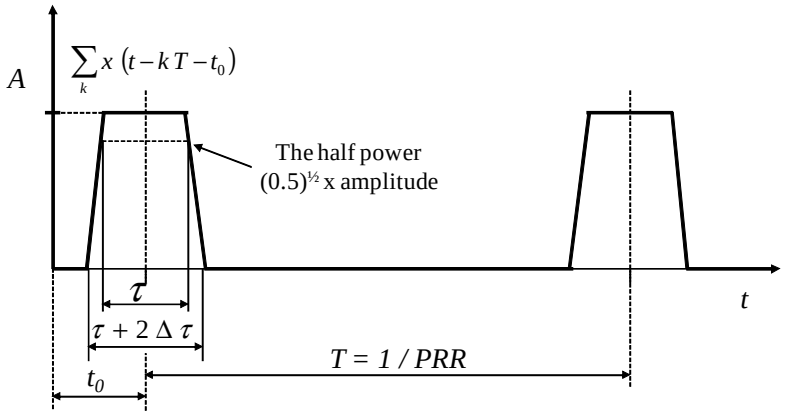

Figure 3b.

The ideal rectangular pulse is defined by Equation 2.3 .

$$x(t) = A\,\mathrm{rect}\left(\frac{t}{\tau}\right) = \begin{cases} A, & -\frac{\tau}{2} \le t \le \frac{\tau}{2} \\ 0, & t < -\frac{\tau}{2},\ t > \frac{\tau}{2} \end{cases} \tag{2.3}$$

The trapezoidal pulse can be expressed as the convolution of two rectangular pulses as defined by Equation 2.4.

$$x(t) = A\ \mathrm{rect}\left(\frac{t}{\tau}\right) * \mathrm{rect}\left(\frac{t}{\Delta\tau}\right) \tag{2.4}$$

The peak power is for both pulse shapes

$$P_{max,rect} = A^2 \tag{2.5}$$

The average power of the rectangular pulse train is

$$P_{ave,rect} = \frac{\tau}{T} P_{pulse} = \frac{A^2\tau}{T} = \frac{\tau}{T} P_{max} \tag{2.6}$$

The average power of the trapezoidal pulse is obtained in the following way

$$\begin{aligned} P_{ave,trap} &= \frac{\int x^2(t)\,dt}{T} = \frac{2A}{T}\left[\int_0^{\Delta\tau}\left(\frac{t}{\Delta\tau}\right)^2 dt + \int_0^{\frac{T}{2}-\Delta\tau} dt\right] \\ &= \frac{2A^2}{T}\left[\frac{\Delta\tau^3}{3\Delta\tau^2} + \frac{\tau}{2} - \Delta\tau\right] = \frac{\tau}{T}A^2\left[1 - \frac{2\Delta\tau}{3T}\right] \\ &= \left(1 - \frac{2}{3}\frac{\Delta\tau}{\tau}\right) P_{max,trap} \end{aligned} \tag{2.7}$$

When the pulse duration τ_p is defined by the time difference between the half power instants, the duration of the rectangular pulse is

$$\tau_{p,rect} = \tau \tag{2.8}$$

and the duration of the trapezoidal pulse

$$\tau_{p,trap} = \tau - \Delta\tau\left(\sqrt{2} - 1\right) \tag{2.9}$$

The pulse spectrum is obtained as the Fourier transform of the pulse train. Equation 2.10 gives the Fourier transform of a periodic pulse train:

$$\mathrm{F}\left\{\sum_{k=-\infty}^{\infty} x(t - kT)\right\} = \frac{1}{T}\sum_{n=-\infty}^{\infty} X\left(\frac{n}{\tau}\right)\delta\left(f - \frac{n}{\tau}\right) \tag{2.10}$$

In Equation 2.10:

- $X(f)$ is the Fourier transform of a single pulse $x(t)$,
- $\delta\left(f - \frac{n}{\tau}\right)$ is a Dirac impulse function at the frequency $f = n/t$ and
- F{ } is the Fourier transform operator.

A set of discrete spectrum lines thus constitute the spectrum of an ideally periodic radar signal.

Equation 2.11 gives the power spectrum of the periodic radar signal.

$$S(f) = \frac{1}{T^2}\sum_{n=-\infty}^{\infty} |X(nT)|^2\,\delta(f - n\,f_0) \tag{2.11}$$

Equation 2.12 gives the Fourier transform of the rectangular pulse.

$$F\left\{A\,\mathrm{rect}\left(\frac{t}{\tau}\right)\right\} = A\tau\,\mathrm{sinc}(f\,\tau) \tag{2.12}$$

The definition of the sinc-function is

$$\mathrm{sinc}(x) = \frac{\sin(\pi x)}{\pi x} \tag{2.13}$$

Thus the expressions of the spectrum and power spectrum of a periodic rectangular pulse sequence are

$$X_{rect}(f) = \frac{A\tau}{T}\sum_{n=-\infty}^{\infty} \mathrm{sinc}\left(\frac{n}{T}\right)\delta\left(f - \frac{n}{T}\right) \tag{2.14}$$

$$S_{rect}(f)=\frac{A^2\tau^2}{T^2}\sum_{n=-\infty}^{\infty}\mathrm{sinc}^2\left(\frac{n^2}{T}\right)\delta\left(f-\frac{n}{T}\right) \tag{2.15}$$

respectively.

Equation 2.16 gives the Fourier transform of the trapezoidal pulse train.

$$\mathrm{F}\left\{\sqrt{A}\,\mathrm{rect}\left(\frac{t}{\tau}\right)*\sqrt{A}\,\mathrm{rect}\left(\frac{t}{\Delta\tau}\right)\right\}=A\tau\,\mathrm{sinc}(f\tau)\,\mathrm{sinc}(f\Delta\tau) \tag{2.16}$$

Thus the spectrum and power spectrum of a trapezoidal pulse train are

$$X_{trap}(f)=\frac{A\tau}{T}\sum_{n=-\infty}^{\infty}\mathrm{sinc}\left(\frac{n\tau}{T}\right)\mathrm{sinc}\left(\frac{n\Delta T}{T}\right)\delta\left(f-\frac{n}{T}\right) \tag{2.17}$$

$$S_{trap}(f)=\frac{A^2\tau^2}{T^2}\sum_{n=-\infty}^{\infty}\mathrm{sinc}^2\left(n\frac{\tau}{T}\right)\mathrm{sinc}^2\left(n\frac{\Delta\tau}{T}\right)\delta\left(f-\frac{n}{T}\right) \tag{2.18}$$

Graphs of the power spectrum of the two pulse trains are shown in Figure 4 with logarithmic power spectrum scale when $\Delta\tau/\tau=0.2$. (In practice this ratio maybe considerable smaller resulting in almost equal power spectra in practical measurement with a noisy spectrum analyzer).

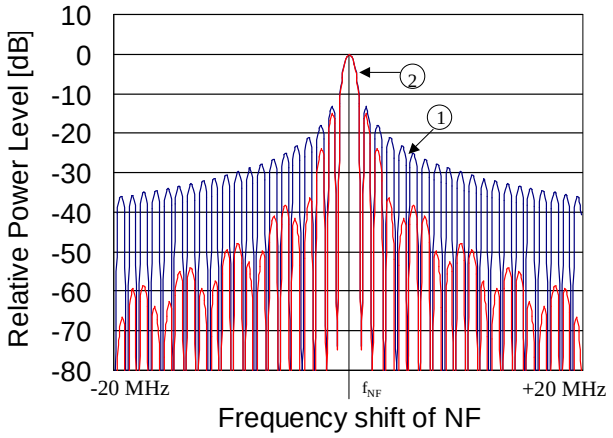

Figure 4. Curve 1 represents rectangular spectrum of pulse and curve 2 a trapezoidal pulse.

2.1.3 Radar pulses and their spectrum and power characteristics

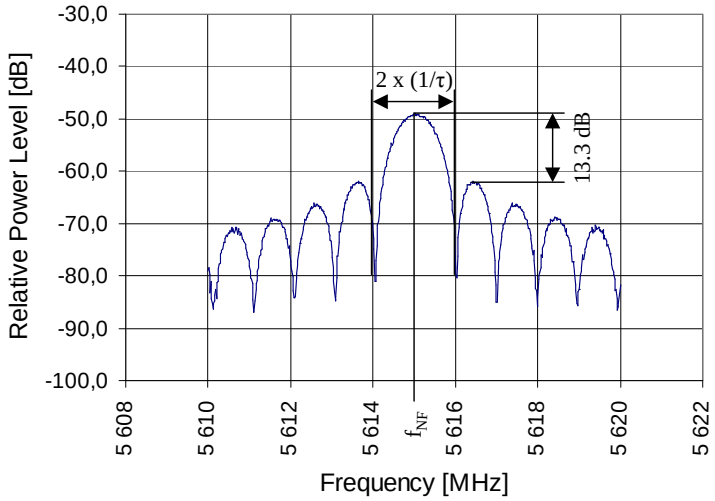

Figure 5. A measured spectrum of the simulated radar signal

In Figure 5 a real measurement of a radar power spectrum with a simulated radar pulse is presented. It is of the form $(\sin x/x)^2$ and represents the power spectral density of the pulse train. $2\cdot(1/\tau)$ equals the bandwidth of the radar transmission. The first sidebands power level is 13.3 dB below f_{NF}.

The key characteristics of this pulse are:

- f_{NF} is the nominal frequency 5.615 GHz,
- τ is pulse duration 1 μs ($1/B_{ref}$=1/1 MHz, frequency difference between *NF* and first zero position of the pulse spectrum),
- f_{PRF} is repetition frequency 1 kHz, frequency difference of two neighboring spectrum lines (can not be seen in this figure) and
- with an ideal rectangular pulse as transmission pulse the power difference between the *NF* power spectrum and the first spectrum side lobe maximum power spectrum is 13.3 dB.

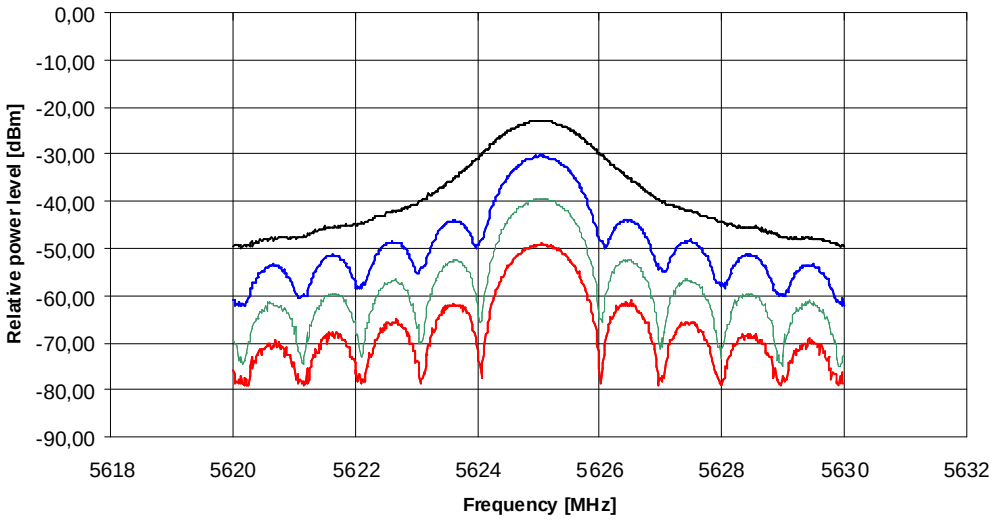

Figure 6. The shape of the measured pulse spectrum with different measuring filter bandwidths.

In Figure 6 the frequency spectrum of a 1µs simulated radar pulse on the SA maxhold display (maxhold is the maximum hold of the SA display) is presented. The curves represent the used 2 MHz, 1 MHz, 300 kHz and 100 kHz measuring filter bandwidth B_{meas} in order from 1...4. The maximum peak power level differences shall in practice approach 10 dB with the exception of curves 1 and 2 where the difference shall be 6 dB. The curve shape of curve 1 shows the radar pulse peak power level. The other curves do not show the correct level but show a more exact curve shape for small bandwidths.

The radiated peak power from the radar's antenna equals the transmitter pulse peak power [dBm] added with the antenna gain [dB], when the transmission pulse of the radar is not compressed and the transmission line loss from transmitter to antenna or transmission line frequency response is insignificant.

2.1.4 Mechanical assembly of the radar and special characteristics of the transmitted radar signal

Due to high transmitted power the mechanical and electrical assembly of radar is a demanding complex. A stable frequency oscillator and a modulator for switching on and off the radar carrier pulse are needed. If the carrier oscillator is incapable of producing the necessary transmit power, an effective amplifier is needed. Additionally a high quality transmission line is needed. The transmission line should withstand high power and pressurization and should attenuate the transmitting power as little as possible. It would be an advantage, if the transmission line attenuates harmonic frequencies of the carrier. Dependence on the used nominal frequency and the antenna lobe requirements often lead to a large antenna structure. A high reflecting surface accuracy of reflector antennas is also required.

Depending on the radar oscillator, a possible amplifier, and the modulator the spectrum of the radiated radio wave can contain components, which are not found in the theoretical spectrum. It is observed that different electrical and mechanical constructions,

needed to generate the final transmitted pulse, generate unwanted frequency components or change the ideal shape of the spectrum. Proposals of power and efficiency produced by different pulse radar types are listed in the ITU recommendation ITU-R M.1314-1 Appendix II [2]. According to this appendix the highest pulse output powers can be generated with crossed-field type equipment (10...5000 kW). This equipment has the highest efficiency of all radar transmitter types, being as high as 35…75 %. The lowest output powers are found in semiconductor type equipment. The appendix also compares sizes of mechanical construction, weight, ruggedness, the expected life cycle and relative acquisition price. The crossed-field type equipment tends to be the best in this comparison.

In the ITU recommendation ITU-R M.1314, Appendix II, it can be noticed that in semiconductor type equipment the power level of non-harmonic interference radiation is the lowest, when comparing to the *NF* power level. Seen from another point of view crossed-field equipment generates the highest output pulse power at the lowest cost. This crossed-field equipment is crossed-filed amplifiers and different magnetrons. According to Appendix II all power sources produce too many harmonic signals with a relatively too high power level. The demand for power levels of harmonic signals is −100 dBc (100 dB lower than the *NF* power level). The antenna solution can still alter the distribution of radiating pulse power in the different parts of the antennas radiation pattern. The ITU recommendation therefore proposes supplying the radar with a filter to reduce harmonic signals. The operating site of the radar mainly determines what kind of power supply is selected for it. The mains and weight of the signal power supply, size and antenna size, for example when using a mobile base, set their own criteria. Furthermore requirements and difficulties with the feed of a rotating antenna must be observed.

2.1.5 Categorization of radars

Radars can be categorized according to their transmission type. Pulse radar is the conventional radar type that transmits a pulse containing fixed *NF* with fixed *PRF*. Traditional surveillance radars are pulse radars enabling measurement of the distance, direction and often also height of a target.

CW (carrier wave) radars are radars transmitting a continuous carrier wave that can determine speed of targets within the radar antenna main lobe. The determination of speed is based on the Doppler shift where the frequency of the echo of the received frequency has changed compared to the transmitted frequency. The measuring of speed is based on this frequency shift. The CW radar can not determine distances. Radars used in traffic control are CW radars. Carrier wave radars can also be used in terrain surveillance (military terrain surveillance radar). Here a detected movement in the area to be observed is for example indicated with a beep.

Distances to targets can be determined with FM-CW radars. When adding FM modulation to the transmission of CW radars it becomes possible to separate one echo pulse from another and then determine distances. FM-CW radars are commonly used as altitude meters in aircrafts.

Radars can also be divided into groups by the location of their transmitters and receivers. In *mono-static* radar the transmitter and receiver are at the same location and establish one entity. This is the operating principle for most radar. Radar with TX and RX at different locations are *bi-static* radars. In bi-static radars sufficient isolation (small leaking of the transmitting pulse into the receiver) between the transmitter and receiver is achieved easily. An expanded version of the bi-static radar is a multiple locations, *multi-static* radar. Jamming of this kind of radar system has proven to be difficult. Also timing of the system is difficult

Here compression means the amplifying of radar pulse energy. This is done to achieve detection of received echo pulses with a satisfactory power level even over long distances and at high interference levels. The output peak energy can not be increased unreasonably high in the transmitter. Decreasing the output peak power and increasing the length of the radar pulse achieve the same outcome. The compressed echo pulse contains more energy than a non-compressed echo pulse. However, receiving of long echo pulses lowers the resolution in distance measurement. Therefore the echo pulse must be decompressed in the receiver. Leading the echo pulse through a matched filter does the decompression. This results in a shorter pulse shape (resolution of measurement accuracy increases) still resulting an energy level equivalent to the stretched output pulse. However this has not required a rising of the output peak power.

The compressed pulse radar is frequency or phase modulated, so that the bandwidth increases. A matched filter truncates the length of the returning echoes but maintains the received energy level. A typical compression is normally between 100…300. This means that the pulse peak power can be reduced with the same amount. Compression of the transmitted pulse can also be used in pulsed radars. With help of that, one gains savings in power, improved resolution in range and reduction of the influence of jamming. In pulse compression radar the output pulse is extended and its peak power is reduced. As a result the same effect with less power is achieved when compared with the peak power of an uncompressed pulse.

2.1.6 Adjacent channels to radar frequencies

If the radar generates unwanted spurious signal frequencies they can be reduced to allowed power levels. A low-pass filter can easily remove harmonic frequencies. However, there are problems in eliminating frequencies caused by spectral growth. The problem is caused because the wanted and unwanted signal are overlapping, so separating the wanted from the not wanted signal is very difficult without affecting the wanted signal. If the used radar frequency is chosen so that adjacent channels are allocated to other radio services, the risk of harmful interference to these services increases.

This subject can also be considered from another viewpoint. If the radar frequency is chosen from other than internationally harmonized bands for radar use, the risk of interference grows significantly. These kinds of radar frequency selections have been made, especially in military radar systems that existed in the former Soviet Union and the so-called Eastern countries after World War II. Both older and more modern radar technology of this kind are still widely in use. Radar signals from these systems are observed over the whole Finnish eastern border region.

The Finnish Communications Regulatory Authority (FICORA), former Telecommunications Administration Center and even former the Radio Department of the Telecom Finland, have been collecting information about interferences described earlier on the eastern and southern border areas. Mapping of radar frequencies has been made from the 1970's until today. The author has participated in this mapping process from its beginning.

The mapping was started because of disturbance of some terrestrial radio relay systems in eastern Finland. The automatization of the Finnish telephone network began in the 1970's / 1980's. At this time also in eastern Finland radio relay systems (240 channel digital TDRRS) were put up to connect the telephone trunk lines. Constant and sporadic interferences were observed in the TDRRSs. At the same time also radar signals that did not belong to this frequency band were observed. Several connections could not be taken into use due to the interference caused by these radars. These connections had to be replaced by connections of a different type. Figure 7 presents typical operating frequencies used by radar

systems with their origin east of Finland. Comparing of the same frequency bands, which are allocated for TRRS and other radio systems in Finland, can also be made from this figure.

The frequency bands marked green in the figure are allocated to radar use. Similarly, bands allocated to TRRSs are marked red and bands for broadcast (BC) operation are marked yellow. Observations of radar, which are in their correctly allocated frequency bands, are marked black. Radar observations marked blue have been observed outside the frequency bands allocated to radar operation. The red dashed line shows, which observed radar transmissions outside the allocated bands, overlap with other radio systems in their allocated frequency bands. These overlaps lead to possible interferences of the other radio systems.

Also it can be observed in this figure that radar frequencies overlap with frequencies used by television (TV) and radio relay systems. When taking into account that radar signal spectra spread widely the risk of interference is significant. Radio interferences of radar spurious transmissions overlapping with TV signals in Band III and Band IV have been observed and investigated by FICORA for decades.

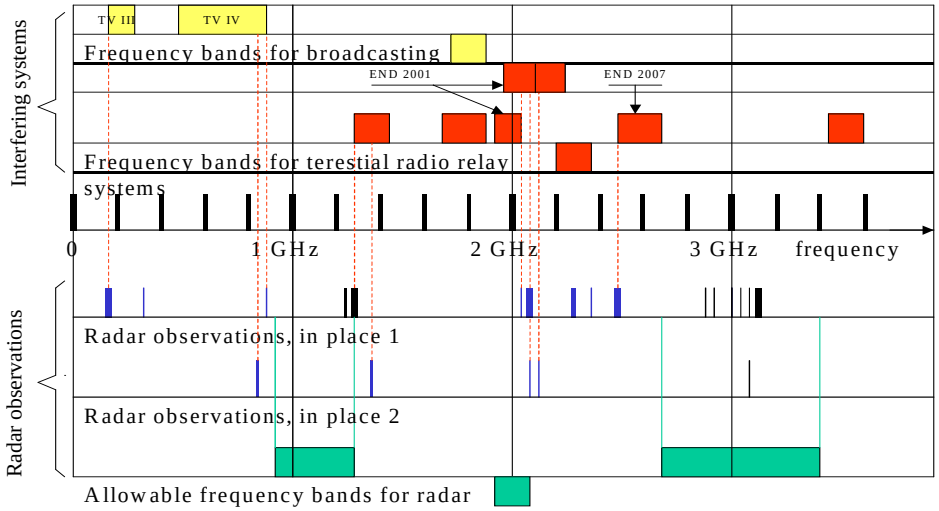

Figure 7. Observations of radar signals and signals from other radio systems

Radars operating in the 160 MHz band have typically been part of radar systems located behind the eastern border of Finland. These kinds of radars have been located on Russian radar stations all along the Russian border. These have disturbed TV viewing in the VHF TV III band near the Russian border. Especially when the TV receiver is mounted with an antenna amplifier and the antenna pointing to the east, viewing of analogue TV broadcasts has been interfered by Russian radar as far as in Jyväskylä and Mikkeli (distances of up to 250 km from the Russian border). Other radio systems interfered by Russian radar has been for example radio systems used by VR Ltd in their freight station operating system (160...170 MHz) in Kotka and Kouvola. Due to communication between the frequency management authorities of both countries the interference situation has got better, but interference still occurs from time to time.

Also radar systems operating in the 800 MHz band have been identified at Russian radar stations. The frequency of these radars is very near to the highest UHF TV channel 69 (855.25 MHz). Interference on this channel has not been observed yet. This is due to the fact

that UHF channel 69 is not in use in Finland so far. Radar systems operating in the 26 cm wavelength band (3.4 GHz) allocated for radar use have been observed in operation in these stations. TRRS operating above 2 GHz are at risk of being interfered by radar systems operating in the same band.

2.1.7 Problems in radar signal measurements

Measurement of the electromagnetic spectrum of radar is difficult not only due to high radar pulse power but also because of its assembly, location, way of operation, user safety and/or other possible limitations. The measurement has to be focused on the radar output signal and its features, when examining the spectrum for all possible interference effects to other radio systems. There is no interest in the returning echo of the radar pulse. The work focuses on examining the shape of the transmitted radar pulse spectrum. Examining the radar spectrum itself, its location on the frequency axis, the differences of levels of various frequency components and their location with respect to *NF* and the effect of the antenna on the signal path do this.

To use a spectrum analyzer (SA) with the largest possible intermediate frequency bandwidth (B_{IF}) for measurement of the spectrum is recommended. This is done to get the signal under measurement to pass through the filter without distortion but the filter being not too wide to reduce the sensitivity of the analyzer (unnecessary noise summing to the signal). The ITU recommendation ITU-R M.1177 [1] for the measurement bandwidth of uncompressed pulse radar defines the SA measurement bandwidth as:

$$B_{meas} \geq (1/\tau) \tag{2.19}$$

where: - τ is the transmitted radar pulse half power (–3 dB) duration

The SA must be set to maximum hold and zero span (a fixed frequency is set at the SA and the sweep is done in the time domain). The measurement antenna has to be adequately wideband to make it possible to measure possible harmonic signals without having to change the antenna. Additionally one needs an adjustable attenuator, a low noise amplifier (LNA), if possible a YIG filter, a fine-tuned band stop-filter (BS filter) and both high-pass and low-pass filters.

When one wants to clarify, how the radar signal is impacting another radio system within a known distance, the measurements have to be conducted in the far field while the radar antenna is rotating. The measurement can also be conducted through the radars internal test point. In this case the antenna impact can not be considered and therefore there are no far field requirements. Neither the possible transmission line filter nor antenna rotation effects will be visible. The radar *NF* and its antennas biggest dimension define where the far field conditions start to be valid. The far field distance [26.pp 28-31] is determined as follows:

$$r = \frac{2D^2}{\lambda} \tag{2.20}$$

where: - r is the distance where the far field begins
- D is the biggest antenna dimension
- λ is wavelength (all dimensions D, r and λ are in the same units)

The measurement should not be carried out starting at the distance where the far field begins because the power level of the transmitter in the main radiation lobe would be usually too

high at the input of measurement equipment. Here a high attenuation of the signal to be measured would be required. For example a far field of a 5.625 GHz weather radar begins at a distance of 0.662 km when the antennas biggest dimension is 4.2 m (for parabolic antenna). In exceptional cases the measurement might be forced to be made in the radar near field area for example at the half far field distance.

The measurement distance should be chosen (optimized) as follows. The measurement point must be at a distance so that the gain of the whole signal path (e.g. antennas, the possible attenuator, the filter, the amplifier and the transmission line) increases to its highest level for proper SA operation. However, the analyzer shall still display correctly. In literature [27] this level has been reported to be (–40...–20 dBm). Very often this range is not achievable and one must settle with a compromise. If the signal peak levels are for example at a level around (–10 dBm) one must be certain that the signals displayed by the analyzer are real signals and not caused by SA non-linearity. Decreasing of the input level of incoming signals can do this check. Here all visible signal levels must be reduced in the same proportion. On the other hand, however, if the signal levels are below (–40 dBm) measurement dynamics is reduced.

One must settle with compromises when there is no suitable measurement site available in the feasible measurement range. Also there can be significant terrain obstacles in the measurement direction. A best possible measuring point would be situated in a lake area. The point of the radar might be located so high in the terrain that the radar antenna main lobe does not hit the measurement antenna. This can happen; if the radar's security construction is limiting the minimum tilt angle to horizontal level (0 degrees) when the required tilt would be below horizontal level. Often using of even horizontal level may be limited due to residential buildings near the radar. This could result in problems because the measurement antenna will not meet the radar main antenna lobe.

The distance of the measurement point must be selected so that no health hazards to humans exist due to too high radar signal power density levels. With the weather radar mentioned before on operating frequency 5.625 GHz the highest average power density may under supervised conditions, in which the measurement staff may operate, be at most 50 W/m^2. The corresponding value for the whole population may be at its highest 10 W/m^2. If the maximum pulse power radiated by the radar is 6.3 GW the mentioned weather radar power density at the far field distance at 662 meters is 1.144 W/m^2. With the far field distance divided into half the power density is 4.567 W/m^2. Sometimes the measurements may have to be conducted with one of the radar antenna's known side lobes. This can be for example 40 dB below the main lobe power. In these cases the radar antenna must not rotate.

The measurements should be conducted with the measuring equipment inside a van with side doors closed (this corresponds nearly a Faraday cage) or the van positioned so that the side door is opposite to the measuring direction. In practice it has been noticed that even though the average power density at the measuring point is within acceptable limits (for example under 0.5 W/m^2) the pulse power causes interference to the measurement without the metallic van body shield. When conducting field measurements outside a car even high quality measurement cables, proper connectors and adapters and equipment shielding do not protect against interference caused by high power densities.

In many types of radar the output power is switched off when the antenna is not rotating. In many of these cases this function can not be mechanically bypassed, without violating safety regulations. This causes difficulties for the measurement process since the rotating antenna main lobe illumination time of the measurement antenna is very short. (This work is focused on studying weather radar. Therefore its technical parameters are used in the examples.) This time can for example be 25 ms per one rotation of the antenna, when the antenna is making one full revolution in 9 s and the antenna main lobe is one degree. All

measurements should be made in this short time. Several of these 25 ms bursts repeated every 9 seconds will be needed to make a comprehensive measurement.

2.1.8 Radar inspection by the authority and its measurements

The use of fixed high power radar is subdued to licensing. The licenses are issued in Finland by the frequency regulator FICORA. The radar license is granted after the radar has passed its inspection. An inspection is also required for all other high power transmitters if interference problems are present. Additionally to radar transmitters all broadcasting transmitters require an inspection (however short term local BC transmitters with an output power under 50 W have not been inspected due to their minimal interference risk).

The inspection does not consider the functionality of the radar receiver. To map possible interference risks the radar transmitter's characteristics are inspected. The inspection targets *NF*, measured radiation power (average peak pulse power), the signal level of harmonics, the levels and locations of non-harmonic signals on the frequency axis and the radiation of *NF* and *SF* signals of the antenna. Additionally before establishing or moving a radar to its place of operation (for example military movable radars) its place of operation is coordinated between the radar operator and the frequency regulator. This is done to prevent a situation where the radar would be too near to another radio system. A worst-case scenario for example would be a radar station placed in line with a terrestrial radio relay system hop or too near a relay station.

2.2 Summary of Chapter 2

Different sources of electromagnetic radiation were presented in this chapter. Also their power levels, the influence of the distance used, ways of use and possible drawbacks were compared. Different radar types have been presented in detail. The radar operational basics, frequency bands allocated for use, use for different purposes, construction mechanics and generation of radar spectrum have been explained.

The author has for several years participated in mapping and measuring of radar based interference in radar operating environments. Based on these measurements the necessity of systematic mapping of radars and their transmissions in view of interferences is shown (accepted inspection of a radar is the key rule in taking it into use). Also possible interferences generated by radar on adjacent channels, on channels not neighboring the *NF* and radar harmonics have been mapped. Additionally to these also most significant problems, like high radar pulse power and wide measurement dynamics, in radar measurement have been treated. Based on these facts it is presented what measurements the frequency regulator has to carry out while inspecting radar stations.

3 MEASUREMENT OF A RADAR SYSTEM

3.1 Echo measurement in radar operational use

The majority of radar measurements comprise measurement of the returning signal i.e. of the echo. In these all possible information included into the echo is tried to be utilized. The most important information utilized from the echo pulse is information about distance of the measured target, direction, speed, height and possible nature of the target. This information is readable instantly from the radar's display but in more precise determination the results have to be calculated and combined to other information available about the target or to earlier knowledge based experience. Numerous calculation algorithms for prediction of more versatile, accurate and reliable results have been developed (and are still developed). The transmitted pulse is often shaped to get more accurate results. One way of this shaping for example is compressing of the transmitted pulse. Also different polarization in transmitting and receiving can be used.

The important elements of the atmosphere for weather radar are interfering targets to the surveillance radar and make its wanted measurement results worse. The echoes received by weather radar are compared to earlier received echoes from known weather patterns. From these the quality of the target, its composition, its size, its movement, its variation and other interesting information is determined. The treatment of the information obtained from the echo consists of a lot of calculation before one gets for example weather maps or predictions qualified for publication.

3.2 Radar spectrum from interference point of view

Searching through databases finds the method recommended by ITU-R [1] for measurement of harmonic and non-harmonic signals. It gives directions for measuring interference radiation of radar and presents measured radiation values. The NTIA Report [3] for measuring interference radiation is also found in the knowledge database.

When transmitting ideal short radar pulses with a constant repetition rate they are seen in the radar spectrum as regularly shaped envelopes on both sides of the *NF*. This is presented in Section 2.1.2 Figure 5. Depending on the oscillator type used in the radar its transmitted spectrum is not regular and symmetric. As described earlier in Section 2.1.3 the crossed field type oscillator produces the most non-harmonic signals. A crossed field oscillator produces the highest pulse peak power without a separate amplifier but it has low suppression of non-harmonic signals. The signals outside the ideal radar spectrum can be very high.

In Figure 8 one measured spectrum shape of a weather radar is shown. The used measurement bandwidth is 2 MHz. The measurement is performed in 400 MHz segments around the *NF* (in the picture *NF* is marked with f_{NF}). After this the results have been processed with a calculating program. This radar is equipped with a harmonic filter that cuts unwanted signals above the *NF* signal. The figure also shows how the spectrum power spreads on frequencies lower than the *NF* and some spurious spectrum components are only 40 dB below *NF* power level. The unwanted signals can be discovered as far as 1.5 GHz below the nominal frequency (*NF*). In this figure the spreading of spurious signal frequency components is a real interference threat.

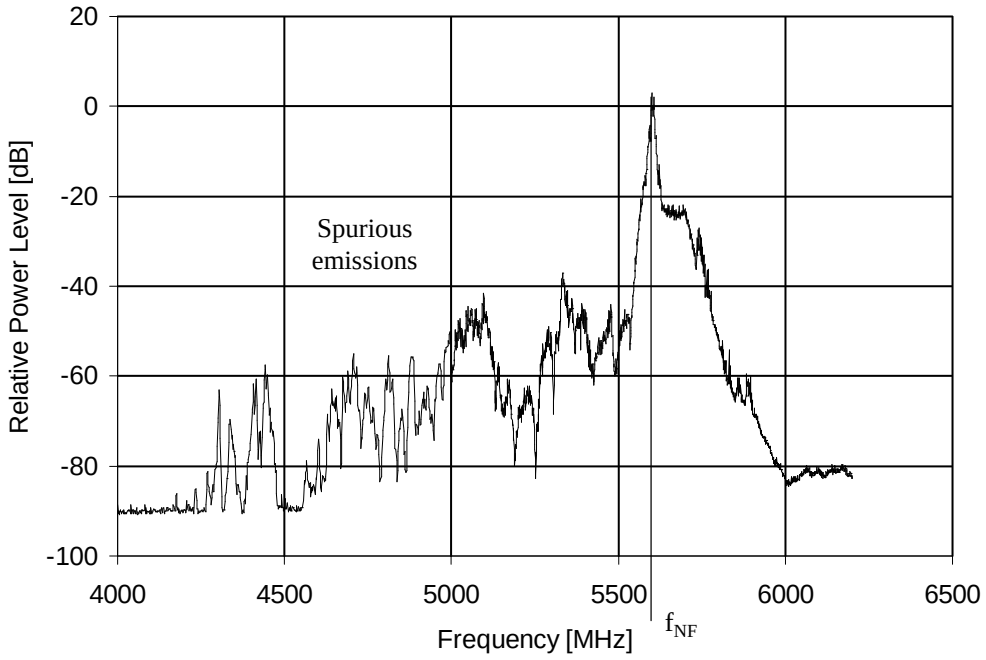

Figure 8. The measured spectrum of a weather radar.

In the table presented in Appendix II one can also see that this kind of oscillator produces harmonic signals. The measurement of these is important since it is known, that they are at their worst only 20...40 dB lower than the *NF* signal level. Usually the harmonic signal occurs on frequencies used by other radio systems and is therefore very harmful. Therefore a harmonic filter with satisfactory attenuation is recommended to be used on the transmitter antenna feeder side of the radar.

After taking into use TDRRSs interferences produced by radar became a problem for terrestrial radio relay systems. In the time of terrestrial analogue radio relay systems (TARRS) the microsecond class spurious pulses of radars made no significant interference inside the 4 kHz wide analogue channels (observations by the author from interference studies 1975...2009). The spuriouses are received as pulses related to the according *PRF* while the radar antenna illuminates the interfered radio system antenna. Radar causes spuriouses into TRRSs because their frequency bands are often adjacent to the TRRS frequency bands. The TDRRSs are very sensitive to short pulse type interferences that radars produce. This is especially when radar pulse peak powers are very high, in the range 1...10 GW.

3.3 Measurement system with spectrum analyzer - measurement routine

3.3.1 Mapping and measurement of an unknown radar

The intention of mapping unknown radar sources at a selected measurement location is to find radar transmissions, determine their directions and measure their frequency, pulse repetition frequency, pulse width, antenna rotating speed and estimate the radiation power and to find out their polarization.

After positioning the measurement vehicle to the best possible location for measuring, the preparations for measurement begin. First all possibly needed measuring equipment are taken out and the measurement system is set up. The implementation of the system is depending on whether the measurement is done on a known radar station, for example a national weather radar station, or is it a mapping of unknown radar at an unknown location. When a radar is measured the implementation of the measurement begins with positioning of the measuring antenna. This can be done either by placing the antenna on a tripod besides the vehicle or on a measuring mast of the vehicle. The mast alternative gives the advantage of large antenna height (up to 10 m) that results in higher signal levels due to elimination of terrain cover attenuation but the disadvantage is longer measurement cable lengths resulting in a higher attenuation. The increase of the received field strength with an elevated measurement antenna is typically larger than the increase of the feeder loss. In a terrestrial radio relay system (TRRS) measurement the measuring antenna must be placed at the same height as the TRRS receiving antenna. In practice this often is impossible. Therefore the effective difference between the antenna height of the measuring antenna and the TRRS receiving antenna height has to be corrected mathematically.

As basis of the measurements presented in this work the author has used horn antennas made by Finnish antenna manufacturer Aerial. The technical values of these are presented in Appendix IV. The measurements have been conducted using HP measurement cables, connectors and adapters [28] and a spectrum analyzer (SA) of type HP 8565 E [29] all manufactured by Hewlett Packard. The measurements can also be conducted with other equipment but these must have the same or better specifications as those presented here.

When measuring unknown radars the measurement cable is connected directly to the SA input. When the measurement preparations (presented later in Section 4.3) have been established the following parameters are set to the SA:

- the nominal frequency (*NF*) to be measured,
- the bandwidth of the frequency band to be measured (SPAN) or the lower and upper frequency limits,
- the IF bandwidth (B_{IF}) and
- sweep time (*ST*).

To make sure that all available energy from a possible radar signal is fed to the detector of the SA (and screen) used for measurement the SA parameters described above have to be set to their extreme values. Since the length of the possible pulse is not yet known one has to be prepared to measure a very short one.

The system usually needs no attenuator because it can be assumed that the signal levels of the unknown radar are not too high at the SA input. The storage of measurement results can be done with either the SA's own memory or by connecting a plotter to the SA or by capturing the data directly to the memory of a computer.

When measuring, i.e. mapping an unknown target, the B_{IF} is set to the highest possible value (for the used SA 2 MHz). With this bandwidth the main spectrum component of a 1 µs pulse spectrum is not distorted significantly in the SA's intermediate frequency (IF) filter. The video bandwidth (B_{VIDEO}) [27] of the SA must be set to an equal or higher value than the B_{IF}. The fastest possible setting is chosen for the *ST* (in this case 50 ms). The lobe width of the measurement antenna, type AU 15 / 1.7...18, for mapping is about 30°. This leads to the need of redirection of the antenna several times in the horizontal plane. If the antenna is redirected every few degrees and the power levels produced by the target to the measuring point are registered one can easily determine the direction of the transmitter. If the back lobe or the minimum between the known side lobes of the antenna is known these

can also be used for determination of the direction of the transmitter. Using the latter way of determination one usually gets more accurate results because the minimum between side lobes always is sharper than the main lobe maximum.

Before the first measurement and before starting the measurement process after modifying the measuring system one has always to calibrate it. The reason for calibration is to obtain the frequency response of the measurement system as reference for the later following relative power level determinations. One can also check the operation of the measuring equipment and connections and the correctness of the power level on the SA display with help of the calibration process (this is checked by calculation using the system parameters and the technical specifications of the measurement equipment).

The calibration is done most easily if one can use a SA possessing a tracking generator (also an external generator is appropriate). As substitute a signal generator possessing frequency sweep mode was used. Disconnecting the antenna cable from the antenna output end of the cable and then connecting it to a signal or tracking generator starts the calibration. All other connections of the setup remain unchanged. The signal generator is set to sweep through the same frequency band as that set to the used SA. The signal generator sweep rate has to be set so low that a coherent power envelope level without interruptions can be achieved on the SA display (Max Hold set) during the measurement. The achieved power level on the SA display (envelope) as function of frequency is the system calibration envelope. Later measurement results can always be corrected with help of the calibration envelope. When the power level of the calibration envelope is known at a certain frequency on the SA display the power level at the antenna connector is also known. The sweep time of the SA is held at 50 ms during the calibration process.

When the antenna has been reconnected to the system the measurement process itself can take place. The SA display is set to View mode and it is observed if signals in the selected frequency band, in the selected direction and with the selected polarization can be detected. When measuring an unknown radar signal one can always assume that the radar antenna is rotating and the persons performing the measurement can not influence the operation of the radar (for example a radar station behind national border). In this case the lobe of a rotating antenna with a rotation speed of 9 seconds per rotation illuminates the measurement system antenna for 25 ms when the radar antenna lobe width is 1°. The rotation of the radar antenna and the SA sweep time (for example 50 ms) are not depending on each other. This causes the measurement antenna illumination and the SA sweep sequence to coincide at random times. It is also possible that coincidence is realized already on the first revolution of the antenna. The whole mapping of the frequency band to be investigated, however, is done first after a satisfactory amount of antenna rotations (the power envelope level without interruptions is seen on SA display). The amount of rotations is depending on the width of the frequency band to be measured. Additionally the time between sweeps of the SA (fly back (*FB*)) is useless time for the measurement and the measurement does not advance during this time.

When a radar transmission is observed its direction is tried to be determined by turning the antenna. The polarization is determined by testing and in this case the work proceeds in 9-second intervals. When these determinations are done the mapping of the spectrum begins. The *NF* of the observed radar transmission and the frequency band needed for mapping are set on the SA. Also the SA display is set to Max Hold mode. After this one has, due to the rotation of the radar antenna, to wait for the continuous power envelope curve without interruptions and the maximum radar signal power having been achieved on the SA display. After this the rough mapping is done and a picture of the radar transmission spectrum is available. However, the usable dynamics is not very high. It is only the difference between the signal peak power level and the noise power level of the SA. The

intention of this mapping is not to get complete results about the radar spectrum, but as the name says to map if some transmissions do exist and if so from which direction and with what approximate values they appear. If it is necessary to get more accurate values the measurements must be conducted as measurements of a known radar system described in Chapter 4.

A mapped radar spectrum is always treated like a known radar system. An example of a mapping log is shown in Table 1:

Table 1. Radar observations from behind the Russian border. Observation point Rannisvaara, Eastern Lapland 1991.

Date	Time/GMT	Frequency/GHz	Level/dBm	Direction/°	Amplifier	pol.	Object	Figure
24	18.00	1.920					link	
	18.27	2.492	–18	160	x	V	radar	2.
	18.33	2.557	–60	160	x	V	radar	2.
		2.678		160	x	V	radar	2.
	18.40	2.471	–20	160	x	H	radar	3.
	20.15	0.860	–18		x	V	radar	4.
	20.45	3.042			x		radar	

As can be seen from Table 1 there are several radar transmissions observed from direction 160° (0° corresponds to North). They are in the same frequency band, but probably at different distances. Their measured power levels differ depending on the distance and propagation conditions. Also their polarizations may differ. The accuracy of the direction towards the radar stations is usually ± 5°, which is a satisfactory result when examining radar transmissions. When later on conducting the known radar measurement the radar station is found easily with these values. At this time the radar station is tried to be determined and located as accurately as possible.

The same radar can appear on different frequencies varying about 20 MHz and with different power levels at different times but at the same location. In this case the identification marks of the radar are used for location of the radar. These identification marks are rotation speed of the antenna (very high accuracy and always constant with the same radar), the *NF*, the *PRF* and pulse length τ, that are determined from the behavior of spectrum. The envelope of the spectrum is called the radar "finger mark". It also is a good identification mark.

The middle flow in Figure 9 shows how the mapping procedure itself proceeds in time order. On the right necessary technical resources are displayed that at least are required for a satisfactory measurement result in the different parts of the measurement. On the left the parameters based on a successful measurement are shown (this flow chart continues in Chapter 4 in connection with the time domain parameter study).

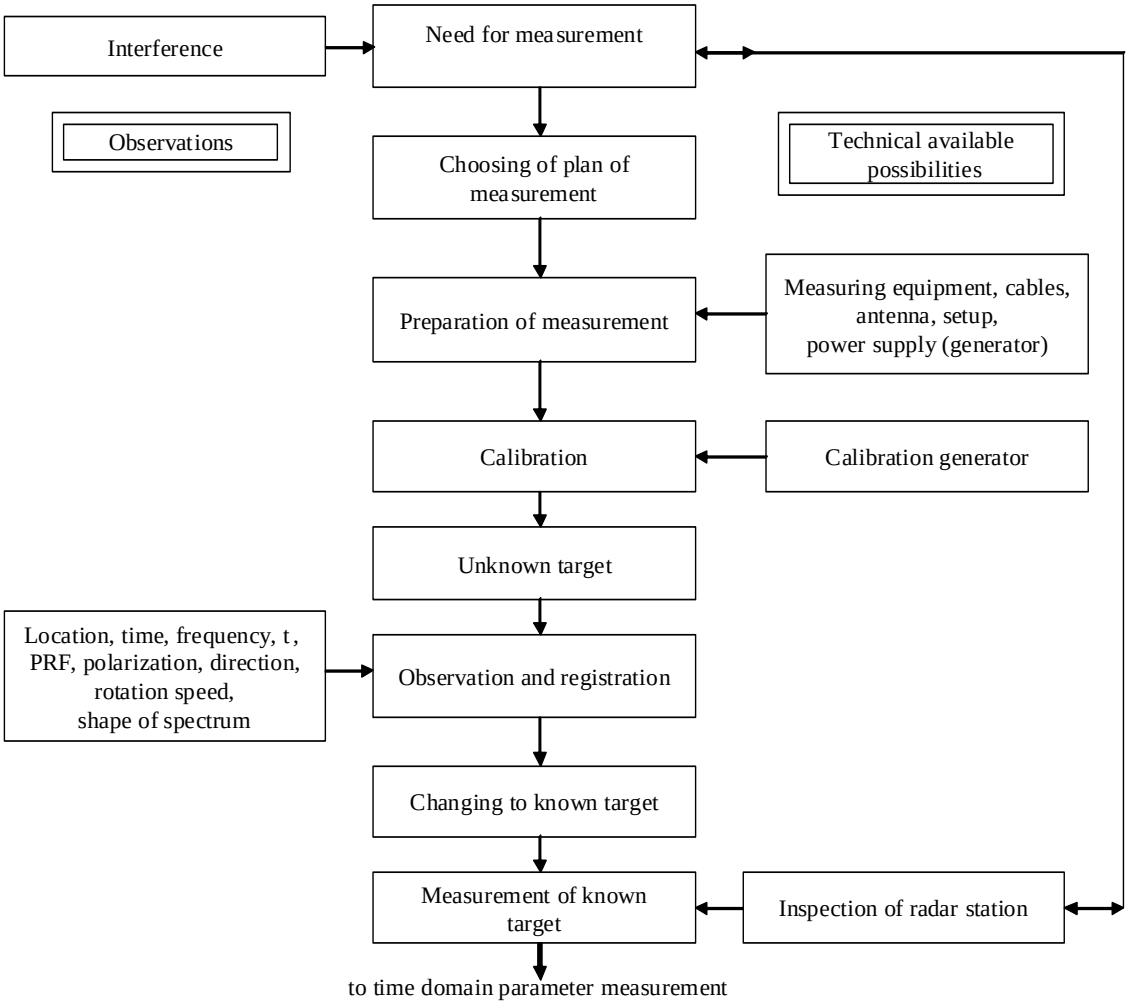

Figure 9. Flow diagram of the measurement procedure of an unknown radar system.

3.4 Summary of Chapter 3

This chapter states the reasons for why the radar pulse itself is the most important object for this work and not the echo pulse that has been ignored. The use of terrestrial analogue radio relay systems has decreased in favor for terrestrial digital radio relay systems. The interference into TDRRSs has emphasized the significance of one interference source, the radar transmissions. The spectrum of radar transmissions has been of high interest in this work. This chapter focuses on presenting the measurement of an unknown radar transmission, the measures to be taken based on these measurement results and how the measurement process proceeds both as text and as a flow chart. Also the measurement equipment and some radar measurement observations at a certain location are presented.

4 NEW TWO-STEP RADAR SPURIOUS EMISSION MEASURING SYSTEM

If radar antenna features should be considered or if antenna rotation can not be disabled, or if the investigated radar can not be controlled by the investigator, measurements have to be performed with rotating radar antenna. The measurement of this kind of radar under field conditions is very challenging. In this chapter a new approach is presented to the measurement with extended dynamics of the transmitted signal from a rotating radar antenna. A new feature in radar pulse measurement is the introduction of a two-step measurement. In the first step measurement of time domain parameters is performed. These time domain parameters are utilized to set equipment parameters in the second measurement step where the radar signal properties are investigated in the frequency domain.

4.1 Determination of measurement parameters in the time domain

This is the first time when radar signal measurement is performed in two steps. In the first step transmitted radar pulses are examined and their time domain parameters and are determined. Appropriate use of these parameters makes it possible to get satisfactorily reliable results about the electromagnetic spectrum either, the exact shape of the spectrum and pulse peak power or possible spurious radiation. The following measurement parameters are important:

1) $T_{360°}$ is the period of revolution of the radar antenna
2) T_{ill} is the time during which the rotating radar antenna illuminates the measurement antenna on each revolution, in this work called illumination time, and
3) N_P / T_{ill} is the amount of radar pulses received by the measuring equipment during one illumination by the radar antenna.

The antenna period of revolution is measured with a stopwatch or is determined from the SA display. Setting the SA to 0-SPAN mode and *NF* as measurement frequency does the latter. When the sweep time in a single sweep is larger than the period of revolution of the radar antenna the SA display displays two or more antenna main lobe spans on the time-scale (Figure 10). From these (scale size = *ST*) the period of revolution can be calculated. The same is achieved if the radar antenna main lobe occurrence is timed with a stopwatch.

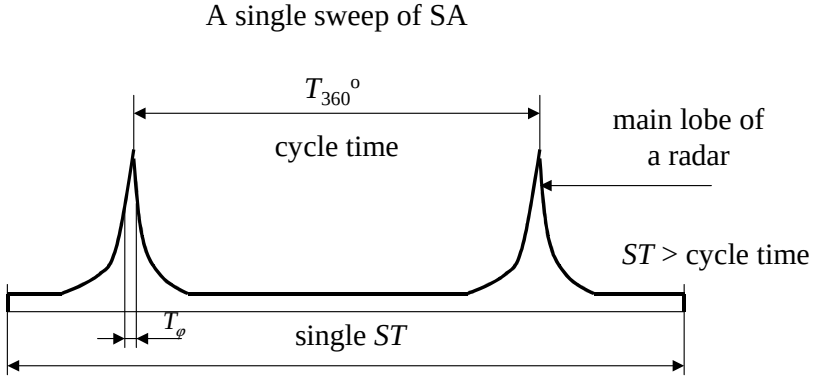

Figure 10. Determination of period of revolution of a radar antenna.

The amount of radar pulses during a single illumination can be calculated when the antenna rotation speed ($1/T_{360°}$) [revolutions/s], the antenna lobe width ($\varphi_{\text{ant.lobe}}$) [°] and the radar pulse repetition frequency (*PRF*) [Hz] (shown in Figure 12) are known. When one antenna revolution (360°) needs $T_{360°}$ [seconds] the radar antenna illumination period during one period of revolution is

$$T_{ill} = T_{360°} \cdot (\varphi_{ant.lobe}/360) \ [s] \tag{4.1}$$

when the lobe width of the antenna is $\varphi_{ant.lobe}$ [°]. The amount of pulses (N_P) during this time is

$$T_{ill} \ [\text{s}] \cdot PRF \ [1/\text{s}] \tag{4.2}$$

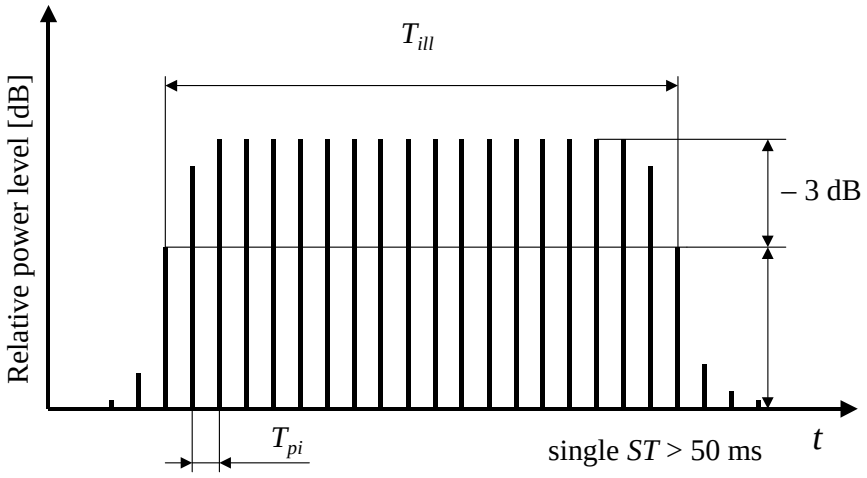

Figure 11. Determination of the radar antenna 3 dB bandwidth ($\varphi_{ant\ lobe}$).

The lobe width (Figure 11) can be determined when it is known how many pulses are received during one illumination, how long the illumination time is and what the *PRF* is. By setting the *ST* so that the single pulses form a cluster on the SA's display while the antenna lobe is limiting the size of the cluster (3 dB lobe width), the amount of received pulses during one illumination can be counted. The illumination time T_{ill} is

$$T_{ill} = N_P \ (-3 \ dB) \cdot T_{pi} \tag{4.3}$$

where:
- T_{ill} is the radar antenna illumination time of the measurement antenna,
- N_P is the amount of pulses during one illumination (at the –3 dB point) and
- T_{pi} is the interval between two pulses (1 / PRF).

From this the antenna lobe width is:

$$\varphi_{ant\,lobe} = \frac{360° \cdot T_{\phi}}{T_{360°}} [°] \tag{4.4}$$

where: - $\varphi_{ant\,lobe}$ is the radar antenna lobe width (at the 3 dB point)
- $T_{360°}$ is the duration of one radar antenna revolution.

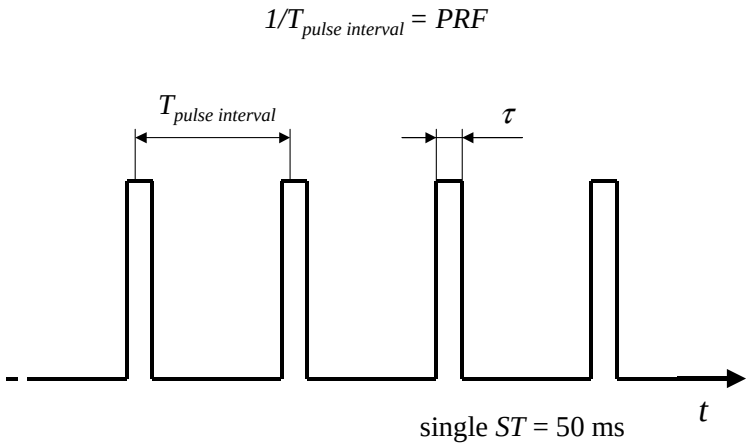

Figure 12. Determination of the PRF.

When determining the *PRF* the SA's *ST* is changed to 50 ms. All other settings remain unchanged. After a successful single sweep (the sweep contains one illumination) the *PRF* is readable from the SA's display (Figure 12),

$$PRF\ [\text{Hz}] = 1 / T_{pi}\ \ [1/\text{s}] \tag{4.5}$$

The radar pulse length τ is defined in Section 2.1.2.

Additionally, the time domain parameter study gives the necessary *FW* size (equals in practice the IF bandwidth of the SA) for the sweep measurement, the *ST* and the total measurement time per measured frequency band. These factors may have to be adjusted to get a reliable and accurate result.

The radar signal in the frequency domain is treated in the second step. The parameters obtained in the time domain parameter study and the available technical resources, that the electromagnetic spectrum characteristics can be measured with, are used. These technical resources and the actual measurement contain:

1) Available measurement antennas,
2) amplifiers,
3) attenuators,
4) filters
5) the SA, used as measurement receiver in this work,

and the specifications of these components, and furthermore

6) received minimum power level.

The specifications of the measurement system include bandwidth, gain, attenuation and noise levels. When comparing with the time domain parameter study, the realization of the

frequency domain measurement is a technical application for extending the measurement dynamics. This is done using the possibilities mentioned before and the time domain parameter study results.

This chapter also treats the problem of how the measurement time is determined and how the choice of measurement bandwidth and *ST* can optimize it.

4.2 The selection of the measurement bandwidth

In this work several different symbols are used for different bandwidths. The different bandwidths are defined as follows:

- B_{meas} is the bandwidth of the measurement as available from the SA. The target value of B_{meas} is B_{ref}
- B_{IF} is the bandwidth of the SA with which the measurement is conducted
- B_{ref} is the bandwidth, that is defined for different radar pulses case by case
- B_c is the frequency shift within the compressed pulse
- $B_{20\text{dB}}$ is the bandwidth measured at the filters –20 dB point
- B_{VIDEO} is the bandwidth of the SA's video filter

In the measurement of radar systems (known or unknown radar signal) special attention has to be given to the selection of measurement bandwidth. When the measurement bandwidth, B_{meas}, is clearly lower than the reference bandwidth, B_{ref}, the peak power level in SA max-hold operation dependence of B_{meas} is 20 dB/decade, while the average noise power level dependence of this bandwidth is 10 dB/decade. For B_{meas}-values clearly higher than B_{ref} most of the spectral content of the radar pulse is inside the measurement bandwidth and the signal peak power level stays constant, while the average noise power level still increases 10 dB/decade when B_{meas} is increased. Behavior of the peak power to noise ratio is 10 dB/decade when $B_{meas} < B_{ref}$, and –10 dB/decade when $B_{meas} > B_{ref}$. B_{meas} is the bandwidth of the measurement.

B_{meas} should always be set equal to B_{ref} when measuring the power level of interference emission. Only when measuring radar spectrum shapes it is recommended to use a narrower measuring bandwidth $B_{meas} = (0.01...0.1) \cdot B_{ref}$.

Typical reference bandwidths of radar are defined as follows:
Pulse radar without compression [1]:

$$B_{ref} = 1/\tau \tag{4.6}$$

where: - τ is the pulse duration.

and with FM compression [1]:

$$B_{ref} = (B_C/\tau)^{1/2} \tag{4.7}$$

where: - B_C is the variation of frequency during the pulse and
- Equation 4.4 is valid, when $B_C > 0$

If the variation of the frequency is not known, it can be roughly estimated from the –20 dB bandwidth of the emitted radar pulse [6], e.g. $B_{20\text{dB}} \approx 2B_C$.

With pulse code compression:

$$B_{ref} = 1/t_{chirp} \tag{4.8}$$

where: - t_{chirp} is the phase coded "chirp" length.

If the bandwidth B_{ref} can not be calculated, it can be determined by measuring the received pulse power of the radar for different B_{meas}-values. The measurement is started with the largest available B_{meas}. When B_{meas} is decreased the measured power change is tracked. The B_{meas}-value that first causes the radar power to decrease can be used as B_{ref}. The SA's selection of B_{IF}-values usually is very coarse (for example 10, 30, 100, 300, 1000 and 2000 kHz). This can cause the power drop to be many dB for a change of the measurement bandwidth. Therefore the value of B_{ref} can not be defined accurately since a B_{IF}-value in the SA equal to B_{ref} is often not found. Usually B_{ref} is in the order of 1 MHz and if it can not be determined more accurate 1 MHz should always be used. During the mapping process of an unknown radar, however, the widest B_{IF} of the SA is used (in this work it has been 2 MHz).

4.3 Study of time domain parameters, conditions for measurement and radar pulse treatment

4.3.1 Treatment of radar pulses in the time domain

When the antenna rotation characteristics of the radar to be measured can not be controlled the radar has to be measured while the antenna is rotating. If the *PRF* of the pulse radar is for example 1 kHz and the pulse length τ is 1µs, the radar transmitter is then transmitting 1 µs long *NF* carrier pulses once every millisecond. During the rest of the time the radar receives echo pulses. The measurement system for the radar signal must be setup so that it is capable of doing the measurement within this 1 µs time when a single pulse occurs. The antenna rotation sets an additional requirement. The measurement has to be conducted when the radar antennas main lobe is illuminating the measurement antenna. Another additional requirement is that only transmitted pulses during the time of illumination coinciding with the SA sweep create components of the radar transmissions spectrum on the SA display. An adequate amount of transmission pulses have to appear during *ST* with the actual FW. The minimum requirement for each frequency window (FW) size to be swept is at least one pulse per sweep. If more pulses than one for each FW bandwidth are available it is possible to speed up the measurement process. Alternatively the frequency range to be measured can be extended. However, the speeding up is limited by the SA characteristics.

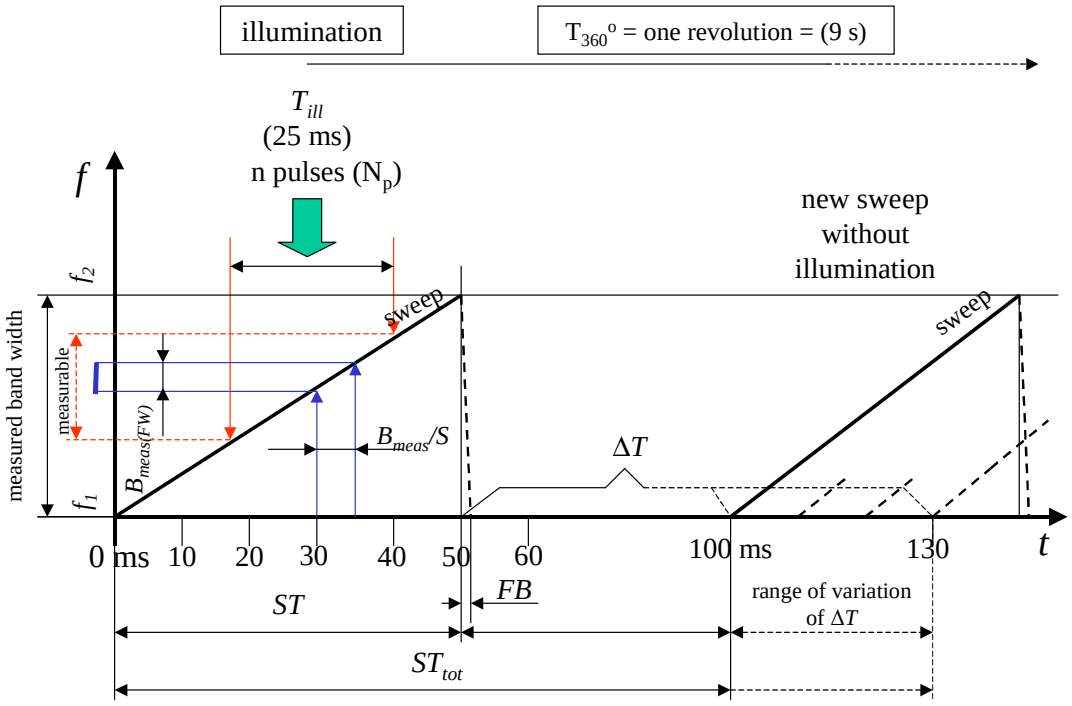

Figure 13. Basic diagram of radar spectrum measurement.

The important parameters in radar measurement (and parameter values of an example radar) are presented in Figure 13. These are radar rotation speed $T_{360°}$ (9 s), illumination time of the radar transmission T_{ill} (25 ms) and radar pulses received during illumination time N_p (25 pulses). The important parameters for the measurement are: bandwidth to be swept ($f_1 \ldots f_2$), fastest sweep time (ST = 50 ms) and size of the frequency window to be swept, FW, (2 MHz = highest suitable usable SA B_{IF}). With these parameters it is possible to measure with a single sweep such a part (50 MHz) from the frequency band f_1 to f_2 that is possible to be swept during one illumination. All radar pulses that coincide with the sweep during one illumination generate spectrum components on the receiver's corresponding frequency band. The measurement can be set up so that the frequency band is swept in chronological order (synchronized sweep) or with a random pattern (unsynchronized sweep).

The fly back time (FB) in Figure 13 is shown as 10 µs long. In practice $FB + \Delta T$ varies in the used SA randomly with every sweep. While FB is constant, ΔT varies between 48 ms and 80 ms. When the ST is short (for example 50 ms…1 s) the FB of the whole sweep is big and its influence is significant. In this case the whole sweep always becomes asynchronous. With a long ST (for example 100…2000 s) the FB of the whole sweep is small and its influence is not significant. If only one single sweep is used the influence of $FB + \Delta T$ to the measurement is non-existent. In this case one can use the synchronous measurement system. To make sure that the ΔT variations do not cause errors to the measurement results of the frequency band under measurement, FW overlapping (10...100 %, even 500 % [9]) is used. This can only be done in the synchronous measurement.

The sweep start delay ΔT of the total sweep ($ST + \Delta T$) is a characteristic of the used spectrum analyzer. It has not been defined in any specification of the measurement equipment. Neither has it been taken advantage of in measurements. The variation of ΔT in the equipment used in this work varies from analyzer to analyzer. The asynchronous

measurement requires a variable fly back ΔT part. This is due to the fact, that if there is no variation between the antenna period of revolution and the total sweep time the measurement can get stuck in one frequency range. Alternatively the measurement might proceed with a constant frequency increase. This would no longer be asynchronous causing furthermore that the calculation of the asynchronous measurement can no longer be applied in this case.

The radar named in the following examples, if not separately mentioned, is a weather radar with the assumed parameters as follows:

- f_C (f_N) is carrier frequency 5625 MHz (typical weather radar frequency range is 5500...5650 MHz),
- τ is pulse length 1 µs (typically used 0.5...2.5 µs),
- *PRF* is pulse repetition frequency 1 kHz (typically used 200...2000 Hz),
- φ is antenna lobe width 1...2°,
- P_{NF} is transmitter output power peak 200 kW,
- revolution of the antenna is 9 s and
- typical radar measurement range is 350 km.

In the following example it is shown how the sweep time and frequency window size of the measurement equipment are chosen. It is also shown how the pulse length and antenna rotation speed effect the measured frequency window size.

Example 1. In Figure 13 the antenna lobe is 1°. The radar antenna illumination time $T_{\varphi ant.lobe}$ = 25 ms. This results in 25 received radar pulses during one illumination ($25\,ms \cdot (1\,pulse/1\,ms)$). The radar pulses are transmitted every 1 ms. The pulse length and power level have no influence in the time domain parameter study if the energy of one pulse is adequate for the measurement equipment to detect and show the spectrum components. The pulse may not be shorter than 0.5 µs. This requires B_{meas} to be at least 2 MHz (the SA largest bandwidth in this work). To get at least one pulse in every *FW* (2 MHz) the frequency band to be swept may not exceed *FW·(2 MHz/1 pulse)·25 pulses = 50 MHz*. Because the radar antenna illumination time T_{ill} (25 ms) is half of the ST (50 ms) the widest frequency band to be swept during one antenna revolution is 2 · 50 MHz = 100 MHz. This, however, can be achieved first after two successive illuminations. So at least double the time will be spent (time of two antenna revolutions of 9 s).

The demand for at least one pulse per 2 MHz bandwidth to be swept can be justified as follows. A certain *FW* (equals B_{IF}) in the measured frequency band is examined. When the sweeping *FW* displays the frequency band in question (*FW* sweeps through the band to be measured with its *ST* = frequency band to be measured divided by *ST* (50 ms)) at least one pulse must be received when the *FW* is on the actual frequency band. If no pulse is received the spectrum components on this frequency band to be measured can not be displayed. No pulse, no transmission, no spectrum! A gap of possible spectrum components is left at this measured frequency but it can be filled during the following illuminations provided that coincidence of the actual FW band and a received radar pulse exists.

When summing up the swept frequency intervals each of bandwidth ($FW = B_{IF}$) it is assumed that the frequency band to be measured becomes gapless when B_{IF} is determined as the SA filter's 3 dB bandwidth. To insure the gaplessness, the B_{IF} intermediate frequency (IF) parts can be summed up of overlapping frequency intervals. When the overlapping for example is 10% of the B_{IF} or the frequency band to be swept the frequency band to be measured is ((0.9·2 MHz/1 pulse)·25 pulses)·2 = 90MHz. This means a slightly narrower but probably more gapless measured frequency band.

If the *PRF* of the radar is 200 Hz, only five pulses can be received during one revolution of the radar antenna. This leads based on the above presentation to a ((2 MHz/1 pulse)·5 pulses)·2 = 20 MHz frequency band that can be measured during one antenna revolution. Equivalently with a 2000 Hz *PRF* the widest frequency band to be measured becomes 200 MHz. End of example.

4.3.2 Limitations of parameters and practical problems in the time domain treatment

If the *PRF*/*FW* -ratio is small, the condition of getting at least one radar pulse into the measured FW during one illumination period will not be fulfilled. The measurement system will see this as a missing pulse. This corresponds in practice to a lower *PRF*. Naturally it is not the case but the radar transmits pulses regularly according to its *PRF*. Due to unsuitable measurement system settings this causes gaps into the displayed spectrum. To avoid this, the SA sweep rate should be decreased. While the radar antenna is rotating several revolutions the measured spectrum shape or the peak power level is becoming more accurate. When the spectrum is monitored in the SA maxhold mode (holds the maximum value on the SA display), the phenomenon explained above looses its significance. The envelope on the SA display becomes gapless but the only disadvantage is the increased measurement time.

Radar pulses can be received continuously according to the *PRF* of the radar, if the rotation of the radar antenna can be stopped and the antenna position can be locked towards the measurement antenna. With the settings of Example 1 the spectrum shape is established in two correctly timed SA sweeps when the ΔT of the total *ST* is assumed to be zero (0). Then the measurement time is 2·50 ms = 0.1 s. If the radar antenna is rotating a total measurement time of 2·9 s = 18 s is required. The measurement time would be 50 ms (when using the SA shortest *ST*) if the radar antenna illumination of the measuring antenna is equal or longer than the used *ST* so the measurement is done in theory during one correctly timed illumination from the radar antenna.

The SA technical capabilities may cause some restrictions to the measurements. The *FW* (equal to B_{IF}) to be swept can not be increased with the SA in this example. The *FW* can be narrowed but at the same time the *PRF* of the radar should be increased or the *ST* should be longer to make it possible to measure an equally large bandwidth. In this case, however, the measurement time and frequency band to be swept becomes smaller and thus the measurement time increases since more radar antenna revolutions are needed. The advantage of narrowing the *FW*, however, is that the noise becomes lower and the spectrum shape becomes more accurate. At the same time the radar pulse peak power level on the SA display is lower. The level shown on the display has to be corrected by $20 \cdot \log\left(B_{ref} / B_{IF}\right)$ dB that is then added to the displayed peak power level.

The maximum *FW* must be at least $1/\tau$ (2 MHz used in this work) because the maximum power levels are measured. If the maximum *FW* is smaller than $1/\tau$, a larger amount of pulses is needed. Otherwise the pulses are received too seldom and the measured spectrum becomes gappy. Narrowing of the *FW* causes the bandwidth to be measured to decrease correspondingly. The amount of radar pulses (*PRF*) can not be increased excessively because the radar use sets limitations to it. Targets at a range up to 150 km can be measured with a 1 kHz *PRF*. This is due to the fact that the echo of the previous pulse must be received before the next pulse is transmitted.

It is good to keep in mind the fact that the spectrum maximum power level determination requires a wide $(\geq 1/\tau)$ measurement bandwidth. The accurate spectrum shape measurement requires a narrow $(<< 1/\tau)$ measuring bandwidth. If the radar antenna rotation speed can be decreased the illumination time of the measuring antenna can be increased and

the amount of pulses received increased. Then it is possible to sweep a wider frequency band with one sweep. This results in a faster measurement. The measurement time due to the same reason, however, becomes longer when the antenna rotation time increases. If the radar station is located abroad the radar *PRF* and antenna rotation speed are not controllable.

With the method described above the measurement time can be optimized in accordance to the width of the frequency band to be measured when considering if one wants to measure the spectrum shape or the spectrum maximum power levels. The result, however, is totally dependent on the radar parameters. These are: repetition frequency, antenna lobe width, antenna rotation speed and the measurement equipment parameters (the sweeping *FW* size, *ST* and intermediate frequency bandwidth possible to use (B_{IF})).

With a single sweep the maximum measurement frequency range (*MMFR*) can be expressed as Equation 4.9:

$$B_{\max}\,[\mathrm{MHz}] = \left(\frac{FW}{N_{pulses}}\left[\frac{\mathrm{MHz}}{\mathrm{pulses}}\right]\right)\cdot\left(\frac{T_{360°}}{360°}\left[\frac{\mathrm{seconds}}{\mathrm{degrees}}\right]\right)\cdot\varphi\,[\mathrm{degrees}]\cdot\left(\frac{PRF}{\mathrm{second}}\left[\frac{\mathrm{pulses}}{\mathrm{second}}\right]\right) \qquad (4.9)$$

The size of the frequency band to be measured is composed of the frequency band parts B_{max} shown in Equation 4.9 observing the possible interleaving of the measured frequency bands.

In the following example the different pulse requirements, the pulse availability and the *ST* effect on the composition of a comprehensive spectrum are compared with help of a simulation. The simulation has been realized by replacing the radar transmitter with a signal generator that generates a signal similar to a radar transmission. Simulation is used here, because of the problem in using real radar in this measurement. The signal generator is connected directly to the SA input, with the output signal level adjusted suitable for the SA. One unsynchronized single sweep is equivalent to one revolution of a radar antenna.

Example 2. It is assumed that the radar *PRF* to be 1000 Hz, the antenna main lobe to be 2° and the antenna rotation time to be 9 s per revolution. This results in receiving 50 pulses with a sweep time of 50 ms. The signal generator simulating the radar transmitter sends (like the radar would transmit) 50 pulses in the sweep time of 50 ms and 500 pulses in the sweep time of 500 ms. The influence of received radar pulses on the spectrum measurement can be compared with the situation where the SA is used in single sweep mode. Here one sweep can be seen as the illumination during one revolution of the radar antenna. Now one can calculate after how many manually triggered single sweeps (simulates the amount of the radar antenna revolutions) the spectrum reaches its final and perfect shape.

When the frequency band to be measured is 10 MHz and the sweeping *FW* size is 30...1000 kHz and *ST* is 50 ms or 500 ms one gets a reference table as follows:

Table 2. The influence of the sweeping *FW* and *ST* to the measurement time (needed amount of antenna revolutions) in an unsynchronized measurement

Frequency range/MHz	Assumed FW/kHz	Total need of pulses	ST/ms	Availability of pulses	Simulated antenna revolutions	Theoretical calculated revolutions
10	30	334	50	50	30	infinite
10	30	334	500	500	2	1
10	100	100	50	50	30	infinite
10	100	100	500	500	2	1
10	1000	10	50	50	30	infinite
10	1000	10	500	500	2	1

The first row of Table 2 contains the following information. When the frequency range is 10 MHz, the *FW* is 30 kHz, and *ST* is 50 ms the simulation with the signal generator and SA shows that the almost complete spectrum shape (a certain exact average proportional part of the perfect spectrum measurement is almost impossible to evaluate) is obtained after 30 antenna revolutions. The minimum amount of needed pulses is $10\,MHz/30\,kHz$ = 334, but only 50 can be received during one revolution. The calculated average proportional part of a completely measured spectrum is 99.9 % after 30 antenna revolutions (explained later) when 50 pulses per revolution are available. For this measurement 30·9 s = 270 s of time is used. In the case the number of received pulses is equal or larger than the requirement, the simulation shows that two illuminations are needed. Theoretically only one illumination is needed. According to the display of the SA (SA resolution) a perfect spectrum is achieved after two sweeps even though the SA display still in holds invisible spectrum components.

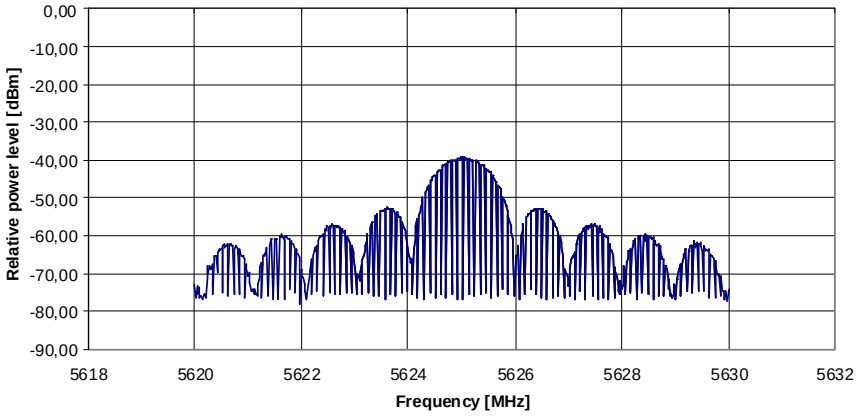

a)

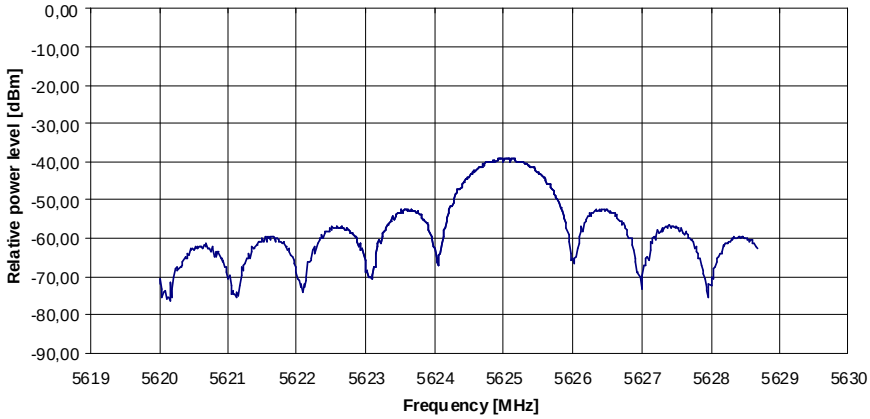

b)

Figure 14
a. Simulated model of the received spectrum shape after one sweep.
b. Simulated model of the received spectrum shape after two sweeps.

Figure 14a shows how the spectrum shape on the SA display is incompletely filled. The black spectrum markings are gaps and the white spectrum markings are filled parts of the spectrum. Figure 14b shows a model of how the spectrum shape of a radar transmitter becomes perfect on the SA display after the second sweep with values given before in Example 2. After receiving the second sweep all spectrum components are shown with the actual resolution of the SA display.

4.3.3 Effect of measurement parameters on the measurement results

It can be shown that the pulse bandwidth of the radar compared to the measurement bandwidth affects the accuracy of the measured peak power level of the received spectrum components and on the other hand the measured spectrum shape. A good approximation value for the peak power level is achieved when $B_{meas} > 1/\tau$. $B_{meas} << 1/\tau$ causes the spectrum shape to be more accurate.

From Equation 4.9 follows that the maximum bandwidth measured during a single sweep is proportional to *FW* and *PRF*. The period of revolution of the antenna has the same effect. The radar antenna lobe width also affects the size of the frequency band to be measured (the wider the radar antenna lobe, the more radar pulses are received during one revolution and the wider frequency band can be measured). The amount of received pulses for a successful measurement in a sweep effects inversely on the size of the frequency band to be measured (the more pulses are demanded, the narrower the measured frequency band will be).

4.3.4 Synchronized sweep

The measuring system for radar spurious components can be realize either by measuring the frequency window step by step or by sweeping the equivalent frequency window. The author has in this work chosen the sweep method. It can be realized either synchronized or unsynchronized.

Figure 15 presents a synchronized sweep with typical weather radar parameters: period of revolution of radar antenna ($T_{360°}$), bandwidth of the SA (B_{meas}) and sweep time of the SA (*ST*). In the synchronized sweep shown in Figure 15 the frequency band measured during one illumination equals *FW*. During the next illumination the *FW* adjacent to the previous *FW* is measured with some possible overlapping. Finally a gapless spectrum of the intended bandwidth will result.

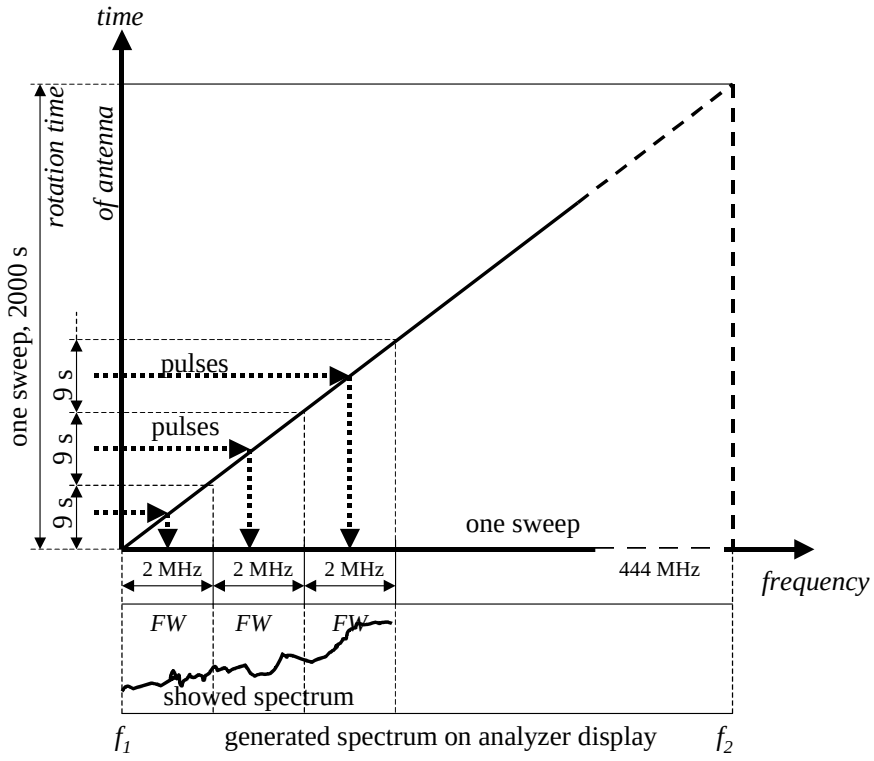

Figure 15. The principle of synchronized sweep measurement.

The *FW* bandwidth of the measuring equipment ($B_{IF} = B_{ref}$) is matched to the antenna period of revolution. This has been done so that the frequency band to be measured is swept systematically with one single SA sweep over the frequency interval $f_1 ... f_2$ when the *ST* and the measurement time are 2000 s. The investigation of the frequency band to be measured proceeds with a speed determined by the period of revolution of the radar antenna and the size of the *FW*.

With the parameter values in Example 2 all radar pulses received during a single illumination will contribute to the spectrum measurements in the 2 MHz *FW* while only one pulse is needed. This waste of pulses results in a longer measurement time but ensures the presentation of a more accurate shape and peak power level of the spectrum. The receiver (the SA used here) uses only the energy of one pulse at a time and shows its spectrum components. When the pulse shape and amplitude stay constant the SA always shows the same spectrum for each separate pulse. Depending on the progress of the sweep the spectrum figure is generated on the SA display in steps, because a maximum B_{IF} is used for sweeping and $B_{meas} \geq 1/\tau$.

The longest sweep time of the SA used is 33 min 20 s. If the antenna of the radar to be measured rotates one revolution in 9 s the antenna has to rotate a total of 222.2 revolutions for the whole measurement procedure. Within the time of the 222 whole revolutions the measurement bandwidth of 2 MHz is measured 222 times giving a total measuring bandwidth of 444 MHz. The measurement bandwidth is the widest possible because all pulses received are at the disposal of the measurement. All other conditions remain unchanged. This measurement system is suitable for determining the spectrum maximum power level when maximum B_{IF} is used for the *FW* and $B_{meas} \geq 1/\tau$. If highest B_{IF} of the SA would be for example 8 MHz the measurement time of the above measurement would

decrease to its fourth, or the measured bandwidth would increase four times with a single sweep. The measurement results would still correspond to the real power level of the spectrum.

The measurement range is not critical but it has to be taken care of that the radar total transmitted power at the SA mixer diode (SA input) does not increase above −20 dBm (it is recommended to use an attenuator). It must be observed that the SA only displays the part of the power level falling inside the *FW* but not for example power levels of harmonic signals. These, however, have influence at the SA mixer diode during the measurement.

If the antenna rotation can not be stopped the SA ST_s is selected as follows:

$$ST_s > \left(W_{meas} / B_{meas}\right) \cdot T_{360°} \tag{4.10}$$

where:
- W_{meas} is the width of the frequency band to be measured,
- $T_{360°}$ is the period of revolution of the antenna,
- ST_s is the single sweep time
- B_{meas} is $(0.01...0.1) \cdot B_{ref}$ and
- B_{ref} = 1MHz.

When knowledge of the exact shape of the spectrum is wanted a suitable value for B_{meas} in Equation 4.10 is $0.01 \cdot B_{ref}$. When knowledge of the pulse peak power is wanted a correction of $20 \cdot \log\left(B_{ref} / B_{meas}\right)$ has to be used with this measurement bandwidth.

Example 3.This example shows the minimum single sweep time is determined. Following assumptions are made. The bandwidth to be measured in single sweep is 1 GHz. The radar rotation time is 9 s and the measurement bandwidth is 2 MHz as before. The sweep time *ST* is then:

$$ST_S > \left(1 \cdot 10^9 / 2 \cdot 10^6\right) \cdot 9\,s = 4.500\,s = 1h\,15\,\text{min} \tag{4.11}$$

In this example all received radar pulses during the illumination time on every revolution of the radar antenna are available in one *FW* to be swept. This measurement is most suitable for determining the shape of the radar spectrum components because a B_{meas} a 100 times smaller than B_{ref} is used.

The measurement time becomes longer than the SA single sweep (2000 s) can provide. Therefore the bandwidth to be measured has to be decreased or B_{meas} has to be increased. The measurement, if possible, should be carried out with the radar antenna halted.

4.3.5 Unsynchronized sweep

If the radar measurement with the radar antenna rotating can not be done with a synchronized sweep it is possible to use an unsynchronized sweep. With an unsynchronized sweep is here meant that the sweep of the frequency band to be measured and the antenna rotation are totally independent of each other. This results in random radar antenna illuminations with respect to the SA sweeps. Also the *FW* within a determined frequency band to be measured $f_{1...}f_2$ occurs randomly with respect to the sweep span of the SA.

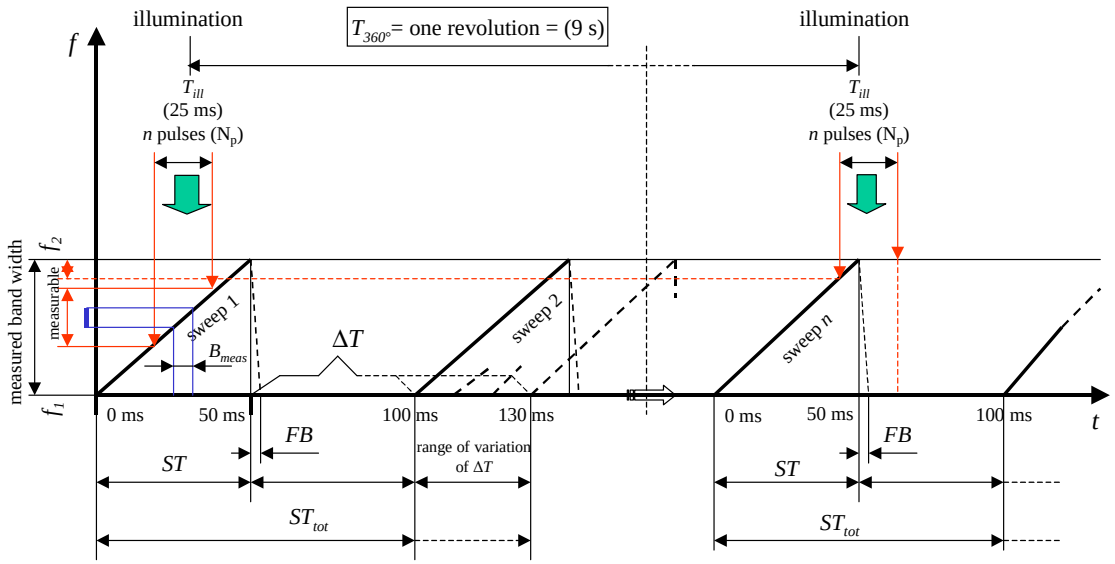

Figure 16a. The principle of unsynchronized sweep measurement.

Figure 16a shows the principle of an unsynchronized sweep, how the spectrum in the frequency interval f_1...f_2 is filled on successive antenna revolutions when *FW* sweeps many times the same frequency interval f_1...f_2.

Figure 16b shows the values needed for mathematical modeling of the unsynchronized measurement method and Example 4 shows their use.

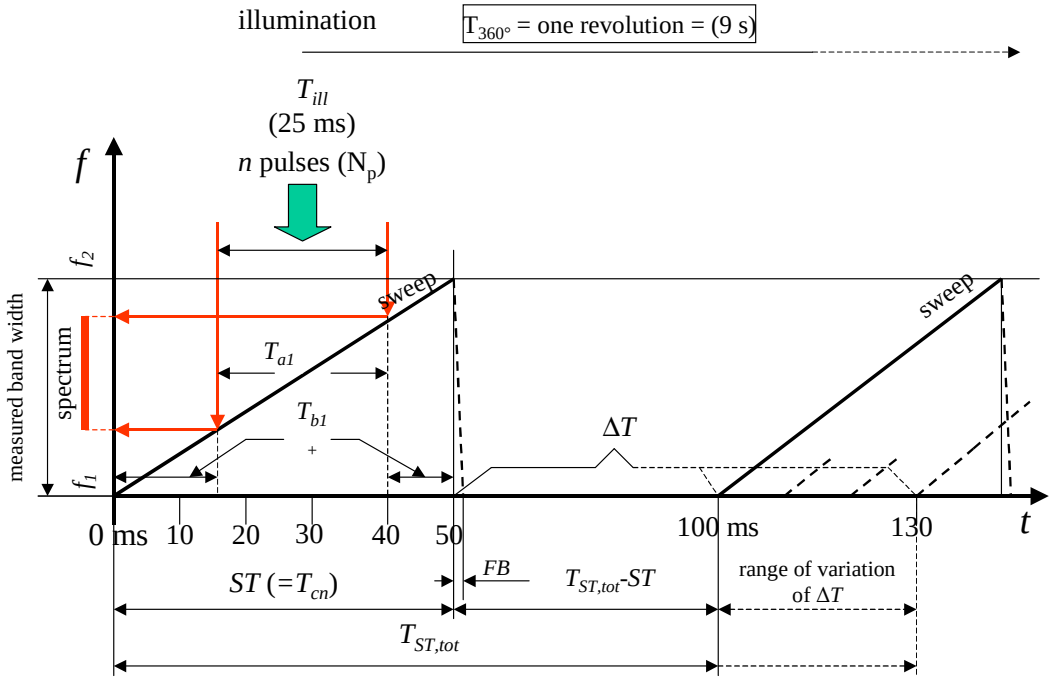

Figure 16b. The most important symbols in the analysis of the unsynchronized measurement.

The symbols in Figure 16b are:

- T_{a1} is the measured part of spectrum after the first illumination,
- ΔT is the delay time between two sweeps,
- FB is the fly back time,
- $T_{st,tot}$ is the overall sweep time (sweep + delay until next sweep starts),
- T_{cn} is the time corresponding the unswept portion of the measurement bandwidth $f_1 \ldots f_2$ after an illumination,
- T_{bn} is the total sum of sweep times needed for the remaining undisplayed portion of the spectrum after n antenna revolutions,
- T_{ill} is the illumination time derived from the radar antenna's beam width and the rotation speed and
- n is the number of antenna revolutions (illuminations).

Example 4. In this example shows how the unsynchronized measurement method advances and what kind of results are obtained (Figure 16b). It is assumed that the radar antenna period of revolution is 9 seconds and the lobe width is 1°. The radar antennas lobe illuminates the measurement antenna:

$$T_{ill} = \left(T_{360} \ / 360°\right) \cdot \varphi_{ant.lobe} \tag{4.12a}$$

where: - T_{ill} is the radar antenna illumination time and
- $\varphi_{ant.lobe}$ is radar antenna width in degrees.

Numerical calculation for Example 4:

$$T_{ill} = \left(9\,s / 360°\right) \cdot 1° = 25\,ms \tag{4.12b}$$

The minimum ST provided by the SA is 50 ms. When the antenna rotates one revolution its lobe (width 1°) illuminates the frequency band to be swept for 25 ms (T_{ill}). Depending on the sweep position of the frequency band on given times the illuminating time hits the SA sweep time randomly. The overall sweep time length consists of 50 ms forward sweep time and 50 ms of random delay (this has been found to be the average value during thousands of measured sweeps) to next sweep ΔT (includes FB, 10 µs). Here ΔT and FB are considered as waste time for the measurement. ΔT varies randomly, but in this calculation a constant value of 50 ms is used (explained in Section 4.3.1). The average fraction of the frequency band remaining unmeasured after n revolutions of the radar antenna can be calculated for the first antenna revolution (n=1) as follows (in terms of needed times for the measurement when the total time is 50 ms = total frequency band to be measured and the measurable time, illumination is at its maximum T_{ill} = 25 ms):

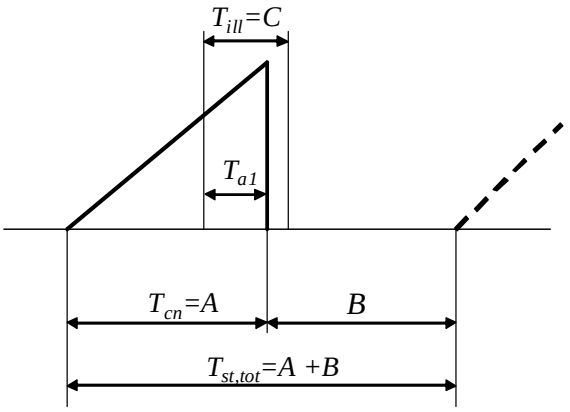

Figure 16c. Simplified scheme for calculation of average unmeasured frequency band.

$$T_{a1} = \frac{A}{A+B} \cdot C \tag{4.13a}$$

where:
- T_{cn} is the sweep time (ST = 50 ms) (equals A),
- T_{a1} is the average intersection of the sweep time and the illumination time,
- $T_{b1} = T_{c0} - T_{a1}$
- $T_{ST,tot}$ (equals $A+B$ in equation)is the total sweep period (100 ms, when ΔT (equals B) is assumed to be 50 ms) and
- T_{ill} is the illumination time (25 ms) (equals C in the equation).

Numerical calculation for Example 4:

$$T_{a1} = \left(\frac{50}{100}\right) \cdot 25[\text{ms}] = 12.5[\text{ms}], \text{ when } \Delta T = 50[\text{ms}] \tag{4.13b}$$

In Figure 16b the first illumination is completely inside the sweep time of 50 ms and it illuminates 25 ms of this time. However, the average overlapping time is 12.5 ms for the first sweep as calculated above. A non-illuminated average time is left after the first sweep:

$$A - T_{a1} = A - \frac{A}{A+B} \cdot C = T_{b1} \tag{4.14a}$$

Numerical calculation for Example 4:

$$T_{b1} = 50[\text{ms}] - \left(\frac{50}{100}\right) \cdot 25[\text{ms}] = 37.5[\text{ms}] \tag{4.14b}$$

Similarly after the second illumination 9 seconds later the average fraction of measured frequency band is ST $(37.5 / 100) \cdot T_{ill} = T_{a2}$:

$$T_{a2} = \left(\frac{A - \left(\frac{A}{A+B} \cdot C \right)}{A+B} \right) \cdot C \tag{4.15a}$$

Numerical calculation for Example 4:

$$T_{a2} = \left(\frac{50 - \left(\frac{50}{50+50} \cdot 25 \right)}{50+50} \right) \cdot 25\,[\text{ms}] = 9.375\,[\text{ms}] \tag{4.15b}$$

After the second revolution on average 28.125 ms of non-illuminated sweep time remains.

T_{a1} = 12.5 ms
$T_{a2} = T_{b1} - T_{b2}$
T_{a2} = 37.5 − 28.125 = 9.375 ms
T_{a3} = 28.125 − 21.09 = 7.035 ms
T_{a4} = 5.24 ms etc
T_{c0} = 50 ms.

After every antenna revolution the average non-illuminated sweep time gets shorter and converges towards zero (meaning the comparable unmeasured fraction of the frequency band to be measured converges towards zero).

The average unmeasured part of the whole frequency band to be measured is after *n* antenna revolutions given by the following equation:

$$T_{bn} = \left(\frac{T_{ST,tot} - T_{ill}}{T_{ST,tot}} \right)^n \cdot T_{b0} \tag{4.16}$$

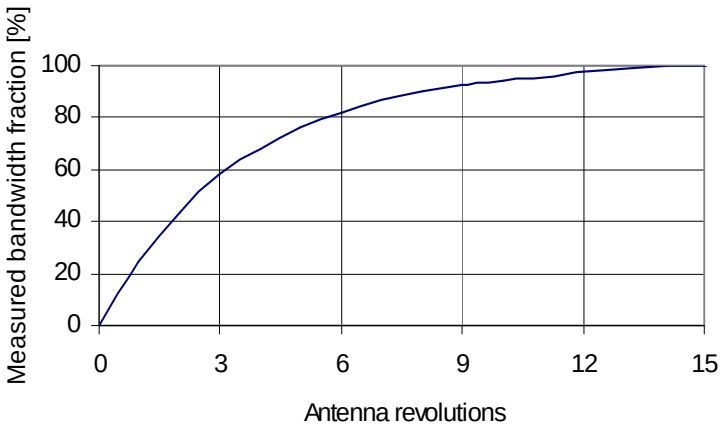

Figure 17. The progress of the measurement of an unsynchronized sweep

Figure 17 shows the average percentage of the total frequency band measured after the given amount of radar antenna revolutions when values from Example 4 are used in Eq. 4.16.

Numerical calculation with Eq. 4.16 shows that after 10 antenna revolutions 94.37% of the frequency band is measured. The time used for this measurement is 10·9 s = 90 s.

The above treatment is valid only if the sweep frequency range and the sweeping *FW* are such that for every swept frequency interval of bandwidth *FW* there is received at least one radar pulse and furthermore that the measurement is really unsynchronized.

4.3.6 Unsynchronized/synchronized sweep - reduced measurement time

If a shortest possible measuring time without causing a distorted measured spectrum is targeted an unsynchronized/synchronized sweep method can be used. With an unsynchronized sweep in this context is meant that the antenna rotation speed and the frequency band sweep are totally independent. Secondly, with a synchronized sweep it is here meant that the sweep time (*ST*) is adjusted, if possible, equal to the radar antenna illumination of the measurement antenna. In this case the whole frequency band to be swept is illuminated on every antenna revolution and the measurement can in theory be swept with a single sweep if an adequate amount of radar pulses are received.

The SA sweep time T_{ST} criteria using various filters for obtaining an undistorted spectrum can be found in radar literature [27] and is expressed as follows:

$$T_{ST} > K_{filter} \cdot W_{meas} / (B_{meas})^2 \tag{4.17}$$

where:
- W_{meas} is the frequency band to be swept
- B_{meas} is the measurement bandwidth
- T_{ST} is the sweep time (*ST*) and
- K_{filter} is a factor depending on filter shape (for Gaussian filter K_{filter} = 3, for rectangular filter K_{filter} = 10…20) [27].

Example 5. The parameters of a radar are known. It is wanted to know how long the measurement time will be when the real spectrum peak power level or the accurate spectrum shape is wanted. The parameters are as follows: The radar antenna rotates and its period of revolution is 9 seconds. The antenna lobe is 2°. The frequency band to be swept is 5 MHz. The *PRF* is 1 000 Hz. The radar pulse length is 1 μs and *ST* is 50 ms.

The illumination (T_{ill}) is given by Eq. 4.18a:

$$T_{ill} = (T_{360} / 360°) \cdot \varphi_{ant.lobe} \tag{4.18a}$$

Numerical calculation for Example 5:

$$T_{ill} = (9[s] / 360[°]) \cdot 2[°] = 50[\text{ms}] \tag{4.18b}$$

that is equal to the *ST* of the measurement equipment. The measurement bandwidth (B_{meas}) is determined as follows:

$$B_{meas} > (K \cdot W_{meas} / T_{ST})^{½} \tag{4.19a}$$

With given values:

$$B_{meas} > (3 \cdot 5 \cdot 10^6 / 0.05)^{½} = 17.32[\text{kHz}] \tag{4.19b}$$

The SA's nearest suitable IF bandwidth (B_{IF}) is 30 kHz which must be used. When a 5 MHz wide frequency band is to be measured with a 30 kHz *FW*, it needs 166.7 pulses per one sweep (5 MHz / 30 kHz = 166.7 pulses). However, the example case gives us only 50 pulses that leads to a need of four antenna revolutions. With a single sweep (50/166.7)·5 = 1.5 MHz is measured. This requires optimization of the amount of pulses, the *ST* and B_{meas}. The optimized values are (depending on the selected B_{meas} the measurement time can be shortened or the measurement dynamics increased for the desired *FW*):

- ST is equivalent to the radar antenna lobe illumination of the measurement antenna = 50 ms,
- the calculated ideal width of Bmeas = 17.32 kHz, so the next higher BIF = Bmeas = 30 kHz must be selected,
- 1 received pulse for every FW bandwidth,
- the measurement is fully conducted in one antenna revolution (the measured bandwidth is 1.5 MHz) and
- the whole 5 MHz bandwidth is measured in 4 antenna revolutions (If FW had been 10 kHz a complete measurement had required 500 radar pulses. This would require 10 radar antenna revolutions).

The selected B_{meas} 30 kHz is best suited for measuring the exact shape of the spectrum when the pulse length is 1 µs or for determining the peak power level of radar with 33.3 µs long pulses.

Flow chart 2 in Figure 18 shows how the time domain parameter study progresses using two different measuring methods (and their combination). In the upper left corner the starting data producing the necessary parameters for use of the time domain parameter study are given. On the right hand side the treatment of the measurement triggering radar pulse is shown. The operation continues in either of two branches: the synchronized or unsynchronized measurement. Both will result in the parameters for the frequency band measurement.

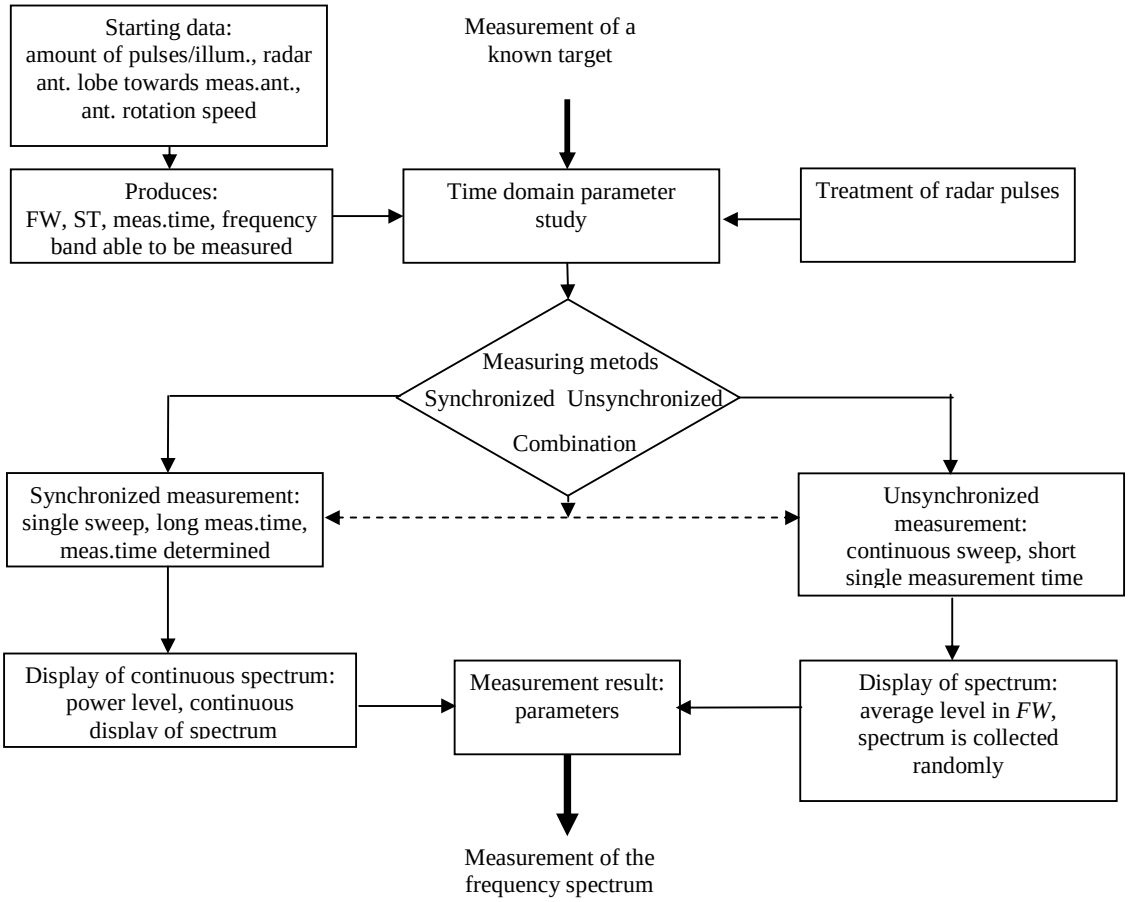

Figure 18. Flow chart 2 is showing the progress of the time domain parameter study.

4.4 Radar spectrum measurements and determination of power level and frequency of spurious emissions

The purpose of this measurement is to determine the nominal frequency (*NF*) of a known radar and the relative power levels of spurious frequency (*SF*) transmissions in frequency domain and their position on the frequency axis. In Section 4.3 the conditions for a successful time domain parameter study in radar measurement is described. Here these conditions are assumed to be valid. The measurement time is not considered regardless whether the exact spectrum shape or peak power level is measured. Neither are the requirements caused by the measurement bandwidth considered, they are assumed to fulfill the conditions. Additionally it is expected that there always is a satisfactory amount of radar pulses available. In this section is explained how the measurement system should be set up to increase the measurement dynamics to 110 dB as required for radar measurements. The largest radar spurious transmission level requirements (harmonic and non harmonic) are −100 dBc.

First a calibration curve is produced as described in Section 3.3.1. After this a maximum pulse power measurement without filter and amplifier is carried out. If it is possible to halt the radar antenna rotation, it is directed towards the measurement antenna in a correct elevation angle for the measurement antenna to be in the radar antenna main lobe.

It is recommended to use an attenuator in the measurement system to set the correct power level to the SA input. The measurement dynamics measuring only with the SA can be between 37...67 dB (difference between the pulse peak power level and the noise power level that are seen on the SA display simultaneously) depending on the SA input level setting and the used measurement bandwidth. In this work the maximum power level at the SA input is chosen to be −20 dBm with the used measurement bandwidth (B_{meas}). Only about ten of these signals can be at the input of the SA simultaneously to minimize the risk of overloading the SA. It must always be ensured that the measurement equipment does not produce internal spurious signals when operating at −10…−20 dBm input level. The possible spurious transmissions are visible within the measurement dynamic range. Here the correctness of the SA display must be checked.

If the radar antenna rotation can not be halted or the operation of the radar is not controllable the measurement must be conducted as described in Section 3.3.2 with a rotating radar antenna. When measuring while the radar antenna is rotating the highest relative power level for the SA max-hold function must be found (the level does not increase over this point during the measurement process).

The high radiation peak power level of radar pulses (up to 10 GW) and the high requirement for low spurious levels (down to −100 dBc) make it difficult to measure the spurious transmissions. This requires a high measurement dynamic range in the order of 110 dB for the measurement system. Additionally it must be taken care of that the signal power level at the SA input does not exceed −10 dBm. For the SA used here the dynamical functionality without distortion is lower than −40 dBm input signal level [27]). Then the second and third order distortion components are about a level of −120 dBm. When the SA input signal level is about −3...−10 dBm the amplification has been compressed by 1 dB.

The requirements for radar signal interference (both harmonic and non-harmonic) attenuation relative to the radar *NF* peak power level [30] are shown in Figure 19.

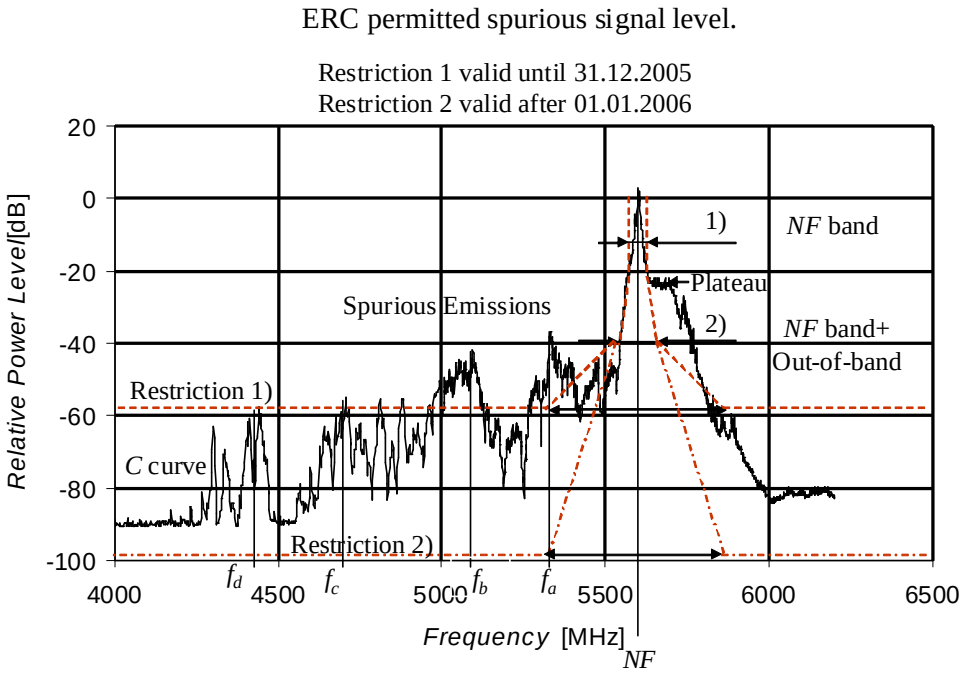

Figure 19. Permitted spurious signal levels of weather radar according to ERC and ITU.

The permitted levels of spurious signals [30] for a 5 GHz weather radar [31] are given by a spectral mask and are defined in Equations 4.20a...4.21d.

Spectral mask:

$$In-band\ domain: \qquad |f - f_C| \in \frac{6.36}{\tau} \tag{4.20a}$$

$$Out-of-band-domain: \qquad |f - fc| \in \left[\frac{6.36}{\tau}, \frac{64}{\tau}\right] \tag{4.20b}$$

$$Spurious\ band-domain\ I: \qquad |f - fc| \in \left|\frac{64}{\tau}, \frac{320}{\tau}\right| \tag{4.20c}$$

$$Spurious\ band-domain\ II: \qquad |f - fc| > \frac{320}{\tau} \tag{4.20d}$$

The spectral mask is defined as straight lines defined by relative spectrum levels at the domain limit frequencies:

$$-At\ \ |f - f_C| = \frac{6.36}{\tau}, \quad 20\log\left|\frac{X(f)}{X(0)}\right| = -20\,dBc \tag{4.21a}$$

$$-At\ \ |f - f_C| = \frac{64}{\tau}, \quad 20\log\left|\frac{X(f)}{X(0)}\right| = -40dBc \tag{4.21b}$$

$$-At\ \ |f - fc| = \frac{320}{\tau} \quad 1)\ 20\log\left|\frac{X(f)}{X(0)}\right| = -60\,dBc\ (until\ 31.12.2005) \tag{4.21c}$$

$$2)\ 20\log\left|\frac{X(f)}{X(0)}\right| = -100\,dBc\ (after\ 1.1.2006) \tag{4.21d}$$

For frequencies farther from the currier frequency than $320/\tau$ depending on the time the radar has been taken into use, the relative spurious level should be lower than either –60 dBc or –100 dBc.

In Figure 19 the measured radar signal spectrum and the spectral mask of allowed spurious signal levels (red dotted line) are shown. The measured spectrum represents the weather radar and the spectral mask is applied to it. A radar station with these measured values would not be approved in an inspection. To be approved this station would need both an additional low pass filter for frequencies above the *NF* and a high pass filter for *NF* or a band pass filter for the *NF* signal.

In this section two differently implemented measurement methods are presented, both following same principles. The basic principle of both measuring methods is that the high power *NF* signal is attenuated to not exceed the measuring equipment maximum input level of −20 dBm and simultaneously amplifying the highest component level of the low power *SF* signals to the same level as the *NF* component at the measurement equipment input. Frequency selective components have been used in the measurement system. The band stop filter (BS filter) and the YIG filter represent the frequency selective components. Signals with different frequencies are attenuated in different ways when passing through the combined frequency selective components.

It must be kept in mind that the measurement setup (Figure 20) must be equal to the measurement setup during calibration for the power level correction to be correct. The actual measurement system presented in Figures 20 and 21 requires a BS filter tuned to the *NF*, a tunable band-pass YIG filter, an attenuator (A) and a low noise amplifier (LNA) before the signal is fed to the SA input. To increase the measurement dynamic range the maximum pulse power has to be attenuated because its peak level determines the power level setting in the SA's input. The attenuation of radar *NF*-signal can be implemented with a tuned stub type multiple stage band-stop filter and the YIG filter controlled by the SA. The *SF* signal is amplified and its power level is matched with the attenuator A so that neither the *NF* or *SF* signal rises too high at the SA input. In this measurement both the attenuator and the amplifier have been checked to have constant loss and gain in the measured frequency range. It is advisable to attenuate the input level with a BS filter as much as it can be amplified by the LNA. In doing so the whole measurement system stays stable and the noise level of the system decreases. The SA's noise factor *F* is quite high. In the SA used for this measurement the noise figure is 27 dB. In the system described above the total noise figure is decreased to 8 dB.

The filter of measuring system setups is problematic. The kind of band stop filter (BS filter) needed in this measurement is not available on the commercial market. Due to their small demand it is no longer economical to manufacture them. There also was no YIG filter available (ITU-R recommendation [1]), which would have been suitable for the SA used in this measurement.

4.4.1 Measurement system 1 for measuring spurious power levels.

The idea of the measurement system is to extend the available measurement dynamic range to enable the determination of the spurious signal power levels. These must, to meet requirements, be more than 100 dB lower than the *NF* signal. Measurement dynamic range in this system means that the maximum input level of signals is reduced and the noise or spurious level at the input is amplified to be readable simultaneously from the SA's display while the highest allowed input level of the measuring equipment is not exceeded. Highest possible dynamic range is achieved when both the highest component of the *SF* signals and the *NF* signal level after attenuation are equally high at the SA's input, for example −20 dBm.

If a YIG filter, a BS filter and an LNA are available the adequate dynamic range is achieved with the measurement system in Figure 20. For tracking the signals to be measured, typical values for a weather radar measurement are used:

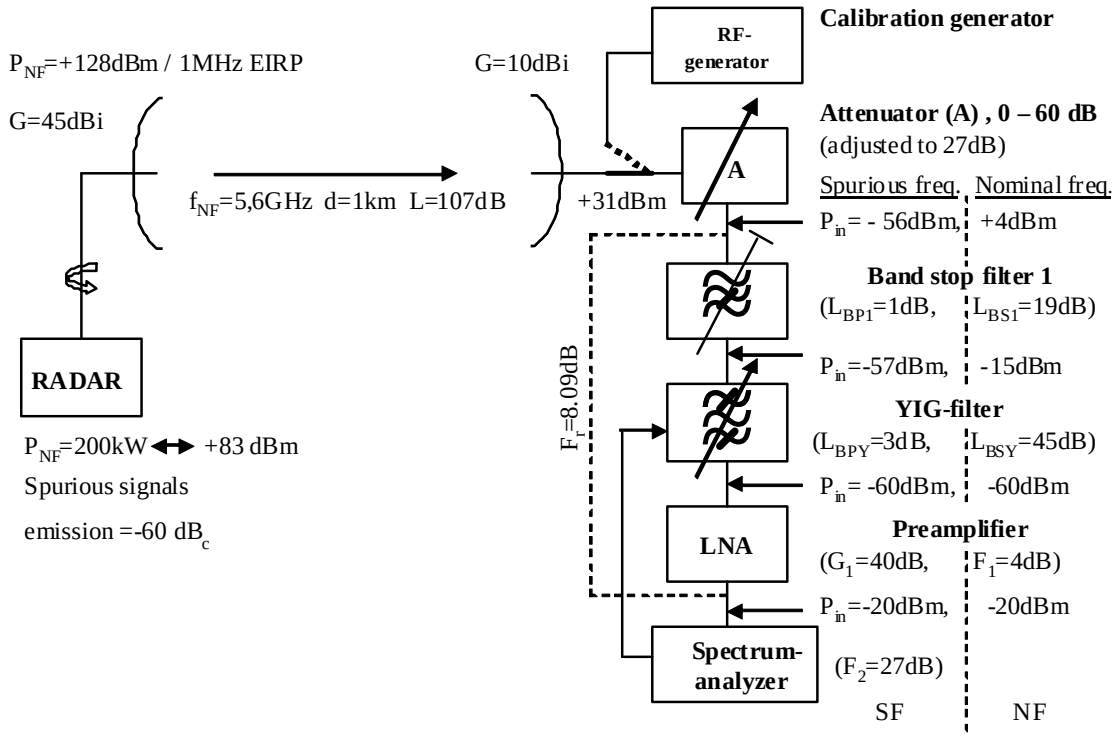

Figure 20. Measurement setup 1.

Figure 20 presents the block diagram of the *SF* signal measurement system. The system comprises one BS filter (band-stop filter 1), a YIG filter and an LNA (preamplifier). All power levels presented in the figure are radar pulse peak powers. Beside the block diagram of the system a radar signal budget for both spurious frequency (*SF*) and the attenuated nominal frequency (NF) signals are shown.

The radar budget presented in Figure 20 can be followed starting at the radar output pulse peak power (+83 dBm) and the assumed maximum power level of spurious signals (here 60 dB lower that the signal level of *NF*). The radar antenna amplifies the signal 45 dB, the one km measurement distance attenuates it 107 dB and the measurement antenna again amplifies it by 10 dB. The *SF* signal either is amplified or attenuated relatively to the *NF* signal depending on whether the signal frequency is higher or lower than the *NF* signal. The amount of amplification or attenuation is dependent on the amount of the frequency difference. Due to the increase of propagation loss (*L*) and the equal measurement system antenna gain (*G*) increase, due to the rising increasing frequency, these almost cancel each other. The impact of the radar antenna gain increase is not taken into account as the spurious level requirement is for the radiated radar signal.

The input power level of attenuator A is +31 dBm with a radar output power level of +83 dBm. In the same point the power level of a spurious signal 60 dB below the NF signal level is –29 dBm. Connector and transmission line losses are assumed to be 0 dB.

By setting the attenuation of attenuator A, the stop-band attenuation of BS1 and the YIG filter, the intention is to achieve the same power level (–20 dBm) of both the *NF* and largest *SF* signal at the input of the SA. With the sample radar in Figure 20 the attenuation of attenuator A is set to 27 dB, the stop-band attenuation of BS1 to 19 dB and the stop-band attenuation of the YIG filter to 45 dB. These attenuation values will lead to a *NF* and *SF* level of –20 dBm in the SA input, when the level difference of these is 60 dB in the received

signal. Another value will lead to other settings. The actual values can be set by observing the spectrum on the SA display. The power level values of the *NF* and *SF* signal of the example radar in different parts of the measurement system 1 are shown in Figure 20. It can be observed that the *NF* signal is attenuated by 51 dB and the *SF* signal is amplified by 9 dB when compared to the filter input levels. It must be kept in mind that the determining factor at the SA's input always is the highest power that creates a maximum −20 dBm power level at the SA input. This is so even when it is not visible on the display.

The calculation of the obtainable measurement dynamic range proceeds as follows:

The overall noise figure of the chain at the input of the LNA, i.e., due to the SA and the low-noise preamplifier (LNA) is given by the Friis' formula:

$$F_{tot} = F_1 + (F_2 - 1)/G_1 \tag{4.22a}$$

where
- F_{tot} is the overall noise factor at the input of the LNA,
- F_1 is the noise factor of the LNA,
- F_2 is the noise factor of the SA and
- G_1 is the absolute value of gain of the LNA

Calculation example for the block diagram in Figure 20:

$$F_{tot} = 2.51 + (501 - 1)/10.000 = 2.56 \Leftrightarrow 4.09\,\text{dB} \tag{4.22b}$$

The overall noise figure reduced (F_r) to the input to the first BS filter is:

$$F_r = F_{3,4} + (F_2 - 1)/G_{3,4} + (F_1 - 1)/(G_2 G_{3,4}) \tag{4.23a}$$

where
- F_r is overall noise factor of the BS-filter - YIG-filter - LNA - SA,
- F_1 is SA noise factor,
- F_2 is LNA noise factor,
- $F_{3,4}$ is total noise factor of YIG and BS filter,
- G_2 is LNA gain,
- $G_{3,4}$ is combined gain of filter amplification
(- the noise factor of each attenuator is its attenuation)

Calculation example for measurement setup in Figure 20:

$$F_r = 2.51 + \frac{(2.51 - 1)}{0.4} + \frac{(501 - 1)}{(0.4 \cdot 10000)} = 6.43 \Leftrightarrow 8.09\,\text{dB} \tag{4.23b}$$

The noise power reduced to the input to the BS filter (i.e., the noise power in the equipment + noise power from the transfer path in the 1 MHz measurement bandwidth) is given by:

$$P_N = 10 \cdot \log(F_r k T_0 B) = F_r + 10 \cdot \log(k T_0) + 10 \cdot \log(B_{meas}) \tag{4.24a}$$

where
- P_N is noise power level,
- F_r is total noise figure of measurement equipment,

- the second term is thermal noise power spectral density level at room temperature, $10 \cdot \log(kT_0)$,
- k is the Boltzmann constant,
- T_0 is the room temperature 290 K and
- B_{meas} =1 MHz is the measurement bandwidth.

Calculation example for measurement setup in Figure 20:

$$P_N = 8.09[\text{dB}] - 174[\text{dBm}] + 10 \cdot \log 10^6[\text{dB}] = -105.91[\text{dBm/1 MHz}] \quad (4.24b)$$

As the signal to be measured must be 10 dB (practical value of an *SNR*) above the noise level to obtain reliable results, the dynamic range (*DR*) of the measurement system becomes:

$$DR_{\max} = P_{NF,inBS} - P_N - SNR_{\min} \quad (4.25a)$$

where
- DR_{max} is maximum achievable measurement dynamics range,
- $P_{NF,inBS}$ is the maximum *NF* signal power level at the input to the BS filter, such that an *NF* power level of (–20 dBm) is not exceeded at the input to the SA (shown in Figure 20),
- P_N the noise power at the input to the BS filter and
- SNR_{min} (10 dB) is the required difference in signal and noise power levels.

Calculation example for measurement setup in Figure 20:

$$DR_{\max} = 4[\text{dBm}] - \left(-106[\text{dBm}]\right) - 10[\text{dB}] = 100[\text{dB}] \quad (4.25b)$$

For comparison, the dynamic range as measured with the SA without the BS filter, YIG filter and LNA is also calculated:

$$\begin{aligned} &\text{Dynamic range without filters and amplifier} \\ &DR_{\max} = P_{NF\,in,SA,\max} - P_{N,inSA} - SNR_{\min} \end{aligned} \quad (4.26a)$$

where
- $P_{NFin,SA,max}$ is the maximum *NF* power level requirement at the SA mixer diode (input),
- $P_{N,in,SA}$ is the SA's noise power + incoming noise power in a 1 MHz measurement bandwidth and
- the wanted signal to noise ratio (SNR_{min}).

Calculation example for a measurement dynamics achieved by just the SA according to Figure 20:

$$DR = \left(-20[\text{dBm}]\right) - \left(-87[\text{dBm}]\right) - 10[\text{dB}] = 57[\text{dB}] \quad (4.26b)$$

If the power level of the *SF* signal is 80 dB lower than the power level of the *NF* signals the attenuator A's value 27 dB can be decreased equivalently 20 dB and the *SF* signal will still not exceed −20 dBm at the SA input. The *NF* signal must also be attenuated by 20 dB to maintain balance between the power levels. The balancing must be done by increasing the attenuation of the BS filter by 20 dB (by retuning the filter) from 19 dB to 39 dB. At the same time the dynamics of the measurement system increases with 20 dB (assuming that the

filter attenuations at SF do not change) (Equation 4.25) to 120 dB. The maximum dynamics 127 dB is possible to achieve with the here presented measuring equipment and with the given measuring distance from the transmitter if the spurious signal is 87 dB below the *NF* signal level. In this case attenuator A must be set to 0 dB attenuation and it can not be decreased from this value.

In case that the *SF* signal level is 100 dB under the *NF* signal level the measuring antenna must be located nearer to the transmitter than assumed in Figure 20. Alternatively a measuring antenna with a higher gain must be used for the *NF* signal power level to be + 44 dBm (when the attenuation of the attenuators is set to 0 dB) at the attenuator A's input. The attenuation of the *NF* filter should be 59 dB. So both signals would be (−20 dBm) at the SA input and the dynamics available would be 44 dBm − (−106 dBm) − 10 dB = 140 dB. This requires the distance to the transmitting antenna to be decreased from 1 km to 0.224 km (distance attenuation *L* decreases) which already is inside the near field and the area of risk to health.

In theory the presented measurement system values can be used. In practice, however, the high radiation field causes errors and interference to the measurement. These appear to the measurement results through connectors, adapters, cables and incomplete shielding level of equipment boxes and due to insufficient connection contacts (the connection attenuation tolerance of all connectors and adapters rises due to the amount of usage times). In practice when measuring under field conditions a satisfactory and useful measuring dynamics of about 110 dB can be achieved.

When measuring *SF* power levels that contain several maximally –20 dBm signal spectrum components, their total power at the SA input can be calculated according to equation $P_{SF,tot} = P_{SF1} + P_{SF2} \ldots + P_{SFn}$. Symbols P_{SF1}, P_{SF2}, ... P_{SFn} mean the separate *SF* maximum signal powers. The result must not exceed (–10 dBm). This means that the total amount of measured *NF* and *SF* signals (–20 dBm) may be about ten. It must be noted that all signals passing the SA front end in the measurement frequency range are fed to the SA detector diode. This means a frequency range of up to several GHz. A too high peak power level causes the detector diode to operate in its non-linear operating range. This makes intermodulation possible. Due to this fact the SA display correctness must be checked when measuring at maximum power levels.

It should be observed that when correcting a power level exceeding the allowed power level (regardless which level is corrected) with attenuator A, it decreases measurement dynamics by the increase of attenuator A's attenuation. If, however, signal level correction can be done by a more effective BS filter (higher band stop attenuation) and amplifier (higher amplification) these increase the dynamics with the amount of the correction. It is also possible to increase dynamics by decreasing the system noise factor by choosing a preamplifier (LNA) with a lower noise figure. The measurement dynamics has been enhanced in this work with this arrangement by decreasing the SA's own noise from 27 dB to the analyzers + amplification systems total noise figure 4.09 dB.

The YIG-filter is a tunable band-pass filter, which is swept so that the 35 MHz pass band coincides with the SA measurement frequency. It can not be used for measurement of the *NF* component, only for measurement of spurious components, as it attenuates the *NF* component by 45 dB.

4.4.2 Measuring system 2 for measuring spurious transmissions.

A practical problem in the realization of measuring system 1 is the availability of a suitable YIG filter. In practice, the measurement shall be conducted without a YIG filter. In this case other methods to prevent the power of the *NF* signal to increase above the –20 dBm limit at the SA's input must be considered.

An alternative measurement system without a YIG filter is presented in Figure 21. Typical values for radar measurement have been inserted. In this measurement two BS filters must be used and the maximum *NF* signal power in the input of the first BS filter must be limited to the following value:

$$P_{peak.\max} \le P_{in,SA,\max} - G_2 + L_{BS1} \tag{4.27a}$$

where:
- $P_{peak..max}$ is the maximum radar signal power level at the input of the first BS-filter,
- $P_{in,SA,max}$ is the maximum power level requirement at the input of the SA,
- G_2 is the gain of the LNA in dB and
- L_{BS1} is the attenuation of the BS filters at *NF* (60 dB).

Calculation example of maximum value for $P_{peak.max}$ in Figure 21:

$$P_{peak.\max} \le (-20[\text{dBm}]) - 40[\text{dB}] + 60[\text{dB}] = \pm 0[\text{dBm}] \tag{4.27b}$$

To get a ± 0 dBm level instead of + 31 dBm at the input of the BS filter the measurement has to be conducted at a larger distance from the radar and / or an antenna with less gain than that described in Section 4.4.1 has to be used.

The lack of the YIG filter has been replaced by using a more effective filter by connecting two BS filters into series. Their attenuation, $L_{BS1,2}$, on the radar's *NF* is as high as 90 dB. After this arrangement the signal power in the input of the of the first BS filter may at its highest be:

$$P_{peak.\max} \le P_{in,SA,\max} - G_2 + L_{BS1,2} \tag{4.28a}$$

where:
- $P_{peak.max}$ is the maximum radar signal power level at the input of the first BS-filter,
- $P_{in,SA,max}$ is the maximum power level requirement at the input of the SA,
- G_2 is the gain of the LNA in dB and
- $L_{BS1,2}$ is the maximum attenuation of two BS filters in series at *NF* (maximum 90 dB).

Calculation example for measurement setup in Figure 21:

$$P_{peak.\max} \le (-20[\text{dBm}]) - 40[\text{dB}] + 90[\text{dB}] = +30[\text{dBm}] \tag{4.28b}$$

The adequately high dynamics with two BS filters connected in series and an LNA but without a YIG filter can be achieved with the measurement setup connection in Figure 21:

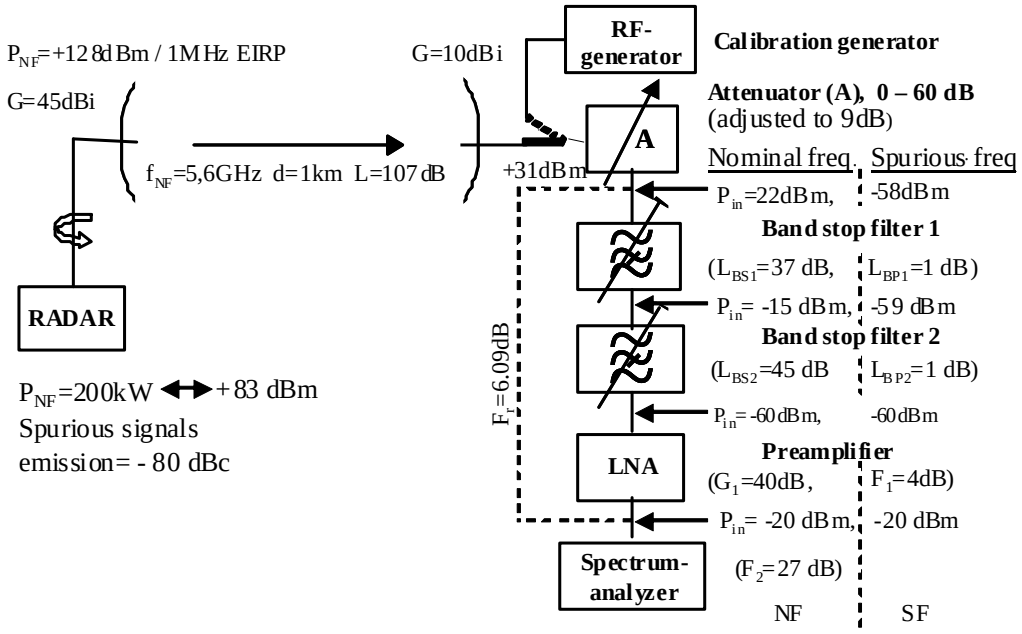

Figure 21. Measurement setup 2

Figure 21 shows the block diagram of the measurement setup with two BS filters connected in series and an LNA without a YIG filter. All given power values are pulse peak power levels. In the setup of Figure 21 the *SF* signal is 80 dB lower than the *NF* signal. In the figure the block diagram for a radar interference radiation measurement with all necessary components and their technical parameters influencing the measurement are shown. In addition to the block diagram the power budget of the radar signal is given. The calculation of measurement dynamics with this setup and the given values advances similarly to the calculation presented earlier in Section 4.4.1.

The circuit (LNA+SA) total noise figure F_r reduced to the input of the LNA has been calculated in Equation 4.22 and is 4.09 dB.

The reduced total noise factor (F_r) of the measuring equipment in the input of the first BS filter is:

$$F_r = F_{3,4} + (F_2 - 1)/G_{3,4} + (F_1 - 1)/(G_2 G_{3,4}) \qquad (4.29a)$$

where
- F_r is system noise factor reduced to the input of the first BS-filter,
- F_1 is the noise factor of the SA,
- F_2 is the noise factor of the LNA,
- $F_{3,4}$ is the total noise factor of the two BS filters (L_{BS1} + L_{BS2} = 1+1 = 2 dB),
- G_2 is the gain of the LNA, and
- $G_{3,4}$ is the total gain of the two BS filters (–1 dB –1 dB = –2 dB)

(- the noise factor of each attenuator is its attenuation)

Calculation example for measurement setup in Figure 21:

$$F_r = 1.58 + \frac{(2.51-1)}{0.63} + \frac{(501-1)}{(0.63 \cdot 10000)} = 4.06 \Leftrightarrow 6.09\,[\mathrm{dB}] \qquad (4.29b)$$

The noise level reduced to the BS filter input is (the sum of the noise level of the measuring equipment and the noise generated on the 1 MHz wide measurement):

$$P_N = 10\log\left(F_r k T_0 B\right) = F_r + 10\log\left(kT_0\right) + 10\log B_{meas} \quad (4.30a)$$

where
- P_N is the reduced noise power level at first BS-filter input,
- the second term ($10\log kT_0$) = −174 dBm/Hz is thermal noise power level spectral density in room temperature (290 K),
- F_r is the reduced total noise figure in the input of the first BS-filter,
- B_{meas} = 1 MHz is the measurement bandwidth,
- k is the Boltzmann constant and
- T_0 is 290 K.

Calculation example for measurement setup in Figure 21:

$$P_N = 6.09[\text{dB}] - 174[\text{dBm}] + 10\log 10^6 = -107.91[\text{dBm/1MHz}] \quad (4.30b)$$

For example with the attenuator value set to 0 dB the *NF* signal level at the SA input is (−19 dBm). When the *SF* signal is 60 dB below the *NF* signal level and +9 dBm at the SA input. To reduce the *SF* signal level below the accepted (–20 dBm) level the attenuator A's attenuation must be set to 29 dB and the *NF* signal must be amplified by 28 dB for the power balance at the SA input not to quake. This gain must be done by decreasing the attenuation of one of the two BS filters by 28 dB (must be retuned).

When the signal to be measured must be 10 dB above the noise power level (*SNR* must be at least 10 dB) to ensure an accurate measurement result, the measuring systems dynamics becomes:

$$DR_{\max} = P_{NF,in,BS1} - P_N - SNR_{\min} \quad (4.31a)$$

where:
- DR_{max} is the highest possible dynamic range
- $P_{NF,in,BS1}$ is the maximum *SF* signal level at the input of the BS1 filter (31 dBm − 29 dBm = 2 dBm),
- P_N is the reduced noise power level at the input of the BS1 filter and
- SNR_{min} is the required signal and noise power level difference.

Calculation example for measurement setup in Figure 21:

$$DR_{\max} = 2[\text{dBm}] - \left(-108[\text{dB}]\right) - 10[\text{dB}] = 100[\text{dB}] \quad (4.31b)$$

If the *SF* signal is 80 dB lower than the *NF* signal (as in the radar budget in Figure 21) the attenuation value of attenuator A must be reduced by 20 dB while increasing BS filter attenuation by the same amount. When the *NF* signal at the first BS filters input rises by 20 dB the measuring dynamics rises by 20 dB from 100 dB to 120 dB. However, 110 dB can be, due to the high RF signal power level, seen as the maximum value for the dynamics in practice. When measurement with more than 110 dB measurement dynamics is desired, the measurement distance must be decreased; the protection of measurement equipment and measurement staff must be checked.

4.4.3 Radar power budgets

The budgets for both *NF* and *SF* frequency radar signals can be displayed in graphical form. In Figure 22 this is done for both measurement system 1 and 2 and for the reference system without any filters and LNA. The radar transmit power level, radar antenna gain, transmission path loss and the measurement system antenna gain are the same in all compared measurement setups. All three measurement systems have the same +31 dBm *NF* signal at the attenuator input and an either 60 or 80 dB lower *SF* signal. Due to low power level and insufficient measurement dynamics of the reference system no *SF* signal lower than (–60 dBc) can be measured with the comparison system.

All *NF* radar pulse and *SF* interference signal power levels shown in the figure are peak powers. In Figure 22 the *NF* level of the measurement system 1 has been decreased by 51 dB (black continuous line) and the *SF* power level increased by 9 dB (red dotted line). If, however, the *SF* power level (here the radiating power under measurement) is for example 80 dB less than the radar pulse peak power one gets to the same (–20 dBm) power level at the SA input when it is passing the attenuator and the filters as explained in Sections 4.4.1 and 4.4.2. The dynamics (blue arrows) is calculated from the difference at the first BS filter input level +4 dBm (measurement system 1) and maximum noise power level (106 dBm) at the same filter input. When one takes into account the 10 dB higher than noise power level as the smallest accurately measurable power (SNR_{min} = 10 dB), one gets a 100 dB dynamics for measurement system 1. The dynamic range of the display is the largest level difference between spectrum components that can be displayed with a specified accuracy.

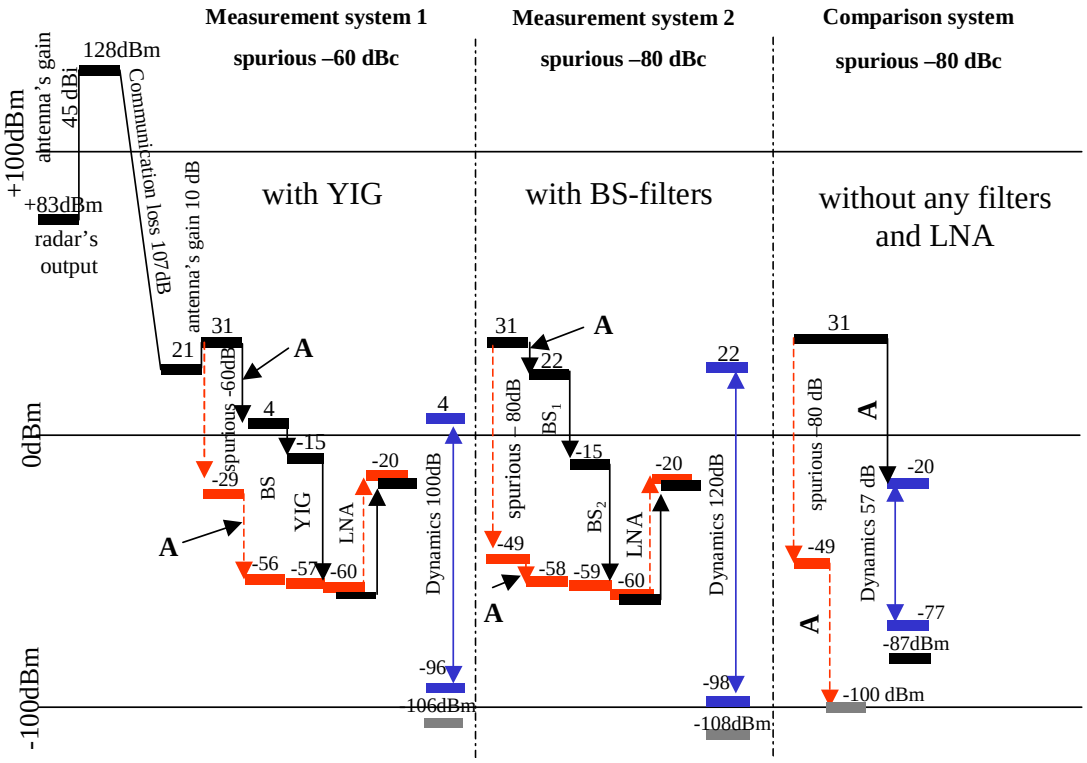

Figure 22. The power budgets and dynamics range of the measurement systems.

Measurement system 2 has been presented in an equal way. The available dynamics in Figure 22 is theoretically 120 dB (measurement distance must be decreased as explained before) while the measurement in this case requires 80 dB.

The dynamics of the reference system is 57 dB. Here the dynamics stays low because no filter is used to tune the power level differences and no amplifier is used to decrease the system noise factor but the input power must be attenuated from +31 dBm to (−20 dBm) with an attenuator. This means a 51 dB loss in dynamics. With the same attenuation value the *SF* power level drops from −49 dBm to −100 dBm which is 13 dB below the SA noise level.

4.4.4 Determination of radar spurious transmissions.

Before it is possible to determine the spurious transmissions power levels relative to *NF* power level from the spectrum picture, the radar *NF* pulse power at the measuring site must be determined. This is most easily done while the radar antenna rotation is halted and accurately pointed towards the measurement antenna both in horizontal and vertical planes. The radar pulse power is measured without BP-filters. Depending on the measurement range and the pulse power the pulse power measurement can be started using an attenuator. An amplifier or attenuator can be added to the system depending on the situation. The radar *NF* center frequency is set to the SA and as B_{meas} is used at least the bandwidth B_{ref} given by $1/\tau$. The correct choice of bandwidth is verified by increasing the SA bandwidth B_{meas} until the measured peak power of the radar no longer increases. The display frequency span (SPAN) is chosen for example as 20 MHz or less but so that the peak power level can easily be determined on the SA display with help of the marker generator (MKR). Mostly (commonly) the determination must be done while the radar antenna is rotating. This causes the needed time due to the antenna rotation to increase before the power level settles to its final value. With these settings one gets a curve as shown in Figure 23. From the transmitted peak power level of the radar the radiating *NF* pulse power can be calculated.

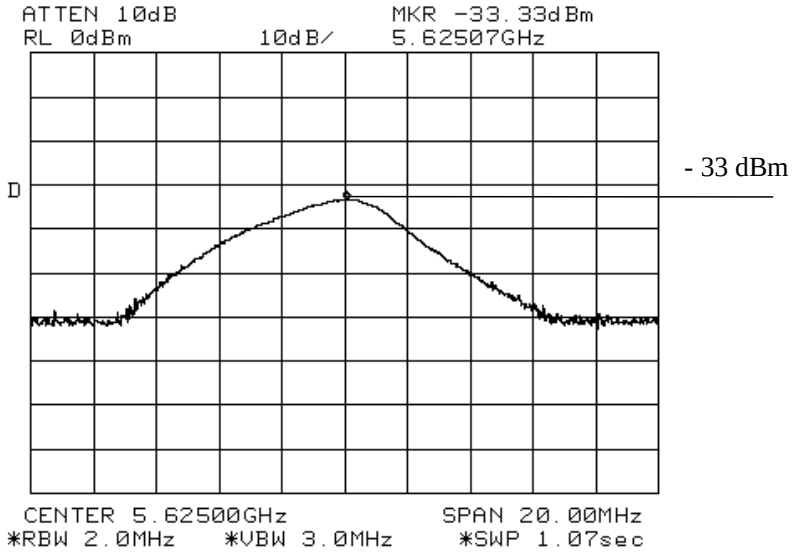

Figure 23. Maximum power on nominal frequency (NF).

In Figure 23 a certain radar with a pulse length of 2 µs is used and its *PRF* is 1 kHz. The radar pulse power (it is assumed here that the transmission path has no obstacles and the transmission path loss is only dependent on measuring distance and used frequency) can be determined from the (−33.33 dBm) (marker level of generator) peak power.

$$\begin{aligned} P_{peak}[\text{dBm}] &= P_d + L_C + L_A \\ -G_{ant} + 32.5 + 20\log f\,[\text{MHz}] + 20\log d\,[\text{km}] &= 126.4[\text{dBm}] \end{aligned} \tag{4.32}$$

where:
- P_{peak} is the radar pulse peak power level,
- P_d is the SA's reading of the measured pulse peak power at the SA input (here (−33.33 dBm)),
- L_C is the measurement cable loss (2.5 dB) and
- L_A is the adjustable attenuation of attenuator (*A*) (here 60 dB).
- G_{ant} is the measurement system antenna gain (here 19.5 dB) and
- the three final terms 32.5 dB, 20log (*f*) and 20log (*d*) define the free space attenuation.

The sum of the first three terms ($P_d + L_C + L_A$) 29.2 dBm is the power level 29.2 dBm at the output connector of the measurement antennas. This value is used as reference value when determining spurious transmission power levels.

The remaining terms of the Equation 4.32 is the free space path loss decreased with the measuring antenna gain:

The calculated power level (P_{peak} = 126.4 dBm) equals a radar pulse EIRP peak power of 4.37 GW.

When using the radar pulse peak power at the antenna connector as a reference it is possible to determine the other possibly occurring component power levels relative to the radar pulse peak level. When determining the final result the effect of the amplifier gains and attenuation of attenuators and filters have to be taken carefully into account. An actual calibration curve must be used on each separate measurement band for which the measurement of *SF* signal powers is going to be carried out.

When a bandwidth of 2 MHz is used in the absolute power value determination in Figure 23 the exact shape of the spectrum is not visible. If one wants to see this spectrum shape, a narrower bandwidth must be used. The spectrum of the radar transmission is in this case shown in Figure 24 (the used measuring bandwidth B_{meas} in this case is 100 kHz when the required B_{ref} is 0.716/2 MHz).

In Figure 24 the radar spectrum shape can be seen more accurately than in Figure 23. The peak power level can be obtained from the detailed spectrum in Figure 24 by adding a correction term $20\cdot\log(B_{ref}/B_{meas})$ = 20·log(0.358 [MHz]/0.1 [MHz]) = 11.1 [dB]. The radar *NF*, the bandwidth B_{meas} of the measuring equipment that equals B_{IF}, the video filter bandwidth B_{VIDEO} (that usually is held same as B_{IF}) and the display frequency span (SPAN) and the used *ST* can be read from Figures 23 and 24. The SA marker (MKR) in Figure 23 has been set to show the pulse peak power.

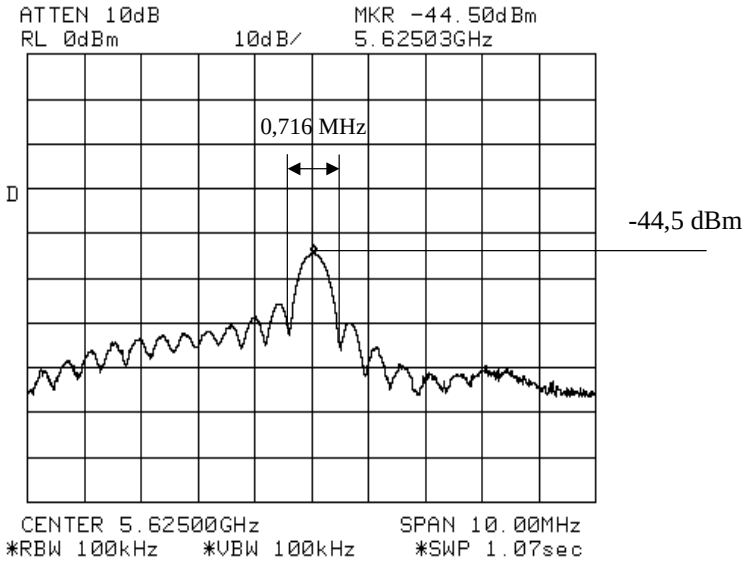

Figure 24. Measured power level on nominal frequency with higher resolution.

From Figure 24 one can determine that the radar pulse length is 2.8 µs. This determination is possible from the distance between the first zero positions. The radar transmission is not symmetrical around its *NF*. This is very typical for example for weather radar spectrum and is not depending on whether a cross field type component, a magnetron or a klystron (like used in this measurement) is used as RF source. A highly accurate determination of B_{ref} from the spectrum shape in Figure 23 is almost impossible or at least is the result inaccurate.

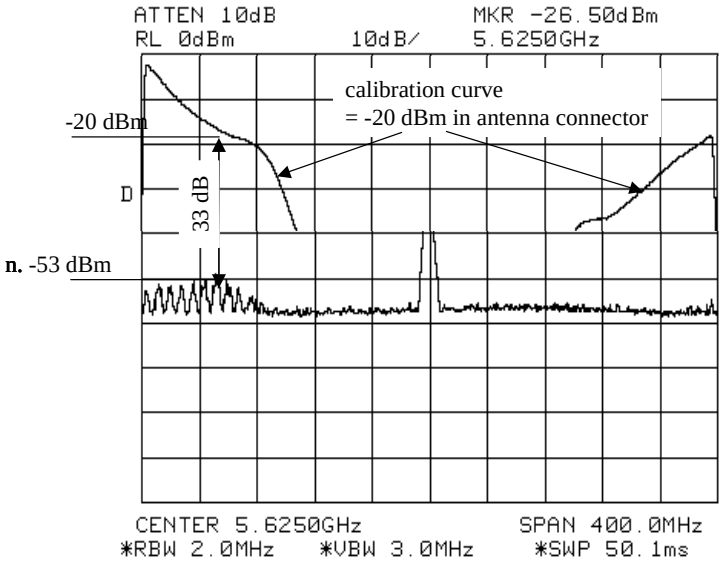

Figure 25. The measurement of the neighboring frequency spectrum with two cascaded BS filters.

Determination of the spurious transmission components within the radar *NF* neighboring frequencies (± 200 MHz) is done when the BS filters, the needed amplifier and attenuator are connected to the circuit. Figure 25 shows spurious transmission components around a *NF* of 5.475 GHz. The calibration curve is inserted into the figure and its level at this display range (400 MHz) is –20 dBm at the antenna connector. The highest spurious power level is determined from the display: –20 dBm – (–33 dB) = –53 dBm. When the 29.2 dBm antenna reference power level at the measurement system antenna connector is used as described before, one can see that the spurious transmission frequency has been attenuated by 29.2 dBm – (–53 dBm) = 82 dB below the *NF*. The spurious transmission attenuation requirement at a distance of at least 150 MHz from the nominal frequency power is 80 dB/1 MHz so this measured radar fulfills the requirement at this frequency.

In the frequency band above the *NF* the spurious transmissions power components are determined similarly. At a frequency 400 MHz above the *NF* the calibration curve is almost straight and its power level is –20 dBm. With the same principle as used in Figure 25 one gets from Figure 26 a spurious transmission attenuation of 29.2 dBm – (–20 – 37) dB = 86.2 dB below the *NF* signal level. The attenuation requirement being 100 dB/1 MHz (meaning measurement on 1 MHz B_{meas}) the radar does not fulfill the requirement on this frequency.

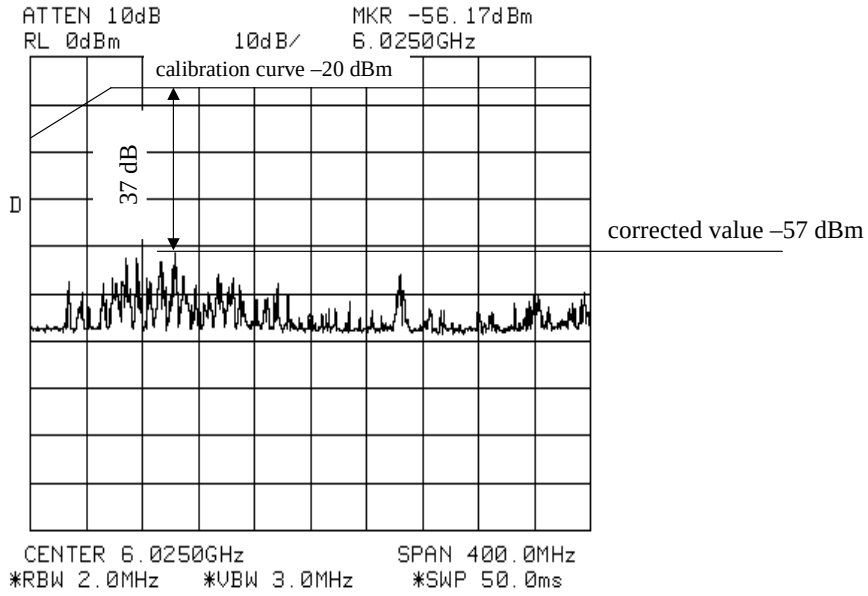

Figure 26. Measurement of spurious transmission above the NF.

In Figure 26 the spurious transmission has been attenuated 86 dB compared to the radar pulse peak power. At the measured frequency range (5.825...6.225 GHz) the highest spurious transmission power is at 5.929 GHz.

The SA display frequency span in this measurement has been selected as 400 MHz to ease the operation. This is due to that the widest possible frequency range to be swept in one sweep, for this SA = 444 MHz when the *ST* = 33 min 20 s, B_{meas} = 2 MHz and the antenna period of revolution = 9 s.

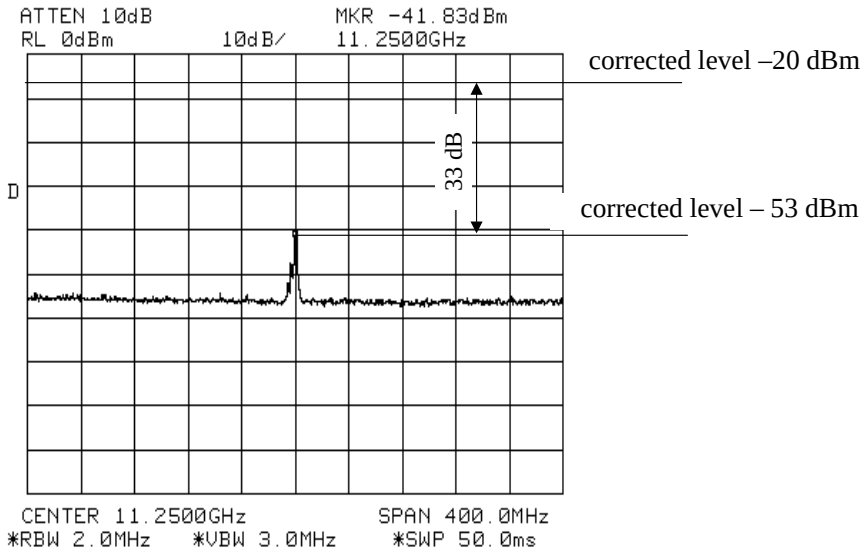

Figure 27. Measurement result of the second harmonic.

In Figure 27 the level of the 2nd harmonic (2·5.625 GHz = 11.250 GHz) is $29.2\ dBm - (-20 - 33)\ dB = 82\ dB$ below the *NF* signal level. This value does not fulfill the attenuation requirement of 100 dB/1 MHz below the radar pulse peak power.

The determination of the 2nd harmonic (11.250 GHz) results in a spurious transmission attenuation of about 80 dBc. The attenuation requirement for frequencies larger than 1 GHz above the *NF* is 100 dB/1 MHz so this radar does not fulfill the requirement at the 2nd harmonic. The gain change of the measurement antenna has been noticed in the calibration curve when measuring the 2nd and 3rd harmonic shown in Figures 27 and 28.

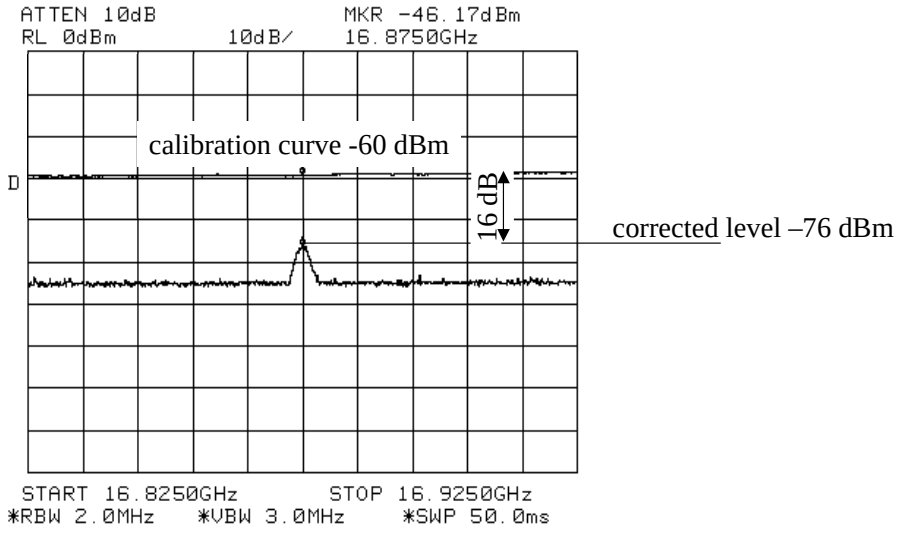

Figure 28. Measurement result of the third harmonic.

In Figure 28 the attenuation of the 3rd harmonic fulfills the attenuation requirement of 100 dB/1 MHz. The relative level is 29.2 dBm – (–60 – 16) dB = 105.2 dBc. The calibration curve on this frequency range is –60 dBm and the frequency of the third harmonic to be determined is 3·5.625 GHz = 16.875 GHz.

4.5 Radiation pattern of the radar antenna

The radar antenna is an important component in radar signal transmission and reception. It has to forward the output power into the desired direction and amplify it by many tens of dB. It must be able to receive weak echo signals and give them reliable directions. The antenna may not have unreasonably big side lobes and its own lobe width must correspond to the required lobe width. Additionally it is required that the antenna has a reliable and steady mechanical construction and that the reflection surfaces of the reflector antenna are accurate. The antenna feed line (that in high power radars normally is a wave guide) must be able to forward high power levels, maintain possible pressurization and to mechanically prevent the rotation of the antenna to be forwarded to the feed line (rotary joint). Additionally the feed line possibly has to function as a low or high pass filter for possible harmonic frequencies above the *NF* component and for other *SF* components. The antenna itself can have different usage requirements. The reflector antenna for example can have the requirement of a parabolic dish, a part of the requirement of a parabolic dish or a part of another mathematical reflector antenna shape. In Nordic environments the antenna must be able to be kept free of snow and ice. Here heating of the reflector and a radome must be used or the whole antenna construction has to be covered with a radome. The radome construction must be made of a dielectrically suitable material. This means that as few as possible metallic or other conductive building materials as possible should be used in the radome. The electrical features of the radome construction must be homogeneous in all possible radiation directions. The attenuation of the radome itself at *NF* must be as low as possible.

4.5.1 Antenna radiation pattern and its measurement.

The measured radiation pattern of a weather radar antenna is shown in Figure 29a. Due to the high pulse power of the radar it is very important to know the direction of the side lobes of the radiation pattern and their attenuation relative to the main lobe. A 40 dB attenuation of spurious levels relative to the pulse power of the main radiation lobe (for example from +128 dBm power) is still +88 dBm. This equals 631 kW maximum radiated pulse power. The highest relative side lobe power level in Figure 29a is 32 dB below the main lobe radiation power level that is +128 dBm at the radar antenna output. In cases, where radiation limitation sectors for radar radiation are determined, due to interference created by radar or possible interference risk, it is important to know the antenna radiation features. High side lobe power levels may interfere with other radio traffic. Their possible limitation requirements may constrain significantly the permitted radar transmit angle.

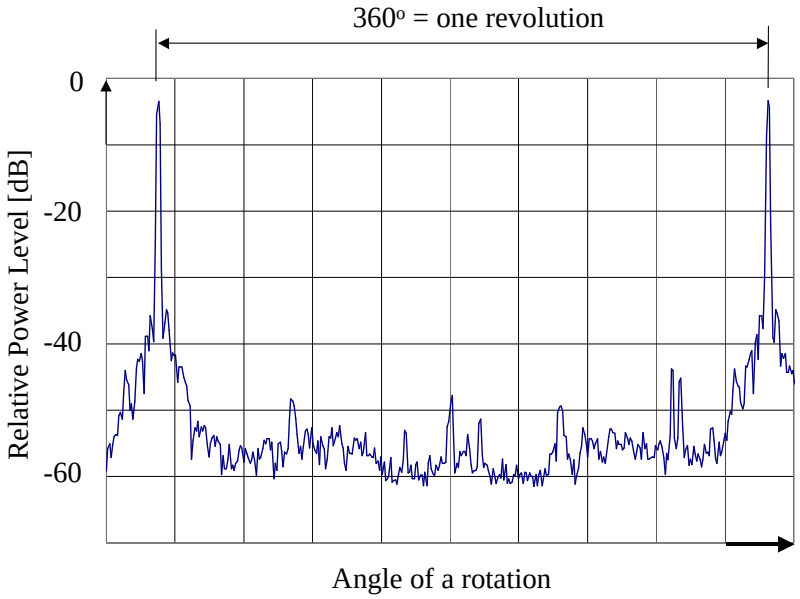

Figure 29a. Measured radar antenna radiation pattern.

When considering Figure 29a it must also be noticed that a high gain side lobe occurring only on one side of the main lobe is not always an antenna feature. Such a side lobe can be generated for example by a reflection to the measurement point from a suitable direction. To verify this, the measuring antenna direction and measurement position must be changeable. If the side lobe direction in the radiation pattern in this case changes, or the side lobe disappears completely, it is a reflection. Side lobes appearing symmetrically around the main radiation lobe are usually antenna features.

Figure 29a contains two main radiation lobes corresponding to a full rotation of the antenna. The presented radiation pattern is measured with the SA operating as an oscilloscope. This function is obtained by setting the SA sweep frequency band to zero (0-SPAN function). Here the SA measures the power level on a fixed frequency as function of time. The sweep setting of the SA must be set to single sweep and the display set to maxhold-mode. Usually the drawing of the curve needs to be repeated for several times. This is needed for the generation of an easily interpretable radiation shape to be displayed on the SA display. By measuring as described above the antenna radiation pattern is not exactly the same as the pattern of the antenna measured under field conditions. The radiation pattern looks just like it should look at the specific measurement site of the possibly interfering radar antenna.

The requirement for a successful measurement is to get measuring dynamics to about 60 dB (see Figure 29a). A filter may not be used in this measurement since it confuses the relative power levels of the measurement and may filter out the main lobe completely. It must be taken care of that the measuring antenna is certainly located inside the horizontal plane of the main lobe for the whole revolution time of the radar antenna. As measuring bandwidth B_{meas} the reference bandwidth of B_{ref} ~ 1 MHz (depends of pulse length) is chosen because maximum power levels are measured.

Usually the antenna direction pattern is presented in a polar diagram as in Figure 29b.

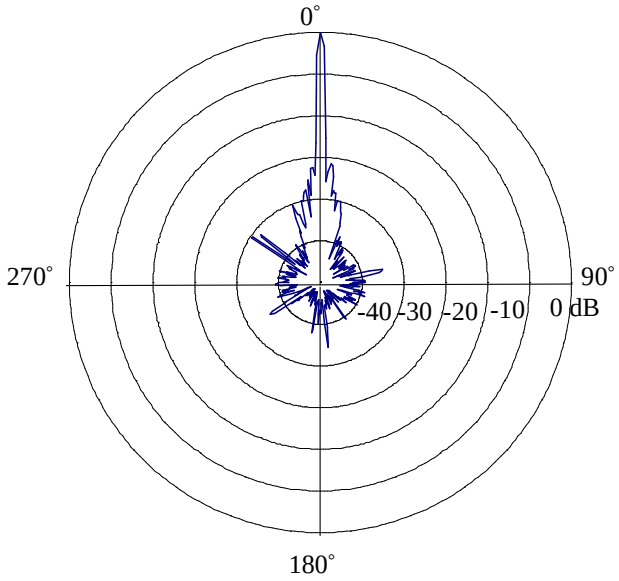

Figure 29b. Polar presentation of a measured antenna pattern of a radar.

4.5.2 Antenna radiation pattern on spurious frequencies.

This measurement can only be done to antennas whose rotation can be controlled. If a slot radiator type antenna (or antenna feed) or dipole group is used as a radar antenna it must be insured that it does not radiate into a direction outside the main lobe direction on another frequency than the *NF*. This is highly possible because (for example with a slot antenna or unbalanced group) the change of feeding frequency affects the speed of the wave inside the waveguide line. The antenna radiation lobe direction change is depending on this change of wave speed. The *SF* due to the change of antenna radiation lobe angle caused by the change of speed can be above or below *NF*. Cross-field type oscillators generate rich *SF* content [2]. Harmonic frequencies do usually cause no trouble under these circumstances because their frequency difference to the *NF* is large.

The antenna itself does not create spurious emissions but can forward them if the radar emission contains them. The spurious emission measurement is conducted with the radar antenna rotation stopped (not always possible). The radar antenna is orientated into different directions in the horizontal plane and a sweeping measurement over the frequency band to be measured is performed. The measurement can be started with the radar antenna pointed towards the measuring antenna and advancing in either positive or negative direction for example measuring at every two degrees up to ±15 degrees (usually done). The maximum angle to be measured depends on how much the *SF* differs from the *NF* signal frequency and how efficiently (degrees/MHz) the lobe turns. This is seen in Figure 8 showing the complete spectrum. The similar measurement is also done symmetrically starting from zero angle into the opposite direction. The first measurement result at the radar antenna zero angle shows the radar maximum power as its P_{NF}.

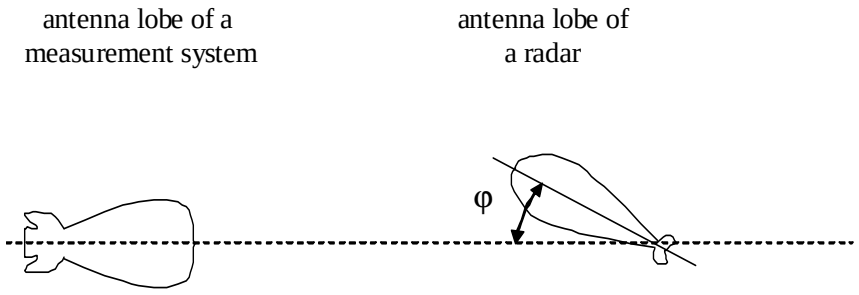

Figure 30. Deviation angle φ of the main radiation lobe of a radar antenna compared to the main radiation lobe of the measurement antenna in the horizontal plane

When changing the radar antenna direction from the zero angle, the measurement shows those spurious emission components that the radar antenna transmits in other directions away from the zero angle and which frequency differs from the *NF*.

The spurious emission components of the radar spectrum can be seen according to the measurement dynamics requirement in measurement setups 1 and 2 (Sections 4.4.1 and 4.4.2). Their power levels can be determined according to the measurements described in Section 4.4.4 but the possible variations from zero direction of the spurious emission components can be detected only with this measurement. It must be noted that the radar antenna radiation pattern measurement is not the same matter as the determining of the direction of spurious emission components. The radar antenna pattern shows the relative powers and the directions into which the antenna radiates the *NF* power. The spurious emission component pattern on the other hand shows the relative powers and directions into which the components differing from the radar *NF* are radiated by the antenna.

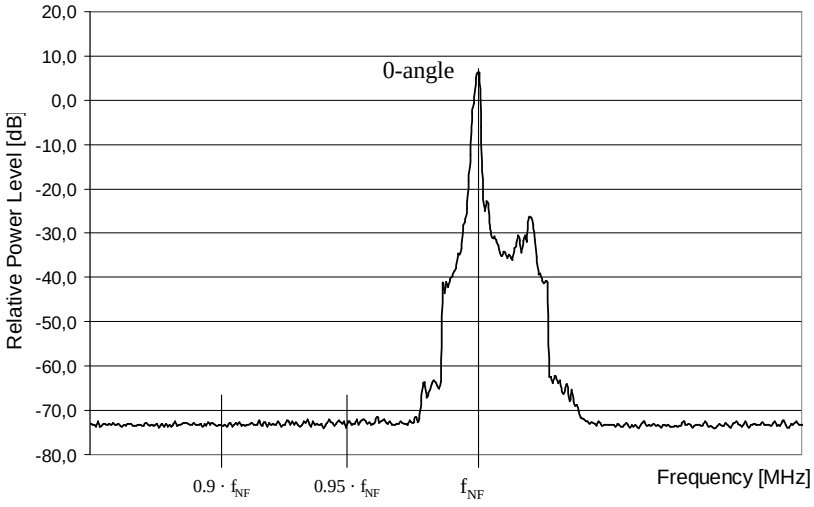

Figure 31. Spurious emission on an antenna 0-angle as function of frequency.

Figure 31 presents the power spectrum measured at some radar's φ-angle being zero. The transmission consists only of the original signal of the radar. The relative peak power level is +5 dB. The possible spurious emission components, that are more than 80 dB below

the nominal frequency (f_{NF}) component, are not visible in this figure because they are below the noise level.

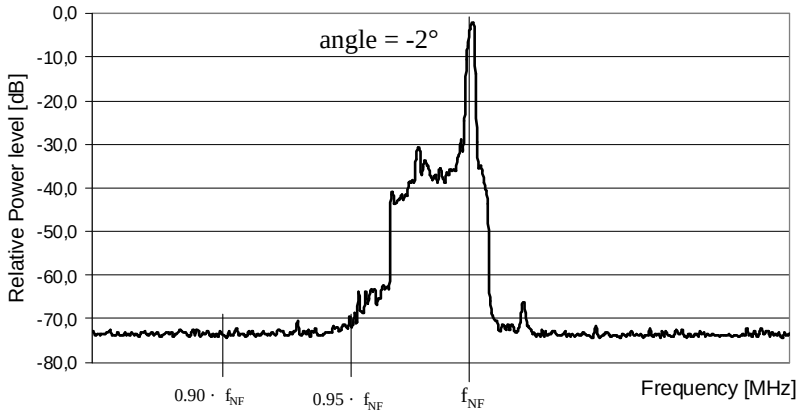

Figure 32. Spurious emission on antenna –2 degrees angle as function of frequency.

Figure 32 shows the spurious emission spectrum when the angle φ is −2°. In the figure it can be noted that with this angle the radar power spectrum contains an *NF* and a leading *SF* component at $0.975 \cdot f_{NF}$, the power levels being 7 dB and 36 dB below the *NF* level for φ = 0 degrees

In Figures 33...37 the position and power level of spurious frequency component emissions are shown and can be compared to the *NF* power with the angle φ = 0 degrees at different radiation angles φ.

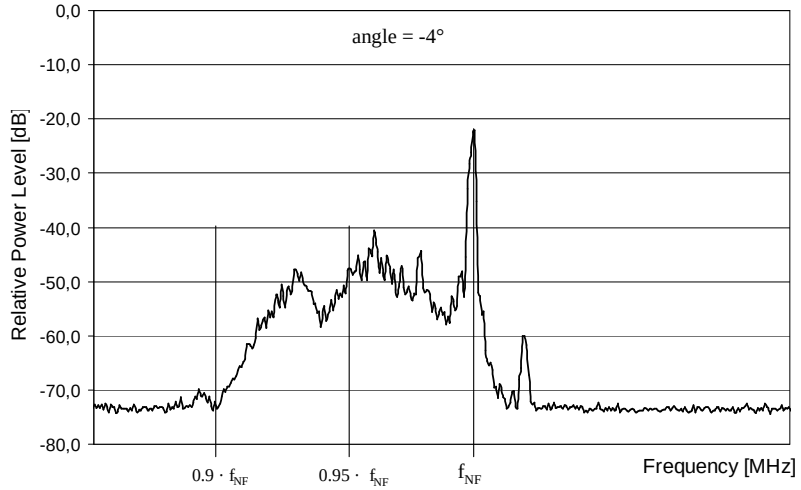

Figure 33. Spurious emission on antenna –4 degrees angle as function of frequency.

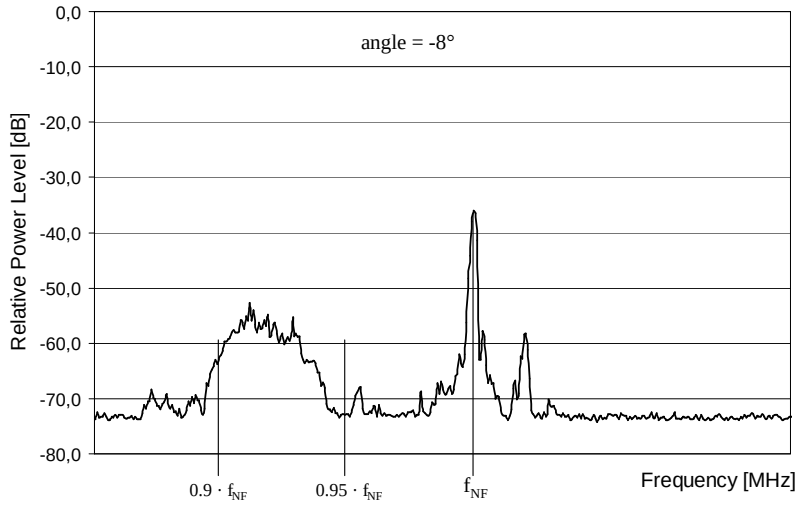

Figure 34. Spurious emission on antenna –8 degree angle as function of frequency.

In Figure 34 most of the *SF* components are around $0.92 \cdot f_{NF}$ at a maximum peak level of –59 dBc. If the radar transmit level is 128 dBm, this corresponds to a *SF* peak power of 7.9 kW.

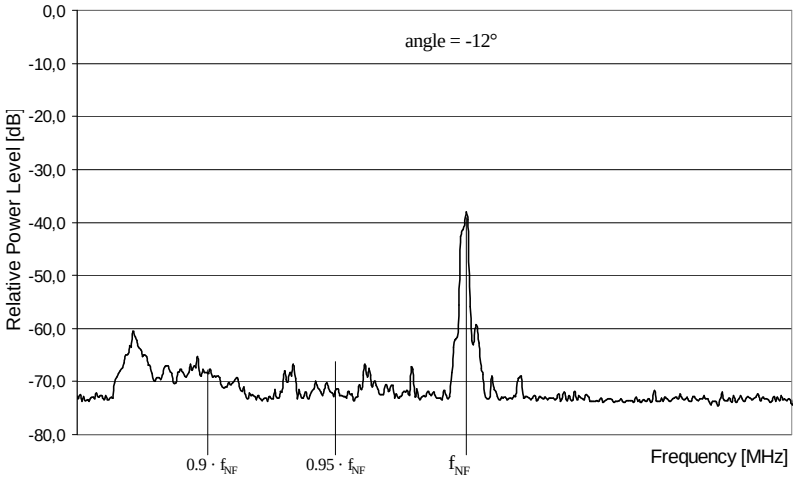

Figure 35. Spurious emission on antenna –12 degree angle as function of frequency.

Figure 35 shows a maximum transmitted *SF* power of 1.58 kW at about $0.87 \cdot f_{NF}$.

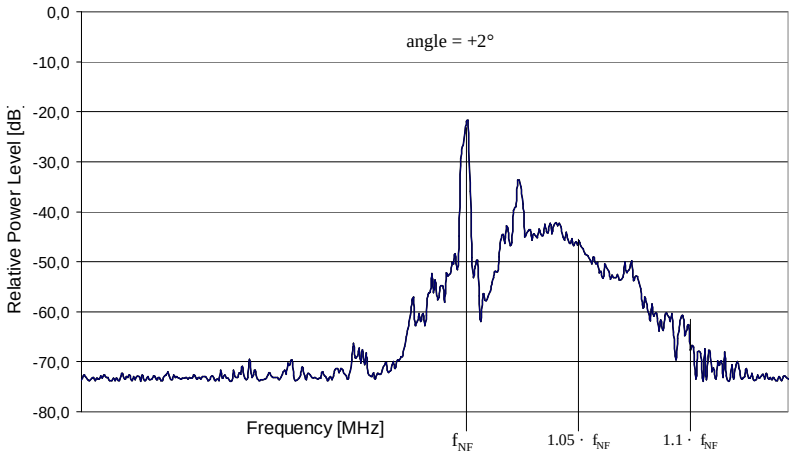

Figure 36. The measured power spectrum when φ = +2 degrees.

Figure 36 shows a maximum transmitted *SF* power of 630 kW at about $-1.03 \cdot f_{NF}$.

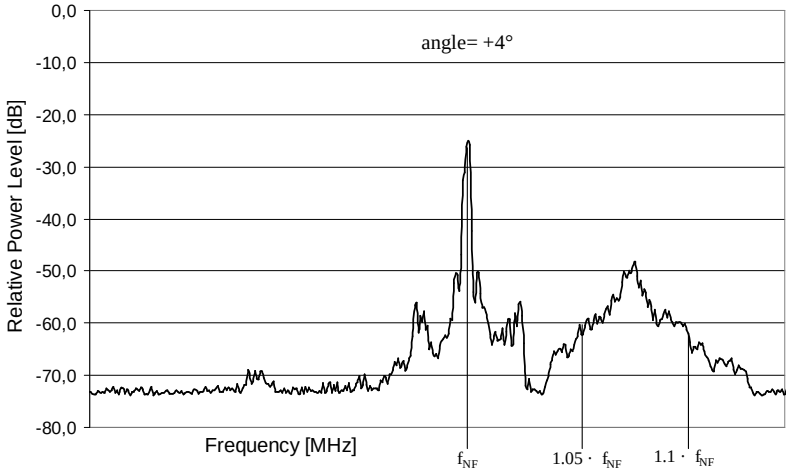

Figure 37. The measured power spectrum when φ = +4 degrees.

Figure 37 shows that the spurious emission components above *NF* turn toward the positive antenna angle directions at the antenna. In the +4° direction of the radar antenna the antenna radiates a $(1.075 \cdot f_{NF})$ frequency component 54 dB below the *NF* power level. The spurious emission components below the *NF* turn towards the negative antenna angle direction at the antenna.

There seems to be a clear relationship between the slot antenna radiation direction in the horizontal plane and the frequency of the largest SF spectrum component. This is investigated using the variables defined in Fig. 38.

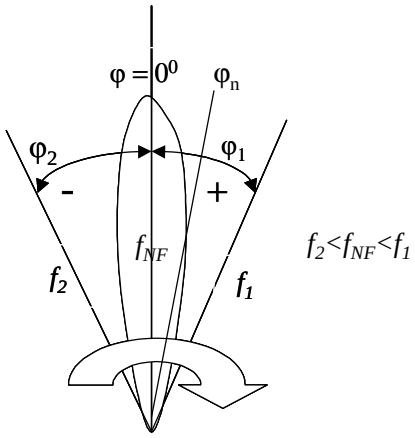

Figure 38. Definition of the frequency of the highest spurious spectrum component in different antenna angles relative to the boresight direction in the horizontal plane.

In Figure 38 φ_n is the radiation angle shift ($\varphi_n = 0$ is the direction of the main lobe maximum at the frequency f_{NF}). The positive direction (+) and the negative direction (–) are as indicated in the figure; f_1 and f_2 are the frequencies of the maximum *SF* components in the directions φ_1 and φ_2.

Figures 31…37 show the general spectral behavior of the maximum peak power *SF* component when a slot-antenna is used. The frequency of this *SF* component will be the lower the smaller the angle φ is. The measured behavior is presented in Figure 39a, which shows an approximately linear dependence. The relative peak power level of the maximum level *SF* component relative to the radar peak power is shown in Figure 39b. The variation of radiation angle higher than the here measured diverts linearly (in Figure 39).

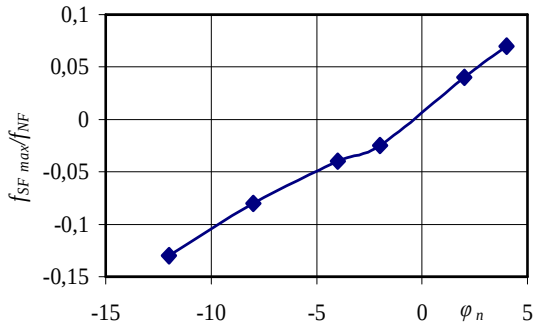

Figure 39a. Measured normalized frequency of the maximum SF component as function of radar antenna radiation angle.

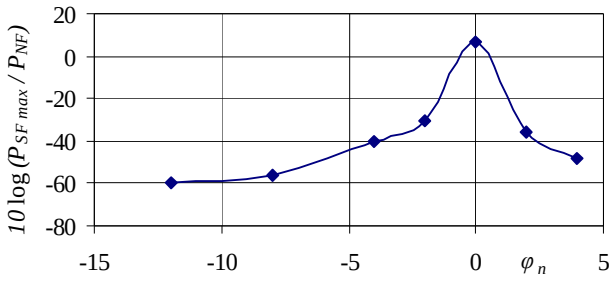

Figure 39b. Peak power level of the largest SF component in different antenna directions.

Figure 39 shows the measured frequency of the maximum SF component and its relative peak power level values as function of radar slot antenna radiation angle. For the *NF* the radiation angle is 0°. For example a −10° radiation angle can be found for spurious emission component whose frequency is $-0.1 \cdot f_{NF}$.

Figure 40 demonstrates that the radar operation sector determined with the *NF* antenna radiation pattern is too optimistic if the radiation pattern on *SF* frequencies is different. It is assumed in a) case that a limitation sector based on the *NF* antenna pattern is between 0°...15°. However, based on the slot antenna measurements shown in Figures 31…37 the antenna radiation pattern change on spurious frequencies requires a ±12° wider limitation sector, thus extending it to −12°...+27°.

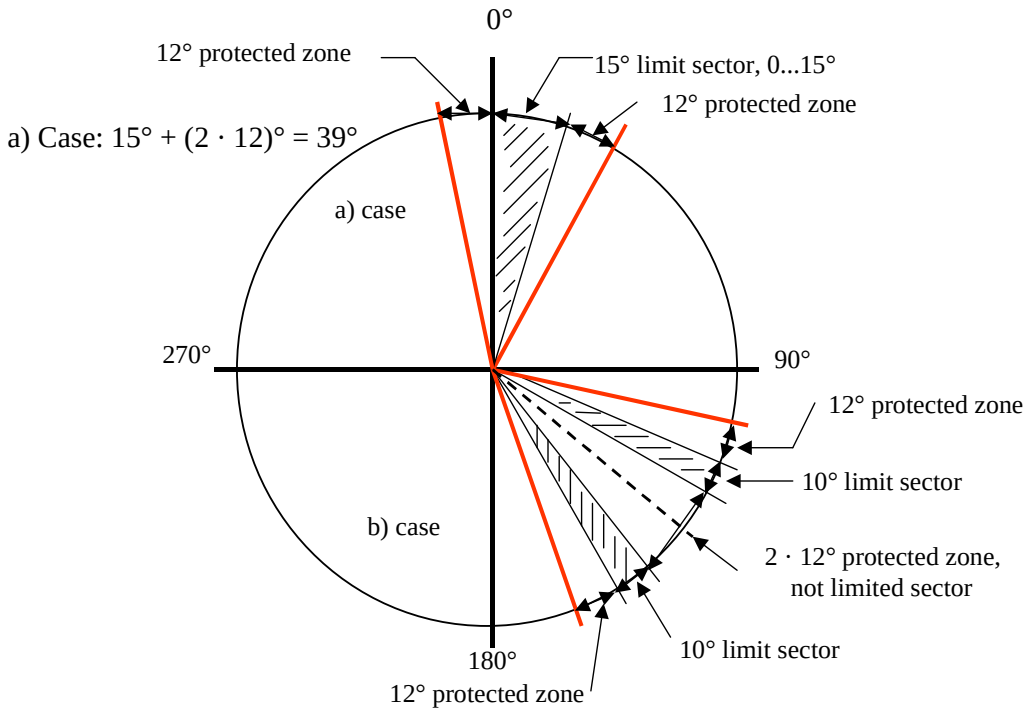

b) Case: (2 · 12)° + (2 · 10)° + (2 · 12)° = 68°

Figure 40. Impact of frequency dependent radar antenna pattern on the permitted operational sectors of the radar.

If the radar use has several limitation sectors (case b) and there is left a non-limited sector in-between them, that is less than 2 times the widest spurious emission radiation angle, (symmetrical diversion of the radiation angle) this sector can not at all be used.

In this chapter it has been shown with help of examples how important it is to prohibit the appearance of all kinds of interference signals due to spurious emissions. The appearance of these is most easily prohibited with suitable low-pass and high-pass filters in the radar antenna feed line. With the present knowledge from filter manufacturers it is known that the manufacturing and the installation of high frequency filters into an already operational system is both extremely laborious and expensive but for achieving the aimed final result extremely important. Therefore the filters should be manufactured and put into place already while manufacturing the radar.

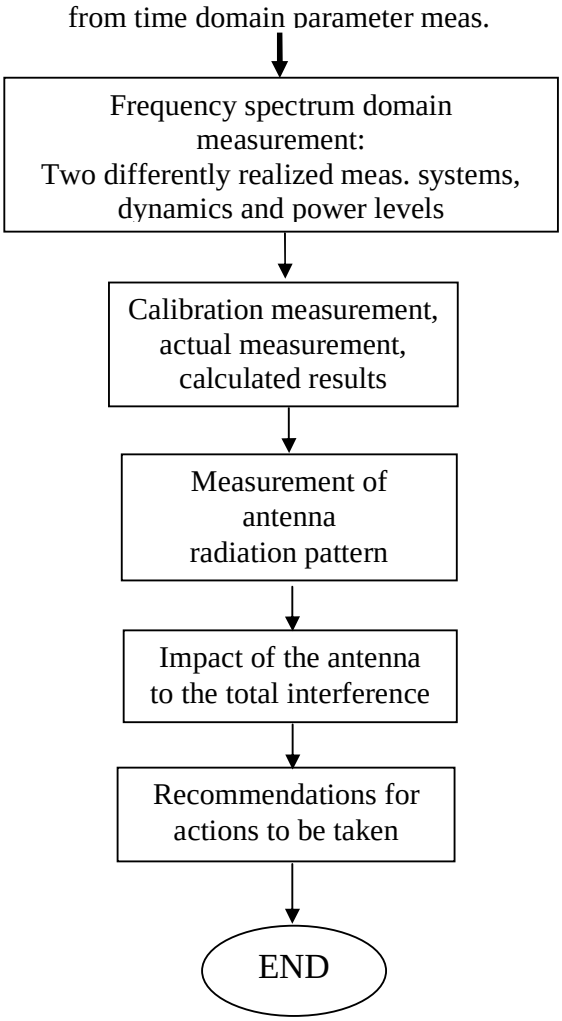

Figure 41. Flowchart 3.

Figure 41 shows how the frequency domain measurement advances and ends in recommendations for actions to be taken. In the radar spectrum measurement one presumes that all necessary parameters produced by the time domain parameter investigation are valid.

It is shown mathematically (Figures 23...28 and their relating calculations) how by calibration the final resulting spectrum of the radar under measurement can be calculated.

Before issuing recommendations the impact of antennas on possible interferences must be estimated.

4.5.3 Formation of the final spectrum shape.

In the following example it is shown how the final spectrum shape (spurious emissions) are obtained by calibration, measurement and combining these two. Figure 44 shows the final spectrum shape.

Example 6. In this example it is shown how the final power response as a function of frequency of the radar signal is obtained. The curves in this presentation are named as follows: $A(f)$ is the calibration curve measured with a BS filter, $B(f)$ is the radar signal spectrum measured with a BS filter and $C(f)$ is the calculated real radar signal spectrum.

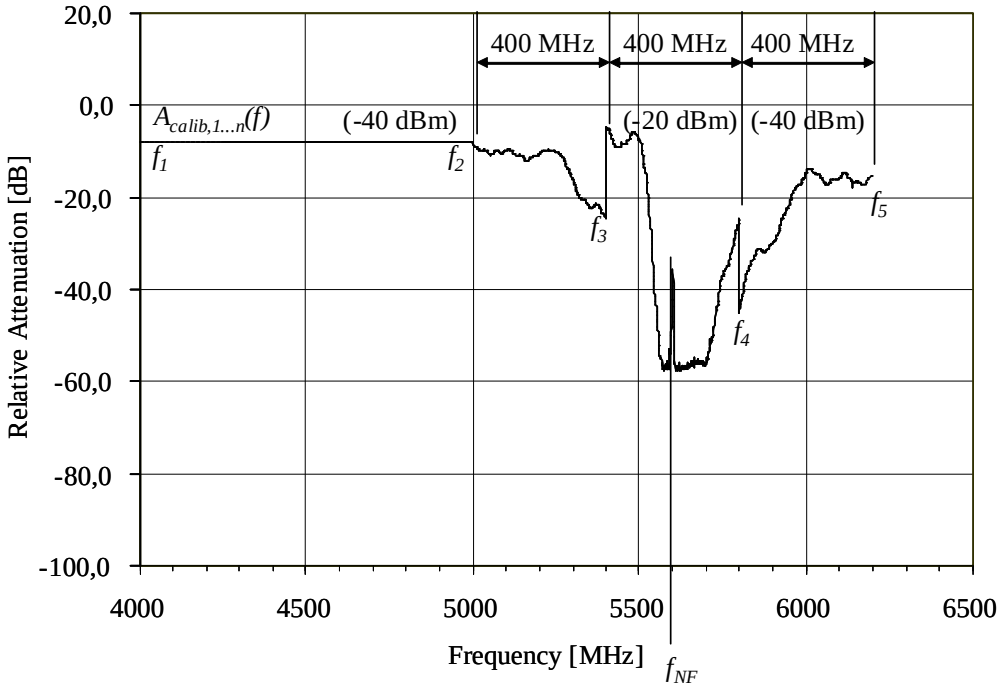

Figure 42. Calibration curve A (f) of the measurement system with BS filter.

The calibration curve of the weather radar in Figure 42 is determined for the complete measurement equipment. According to measurement system 2 (Section 4.3.2) the equipment are an attenuator, BS-filters and low noise amplifier, measurement cables and as measurement equipment the SA. The calibration curve must be created with the same circuit and parameter values as used in the original measurement. This must be done for each frequency band separately using a measurement antenna.

In Figure 42 the curve $A(f)$ is obtained by feeding a sweep signal with suitable power level to the antenna connection point from a signal generator (or tracking generator). Suitable values in this example can be −40 dBm in frequency intervals $f_1...f_3$ and $f_4...f_5$ and −20 dBm in frequency interval $f_3...f_4$. The power level at the SA input may not increase so much that it causes overload effects. After this the measurement is conducted by sweeping a 400 MHz frequency slot in a single sweep with the SA. Because the BS filter attenuation is

more than 40 dB the signal level must be increased by 20 dB for the measurement slot f_3...f_4 to prevent that the signal spectrum in these intervals goes below the SA noise level. This is seen as a 20 dB discontinuity in the curve at the frequency slot f_3...f_4. When a –40 dBm or a –20 dBm signal level is fed to the circuit the SA display power level envelope value corresponds to these values.

The real power level envelope, $C(f)$, can easily be derived from the measured curves ($A(f)$ and $B(f)$) when taking into account the different calibration curves at the various frequency intervals and the measurement system antenna gain as a function of frequency. The combining of power level envelopes is done as follows:

$$C_{calc,n}(f) = -40 - \left(A_{calib,n}(f) - B_{meas,n}(f)\right)\,[\mathrm{dB}], \textit{between } f_1 \textit{ and } f_3 \textit{ as well as } f_4 \textit{ and } f_5 \quad (4.33a)$$

and

$$C_{calc,1}(f) = -20 - \left(A_{calib,1}(f) - B_{meas,1}(f)\right)\,[\mathrm{dB}], \textit{between } f_3 \textit{ and } f_4 \quad (4.33b)$$

where:
- $A_{calib,\ 1...n}$ (f) is the relative power level as function of frequency in the different frequency intervals (Figure 42)
- $B_{meas,\ 1...n}$ (f) is the measured received radar relative power level as function of frequency combined to one single curve (Figure 43) and
- $C_{calc,\ 1...n}$ (f) is the calculated/calibrated received radar relative power level as function of frequency combined to one single curve (Figure 44).

The measured relative power level spectrum $B_{meas,\ 1...n}$ (f) of the radar is shown in Figure 43. The following measurement parameters have been used:

- measurement bandwidth Bmeas is 2 MHz (radar pulse length τ is 1 µs),
- radar PRF is 1 kHz,
- sweep time (ST) is 50...200 ms,
- measurement conducted in 400 MHz frequency slots and
- radar antenna halted and directed toward the measurement antenna.

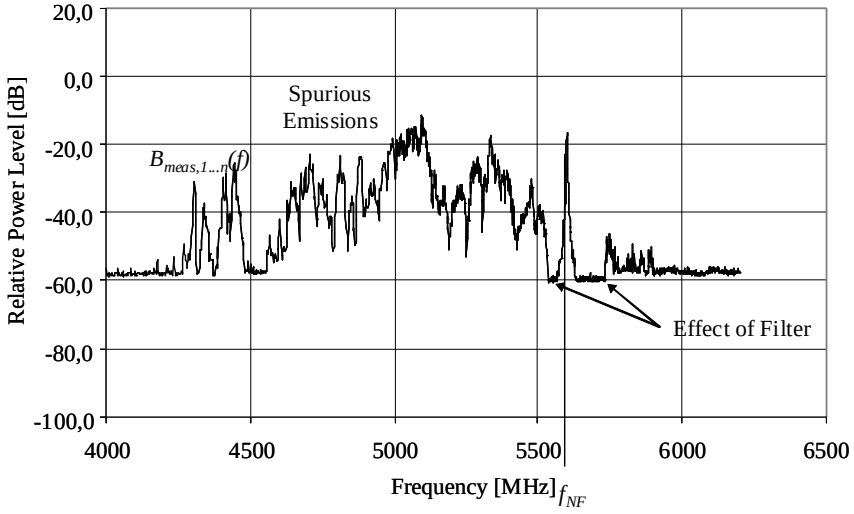

Figure 43. Measured spectrum (curve $B_{meas,\ 1...n}$ (f))

The relative power level of the radar shown in Figure 43 (curve $B_{meas}(f)$) has been measured with the same settings as those used during calibration. In the figure it can be seen that when the *NF* is attenuated with a BS filter, the *NF* relative power level is almost equal to the highest *SF* relative power level. This gives an opportunity to maximize the measurement dynamics when the SA input has the same maximum allowed relative power level for both frequency components (*NF* and *SF*). The dynamic range of the SA display is defined as the largest level difference of two spectrum components that are simultaneously displayed with a given accuracy. The difference between the power levels is obtained when summing the total attenuation of the *NF* signal and the total gain of the *SF* signal on the signal path when they both are on the same power level on the SA display.

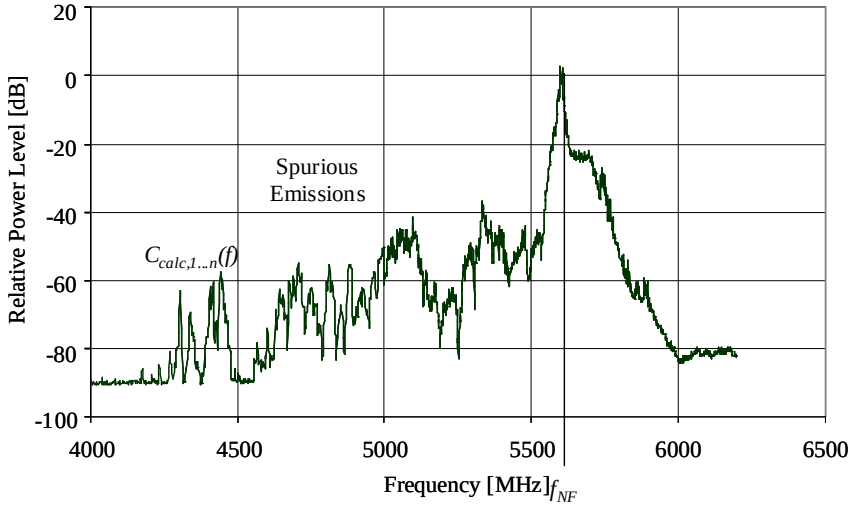

Figure 44. Calculated/Calibrated relative radiating power level spectrum of the radar (curve $C_{calc}(f)$).

From the curve in Figure 44 it can be estimated that the *SF* signal power level is about 90 dB below the *NF* signal power level at the frequency 4.2 GHz (noise level), but only 60 dB level at 4.3 GHz. Spurious signals of this radar do not fulfill the ITU spurious signal attenuation requirement (in this measurement the attenuation is only 59 dB at 1 GHz from *NF*). The requirement is > 100 dB at 1 GHz from the *NF* (this is in the frequency band used by the TDRRS). The flat visible between frequencies 5650...5700 MHz in Figure 63 is not real. It is created due to discontinuity when connecting parts of the curve together.

Because the dynamic range according to Figure 44 only is 90 dB as the signal difference between *SF* and *NF* it can not be determined if the radar spurious signal interferes harmfully a TDRRS on frequencies below 4.2 GHz or not. The achieved dynamics does not correspond with the named max. dynamics. In this case a smaller measurement dynamics is satisfactory for verifying spuriouses. If a higher dynamics is targeted the *NF*-signal level must be lowered and the *SF*-signal level risen. (i.e. BS-filter attenuation and LNA amplification must be risen, the measurement antenna must be changed into a more efficient one or the measurement distance to the target being measured must be shortened.)

4.6 Summary of Chapter 4

In this chapter the most essential measuring methods for determining *SF* radiation peak levels and the results obtained by them are presented. First the time domain parameter study has been presented. This produces the parameters needed for radar spectrum domain measurement. In the time domain parameter study at first a part of the parameters can be defined by the measurements and thereafter the rest can be calculated. In the parameter definitions the various bandwidths are important, so their definitions are given.

The essential part in the time domain parameter study is the availability of radar pulses and their treatment in different situations. The sensitivity of measurement results to the measurement parameters in the time domain leads to the use of two different measurement approaches (synchronized and unsynchronized sweep). Both cases are presented with help of an example. The advance of the time domain parameter study is also presented in a flow chart.

The frequency domain measurement uses the parameters received from the time domain parameter study. In the actual frequency domain measurement all the needed parameters are expected to be appropriate and valid. Based on the above two slightly different measuring methods are presented. With both methods it is possible to determine spurious emissions of the radar within the required measurement dynamics. The measurement methods have been described mathematically using practical examples. The power budgets of both measurement methods and a reference measurement system have been presented.

The impact of the radar antenna on the transfer of spurious signals is presented. The antenna patterns of both the *NF* signal and the *SF* signals have also been presented with help of an example. Measures for reducing the impact of spurious signals have been proposed. These include measures to be taken into account in their effects and to prohibit them. The advance of the frequency domain measurement and the impact of the radar antenna are also presented in a flow chart.

5 A MODIFIED MEASURING SYSTEM FOR DETERMINATION OF RADAR INTERFERENCE LEVEL IN TDRRS

In Chapter 4 a new implementation of a measurement method for investigation of radar spurious radiation was presented and the impact of the radar antenna radiation pattern on this measurement system was investigated. In Chapters 5 and 6 the modification of the new measurement system for the investigation of radar impact to radio communication systems under real field conditions.

In terrestrial radio communication systems (e.g. TDRRS, RLAN, WIMAX, UWB) there may, in addition to propagation phenomena, occur irregular disturbances, which cause occasional or continuous transmission outages. Often the cause of disturbance turns out to be a radar, either its NF-component or an SF-component. This chapter presents the frequency bands allocated to TDRRSs, the performance requirements put on digital errors in TDRRSs, signal presentations and error mechanisms and other signal characteristics as far as they are needed in the investigation of disturbance impact on the radio link. By radio link budget calculations on a measurement system improved step by step it is shown how an appropriate dynamic range is achieved for measurement of radar signal components impacting TDRRS transmission performance.

In reality, this measurement system should be used to verify the protection distance between a radar and a radio communication system, e.g. a TDRRS. This protection distance is obtained by theoretical calculations as presented in Chapter 6. To the author’s knowledge this approach to the determination of the protection distance and the verification of it by measuring the radar radiation on the TDRRS channel has not bee published earlier.

5.1 Evolution of terrestrial radio relay systems

According to literature [32] a Terrestrial Radio Relay System (TRRS) is defined to be a fixed or partly fixed two-way radio connection. TRRS's are used for forwarding telephone and data traffic and radio and TV signals between two terminal stations using repeater stations, if necessary.

Finland's first radio link span was taken into use in Oulu in 1954. The former Oulun Puhelin Oy operated a radio link span (General Electric's link equipment) offering 5 speech channels and was used to replace the wired land lines between Oulu and Utajärvi which were heavily loaded by traffic to a hydro-electric power station under construction. The first radio link span of the only national telecom operator at the time (Posti- ja lennätinlaitos) was taken into use between Hyvinkää and Mäntsälä in 1959.

What was the evolution stage of telecommunication techniques when the first radio relay systems were taken into use in Finland? When comparing the introduction time of radio relay system with to the development of other communication techniques one can find, that in 1965 in Finland there were 169 telephone connections per 1000 inhabitants, 380 radio receivers per 1000 inhabitants and 142 TV receivers per 1000 inhabitants. The first TV broadcasts in Finland started in 1955. Mobile telephones or mobile telephone networks in competition with each other not to speak about multiple mobile network operators could not be believed of at that time.

The development of radio relay systems begun at the electronics department of Suomen Kaapelitehdas in Salmisaari at the beginning of the 1960's [33]. Their assortment included single channel radio relays and 150/360 MHz frequency band base stations for vehicle mounted stations. Type SV1100 was used for forwarding speech and SV1400 for

forwarding data. Their first multi-channel radio relay system for the UHF band (type FM 24-400) was introduced in 1966 and for the SHF band (type FM 120-7000) in 1968. The systems were of course analogue. The FM 24-400 (24 channel 360 MHz frequency band relay system) was partly implemented with vacuum tubes since UHF band power transistors were not yet available to affordable prices.

Radio relay systems between Finland and Sweden were established at the beginning of the 1960's starting in Helsinki and continuing via Nuuksio, Pusula, Salo and Turku to Stockholm. In the beginning of the 1970's a connection between Vaasa and Umeå (Sweden) was established.

In 1974 the first generation of digital radio relay systems, PCM 30-400 (pulse code modulation) using binary FSK modulation was developed as a modification of the FM 24-400. The manufacturer had already formed to be Nokia Oy. In the years 1965...1976 a total of 3729 radio link equipment (TX / RX pairs) were produced in Finland by Nokia Oy. After the second digital radio relay generation TU 5800 in 1977 there has been a huge development of TRRSs. One nowadays bumps into radio relay systems almost everywhere: where a mobile or portable phone works one can probably find a radio relay terminal at the base station site. Nokia has not been the only supplier of radio relay systems in Finland. Its competitors have been and partly still are international manufacturers like Ericsson, Siemens, Nera, NEC, Thompson, Waves, Avantek, Telettra, Autophon etc.

In 1972 the first radio relay system between Finland and the former Soviet Union was built between the Pääjärvi forest collective combine and Kuusamo after Finns had started building of the Pääjärvi collective combine. The radio relay system was realized with three parallel one channel radio relay systems. Two channels were used for speech and one for a telex connection. The radio relay systems equipment comprised radio relays of Nokia of the types SV1100 and SV1400 operating in the 150 MHz band. The Finnish antenna manufacturer Aerial Oy, just starting its business, manufactured the antennas needed in the radio relay systems including their special features (a corner reflector antenna was used for the first time in Finland). The Pääjärvi link span used in the beginning two hops from Kuusamo to Ruka and continuing to Pääjärvi. After raising the power of the radio relay transmitter with an amplifier especially designed for this link, only one 102 km hop was needed between Kuusamo and Pääjärvi.

The triumphal march of radio relay systems was not always a triumph. When advancing the Finnish long distance trunk network the coaxial cable was a serious competitor to radio relay systems and it displaced at least a part of radio relay spans. Later when fiber optics took over the connections with its superior transfer capacity the faith of radio relay systems seemed to be sealed.

It, however, proved to be otherwise. For several years Nokia supplied small quantities of radio link terminals (TX/RX). In January 2004 the Nokia FlexiHopper product family, that was released in 1999 reached the production quantity of 100 000 units. The links are operating in the 12, 13, 18, 23 and 38 GHz frequency bands and they are used to connect mobile telephone networks to the wired line network. The typical operating range is 3...6 km and the capacity is four times 2 Mbit/s that offers four times 30 speech channels for use. Additionally the RF part of the link is one entity that includes an integrated planar antenna. This makes it more favorable and faster to insert into an existing infrastructure when the alternative would be installing fiber optic cables and even excavate streets to install them. The Nokia MetroHopper product family (also launched in 1999) with a smaller operating radius operates in the 58 GHz band. It also offers four times 2 Mbit/s capacity with an operational range of 0.3...0.6 km and four times 30 speech channels. Radio relay systems based on analogue technique are no longer produced in Finland.

5.2 TRRSs and their users and their number in Finland.

In the radio frequency regulation 4J/2007M published by the Finnish Communications Regulatory Authority [25] there are several frequency bands allocated for TRRS's. A brief overview of frequency bands, purpose of use, users and number of terminals (spans) for TRRS's operating above 1 GHz is presented below:

PMP 1400 (point to multipoint), frequency band 1375...1430 MHz
Used in northern and eastern Finland to substitute wire lines between junction centers and local exchanges. Telia-Sonera is operating about 60 spans. Networks are no longer expanded, only their maintenance is carried out.

DRS 1800 (Digital Radio System). 1705...1870 MHz.
Used in northern and eastern Finland to replace fixed wire lines between junction centers and local exchanges. A couple of tens of spans are operated by telecom operators, VR (the state owned rail road company) and the defense forces. These will give way to GSM [25]. The frequency range above 3 GHz is already at risk.

DRS 2000. 1910...2100 MHz.
The telephone trunk network in northern and eastern Finland. Tens of spans. These will give way to IMT 2000 (3G) [25].

DRS 2100. 2030...2280 MHz and DRS 2600. 2500...2690 MHz.
Telephone trunk network connections, over 100 spans operated by telecom operators, VR and the defense forces, etc. These will give way to IMT 2000 [25].

Fixed access network, 3410...3600 MHz.
In big cities and in rural areas to replace subscriber wire lines. Thousands of connections operated by telecom operators.

Broadcast radio relay systems, 3600...4200 MHz.
Both analogue and digital program distribution links (for example for TV program transmission). Several hundred spans all over the country operated by Digita Oy.

DRS 6200, 5900...6450 MHz.
Reserved for high capacity radio relay systems. The band is not in use at present.

DRS 6800, 6450...7100 MHz.
High capacity radio relay systems. A few spans operated by Telia-Sonera.

DRS 7300, 7100...7450 MHz and DRS 7600, 7450...7750 MHz.
High capacity radio relay systems. Several tens of spans operated by telecom operators and the defense forces.

FMTV 8000, 7750...8200 MHz.
Fixed and mobile broadcast radio relay systems (for example for transferring TV programs). Tens of spans all over the country operated by Digita Oy and YLE (the Finnish Broadcasting Company).

8200...8500 MHz.
Band reserved for radio relay system operation. Not in use at present.

Fixed access network, 10.5 GHz.
In use only in Helsinki.

Medium capacity (34 Mbit/s) radio relay systems, 13 GHz
Hundreds of trunk network spans operated by telecom operators and the defense forces.

15.0; 18.7 and 23 GHz.
Use as above. Thousands of spans.

Fixed access network, 26 GHz.
In use only in Helsinki.

Mobile telephone base station connections, 38 GHz and 58 GHz.
Used in southern Finland.

In future (within the next 15...20 years) radio link frequencies below 6 GHz are endangered from the frequency needs of the mobile telephone network service (4G) and other mobile services. Also in the frequency range below 10 GHz preparations for the future ultra wide band (UWB) frequency needs are made. These needs are already discussed in the ITU and in the CEPT.

5.3 Topological and economical location needs of TRRS's

Differing from conventional telephone lines, where physical wire lines were built between two locations with pole line, open wire, air cable or coaxial cable or buried cable following public roads, radio relay systems (link span) has other location requirements. The antennas of the link span must at both ends be located so high that their first Fresnel zone stays free during standard propagation conditions. To realize this link masts at both ends are usually required. To keep the mast heights reasonable natural benefits provided by the terrain are used. Masts can be built at high terrain levels, on ridges, on top of water towers, on eskers and on mountains to reduce mast heights. This location of the site usually creates the need of a feeder connection to the exchange, which usually is located in a population centre. The need of connection may also branch into several places where for example YLE distribution link towers have been built at the most important branching points. Link spans built into the archipelago are, on the contrary, tied closely to the topography of the region of operation.

Figures 45 and 47 show the locations of individual radio links of the radio relay systems of different operators in Finland. Figure 49 shows the locations and coverage areas of weather radars operated by the Finnish Meteorological Institute. Figures 46, 48 and 50 show link and radar station outer construction.

According to the link span maps it is difficult to find a spot for a radar station that produce spurious emissions. At almost all thinkable radar station spots a link station is too near or one of the link spans runs through a sector in line with the radar transmission. The location of radar stations must be planned so that complete radar coverage is achieved but must unconditionally be implemented with equipment that produce no spurious transmissions or will suppress spuriouses with effective filters (acceptance requirement in the inspection measurement by FICORA).

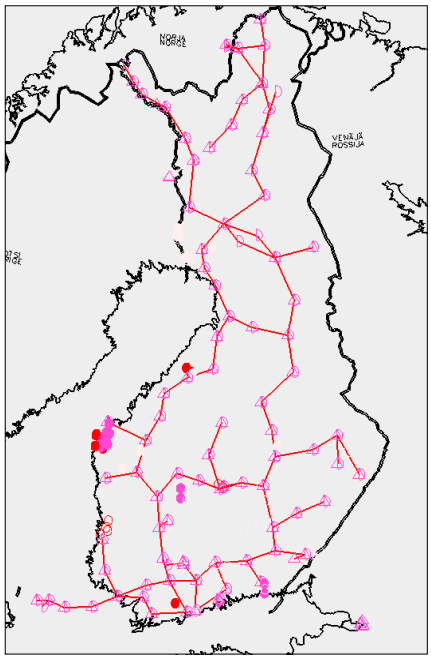

Figure 45. The program distribution radio link networks, operated by Digita on 3.6 - 4.2 GHz. The connections are partly analogue, partly digital. Link span lengths are on average less than 100 km.

Figure 46. A TRRS tower

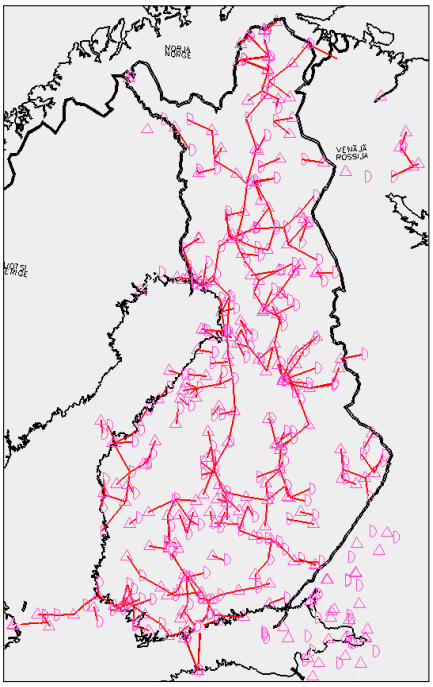

Figure 47. The high capacity radio link networks operated by telecom operators and the defense force in the 7.3 / 7.6 GHz frequency bands. Span lengths are at an average less than 50 km.

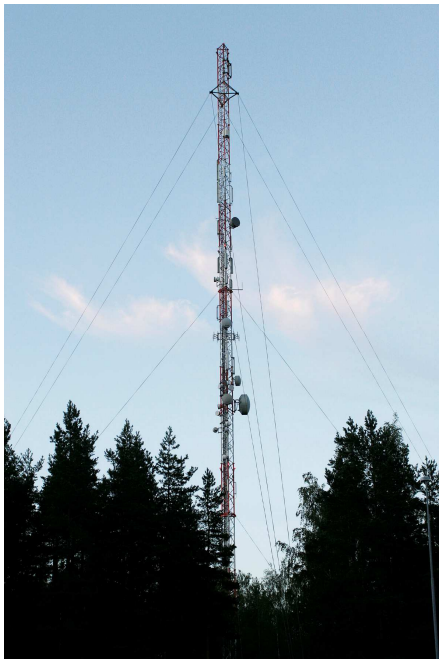

Figure 48. Army link mast.

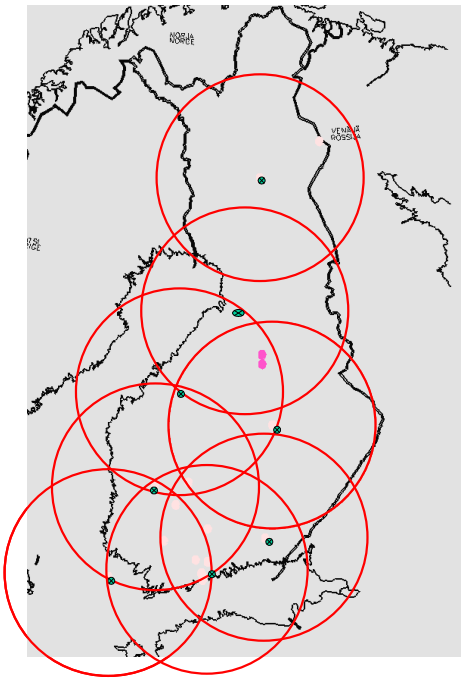

Figure 49. The station locations of weather radars and their coverage areas. Measurement range set to 200 km. The 5250...5280 MHz frequency range is reserved for weather radar.

Figure 50. A weather radar station

If a weather radar spurious transmission spectrum extends 1.5 GHz below its *NF* the broadcast links start getting interfered. Equally the spreading of the spurious transmission spectrum upwards causes the high capacity links to start getting interfered.

5.4 Special features of terrestrial radio relay systems

A radio link network usually is a static network with fixed station sites. Due to this highly directional antennas can be used. This reduces interference coming from sources not in line to the span. Due to highly directional antenna the same frequency can be used several times at the same station than would be the case with antennas with a wide main lobe. The disadvantage of highly directional antennas is that the mast must be equipped with an anti torsion mechanism at the top which increases the masts construction costs. The narrower the antenna lobe, the greater the risk of losing the transmitter antennas lobe at the receiving antenna, due to torsion of masts. The torsion of the mast forth and back can be caused for example by high wind speeds in the mast where the wind load relative to the vertical axis is unsymmetrical. Also heavy ice and rime layers cause twisting of masts. Also refraction changes can cause outage of a link connection when the direction of transmitter and receiver antenna lobes change so that the radio wave does not hit the antenna of the opposite station. Multipath propagation also causes problems when the reflected and delayed signal components either enhance or more usually attenuate the main signal when the fields are summed in the receiving antenna. This interference can be reduced by applying space diversity. This, however, raises the start-up costs because an additional antenna and a diversity combiner must be installed.

Nowadays link networks mainly use frequency bands above 3 GHz, so the influences from interference signals from other electrical appliances are small. EMSEC [34] has been doing interference measurements in Finland, for example on interference power field intensities of sparking between the electric locomotive collectors and the overhead contact line. According to the measurements the interference field strength reaches its maximum in the frequency range from 160...400 MHz. At frequencies above 2 GHz almost no interfering field strengths were discovered.

Output powers from TRRS's are low, at their highest in the range of a few watts. When the attenuation between antennas outside the foresight direction is high, typically more than 100 dB, the transmitter cross modulation signals usually cause no problems.

Due to the fixed position of link stations all input levels in a star point (where link connections from different directions combine) can be adjusted to be almost equal and of adequately low level. This is done to enable controlling of cross modulation between the different received signals.

High level interferences of far away systems seldom occur, because the path attenuation of a radio transmission is proportional to the square of frequency and to the square of distance.

The special features presented above are valid for both analogue and digital radio links.

5.5 Quality requirements of digital paths

The Finnish Standards Association's (SFS) standards have been followed in the presentation in this section.

5.5.1 Area of application

SFS has published the standard SFS 5626 [35] concerning quality requirements for digital connections. The standard defines quality requirements of a digital 64 kbit/s connection from subscriber A to subscriber B using a reference path.

The quality requirements are based on digital errors, slips, jitter and wander, delay, and availability of a digital hypothetic reference path.

5.5.2 Digital hypothetic reference path

The digital hypothetic reference path is a model that can be used for determination of quality requirements of a digital connection in such a way that makes it possible to reach the total quality of service of a telecom network. The model has been published in ITU recommendation G.801 [36].

5.5.3 Digital errors

With a digital error is here meant the inconsistence between a single signal element of transmitted signals and the corresponding received digital signal element. Depending on how the errors are generated the errors can occur as random single errors or as error bursts having random length and density. The error performance requirements relates to a 64 kbit/s circuit switched duplex connection in a PDH network (SDH networks have own definitions). The requirements are defined by the error rate in a certain time frame T_0 measured during a long time frame T_L when the connection is in availability state. The following error rates and time frames T_0 are used in the definition:

- (degraded minutes: time frame T_0 = 1 min, error rate worse than $1 \cdot 10^{-6}$, is not included in ITU recommendations),
- severely errored seconds: time frame T_0 = 1 s, error rate worse than $1 \cdot 10^{-3}$ (at most 9 consecutive seconds) and
- error-free seconds: time frame T_0 = 1 s, zero errors.

The digital hypothetic path of 27 500 km must fulfill the following error performance requirements:

- (the fraction of degraded minutes must be less than 10 %, is not included in ITU recommendations),
- the fraction of severely errored seconds must be less than 0.2 % and
- the fraction of errored seconds must be less than 8 %.

The quality requirements are allocated to the different parts of the connection allowing them a certain percentage of the required values of whole connections. For this the reference connection is split into parts and quality levels according to Figure 48 and Table 3. The values in the table are allowed percentage (time percents) of degraded minutes, errored seconds and severely errored seconds.

The local grade and medium grade are associated with both ends of the connection. Additionally a common 0.1 % has been reserved for the severely errored seconds at the medium and high grade sections for extremely unfavorable conditions (radio relay systems and satellites).

The national splitting into parts of the error handling capability at different levels of a digital network is presented for Finland in the standard SFS 5627 [37].

Table 3. Error performance requirements on a 50 km hop for different quality levels.

Performance level	Local grade	Medium grade	High grade
Degraded minutes	1.50%	1.50%	0.20%
Errored seconds	1.20%	1.20%	1.15%
Severely errored seconds	0.02%	0.02%	0.001%

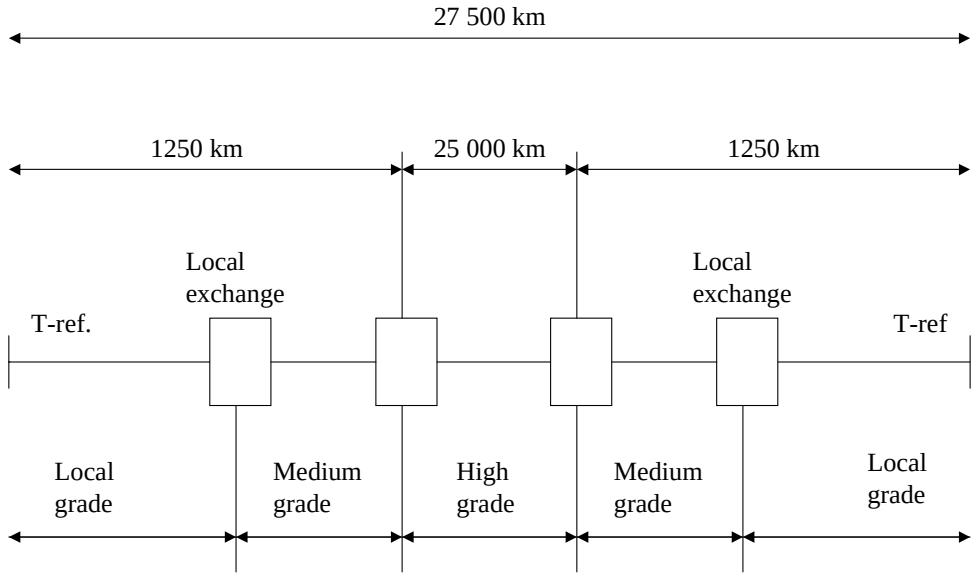

Figure 51. The splitting of error performance requirements on the various transmission quality parts of the ITU-T hypothetical reference path.

5.5.4 Slips

A slip is defined as repeating or non-appearance of a single bit or a certain group of bits occurring at any junction exchange of a digital network. Performance requirements are presented in ITU recommendation G.822 [38].

The allowed average density of slips:

When values are given for the average slip density of an international digital connection, the reference connection according to ITU recommendation G.801 is used. Finland is assumed to form one synchronizing area that operates plesiosynchronously on international connections as defined in [39].

The allowed average slip densities are given in Table 4:

Table 4 Requirements on slip density in HDRP

Average slip density	Fraction of total time
< 5 slips in 24 hours	98.9 %
>5 slips in 24 hours and < 30 slips in one hour	< 1 %
> 30 slips in one hour	< 0.1 %

5.5.5 Jitter and wander

With jitter and wander is meant the deviation of the significant instants of digital signals from the ideal periodic instants ($1/R_S$) from their nominal positions. Wander is the slowly varying part and jitter is the rapidly varying part of this phenomenon.

In the standard SFS 5647 the performance requirements for jitter and wander of junction of the network are presented. For transmission systems the similar characteristics are presented in the transmission system standard [39].

5.5.6 Delay

Delay appears in harmful quantities in international connections. The performance requirement in speech transfer is presented in ITU recommendation G.114 [40].

5.5.7 Availability

The availability of the network (ITU recommendation G.106 [41]) means the capability of being operational in the required way at an arbitrary moment of time or at any time in an arbitrary time slot. The connection is considered to be in a non-availability state when the error rate of all seconds is worse than $1 \cdot 10^{-3}$ during ten consecutive seconds. The connection is seen to return into availability state when the error rate of all seconds is better than $1 \cdot 10^{-3}$ during ten consecutive seconds. These ten seconds are included in the non-availability time.

The availability of the network is also affected by equipment failure, power supplies and transmission equipment, cable faults, the operation of fault repairing organization, interferences occurring on the transmission path and both backup and protection systems

5.6 Interference criteria of TRRS's

The block diagram of a typical radio link connection is shown in Figure 52. In this figure a 4PSK radio communication connection is presented with typical devices and parameter values.

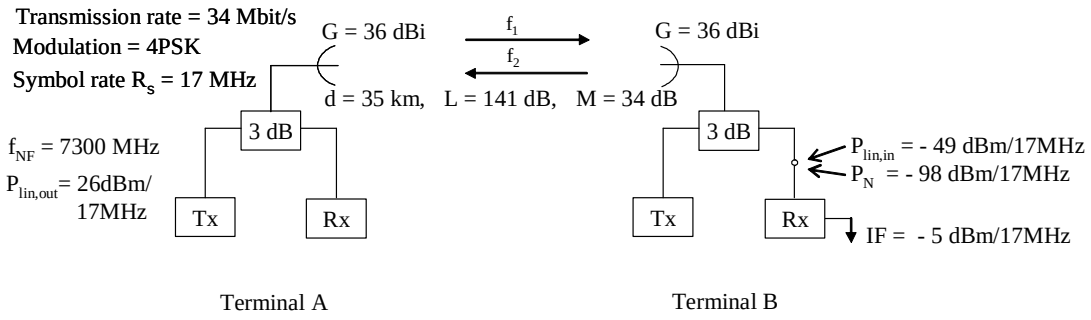

Figure 52. Link budget and radio link block diagram of the investigated TDRRS.

Following assumptions are made:

- the carrier frequency f_{NF} of the link is 7300 MHz, (the frequencies of the two connection directions, f_{NF1} and f_{NF2} , are different)
  - the link output power, $P_{lin,out}$, of the transmitter is 26 dBm and the signal bandwidth is 17 MHz
  - after the transmission path attenuation (L), antenna gain (G), feed line and splitter attenuation the input signal level of the receiver, $P_{lin,in}$, is –49 dBm and the signal bandwidth is 17 MHz,
  - at the same point the noise power level, P_N, is –98 dBm on the 17 MHz bandwidth (equipment parameter) and
  - the assumed connection length, d, is 35 km and the flat fade margin M is 34 dB when a *SNR* requirement of 15 dB is taken into account.

  The interference criteria for the investigated link can be described as follows:

  - In a dense radio link network, where the links are operating in an interference limited environment, the long time interference may deteriorate the required flat fade margin of the radio link by a maximum of 1 dB.
  - In the case of long time interference the interference power level must be 6 dB below the receiver's noise power level. This means that the signal to interference ratio (C/I) under normal propagation conditions must be:

$$C/I = M + C/N\left(10^{-3}\right) + 6\left[dB\right] \tag{5.1}$$

where:
- M is the actual flat fade margin,
- C/I is the carrier to interference ratio where
- C is the received TDRRS power level (The definitions of C is valid in the whole thesis)
- I is the interference peak power level (The definitions of I is valid in the whole thesis)
- $C/N(10^{-3})$ is the signal to noise ratio at which the error rate is 10^{-3} where
- N is the noise power level in the receiver filter output, and
- in a very short temporary interference situation the signal to noise ratio may be (< 1 % of the time):

$$C/I = C/N\left(10^{-3}\right)[dB] \tag{5.2}$$

If the interfering transmitter is a radar transmitter the long time interference criteria is always used.

Table 5. Required signal to noise ratio for different modulation systems at bit error ratio of 10^{-3}.

Modulation systems	$C/N(10^{-3})$
4PSK	14 dB
16QAM	23 dB
32QAM	25 dB
64QAM	29 dB
128QAM	32 dB

The $C/N(10^{-3})$ values given in Table 5 do not comply fully with theoretical values in an AWGN-channel, but they are values observed in practical measurements with radar interference present [42]. These values have been found satisfactory for measurements by the frequency regulator. A theoretical treatment of the impact of pulsed interference on 2PSK is given in [43].

The interference power budget and the TRRS link power budget are shown in Figure 53.

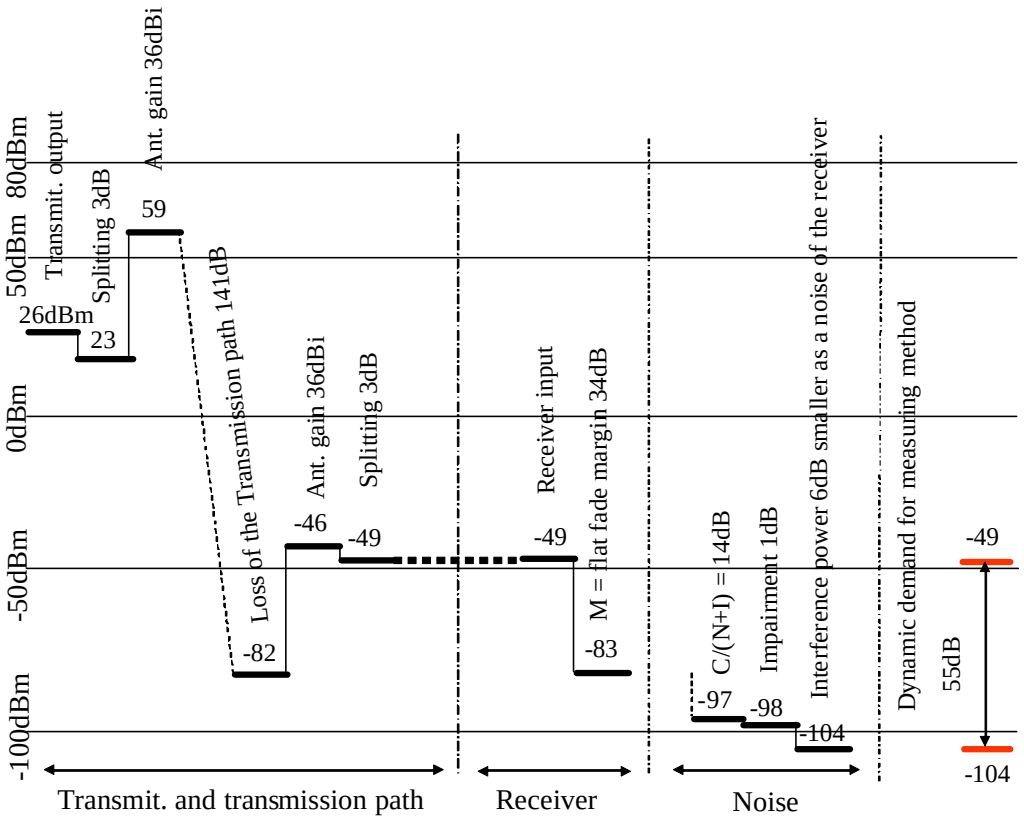

Figure 53. The impact of interference to the link budget.

In Figure 53 the power budget of a radio link is shown starting from the transmitter's output power level and ending at the –83 dBm power level (including a 34 dB flat fade margin) at the radio link input. The noise power level at the radio link input is during a non-interfering state 14 dB lower than the signal of the link –97 dBm. This can be regarded as the maximum power level of interference signals. When interference occurs on the transmission path inside the frequency band of the radio link while the flat fade margin already is used up, then the total disturbance power level (interference level –104 dBm in the figure) raises to –97 dBm with a 14 dB *C/(N+I)* ratio. If the interference level still increases the operation of the link begins to deteriorate. The interference in the link is seen as an increase in error rate that causes speech quality degradation.

Due to fading the flat fade margin of 34 dB decreases to 0 dB when the signal power level decreases from –49 dBm to –83 dBm. If the fading still increase, the carrier to total disturbance ratio (*C/(N+I)* = 13 dB) starts to decrease and the link receiver goes into non-availability state. Recovery from non-availability state requires 10 consecutive non-interfered seconds. When, for example, a radar interferes the link receiver, the link gets no possibility of recovering from the non-availability state due to the radar antenna rotating at 9 seconds per rotation (this is shorter than the required 10 successive seconds).

5.7 The interference mechanism of TDRRS

As mentioned before short radar pulses do not cause much interference in analogue TRRS's narrow speech channels (300...3400 Hz). In digital radio systems the situation is different. The interference mechanism of a TDRRS or other similar digital radio system can be described as follows:

Let's assume a 4-state phase modulation (4PSK). The modulation can be represented at the decision sampling instant as one of four vectors, each corresponding to a unique combination of two bits (Figure 54).

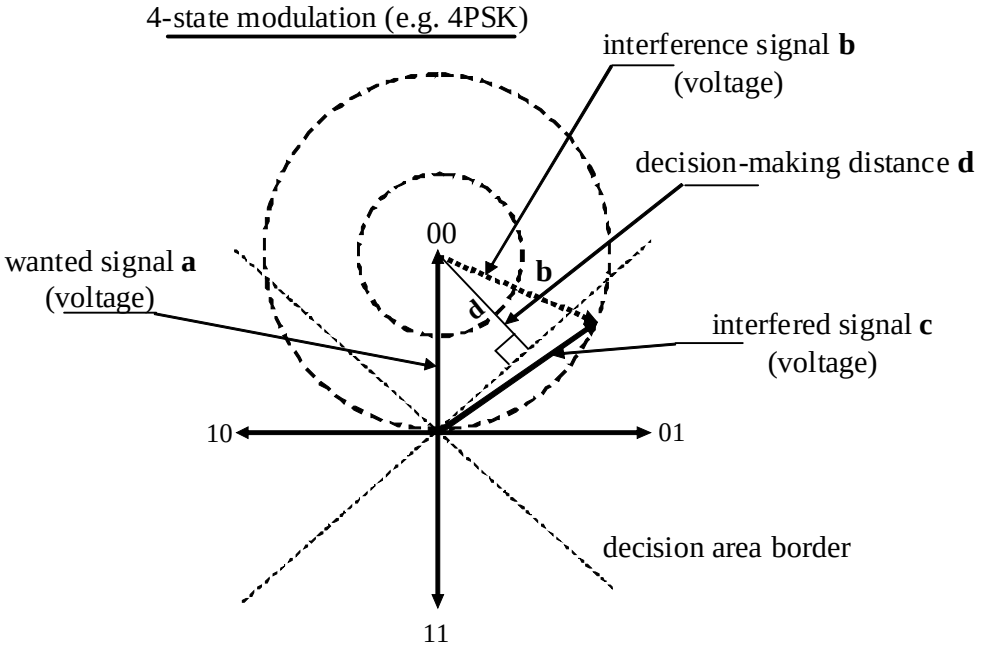

Figure 54. Phasor diagram of interfered 4PSK.

The diagram shows how the interference vector **b** (interference signal vector) is summing to the vector **a** representing the wanted signal with their amplitudes and phases. If the frequency of the interference differs from the center frequency of the radio link the interference vector starts rotating with the vector **a**'s current symbols vertex as its center point. The rotation direction is clockwise if the interference frequency is higher than the center frequency of the radio link. Similarly it is counterclockwise if the interference frequency is lower than the center frequency of the link. The rotation speed is depending on the frequency difference. If no frequency shift is present the interference vector stays in a constant direction. If the amplitude of the interference stays constant the length of the interference vector stays constant. When the interfered signal **c** level vector exceeds the decision area border the detected symbol becomes false. The interference signal in this example is assumed to be an unmodulated sine wave (an unmodulated pulsed spurious signal of the radar) and noise is negligible.

When the radar transmits several sine-shaped spurious pulsed signals with the pulse repetition frequency (*PRF*) the sum vector is formed from all signals contained in the intermediate frequency band. This means that at the vertex of the actual 4PSK-signal is the center many interference vectors of different length and rotation frequency. The interference vector is the sum of all these vectors.

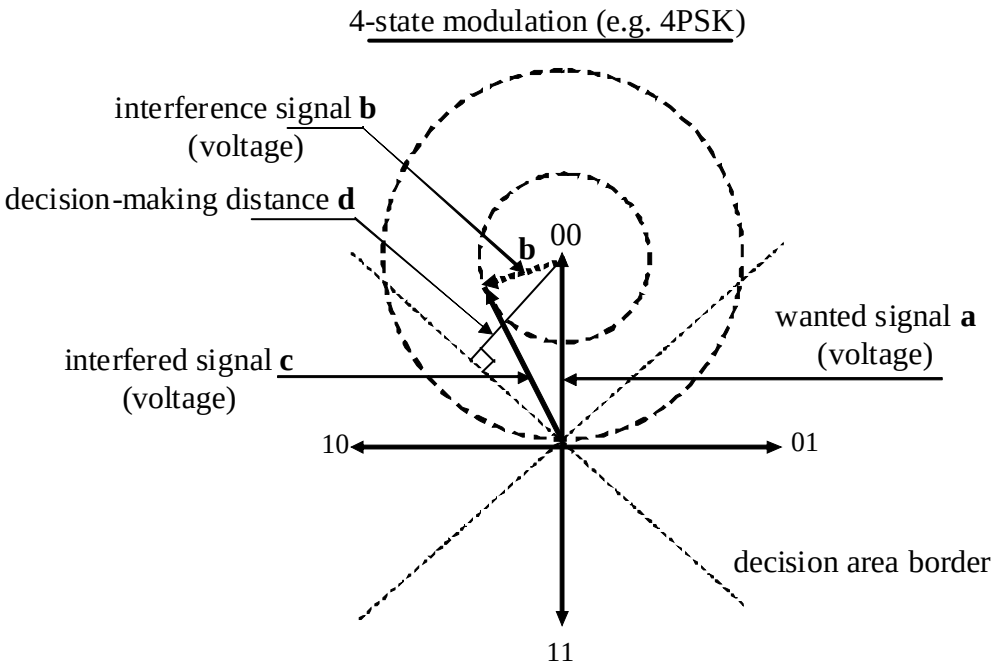

Figure 55 Phasor diagram at decision instant of 4PSK with interference not alone causing symbol error

Figure 55 shows a situation where the interference does not cause decision errors when noise is negligible. This is the case when the signal vector **a** is more than 3 dB higher than the interference signal vector **b** $20 \cdot \log(|b| / |a|) < -3$ dB. In this situation the sum vector vertex will stay in the correct decision area regardless of the phase of the interference vector, and an erroneous decision will not be made. For stronger interference it depends on the phase of the interference, whether the decision is correct in 4PSK.

As reference system 4PSK modulation has been used in Figure 54. When using 2PSK the interference signal must be higher than the wanted signal to make decision error interpretation possible. In 2PSK the $C/(N+I)$ maximum value is < 0 dB. The maximum interference to signal ratio in dB making data errors improbable are given in Table 6.

It should be kept in mind, that:

- Signal vectors, noise, and interference vectors represent sample values at the decision circuit input (includes impact of reception filter).
- With 2PSK even higher interference can be tolerated without causing decision making errors, when the direction of the interference vector is not orthogonal to the decision area border.

According to Figure 54 the interference signal vector **b** causes a symbol error when the sum vector crosses the decision area border. In Figure 55 the interference vector **b** does not create a sum vector crossing of the decision area border. However, the interference vector **b** might, while summing up with the wanted signal vector, cause the sum vector to be attenuated so that a erroneous symbol decision may occur due to noise, or it is increased so much that non-linear effects occur.

Table 6. The theoretical (noiseless transmission) maximum interference to average signal power–value in dB for different modulation methods.

Modulation systems	I/C [dB]
2PSK	±0.0
4PSK	–3.0
8PSK	–8.4
16QAM	–10.0
64QAM	–16.2

To make it possible to estimate if an outside signal causes harmful interference to the TDRRS both the system link budget must be calculated and the interfering signal level must be measured. The measurement of an interfering signal level (for example spurious emission of radar) has been described in Section 4.3.4 "Determination of radar spurious transmissions."

The target pulse shape of a TDRRS using linear modulation has usually a raised cosine spectrum shape. Raised cosine filtering is a form off so called Nyquist filtering, where sampling of the channel impulse response with symbol rate R_S produces only one sample differing from zero.

As digital circuits generate almost ideal rectangular pulses, not impulses, a so called sinc corrector is needed to correct the spectrum shape. The total filtering is normally split equally between the radio link transmitter and receiver.

The transmission pulse spectrum and the pulse shape in the output of the receiver filter are as follows, [44]:

$$X(f)=\begin{cases} T, & |f|\le(1-\alpha)\frac{1}{2T} \\ \frac{T}{2}\left[1+\cos\left(\frac{\pi}{\alpha}\left(|f|T-\frac{1}{2}(1-\alpha)\right)\right)\right], & (1-\alpha)\frac{1}{2T}<|f|\le(1+\alpha)\frac{1}{2T} \\ 0, & |f|>(1+\alpha)\frac{1}{2T} \end{cases} \tag{5.3a}$$

$$x(t)=\operatorname{sinc}\left(\frac{t}{T}\right)\frac{\cos\left(\pi\alpha\frac{t}{T}\right)}{1-\left(2\alpha\frac{t}{T}\right)^2} \tag{5.3b}$$

where: - f is the frequency
- T is the symbol duration (= $1/R_S$)
- α is the spectrum roll-off parametric identifying the total bandwidth

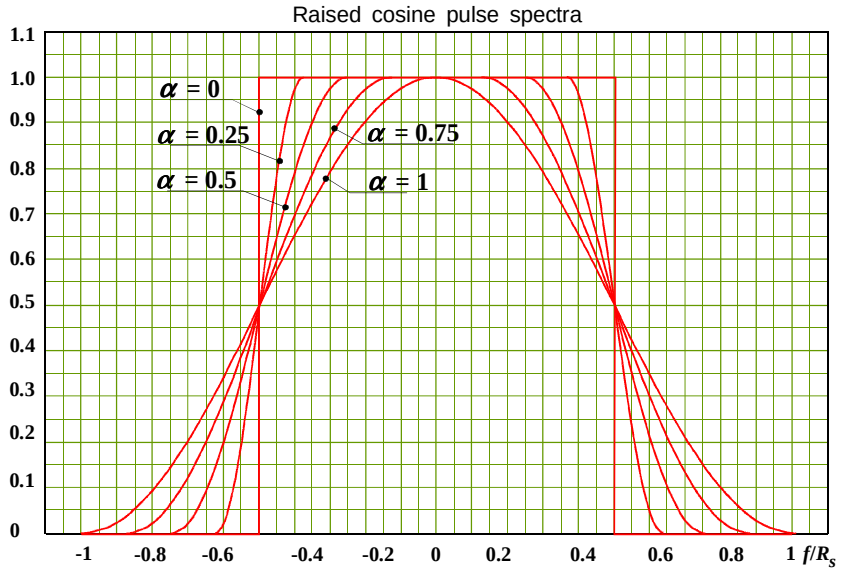

Figure 56a. Raised cosine pulse spectrum.

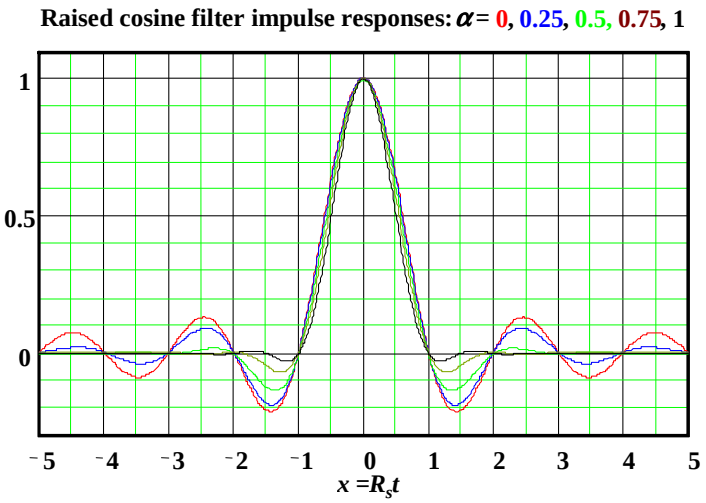

Figure 56b. The equivalent low-pass impulse response of the pulse with raised cosine shaped spectrum.

For determination of a link budget the following basic attributes are needed to make it possible to perform a digital broad band signal power measurement:

- measurement is done with an SA,
- B_{meas} is the measuring bandwidth,
- symbol rate $R_S = R_B / \log_2 N_S$,
- N_S is the size of the symbol set,
- power spectral density $S(f_c)$ is P_{tot} / R_S ,
- total average power level $P_{tot} = P_{meas} + 10 \cdot \log(R_S/B_{meas})$, when $B_{meas} << R_S$ and
- f_c is the TDRRS carrier frequency.

5.8 Measurement of radio link interference

Because the radiation pattern of radio link antennas and the transmission characteristics of the receiver filter play a significant role in the radio link getting interfered the interference measurements should be carried out using the TDRRS link receiver as measurement receiver according to the measurement setup shown in Figure 57.

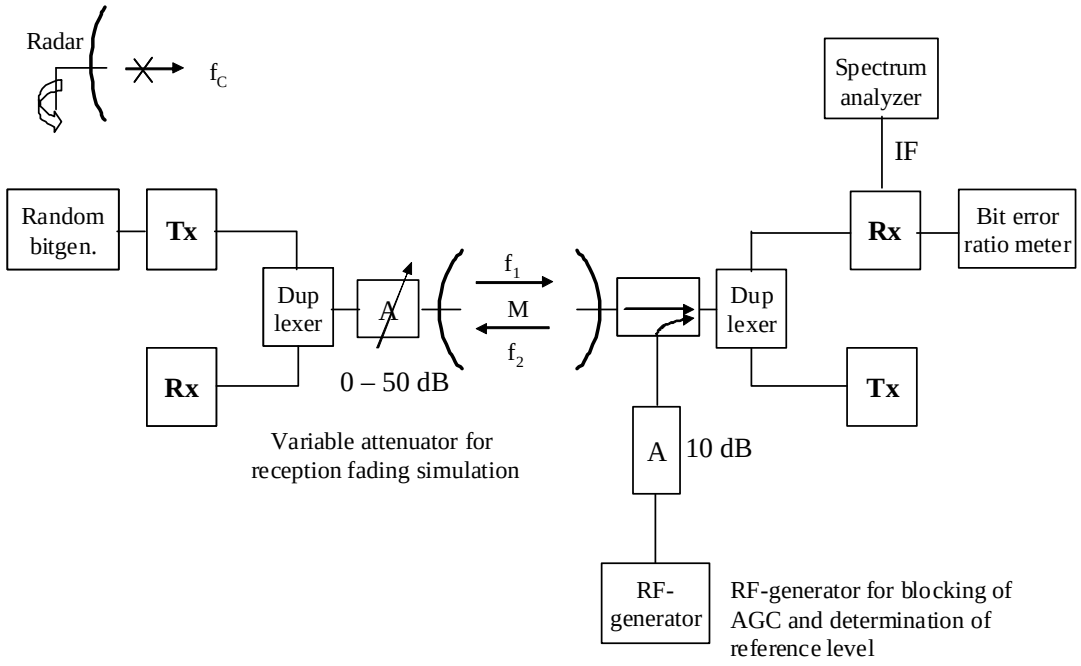

Figure 57. Basic measurement setup of interference measurement.

With the link interference measurement system presented in this work the intention is to approach the measurement problem step by step (Fig 58...Fig 60) and prove how the own received power level of the radio link and the signal level of the possible interference reach a satisfactory and reliably readable level difference (55 dB, from Figure 53).

The dynamic range of the measurement signal, DR_{sig}, is in this context defined as the difference between the peak level of either the received radar signal, $P_{NF,in}$, or TDRRS signal, $P_{lin,in}$, (in practice the average power level) and the peak level of the strongest radar SF-signal in the TDRRS transmission channel, $P_{SF.\max}$, (Eq. 5.4)

$$DR_{sig} = \max\left\{P_{lin,in}, P_{NF,in}\right\} - P_{SF,\max} \tag{5.4}$$

The dynamic range of the measurement system, *DR*, is defined as the difference between the SA maximum input level, $P_{SA,\max}$, and the average level of the measurement noise level, $P_{N,.sys}$, reduced to the SA input. Both levels can be reduced to some other point in the system (Eq. 5.5)

$$DR = P_{SA,\max} - P_{N,sys} \qquad \text{……(5.5)}$$

For a successful measurement must the dynamic range of the signal increased with the minimum SNR for an accurate result of the spurious signal level, $SNR_{\min}$, be inside the dynamic range of the measurement system. This can be expressed with the three following inequalities:

$$DR_{sig} + SNR_{\min} \le DR \tag{5.6a}$$

$$\max\left\{P_{lin,SA}, P_{NF,SA}\right\} \le P_{SA,\max} \tag{5.6b}$$

$$P_{SF,\max} - SNR_{\min} \ge P_{N,sys} \tag{5.6c}$$

If the above inequalities are not fulfilled special measures must be taken e.g. selective attenuation of the radar NF-signal, amplification of the SF-signal and improvement of the noise properties of the measurement system as was done with the system described in Chapter 4.

The basic block diagram of the interference measurement setup is presented in Figure 57. Figures 58, 59 and 60 it is shown how measurement dynamics can be increased with several practical measures.

Attention must be paid to the fact, that the transmission directions have different frequencies (f_1 and f_2). This leads to different loss behavior between the two different directions.

5.8.1 The interference measurement without the radio link antennas and receiver (step 1).

In Figures 58, 59 and 60 three different block diagrams for interference measurement are presented with typical TDRRS parameter values.

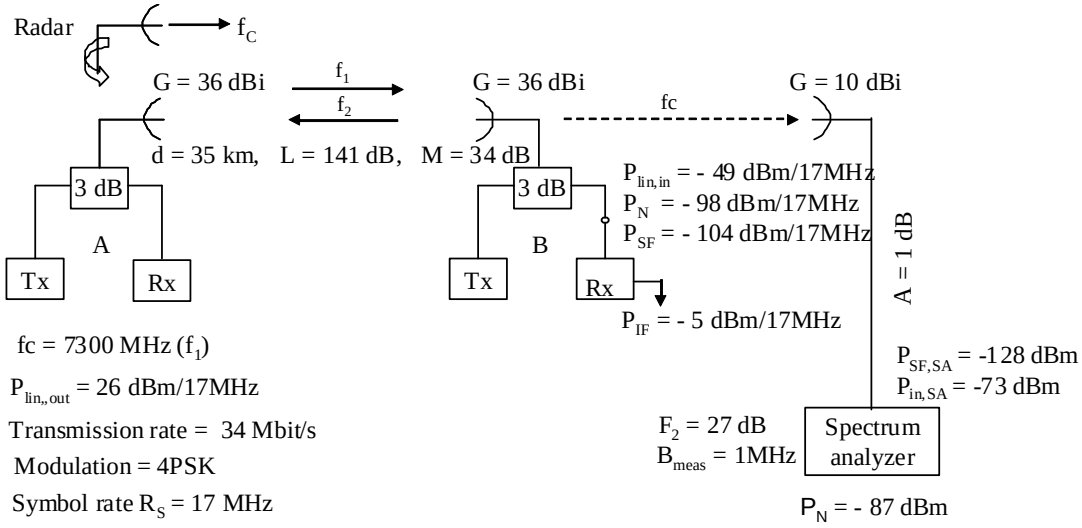

Figure 58. Interference measurement setup in Step 1.

Step 1: A typical radio link connection is assumed as presented in Figure 58 where the occurring interference should be measured with an SA and own measuring antenna. The antenna gain is 10 dB and the feed line attenuation is 1 dB while the SA's noise figure typically is: F = 27 dB and the measurement bandwidth B_{meas} is 1 MHz.

At the SA input the measured transmission power level $P_{in,SA}$ is:

$$P_{in,SA} = P_{lin,out} - A_{splitter} + G_{lin,ant} - L + G_{meas,ant} - A \tag{5.7a}$$

where: - $P_{in,SA}$ is the power level of the TRRS at the SA input,
- $P_{lin,out}$ is the output power level of the TDRRS transmitter,
- $A_{splitter}$ is the TX branch attenuation in dB of the duplex filters,
- $G_{lin,ant}$ is the gain in dB of the TDRRS transmitter antenna,
- L is the transmission path loss in dB,
- $G_{meas,ant}$ is the reception antenna gain in dB of the measurement system and
- A is the attenuation in dB of the measurement system antenna cable.

Calculation example for Figure 58:

$$P_{in,SA} = 26[\text{dBm}] - 3[\text{dB}] + 36[\text{dB}] - 141[\text{dB}] + 10[\text{dBi}] - 1[\text{dB}] = -73[\text{dBm}] \quad (5.7b)$$

Equation (5.4) shows the power budget of the radio link from the transmitter to the SA input.

The noise power P_N of the SA on the measurement bandwidth (=B_{meas}) is:

$$P_{N,SA} = F + 10 \cdot \log(kT_0) + 10 \cdot \log(B_{meas}) \quad (5.8a)$$

where: - $P_{N,SA}$ is the total noise power level at the SA input,
- F is the noise figure of the SA,
- k is Bolzmann's constant 1.380 10^{-23} JK^{-1},
- T_0 is the temperature 290 K and
- B_{meas} is the SA measurement bandwidth.

Calculation example for Figure 58:

$$P_{N,SA}[\text{dBm}] = 27[\text{dB}] + (-174)[\text{dBm}] + 10 \cdot \log 10^6[\text{dB}] = -87[\text{dBm}]/1\text{MHz} \quad (5.8b)$$

The average TDRRS signal is only 2 dB above noise level and therefore not reliably detectable −85 dBm − (−87 dBm) = 2 dB. This means that it is impossible to measure the *SF* signal reliably.

$$DR_{sig} = \max\{P_{lin,in}, P_{NF,in}\} - P_{SF,\max} = P_{SF,\max} + X - P_{SF,\max} = X \ , \quad (5.9)$$

and the dynamic range of the measurement system when $P_{SA,\max} = 0$ dBm and $P_{N,sys} = -87$ dBm is, (when $X = P_{NF} - P_{SF}$)

$$DR = P_{SA,\max} - P_{N,sys} = 0 - (-87) = 87 \text{ dB} . \quad (5.10)$$

Thus Eq. 5.6a is fulfilled if the maximum radar SF component in the TDRRS channel is larger than −87 dBc.

The inequality in Eq, 5.6b can in this case be written in the form

$$P_{NF,SA} = P_{SF,\max} + X \le P_{SA,\max} \rightarrow -128 + X \le 0 \rightarrow X \le 128 \text{ dB} . \quad (5.11)$$

Thus the maximum SA input level will not be exceeded if the maximum SF-level is larger than −128 dBc. However, the assumed maximum SA input level will in practice exceed the specified maximum level for linear SA operation. As this is a rather narrow-band

measurement this will not cause problems, but it must always be checked that the measured component is in the radar signal and not generated by the SA.

The inequality in Eq. 5.6b can in this case be written in the form

$$P_{SF,\max} - SNR_{\min} \geq P_{N,sys} \rightarrow -128 - 10 \geq -87 \text{ dBm} \tag{5.12}$$

Thus this inequality is not fulfilled. In this measurement system a radar signal fulfilling the ITU recommendation has a dynamic range exceeding the dynamic range of the measurement system and an SF-signal that would just not impact on the TDRRS performance cannot be measured due to the high noise of the measurement system.

5.8.2 Interference measurement with an SA using a low noise preamplifier (LNA) and a band-stop (BS) filter, (step 2).

Because the dynamic range of the above measurement system (Step 1) does not fulfill the requirement the measurement system is improved with an LNA and BS filter as shown in Fig. 59.

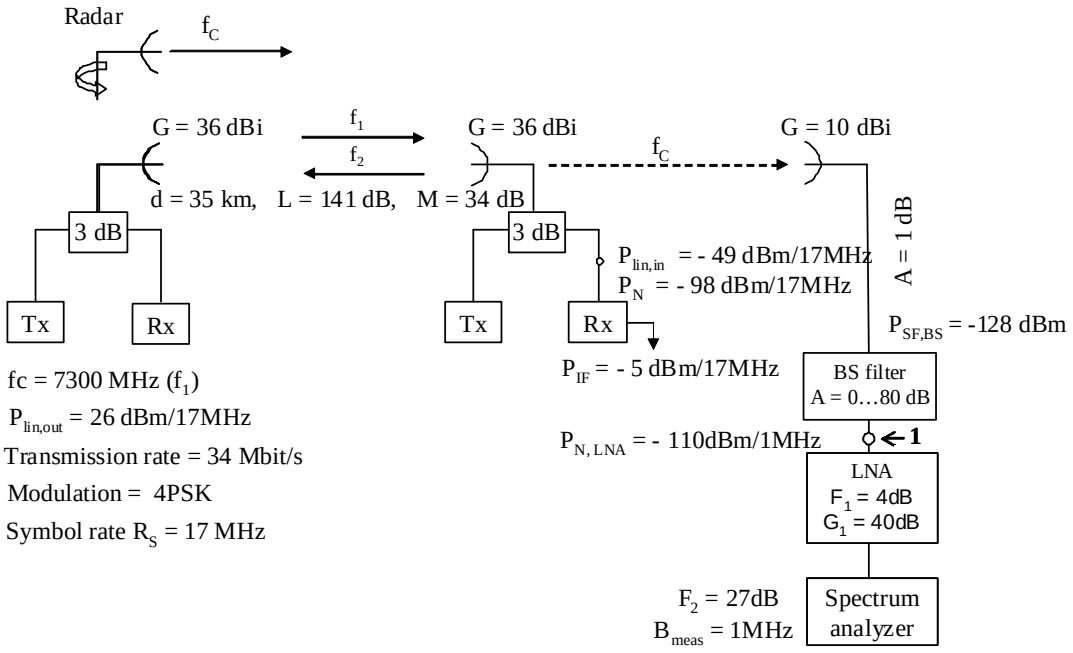

Figure 59. Interference measurement setup in Step 2.

The noise figure of the LNA is F_1 and its gain G_1 noise figure F_1 is 4 dB and its gain G_1 is 40 dB and the SA noise figure F_2 is 27 dB.

The total noise factor F_r of the measurement system at point 1 can be calculated from the following equation:

$$F_r = F_1 + (F_2 - 1)/G_1 \tag{5.13a}$$

where: - F_r is the combined noise factor of the SA and LNA at the LNA input,
- F_1 is the noise factor of the LNA,

- F_2 is the noise factor of the SA and
- G_1 is the gain of the LNA
- (noise figure F = noise factor in dB)

Calculation example for Figure 59:

$$F_r = 2.51 + (501-1)/10000 = 2.56 \Rightarrow 4.08\,[\mathrm{dB}] \tag{5.13b}$$

The P_N of the SA with $B_{meas} = R_S$ = 17 MHz is reduced to the LNA input (point 1):

$$P_{N,LNA} = F_r + 10\log(kT_0) + 10\log(B_{meas}) \tag{5.14a}$$

where: -$P_{N,LNA}$ is the total noise power at the LNA input,
-F_r is the noise factor of the cascade LNA and SA,
-k is Bolzmann's constant,
-T_0 is the standard room temperature (T_0 = 290 K) and
-B_{meas} is the SA measurement bandwidth.

Calculation example for Figure 59:

$$P_{N,LNA}\,[\mathrm{dBm}] = 4.1\,[\mathrm{dB}] + (-174)\,[\mathrm{dBm}] + 10\cdot\log 10^6\,[\mathrm{dB}] = -110\,[\mathrm{dBm}]/1\mathrm{MHz} \tag{5.14b}$$

The noise power level obtained in Section 5.8.1 (–87 dBm) is now reduced to (–110 dBm). When in Section 5.8.1 the link signal in the measurement system was 2 dB over the noise power level, in this measurement setup (5.8.2) the link signal power on the SA display is now $P_{in,SA} - P_{N,in} = P_{in.LNA} - P_{N.LNA}$ = (–85dBm) – (–110dBm) = 25 dB above noise power level (the signal of the link transmitter has remained unchanged, only the noise power level has decreased).

The dynamic range of the measurement signal in the measurement system input is

$$DR_{sig} = \max\{P_{lin,in}, P_{NF,in}\} - P_{SF,\max} = P_{SF,\max} + X - P_{SF,\max} = X\ , \tag{5.15}$$

and the dynamic range of the measurement system in the measurement system input is

$$\begin{aligned} DR &= P_{SA,\max} - G_{LNA} + L_{BS} - P_{N,sys} - L_{BP} \\ &= 0 - 40 + L_{BS} - (-110) - L_{BP} = 70\ \mathrm{dB} + L_{BS} - L_{BP} \end{aligned}\ . \tag{5.16}$$

Thus Eq. 5.6a is fulfilled if X is less than 70 dB + $L_{BP} - L_{BS}$. Especially, if X = 100 dB the needed difference between the BS-filter attenuation of the radar NF-signal and the attenuation at SF is 30 dB.

The inequality in Eq. 5.6b can in this case be written in the form

$$\begin{aligned} &P_{NF,SA} = P_{SF,\max} + X - L_{BS} + G_{LNA} \le P_{SA,\max} \rightarrow -128 + X - L_{BS} + 40 \le 0 \\ &\rightarrow X - L_{BS} \le 88\ \mathrm{dB} \end{aligned}\ . \tag{5.17}$$

Thus, if X = 100 dB the needed BS-filter attenuation is only 12 dB.

The inequality in Eq. 5.6b can in this case be written in the form

$$P_{SF,\max} - L_{BP} - SNR_{\min} \geq P_{N,LNA} \rightarrow -128 - 1 - 10 \geq -110 \text{ dBm} \qquad (5.18)$$

Thus this inequality is not fulfilled. Also another basic problem remains, this measurement system has an antenna which cannot easily be put on the same height as the TDRRS antenna, and its gain pattern is also very different.

5.8.3 Interference measurement using the radio links own antenna and receiver (Step 3).

The best and most appropriate measurement of radio link interference levels is to use the own antenna of the radio link and as preamplifier to use the link receiver. Additionally to satisfactory measuring dynamics one also gets the impact of the antenna side lobe attenuation and the attenuation of the receiver filter into the measurement results. These often have a significant effect on the interference of radio link connections.

In this method the TDRRS transmitter is switched off and instead a local sine oscillator is connected to the TDRRS receiver. It is important for the measurement that the AGC function can be deactivated or locked to a certain level with help of a signal from an external RF generator. Its power is the same as the TRRS power at the feed point. This is necessary because of the requirement of keeping the TRRS receiver operational point in the linear part of its operating range at an optimum value. Otherwise the receiver gain will increase to its maximum value, when the DRRS transmitter is switched off for the interference measurement.

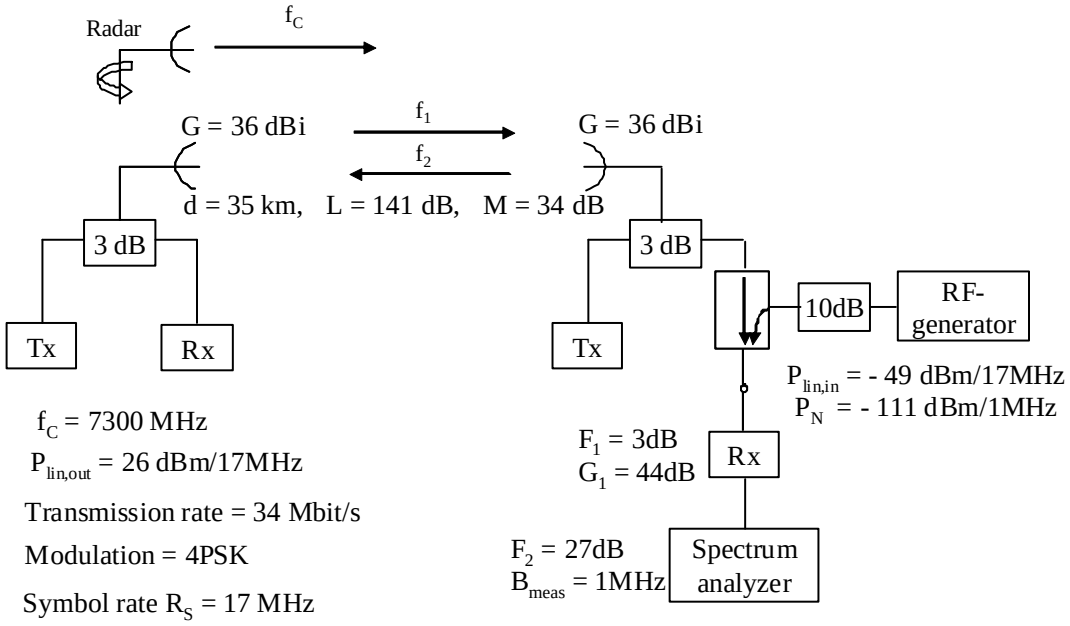

Figure 60. Interference measurement setup in Step 3

In the following analysis the parameter values of the example system are used.

The total noise factor F_r of the receiver (in Figure 60) based on the SA and the link receiver characteristics can be calculated as shown in Section 5.8.2 when the link receiver gain G_1 is (−5 dBm) − (−49 dBm) = 44 dB and its noise figure F_1 is 3 dB.

$$F_r = F_1 + (F_2 - 1)/G_1 \tag{5.19a}$$

where: - F_r is the total noise factor generated by the TDRRS and SA at the Rx input,
- F_1 is the noise factor of the TDRRS receiver, 3 dB
- F_2 is the noise factor of the SA and
- G_1 is the gain of the TDRRS receiver.

Calculation example with the noise figure values in Figure 60
- (noise figure F_N = noise factor in dB)

$$F_r = 2.00 + (501 - 1)/25119 = 2.02 \Rightarrow 3.05[\text{dB}] \tag{5.19b}$$

The noise power $P_{N,SA}$ of the measurement system with the 17 MHz measurement bandwidth B_{meas} is:

$$P_{N,Rx} = F_r + 10 \cdot \log(kT_0) + 10 \cdot \log B_{meas} \tag{5.20a}$$

where: - $P_{N,Rx}$ is the reduced total noise power sum at the Rx input,
- F_r is the total noise factor of the measurement system,
- the second term is the thermal noise power collected on the TDRRS connection for 1 Hz measurement bandwidth and
- B_{meas} is the measurement bandwidth in Hz.

Calculation example using block diagram parameters in Figure 60 $P_{N.Rx}$ is:

$$P_{N,Rx}[\text{dBm}] = 3.0[\text{dB}] + (-174)[\text{dBm}] + 10 \cdot \log(10^6)[\text{dB}] = -111[\text{dBm}]/1\text{MHz} \tag{5.20b}$$

The received power level $P_{in,SA}$ at the TDRRS receiver input is –49[dBm] (from Figure 60).

In this case the radar NF-signal is attenuated by the TDRRS channel filter in the branching system and also by the receiver filters. It is assumed that its level is negligible compared to the local oscillator signal level. The dynamic range of the measurement signal in the measurement system input is

$$DR_{sig} = \max\{P_{lin,in}, P_{NF,in}\} - P_{SF,\max} = P_{lin,in} - P_{SF,\max} = -49 - (-104) = 55 \text{ dB}, \tag{5.21}$$

and the dynamic range of the measurement system in the measurement system input is

$$DR = P_{SA,\max} - G_l - P_{N,sys} = 0 - 44 - (-111) = 67 \text{ dB}. \tag{5.22}$$

Thus Eq. 5.6b is fulfilled.
The inequality in Eq. 5.6b can in this case be written in the form

$$P_{lin,SA} = P_{lin,in} + G_l \le P_{SA,\max} \rightarrow -49 + 44 \le 0 \text{ dB}. \tag{5.23}$$

Thus, the inequality is fulfilled.
The inequality in Eq. 5.6b can in this case be written in the form

$$P_{SF,\max} - SNR_{\min} \ge P_{N,sys} \rightarrow -104 - 10 \ge -111 \text{ dBm} \tag{5.24}$$

Thus this inequality is not fulfilled. However, if one considers that a SNR_{min} = 7 dB is satisfactory; this measurement system fulfills all three inequalities. As earlier was stated it must be checked that the measured signal is not a spurious response generated by the SA.

It should be noted that the ITU-R requirement on radar spurious emission levels are defined for a reference bandwidth while the measurement described in this chapter should give information about the true peak power level of the radar signal passed through the TDRRS receiver filters. In most cases the TDRRS receiver filter bandwidth contains all significant energy of the interfering radar signal. The radar NF-signal and all SF-components are basically deterministic signals with a rectangular envelope. The conversion problem is to find the relationship between the peak value on the measurement bandwidth and the pulse amplitude. The same problem is not significant in Chapter 4, because ITU-R M1177 defines a measurement bandwidth equal or smaller than the radar reference bandwidth which is much smaller than the effective pulse bandwidth (say 99 percent power bandwidth) and gives simple reduction formulas for that case.

A theoretical investigation has been made to find out the difference between the measured radar interference peak level and the peak level of the unfiltered radar interference. It is assumed that the radar interference pulse is a rectangular sine pulse and the measurement filter has a rectangular frequency response. For instance a $1/\tau$ measurement filter bandwidth results in a level 1.18 dB lower than the radar pulse peak level, while a $2/\tau$ measurement filter bandwidth results in a measured peak level 1.43 dB higher than the radar pulse peak level. A more realistic measurement filter model might somewhat change these values. In practice this can be considered by a corresponding change of the X-value obtained with the measurement system presented in Chapter 4.

5.9 Summary of Chapter 5

At the beginning of Chapter 5 the history, development, frequency ranges, their means of operation and users of radio links have been described. The special features and their economical advantages when compared to fixed line connections are also described.

Quality requirements for digital radio relay systems have been defined. This has been done when interference of links has been studied.

Also the link connection interference criteria have been described both with a measurement setup and link budget. Furthermore the measurement dynamic range has been estimated. The nature and impact of the interference have been described by an example using QPSK.

The focus is on the measurement of link interferences in this chapter. Three different measurement setups have been presented. The chapter contains a presentation how the needed measurement dynamic range has been achieved by a step by step approach. Both the power and noise power levels have been mathematically presented for each measurement setup separately.

6 ESTIMATION AND CHECKING OF THE PROTECTION DISTANCE BETWEEN RADAR TRANSMITTER AND TDRRS RECEIVER

In this chapter the behavior of the bit error rate of a certain TDRRS exposed to radar disturbance is explained. An example of measured radar interference is shown. A theoretical method for estimation of the protection distance is presented. This method is based on a maximum allowed radar interference level depending on the modulation method and on radio link budget calculations where the TDRRS receiver antenna radiation diagram obeys the ITU-R Recommendation F.699 [45]. The radar propagation mechanism is modeled either as free space propagation, diffraction propagation, or tropo-scatter propagation.

The verification of the protection distance in a field configuration is based on interference measurements with the measurement method presented in Chapter 5. Due to the average nature of the used propagation models the verification is very important. However, there has been no possibility to perform such verification measurements within this work.

6.1 The occurrence, identification and effect on bit error rate behavior of radar interference in TDRRS measurement.

The interference caused by radar is easily identified. This is because the interference signal is burst like due to the radar antenna rotation. Each burst contains some pulses depending on the radar antenna lobe width and the *PRF*.

When the TDRRS bit error rate as function of the received TDRRS power level is studied by measurements one gets a result schematically presented in Figure 61. The location and numerical values of the star points are only indicative.

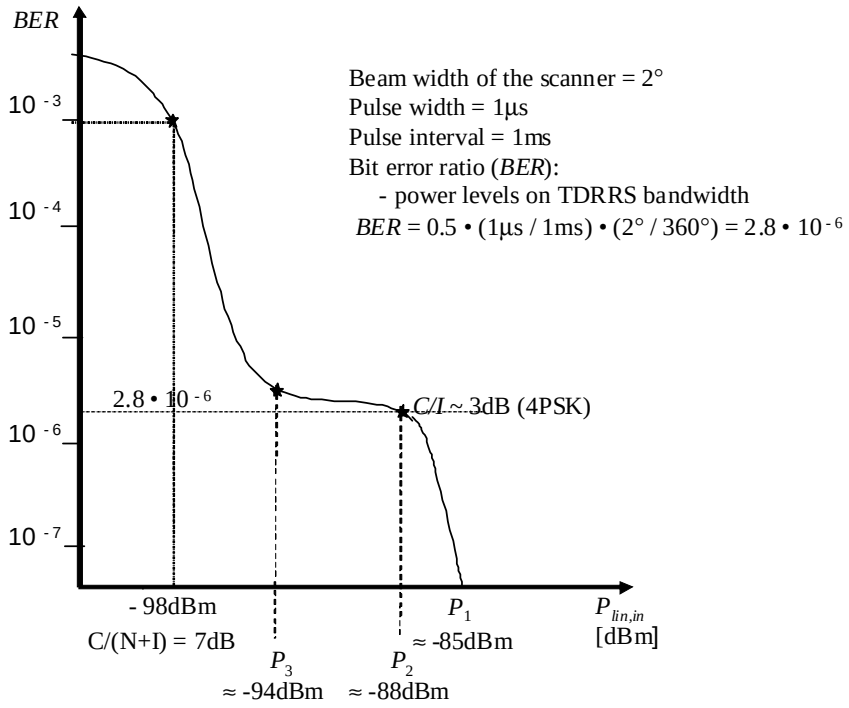

Figure 61. The effect of the radar interference on the measured bit error rate curve.

The graph shows a typical TDRRS error behaviour in a channel containing Gaussian noise and pulsed constant peak level radar interference as function of TDRRS signal level. It is assumed instantaneous receiver recovery after each interference pulse.

In the BER-curve occurs an almost horizontal portion that can be interpreted in the following way:

It is assumed that in non-fading conditions the input level at the TDRRS receiver is −49 dBm and the interference peak power level created by the radar is P_2.

When fading occurs, the received power level decreases and approaches the radar interference signal level. At power level P_1 the signal to interference ratio (C/I) approaches 3 dB (which can cause symbol decision errors in 4PSK modulations even without noise as demonstrated in Section 5.6). The received power level at this point is so high that the noise by itself is not yet significantly causing errors. With the power level continuing to decrease the amount of errors rises until the reception power level reaches power level P_2 where $C/I = 3$ dB. After this the radar pulse "destroys" all bits when it illuminates the TDRRS receiver antenna. In this case the error rate is 0.5·average error rate (because on average only half of the bits are destroyed). When the received power level still continues to decrease, the error rate of the TDRRS during radar illumination stays at 0.5·average error rate. This is practically independent of the received power level. This causes an almost horizontal part in the curve. The average error rate (in the considered case $2.8 \cdot 10^{-6}$) on this portion is depending on the duration and *PRF* of the radar pulse and the radar antenna lobe width as the calculation assuming immediate recovery after each radar pulse in Figure 61 shows.

When the received power level has decreased to the level P_3 the receiver noise begins to create errors between the radar pulses. If the received power level is still decreasing and falling below P_3 the amount of errors due to noise increases rapidly. At the same time the errors caused by radar remain at a constant level and become insignificant. With the received power level still decreasing, the slope of the error rate curve follows the shape of the normal error rate curve as in non-interference cases. Due to this the lower part of the curve is shifted to the right.

6.2 Radar signal interference in TDRRS investigated in the time domain.

In this section the impact of an interfering radar signal on TDRRS error behavior on bit level is treated in the time domain using parameter values from Example 7.

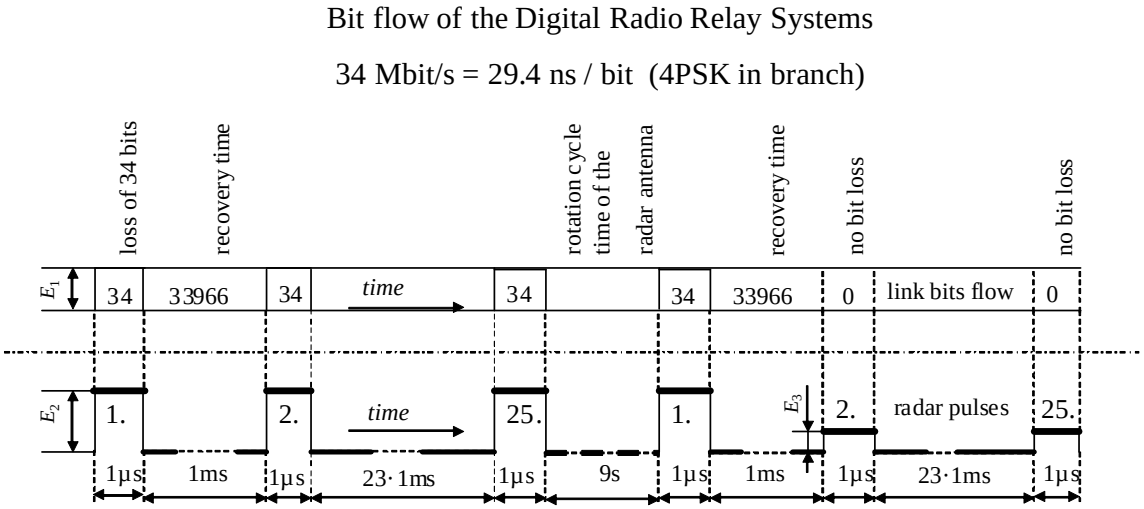

Figure 62. The interfering of a digital link shown in the time domain.

Example 7. In the following example it is shown bit by bit how a radar pulse may interfere a TDRRS. Also the example gives the typical parameters for a 4PSK link. It is assumed that the radio link recovers immediately after the interference pulse. The following technical parameters are assumed for a TDRRS link:

- Bit rate is 34 Mbit/s,
- symbol rate (R_s) is 17 MBd,
- modulation is 4PSK,
- bit length is 29.4 ns.
- flat fade margin is 34 dB and
- required *C/(N+I)* ratio is 14 dB.

Technical parameters of the radar:

- pulse length is 1 µs,
- *PRF* is 1 kHz,
- antenna lobe width is 2° and
- antenna rotation time is 9 s per revolution.

The TDRRS carrier frequency may be at any carrier frequency in the allocated frequency band and the radar spurious emission is on the same frequency.

Figure 62 shows the TDRRS bit flow (upper part) and interfering pulses produced by the radar (lower part) in the time domain. The zeroes and ones of the TDRRS bit stream are assumed to occur with the same probability (0.5). The radar antenna illuminates the link antenna 25 ms during each revolution.

When the radar spurious signal (at level E_2) is in the TDRRS frequency channel (TDRRS signal level E_1), its impact is depending on the ratio of E_1 and E_2. If the E_1 and E_2 ratio is smaller than 3 dB the radar pulse will destroy all bits that coincide with the radar pulse. Depending on the polarity of the radar signal the destroyed bits in the two-level bit stream become either ones or zeros. Because the radar pulse is much longer than one single bit, one radar pulse is capable of destroying 34·29.4 ns long bits. When the bit flow is statistically 50 % of time ones and 50 % of time zeros the demolition only applies to half of the bits (17 bits, but not consecutive bits). According to the radar *PRF* the next interfering pulse follows in 1 ms.

Between two pulses the TDRRS receiver has 1 ms time to recover from the outage caused by destroyed bits. Depending on the TDRRS error correction capability it either is disturbed or not disturbed by the destroyed bits. In addition the error correction capability affects whether the TDRRS receiver is capable of recovering within the 1 ms until next pulse arrives. After receiving 25 interfering pulses it takes 8.975 seconds before the next pulse burst arrives. The TDRRS also has this time to recover. If the system goes into non-availability state it can not recover from it because it receives every nine seconds (time of one antenna revolution in this example) a new interference pulse burst. The requirement for availability state is 10 consecutive seconds not containing severely errored seconds (as explained in Section 5.4.7).

If the synchronization is maintained during interference time, the BER in this example is $1.25 \cdot 10^{-5}$, meaning that no SES occurs but worsened minutes occur. If synchronization is lost the situation is different (in SDH systems the situation may be different). However, every ninth second will be an errored second.

When the radar spurious pulse power level (E_3) is more than 3 dB below the signal level (E_1) the interference becomes insignificant. The TDRRS returns, if possible, to availability state and begins normal operation (if fully recovered = severely errored seconds occur less than every 10 seconds).

The radar pulse length can under certain circumstances be 40 µs or longer. If the radar *PRF* stays at 1000 Hz the 40 µs radar pulse can destroy $0.5 \cdot (40 \cdot 34) = 680$ TDRRS bits. If there is an outage and the recovery time is longer than 1 ms much more error correction capability is required. The improvement of the error correction capability at the TDRRS adds the amount of bits used for correction but holds the amount of bits used for communication at a constant level (payload symbol rate stays at the same level). The radio transmission frame must allow this which leads to an increase of the total bit rate.

When the radar antenna rotation speed increases the amount of radar pulses illuminating the TDRRS antenna decrease but the recovery time between revolutions gets shorter and vice versa. The example radar can, while rotating or in operation (for example in electrical scanning), scan in many different ways so that the interfering signal does not reach the TDRRS antenna at regular intervals. The radar can also vary its pulse length, pulse repetition rate, polarization and output power. This causes the possibility for the interference effect to change. If the radar is positioned near the possibly interfered TDRRS or its pulse power is being very high (max. 10 GW) even the radar antennas side lobes can cause interferences. It is thus possible that the TDRRS described in the situations above has no time at all to recover. If the condition is as described before even farther located digital radio systems in the same frequency band are in danger of being interfered. If possible, such conditions should be avoided.

6.3 Interference caused by radar signals in the TDRRS investigated in the frequency domain

The possibly harmful interference to a TDRRS (for example radar signal) is easily seen in the frequency domain when examining the link and noise budget in Figure 53. When the interference power level (including noise) grows from −104 dBm to −97 dBm the disturbing signal level is the same as the radio link input noise power level. After this when the signal to disturbance ratio continues to decrease below 14 dB (4PSK) the possible interference degradation of the TDRRS begins. During fading this limit can vary within 34 dB.

Example 8. A radar signal, with the parameters from Example 7, equipped with a magnetron without filters (weather radar with *NF* = 5.625 GHz) may cause spurious signals in TRRS frequency band 3.600...4.200 GHz, see Figure 8. The part of radar spectrum spreading onto the TDRRS channel has a noise-like impact. When increasing, it decreases the flat fade margin value thus decreasing the signal to noise and interference ratio $C/(N+I)$ as in Figure 53.

6.4 Interference measurement and interpretation of the results

The following example shows by means of measurement in practice how the interpretation of measuring results can be completely faulty if the measurement bandwidth is not chosen adequately. The presented measurement is from a real interference case between a radar and a TDRRS radio link.

Example 9. The TDRRS spectrum when interfered by a radar signal is measured with an SA (Figure 63) and also theoretically analyzed in this example.

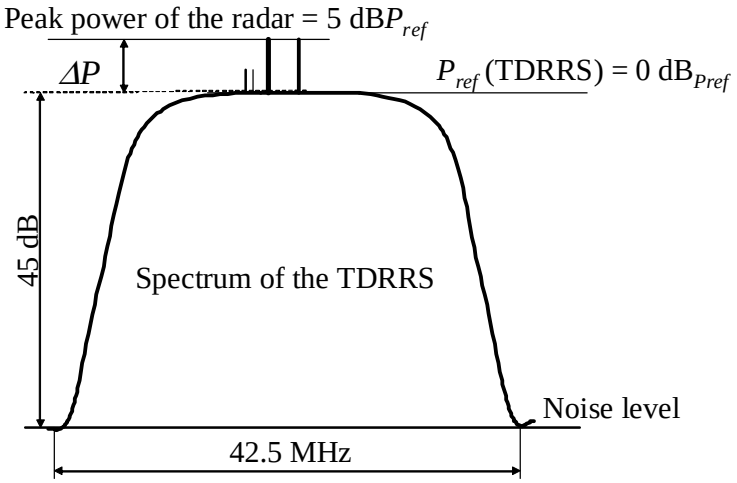

Figure 63. The radar interference spectrum on top of the frequency spectrum of a TDRRS as seen on the SA display.

SA settings: - B_{meas} is 300 kHz,

The interfered TDRRS signal:

$$R_S = \frac{R_B}{log_2(N_S)} \tag{6.1a}$$

where: - Bit rate R_B is 155 Mbit/s ,
- Modulation is 64 QAM, that gives the number of bits in a symbol N_S = 6 and
- Symbol rate = R_S .

Numerical calculation for Example 8:

$$R_S = \frac{155\ [\text{Mbit/s}]}{6} = 25.8\ [\text{MBd}] \tag{6.1b}$$

The FM compressed transmission of a radar (Equation 4.4):

- –20 dB bandwidth of the spectrum B_{20dB} = 5.5 MHz
- pulse length τ = 40 µs.

The frequency shift during the pulse duration [1]:

$$B_c \approx \frac{B_{20dB}}{2} \tag{6.2a}$$

Numerical calculation for Example 9:

$$B_c \approx \frac{5.5[\text{MHz}]}{2} = 2.7[\text{MHz}] \tag{6.2b}$$

The bandwidth B_{ref} is [1] (Equation 4.4):

$$B_{ref} = \left(\frac{B_c}{\tau}\right)^{0.5} \tag{6.3a}$$

Numerical calculation for Example 9:

$$B_{ref} = \left(\frac{2.7[\text{MHz}]}{40[\mu\text{s}]}\right)^{0.5} = 0.26[\text{MHz}] \tag{6.3b}$$

The maximum level of the TDRRS spectrum in Figure 63 is set to be the reference level P_{ref}. As shown in the figure the radar signal peaks (*RSP*) are 5 dB above the reference level.

The nearest available measurement bandwidth of the used SA is B_{meas} = 0.3 MHz. A laboratory test was made to determine the relationship between the measurement bandwidth and average and peak power levels was made with the used SA (HP8564E). A 150 Mbit/s 64QAM-signal was generated with an R&S signal generator (R&S SMJ 100A Vector Signal Generator) on 4.2 GHz. The modulating signal was a pseudo-random bit stream (PBRS23) and the pulse spectrum shape was root raised cosine with the roll-off parameter α = 0.25. Following observations were made:

1) on measurement bandwidths less than 0.3 MHz the peak power level in SA max-hold mode has an almost ideal linear dependence of the measurement bandwidth. For larger bandwidths the power increase is slightly less than linear.
2) on the measurement bandwidth 0.3 MHz the measured max-hold level is 9 dB below the average power level of the 64QAM-signal and 17 dB below the peak power level of that signal. The latter value is based on the signal generator display information.

The theoretical total average power level of the radio link transmission is:

$$P_{lin,ref} = P_{ref} + 10 \cdot \log\left(\frac{R_S}{B_{meas}}\right) ; \ when \ \ B_{meas} < R_S \qquad (6.4a)$$

where: - the reference level and the differences to the reference level are shown in Figure 63 and
- adding of the logarithmic term gives the total peak power level corresponding to the measurement bandwidth.

Numerical calculation for Example 9:

$$P_{lin,ref}\left[dBP_{ref}\right] = 0\left[\mathrm{dB}P_{ref}\right] + 10 \cdot \log\left(\frac{25.8}{0.3}\right)\left[\mathrm{dB}\right] = 19.3\left[\mathrm{dB}P_{ref}\right] \qquad (6.4b)$$

The observed peak power level is thus 2.3 dB lower.

Radar transmission peak power level:

$$P_{radar,ref} = P_{ref} + \Delta P + 20 \cdot \log\left(\frac{B_{ref}}{B_{meas}}\right) \qquad (6.5a)$$

where: - reference level P_{ref} and difference to reference level ΔP are shown in Figure 63 and
- adding of the logarithmic term gives the total power level corresponding to the measurement bandwidth.

Numerical calculation for Example 9:

$$P_{radar,ref}\left[\mathrm{dB}\right] = 0\left[\mathrm{dB}P_{ref}\right] + 5\left[\mathrm{dB}\right] + 20 \cdot \log\left(\frac{0.26}{0.3}\right)\left[\mathrm{dB}\right] = 3.76\left[\mathrm{dB}P_{ref}\right] \qquad (6.5b)$$

6.4.1 Interpretation of measured results

The measured peak power level difference of the TDRRS signal and the radar spurious signal is $P_{lin,ref} - P_{radar,ref}$. According to Example 9 with the numerical values inserted the power level difference is 17 dB P_{ref} (Equation 6.4b) − 3.76 dB P_{ref} (Equation 6.5b) = 13.2 dB.

The result according to the spectrum in Figure 63 shows the radar spurious signal level to be 5 dB higher than the signal level of the TDRRS. However, according to the calculations above, the radar spurious signal level is 15.5 dB lower than the TDRRS signal.

The difference is completely depending on the selected measurement bandwidth. Depending on the demanded peak signal to noise ratio the TDRRS either goes into error state or not. In this example the *C/N* ratio required for 64QAM is according to Table 5 29 dB (with a bit error rate of 10^{-3}). This corresponds to a peak signal to noise ratio 29 dB + 8 dB = 37 dB. With the values in this example the TDRRS operation will probably be harmfully interfered by the radar spurious signals. This is valid for errored seconds, the generation of severely errored seconds depends on the TDRRS recovery time.

6.4.2 Theoretical method for estimation of protection distance between a radar and a TDRRS

The following example shows how the radar minimum distance is determined for a radio link in different TDRRSs interfered by a radar with given parameters when using free space attenuation and ITU diffraction and Siwiak's scatter attenuation models.

Example 10. The minimum distance of a radar to a TDRRS receiver for not causing harmful interference is estimated with the following parameters of the interfering radar and TDRRS:

- let the link span and the radar be in same direction,
- radar *NF* is 5.625 GHz,
- equivalent radiated radar peak power level is +128 dBm,
- *X* is the required power level difference between *SF* and *NF*,
- TDRRS f_{NF} is 4200 MHz and
- modulation method is 4PSK or 64QAM, bit rate 34 Mbit/s.

4PSK:

When the required signal level at the receiver input under standard propagation conditions of the TDRRS (f_{NF} is 4.200 GHz) is $P_{rx} = -49$ dBm, the flat fade margin being M = 34 dB and the $C/(N+I) = \Gamma$-ratio requirement being 14 dB (as shown in Figure 64) the spurious signal may not exceed

$$P_{SF,max} = P_{rx} - M - \Gamma - 7 \, . \tag{6.6a}$$

The term 7 comes from the fact that a spurious signal with a level 6 dB less than the noise level will increase the total disturbance by about 1 dB. It is assumed that this interference level would not cause significant increase of SES- and ES-values. If the actual spurious level is

$$P_{SF} = P_{NF} - X \tag{6.6b}$$

the maximum *NF* level at the TDRRS input of

$$P_{NF,max} = P_{SF,max} + X \, . \tag{6.6c}$$

If the radar *SF*-level just fulfills the requirement to be –100 dBc, this results in a maximum *SF*-level at the input of the TDRRS receiver of –4 dBm. The attenuation due to the distance between the radar and the TDRRS receiver and the direction dependent gain of radio link antenna must together attenuate the radar pulse peak power at *NF* to below $P_{NF,max} = -4$ dBm at the TDRRS input.

In Figure 64 the basic data for determination of the minimum distance *d* of a radar from a TDRRS receiver is shown.

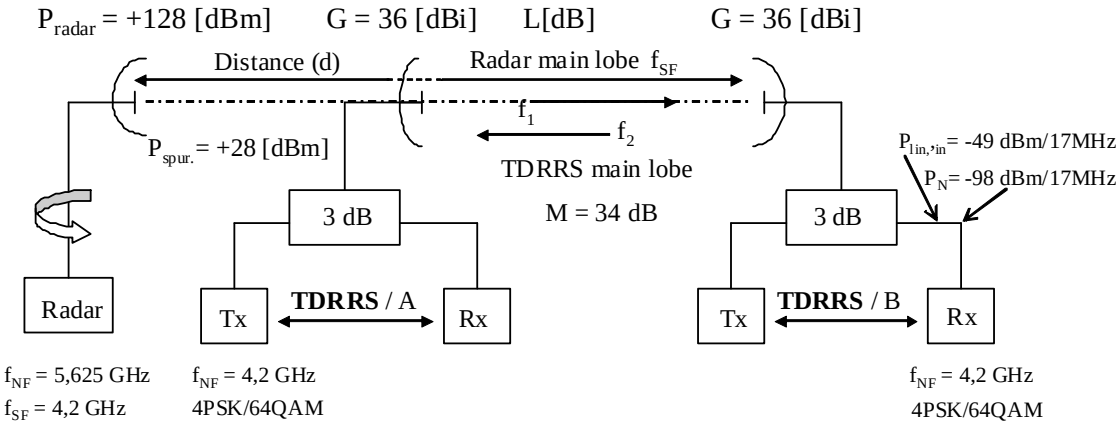

Figure 64. Block diagram and power budget parameters of a TDRRS interfered by a radar located within the TDRRS receiver antenna main lobe.

With help of the radar / link budget the required propagation loss *L* is determined. The radar spurious signal at the TDRRS input should not exceed –4 dBm. With values in Figure 64 –4 dBm is achieved when a balance equation is fulfilled:

$$P_{N,lin,\max} = P_{SF\max} + X = P_{radar} - L + G_{lin,ant} - A_{dup} \tag{6.7a}$$

where:
- $P_{N,lin,max}$ is the maximum *NF* power level at the link receiver input,
- $P_{SF,max}$ is the maximum *SF* power level at the link receiver input,
- *X* is the difference between *NF* and *SF* signal level
- P_{radar} is the maximum radiated *NF* power at radar antenna,
- *L* is the loss depending on the chosen situation (using free space attenuation when the radar propagation path is within line-of-sight or using ITU-R P.530- 12 diffraction loss model in the non-line-of-sight case or Siwiak's scatter loss model [48],
- $G_{lin,ant}$ is the radio link antenna gain at link station B (includes feed line loss),
- A_{dup} is the duplexer attenuation at the receiver side,
- the radar is within the main lobe of the TDRRS B-antenna.

Solving for *L* gives:

$$L = P_{radar} - P_{SF,\max} - X + G_{lin,ant} - A_{dup} \tag{6.7b}$$

Numerical calculation for Example 10 when 4PSK is used.
The maximum spurious level is obtained with Eq. 6.6

$$P_{SF.max} = -49 - 34 - 14 \ -7 = -104 \text{ [dBm]} \tag{6.7c}$$

When the radar maximum spurious level fulfills the ITU requirement *X* = 100 dB the minimum required path loss is:

$$L = 128[\text{dBm}] - (-104)[\text{dBm}] - 100[\text{dB}] + 36[\text{dB}] - 3[\text{dB}] = 165[\text{dB}] \quad (6.7d)$$

64QAM:

It is assumed that the received power level is the same as in 4PSK ($P_{lin,in}$ = –49 dBm). The receiver noise figure is also assumed to be the same. The bit rate is also unchanged which means that the signal bandwidth and thus the noise power level is reduced by $10 \cdot \log(N_{bit,64QAM}/N_{bit,4PSK}) = 10 \cdot \log(6/2) = 4.77$ dB. Then

$$P_{N,64QAM} = P_{N,4PSK} - 10 \cdot \log\left(N_{bit,64QAM} / N_{bit,4PSK}\right) \quad (6.8a)$$

This implies a change in the flat fade margin:

$$M_{64QAM} = P_{lin,in} - P_{N,64QAM} - \Gamma_{64Q4} \quad (6.8b)$$

The maximum spurious level is obtained with Eq. 6.6

$$P_{SF,max} = -49 - 24.8 - 29 - 7 = -109.8[\text{dBm}] \quad (6.8c)$$

When the radar maximum spurious level fulfills the ITU requirement X = 100 dB the minimum required path loss is with:

$$L = 128[\text{dBm}] - (-109.8)[\text{dBm}] - 100[\text{dB}] + 36[\text{dB}] - 3[\text{dB}] = 170.8[\text{dB}] \quad (6.8d)$$

The L-values are composed of three terms:

$$\text{propag.att.} = \text{constants} + \text{influence of freq.} + \text{influence of distance} \quad (6.9)$$

Literature provides many propagation models for calculating (or estimating) propagation loss. Some of the most typical models are listed as follows:

- free space attenuation model, used when no obstacles are present in the signal path (line of sight free),
- ITU diffraction attenuation model ITU-R P.530-12 [46], beyond horizon propagation model,
- ITU beyond the horizon attenuation model ITU-R P.1546-2 [47], (by extrapolation this model is valid up to 5...6 GHz) and
- the Siwiak [48] empiric tropo scatter attenuation model (also curves), beyond horizon propagation model.

The free space attenuation (L_{fs}) model is given by

$$L_{fs} = 32.45 + 20\log(f) + 20\log(d) \quad (6.10a)$$

where:
- the constant 32.45 dB is used with frequency in [MHz] and distance in [km],
- f is the frequency in MHz and
- d is the distance in km.

This gives the minimum distance between the radar and the TDRRS receiver:

$$d = 10^{0.05\left(L_{fs} - 32.45 - 20\log(f)\right)} \tag{6.10b}$$

Calculation example with numerical values from Example 10:

4PSK: $$d = 10^{0.05\left(165 - 32.45 - 20\log(4200)\right)} = 1009.8\,\text{km} \tag{6.10c}$$

64QAM: $$d = 10^{0.05\left(170.8 - 32.45 - 20\log(4200)\right)} = 1969.0\,\text{km} \tag{6.10d}$$

The distances calculated here are only valid if the TDRRS and radar antenna radio waves are refracted along the Earth's surface and there are no obstacles in the propagation path. In this situation the *k*-value of the atmosphere increases towards infinite. The *k*-value might even turn negative. This would mean that the propagating radio signal would curve towards earth surface and may reflect from the surface. This makes it possible for the signal to travel long distances by hopping along the surface while attenuating almost as in free space propagation.

The obtained values are purely theoretical distances and they do not correspond to normal operating ranges. However, long connection distances may occur at some small time percentage (for example 0.1 % of time) when super-refraction causes infinite or negative k-values to occur. During normal propagation conditions a radar signal propagates with far higher attenuation if traveling beyond the horizon than in free space. Under typical conditions in Finland with practical antenna heights it turns out that a radar station may be located a few ten kilometers beyond the radio horizon. This is due to the effect of the diffraction and tropospheric scattering attenuation beginning to increase rapidly beyond line of sight. The free space attenuation distance slope is 20 dB / decade. According to Siwiak [48] at 5.0 GHz measurements show that the attenuation distance slope is 70...80 dB / decade (±10 dB) for scattering beyond the radio horizon.

It is more realistic to calculate the radar minimum distance due to spurious interference with the free space model up to the radio horizon and beyond the radio horizon with for example the ITU P.617-1 [49] diffraction model.

The total path loss on a beyond the horizon path using the excess diffraction loss according to [46] can be estimated from the equation

$$L = L_{fs} + L_{diff} = 32.45 + 20 \cdot \log(f) + 20 \cdot \log(d) + 10 + 20\frac{c}{R_{F1}}\left[\text{dB}\right] \tag{6.11a}$$

where:
- f is the TDRRS carrier frequency in MHz,
- d is the distance between the radar transmitter and the disturbed TDRRS receiver in km,
- c is the height of the leading obstacle above the virtual line-of-sight in m and
- R_{F1} is the radius of the first Fresnel-zone at the leading obstacle in m.

The *c*-parameter is obtained by trigonometric analysis on a simplified path geometry shown in Figure 65, where it is assumed that the obstacle is on the height *h* and the antennas on heights h_t and h_r above the reference earth with the equivalent radius R_{eq}. The expression for *c* is

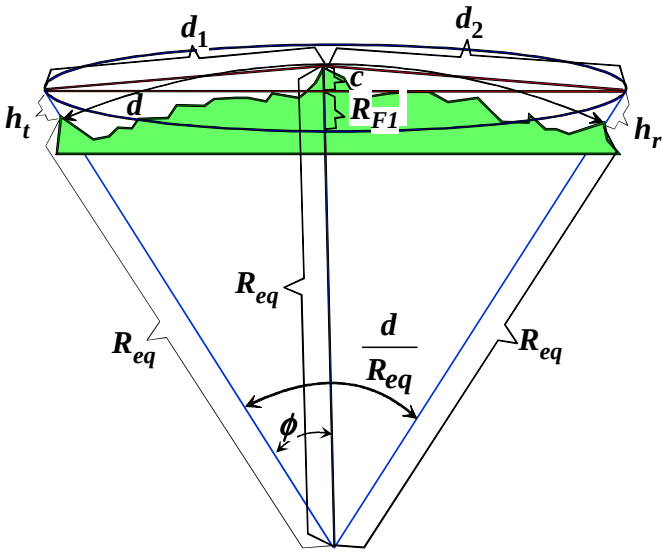

Fig. 65. Radio link geometry for the estimation of excess diffraction loss according to ITU-R Rec. P530.

$$c = 2\left(R_{eq} + h_r\right)\sin^2\left(0.5\Phi\right) - h_t + h \tag{6.11b}$$

$$\Phi = \arctan\left(\frac{h_t - h_r + 2\left(R_{eq} + h_r\right)\sin^2\left(\frac{d}{2R_{eq}}\right)}{\left(R_{eq} + h_r\right)\sin\left(\frac{d}{R_{eq}}\right)}\right) \tag{6.11c}$$

and the expression for the radius of the first Fresnel zone is

$$R_{F1} = \sqrt{\frac{\lambda d_1 d_2}{d_1 + d_2}} \tag{6.11d}$$

where: - λ is the wavelength of the carrier wave and

$$d_1 = \sqrt{\left(h_t - h\right)^2 + 2\left(R_{eq} + h_t\right)\left(R_{eq} + h\right)\sin^2\left(\frac{\Phi}{2}\right)} \tag{6.11e}$$

$$d_2 = \sqrt{\left(h_r - h\right)^2 + 2\left(R_{eq} + h_r\right)\left(R_{eq} + h\right)\sin^2\left(\frac{d}{2R_{eq}} - \frac{\Phi}{2}\right)} \tag{6.11f}$$

Under the same assumption as above of having the same received power level and bit rate in all modulation methods and the same noise figure and applying the same calculation methods for achieving the required radar signal path loss and minimum distance as before (Equations 6.11a…6.11f) the minimum distances under free space propagation conditions and in diffraction conditions according to [46] in Table 7 are obtained.

Table 7. Minimum distance between interfering radar and TDRRS receiver

Modulation system	Γ/dB	M/dB	L/dB	Free-space Distance / km	ITU-R P.530-10 Distance / km
4PSK	14	35	165	1010	68.8
16QAM	23	29	169	1601	72.4
32QAM	25	28	170	1797	73.3
64QAM	29	24.8	170.8	1970	74.0
128QAM	32	22.4	171.4	2111	74.7

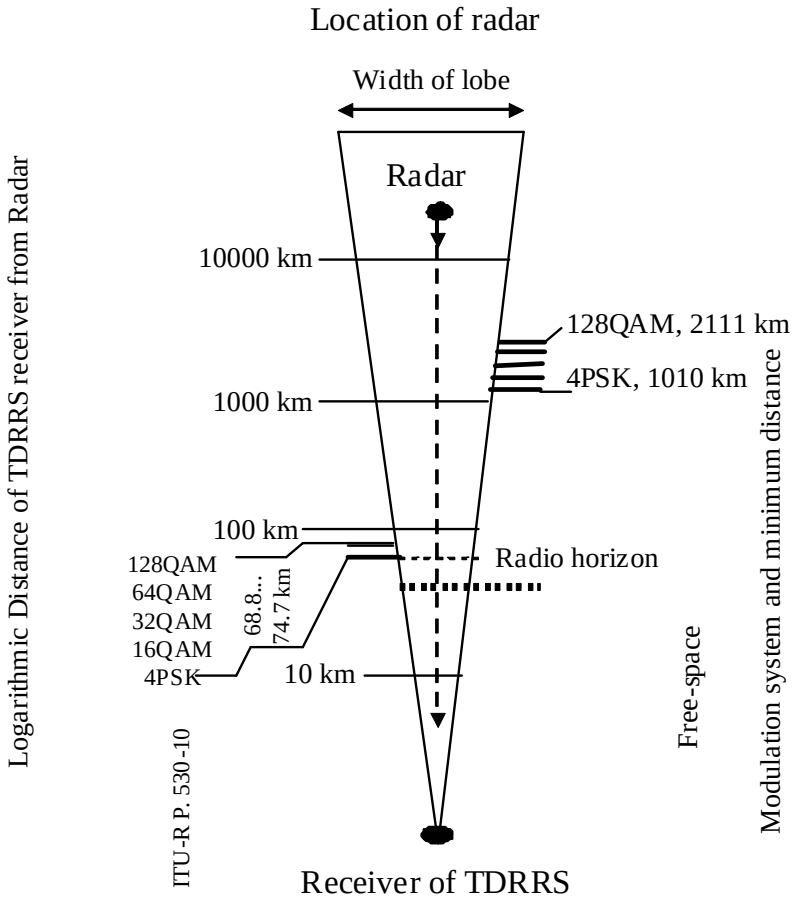

Figure 66. Minimum interference distances for free space loss and for diffraction attenuation from radar to link when link modulation is 4PSK…128QAM

The minimum distances between an interfering radar with in the TDRRS receiver antenna main lobe are graphically shown in Figure 66. The figure shows clearly, how huge the difference is between free space loss and the diffraction attenuation model. In the diffraction model the attenuation increases very fast beyond the horizon.

Outside the TDRRS receiver antenna main lobe direction the minimum radar distance will depend on the antenna radiation pattern. It is given by the expression

$$L = P_{radar} - P_{SF,\max} - X + G_{lin,ant}(\theta) - A_{dup} \tag{6.12a}$$

where: θ is the direction of the radar with respect of the TDRRS receiver l.o.s. direction. The minimum distance of the radar as function of θ is determined as before.

The following example shows how the interfering radars minimum protect distance is defined when an ITU reference link antenna is used. The minimum distance towards the TDRRS is presented both graphically and in table form.

Example 11. It is assumed, that the TDRRS (modulation method 64QAM) is located in Helsinki (A station) and its antenna is directed toward north (B station). The distance between stations A and B is 50 km. At both ends of the link span the antenna height is 100 m and the radar antenna height is 10 m. Further, it is assumed that the TDRRS receiver antenna radiation diagram is that given in ITU-R Recommendation F.699 [45]. When $D/\lambda \leq 100$ the antenna radiation pattern is then:

$$G(\theta) = \begin{cases} G_{\max} - 0.0025\left(\dfrac{D}{\lambda}\theta\right)^2, & |\theta| \in [0, \theta_m) \\ G_1, & |\theta| \in \left[\theta_m, 100\dfrac{\lambda}{D}\right) \\ 52 - 10\cdot\log\left(\dfrac{\lambda}{D}\right) - 25\cdot\log(\theta), & |\theta| \in \left[100\cdot\dfrac{\lambda}{D}, 48\right) \\ 10 - 10\cdot\log\left(\dfrac{\lambda}{D}\right), & |\theta| \in [48, 180) \end{cases} \tag{6.12b}$$

$$\theta_m = 20\cdot\frac{\lambda}{D}\sqrt{G_{\max} - G_1} \tag{6.12c}$$

$$G_{\max} = 7.7 + 20\cdot\log\left(\frac{D}{\lambda}\right) \tag{6.12d}$$

$$G_1 = 2 + 15\cdot\log\left(\frac{D}{\lambda}\right) \tag{6.12e}$$

where:
- θ is the horizontal angle compared to pattern in degrees
- D is the parabolic antenna reflector diameter in m
- λ is carrier wavelength in m
- G_{max} is the antenna pattern gain in dBi
- G_1 corresponds to the maximum gain of the first side lobe.

In the example it is assumed that the bore-sight gain of the TDRRS antenna is 40 dBi and the radar EIRP is 128 dBm. The D/λ–ratio can be determined from Equation 6.13a:

$$G_{\max} = 7.7 + 20 \cdot \log\left(\frac{D}{\lambda}\right) \rightarrow \frac{D}{\lambda} = 10^{0.05(G_{\max} - 7.7)} = 10^{0.05 \cdot (40 - 7.7)} = 41.2 \quad (6.13a)$$

From this follows that

$$G_1 = 2 + 15 \cdot \log\left(\frac{D}{\lambda}\right) = 2 + 15 \cdot \log(41.2) = 26.2 \ [\text{dBi}] \quad (6.13b)$$

and

$$\theta_m = 20 \cdot \frac{\lambda}{D} \cdot \sqrt{G_{\max} - G_1} = \frac{20}{41.2} \cdot \sqrt{40 - 26.2} = 1.80° \quad (6.13c)$$

$$100 \cdot \frac{\lambda}{D} = \frac{100}{41.2} = 2.43° \quad (6.13d)$$

The radiation pattern is shown in Fig. 67.

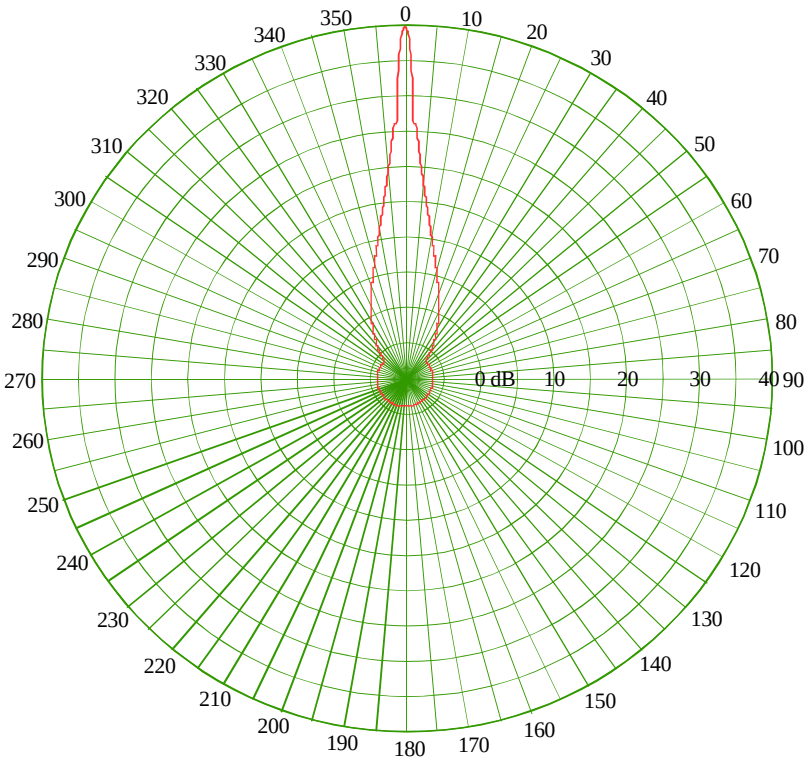

Fig. 67 Radiation diagram of the ITU reference antenna.

In this example the radar *NF* is assumed:

i) to be inside the TDRRS signal bandwidth, (This situation may occur if the radar is located in another country)
ii) to be offset so that the TDRRS receiver filter attenuates the radar signal by 25 dB,
iii) to be offset so that the TDRRS receiver filter attenuates the radar signal by 40 dB.

In this case the maximum level of the radar signal in the TDRRS receiver input may be

$$P_{NF,lin,\max} = P_{radar} - L_{path} + G_{lin,ant} - A_{dup} \tag{6.14a}$$

From the above expression the required minimum path loss of the radar signals:

$$L_{path} = P_{radar} - P_{NF,lin,\max} + G_{lin,ant} - A_{dup} \tag{6.14b}$$

The maximum radar peak power level in the TDRRS receiver input is now given by the expression

$$P_{NF.lin,max} = P_{rx} + L_{rx\text{-}filter} - M - \Gamma - 7 \tag{6.15a}$$

This gives finally the required minimum path loss of the radar signal:

$$L_{path} = P_{radar} - P_{rx} - L_{rx\text{-}filter} + G_{lin,ant}(\theta) - A_{dup} + M + \Gamma + 7 \tag{6.15b}$$

Assuming a worst case with free space propagation regardless of the distance the minimum distance of the radar from the disturbed TDRRS receiver is given by Equation 6.16a

$$d = 10^{0.05\cdot\left(L_{path}-32.45-20\cdot\log(f)\right)} \tag{6.16a}$$

With the above and earlier defined system parameters for 4PSK the following numerical values are obtained in the TDRRS bore sight direction:

$$L_{path} = 128-(-49)-0+40-3+35+14+7 = 270 \text{ dB} \tag{6.16b}$$

$$d = 10^{0.05\cdot(270-32.45-20\cdot\log(4200))} = 179600 \text{ km} \tag{6.16c}$$

The result shows that under super-refractive propagation conditions there is no possibility for co-existence of radar and co-channel radio communication systems. This is also true for other direction than bore sight of the radio link receiver antenna.

Next the minimum protection distances are investigated when tropospheric scattering is the main propagation mechanism. The EIRP power level of the radar *NF* signal at the TDRRS antenna output is assumed to be 59 dBm. The path loss is estimated using Siwiak's tropo-scatter loss model [48]. The path loss expression is

$$L = 20\cdot\log\left(\frac{h_r h_{lin}}{(1000d)^2}\right)+10\cdot\log\left(\frac{1+\left(\frac{d}{d_{hor}}\right)^7}{1+\left(\frac{d}{d_{hor}}\right)^3}\right) + 22+\frac{f}{2000}\cdot\log\left(\frac{100}{f}\right)-\frac{d}{13+77\left(\frac{d_{hor}}{d}\right)} \tag{6.17a}$$

where - d_{hor} is the sum of the distances to the radio horizon of both antennas,

$$d_{hor} = 3.571\cdot\sqrt{k}\cdot\left(\sqrt{h_r}+\sqrt{h_{lin}}\right) \tag{6.17b}$$

In Equations 6.17a and 6.17b the variables are the following:

- h_r is the radar antenna height above a reference level in m,
- h_{lin} is the TDRRS receiver antenna height above the same reference level in m,
- d is the distance between the radar antenna and the TDRRS receiver antenna in km
- f is the *NF* of the TDRRS in MHz and
- k is the tropospheric refraction factor, k = 1.6 in this example.

Additionally it is expected that other TDRRSs must not be taken into account.

When the path loss is known, the minimum radar protection distance can be solved numerically from Equation 6.16. The path loss is shown for a few frequencies in Figure 68.

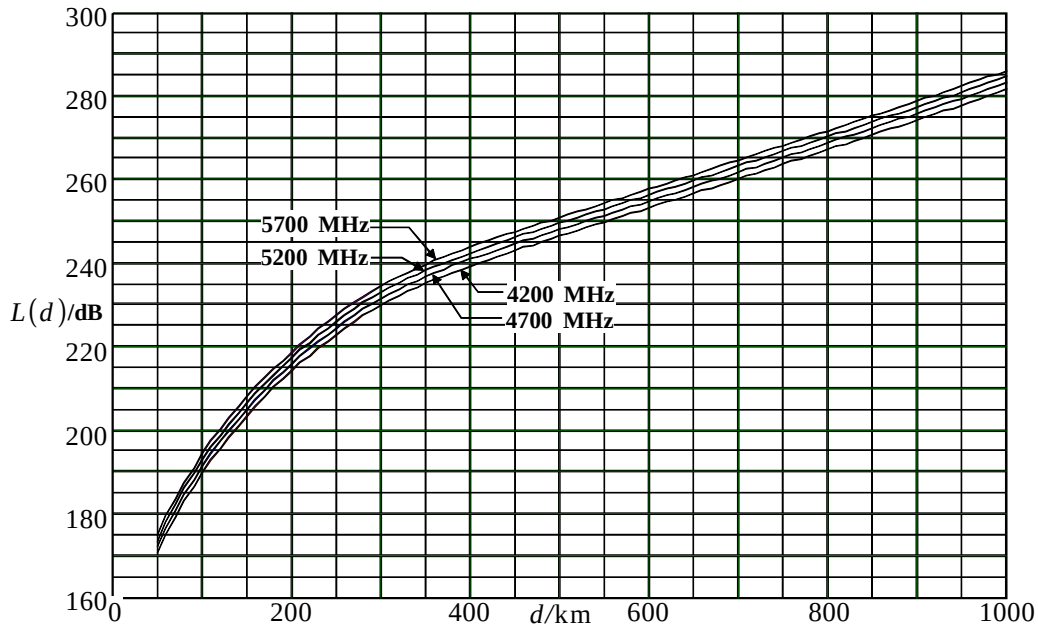

Figure 68. Troposcatter path loss with Siwiak's propagation model.

Calculation of minimum co-channel radar protection distance has been performed for different TDRRS modulation methods assuming a constant bit rate and for three radar NF-values giving 0 dB, 25 dB and 40 dB attenuation in the radio link receiver filter. The minimum protection distances for 64QAM are given in Table 8 and graphically shown in Figure 69, where they are overlaid on a map of Finland. Corresponding results for 4PSK, 16QAM, 32QAM, and 128QAM are given in Appendix 6.

The red curve Figure 69 shows that if a 64QAM receiver is located in Helsinki with the bore-sight direction to the north, the use of the example co-channel radar should be prohibited in a large part of Finland. A frequency off-set giving 25 dB filter attenuation would improve the situation, but still a minimum radar protection distance of 550 km in the bore-sight direction and 150 km in the west and east directions (blue curve). A frequency off-set giving 40 dB filter will give minimum radar protection distance of 350 km in the bore sight direction and 100 km in the west and east directions (black curves). However, the ITU antenna radiation pattern is rather pessimistic, and in practice the minimum protection distances are somewhat smaller. In super-refractive propagation situations the interference situation is much worse.

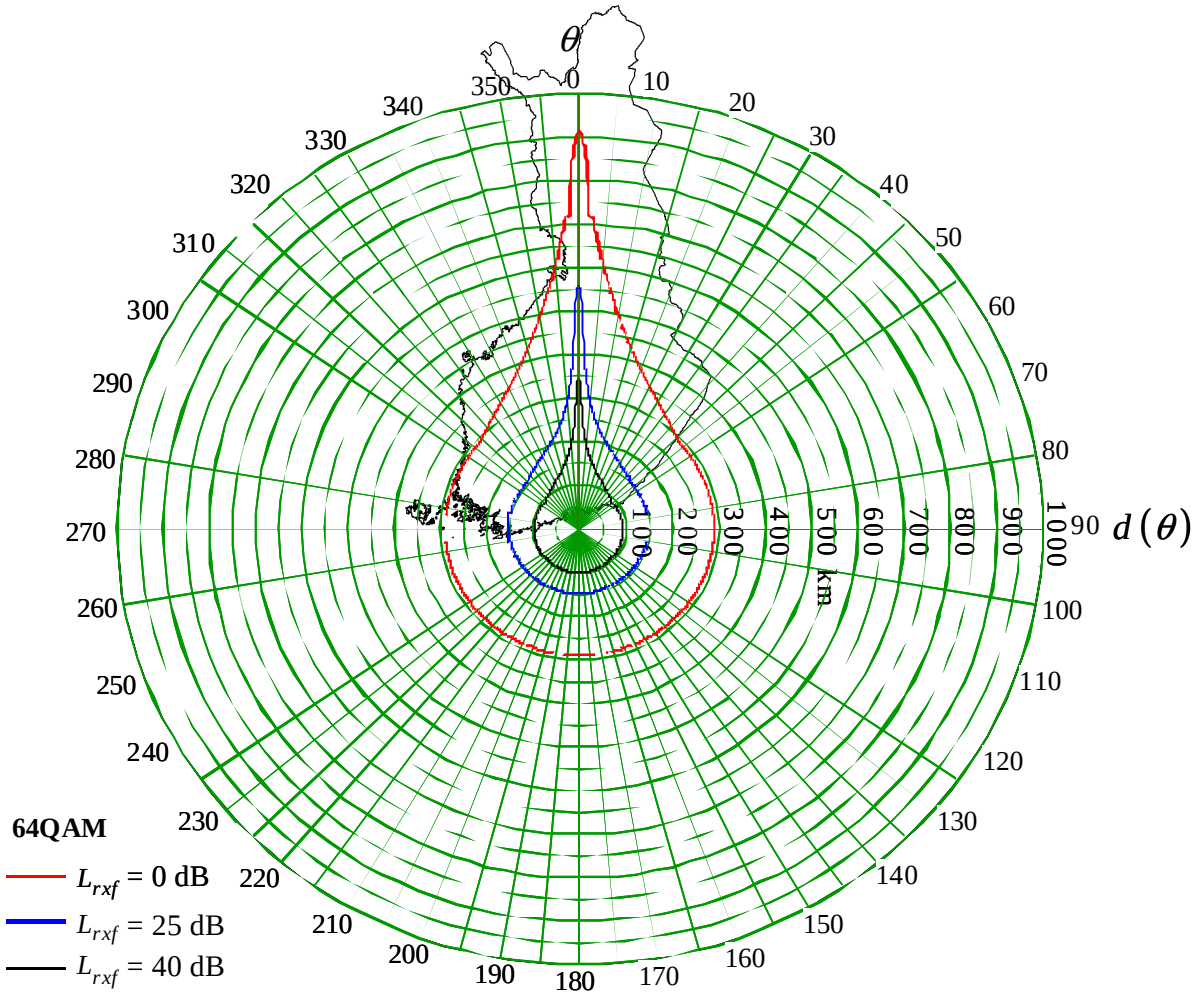

Fig. 69. Radar protection zones with 64QAM.

Table 8. Protection zone radii for 64QAM

θ	$G(\theta)$/dBi	L/dB (L_{rxf}=0)	d/km (L_{rxf}=0)	L/dB (L_{rxf}=25)	d/km (L_{rxf}=25)	L/dB (L_{rxf}=40)	d/km (L_{rxf}=40)
0°	40.0	274.8	911	249.8	553	234.8	348
±1°	35.8	270.6	852	245.6	491	230.6	307
±1.5°	30.5	265.2	777	240.2	415	225.2	266
±(1.8°…2.43°)	26.2	261.0	717	236.0	362	221.0	239
±5°	18.4	253.2	603	228.2	288	213.2	196
±10°	10.9	245.7	492	220.7	237	205.7	160
±20°	3.3	238.1	387	213.1	195	198.1	129
±(48°…180°)	–6.1	228.7	291	203.7	152	188.7	97

6.5 Checking the minimum radar distance by measurements

As the local radio wave propagation characteristics (e.g. terrain profile, climate type etc.) may differ from those where the scattering loss and diffraction loss models are derived, it is essential to check by measurement the radar interference level of a radar located according to the protection distance estimate.

This measurement can be done with the measurement system described in Chapter 5 (Step 3). This system is modified from the new system described in Chapter 4 where the BS-filter and LNA are replaced by the interfered TDRRS receiver antenna system and receiver RF and IF parts. Then the propagation path of the radar interference remains unchanged in the check measurement and the dynamic range of the measurement system is sufficient.

Although a checking measurement is highly desirable, it has still not been possible to perform such a measurement. This would require cooperation between the measuring party and the TDRRS operator.

6.6 Summary of Chapter 6

The chapter starts with a description of the impact of an interfering radar on the bit error rate performance of a TDRRS radio link. An example demonstrates how a plateau is created in the BER vs. received TDRRS level behavior when the interference level exceeds the TDRRS noise level. For proper transmission quality a higher receive level corresponding to the width of this plateau is necessary.

The error generation by strong radar interference is studied on bit level in a simple time domain analysis. Assuming immediate performance recovery after each radar pulse a BER estimate is easy to obtain, if the recovery time is larger the BER estimation is difficult. With recovery times causing severely errored seconds the TDRRS will go in unavailability state due to too strong radar interference. The investigation of radar interference in the frequency domain is studied with a measured interfered TDRRS signal spectrum.

A theoretical approach to the determination of the minimum distance of a radar to a TDRRS receiver is based on the assumption that the impact of the interference is negligible if its level is at least 6 dB lower than the TDRRS receiver noise power level. From this a minimum loss of the radar signal is derived for each type of TDRRS modulation. The minimum distance is obtained via the radar link power budget assuming free space and diffraction or scatter loss propagation models. Numerical results are given and presented in graphical form for four linear modulation methods using a TDRRS reference antenna pattern defined by ITU and assuming co-channel radar operation.

The radar measurement described in Chapter 4 and modified as described in Chapter 5 can be used to check the sufficiency of the minimum distance obtained by the theoretical method described in this chapter. However, it has not been possible to perform such tests. This checking is in practice important and should be a topic for further research.

The procedure of estimating and checking the protection distance between a radar and a TDRRS radio link can be summarized as follows:

- Definition of DRRS characteristics
  - carrier frequency
  - modulation method
  - bit rate
  - radio link budget
- Determination for maximum allowed radar interference level

- it is assumed that a level that is 6 dB below the noise level in the reference point would not increase significantly the amount of SES or ED in the TDRRS

- Estimation of the protection distance
  - measuring the highest interference level of the radar in the actual TDRRS channel using e.g. the new measurement system described in Chapter 4.
  - calculated with the radar link budget using free space propagation loss in a free space propagation situation
  - calculated with the radar link budget using the ITU-R Recommendation P530 diffraction loss model or Siwiak's troposcatter model and using the model that gives the larger protection distance.
- Checking the sufficiency of the implemented protection distance
  - Measuring the radar interference level within the TDRRS channel using the modified version of the new measurement system described in Chapter 5.
  - If necessary, the protection distance may be changed.

7. SUMMARY

7.1 Research items

In this work a new measurement system for measuring radar spectrum has been developed. The measurement procedure consists of two stages, the time domain parameter study and the spectrum measurement. In the first stage the availability of radar pulses and their properties are analyzed in the time domain. This also creates needed parameters for the second stage of the measurement. In that stage the frequency spectrum generated by real radar pulses is measured resulting in the power level of SF-components relative to the NF component power level.

The measurement system presented in this work is suitable for checking the predicted area of interference of the radar to TDRRSs. The prediction is based on both calculating and measuring of absolute and relative power levels. This is done for both the interfering and the interfered transmission at the same measurement point.

7.2 Application of the new measurement system

The measurement system created by the author is based on frequency sweeping and complies with ITU recommendations concerning measurement of radar spurious emission. The dynamic range of this system meets and exceeds ITU recommendations. The ITU requirement for spurious transmissions of weather radar, operating in the C-band, is at its tightest (–100 dBc) when the *SF* is at least 320 MHz lower or higher than the *NF*. This measurement system has been applied successfully for measuring weather radar *SF* spectrum. The maximum peak pulse power level of weather radar can be up to 10 GW. When used without output filters, this radar can according to measurements produce a relative power level of (–60 dBc) at a frequency deviating 1 GHz from the radar *NF*.

In this work this new measurement system has been used to measure weather radar *SF* spectrum. The weather radar interference area has been determined assuming a TDRRS using a set of QAM-modulation methods. As propagation models the free space propagation model has been chosen up to the point of radio horizon and the ITU-R P.530-12 diffraction model and Siwiak's tropo-scatter model for beyond horizon propagation. These propagation models have been used in frequency planning by the Finnish Communications Regulatory Authority (Equation 6.11). Also propagation path loss curves for tropospheric scattering by Siwiak [48] have been used in radar frequency planning.

7.3 Comparison of the new measurement method with previous measurement methods

The new measurement system has been implemented by using simpler measuring devices than is usually done for this kind of measurement. The system has proven capable for field operation and gives satisfactory accuracy which makes this new system very useful for radar inspection measurements carried out by the frequency regulator. Because of its field capability and simplicity of measurement equipment the measurement system has also proven to fulfill the measurement requirements of wide frequency range interference measurements. These requirements are often set by measurement locations (towers etc.).

This measurement system makes it possible to estimate and optimize the time needed for measurement.

This measurement system has also been used in rural environments where electric mains are not available. Due to the field capability of the measurement equipment transportation has been no problem. The measurement system can be powered with help of a movable generator.

The new method presented here and other existing measurement methods are all based on the same principle that is outlined in the ITU Recommendation [1]. The high-level *NF* component is attenuated and the *SF* components are amplified so that they reach the same level at the SA input (the total maximum input level of the SA). Thereby the power level of each *SF* component relative to the peak *NF* level is easily readable (the sum equals the sum of *NF* attenuation and LNA gain). Correspondingly the measurement dynamics is the readable as the difference between the *NF* power level and the noise power level of the measurement system.

The time domain parameter analysis in the new method is a new feature. The new method also outlines how unknown radar emissions are mapped. Neither the ITU recommendation nor the other methods treat these aspects.

In many previously measurement systems a YIG-filter is used to attenuate the *NF*-component. As YIG-filters have poor field capability the new method uses only tunable band-stop filter to suppress *NF*.

ITU uses in its method two different antenna solutions, either measuring without or with the radar antenna. ITU Recommendation SM-329-10 presents a measurement system block diagram where the radar signal is taken from the radar antenna feeder line [5]. In the new method the radar antenna is always included with the measuring site in the antenna far field, thus taking into account the antenna characteristics in the measurement result.

In the ITU method the measurement is made on discrete frequencies in the SA 0-span mode. In the new method a swept measurement is made in the SA max-hold mode. With synchronized sweep the entire frequency range can be measured with a single mid-frequency setting (depends on the SA limitations).

User experience of the new method shows sufficient field capability and the measurement system enables radar equipment inspections and disturbance investigations that the regulatory authority performs. The implemented system is dimensioned to allow the use of simple, cheap and field capable equipment. The measurement accuracy is estimated to be ±3 dB. For the ITU measurement system a ±2 dB accuracy is promised. DTIC states an accuracy of ±1 dB [9] for their system when every frequency point measurement lasts for 5 minutes. Field capability information of other systems is not given.

The shortest possible measurement time is achieved when the SA sweep is synchronized to the radar antenna rotation. In this case the sweep starts during a new illumination from the frequency where is stopped at the end of the previous illumination. In the NTIA report 94-313 [4] the same measurement time is achieved with a single sweep over the full frequency range using SA max-hold mode. With a 2 MHz *FW* and a 444 MHz frequency range the measurement lasts 2000 s. With the DTIC measurement method [9] the same frequency range is measured in 18.5 hours.

The dynamic range of the ITU and NTIA measurement methods estimated to 120...130 dB. The calculated dynamic range of the new method is 140 dB. However, due to signal leakage in the measuring equipment the achievable dynamic range is in order of 120 dB.

It is shown in detail in this work how the interfering of a TDRRS by a radar signal progresses when the new measurement method is applied. Corresponding applicable methods have been proposed by NTIA [7], CCIR [11], and Telecom Denmark [12]. The

presentation of new method in this work gives a much more detailed application description including calculations and as an application the checking of the theoretically calculated protection distance to a radar station. The unconditionally highest dynamic range of the interference measurement is obtained by using the TDRRS receiver antenna and RF stage as LNA otherwise using the equipment in the new measurement system.

The new measurement system can be easily modified for other tasks. In this work it has been adapted for measurement of radar interference into TDRRS receivers.

7.4 Accuracy and limitations

The accuracy of the measurement is estimated by the measurement error. This is influenced by errors caused by the system equipment and the persons performing the measurement. The accuracy of the measurement system presented in this work can be evaluated separately for time domain parameter measurements and spectrum measurements. First one can estimate the errors caused in the time domain parameter measurement. These can be either true or false'. For example lack of a pulse would be a fatal error when the correct result would require this pulse. Second, in unsynchronized spectrum measurements errors may occur if the measurement time used is too short (the measurement result has no time to settle). An unnecessary long measurement time may collect irrelevant spectrum components on the SA display, when using the MAX-HOLD mode (sparks etc.). Errors in the frequency domain are caused by inaccuracy of the measurement equipment. SA overload may cause errors in the relative measurement results. Also the out of band steepness of the filter can cause errors due to its abnormal behavior.

When estimating the relative measurement result, errors are caused for example in reading measurement values. Additionally, most measurement system errors become insignificant, when seen relative to each other (drift of equipment).

An absolute error, that in reality is not known exactly, can be estimated from the square root of the sum of the single squared independent errors. Single errors in this measurement system under these circumstances can be caused by several reasons:

- Do the time domain parameters correspond to the measurement system settings in the frequency domain
- or can they be adjusted to meet each other,
- accuracy of the measurement equipment (SA) and its own noise figure,
- overload of the measurement equipment (SA),
- accuracy of the attenuator,
- accuracy of the filter and its calibration curve,
- accuracy of the amplification curves of amplifiers and antennas,
- accuracy of loss of cables, connectors and adapters and
- the readout accuracy of measurement equipment when operating on recommended power levels.

It is difficult to estimate the accuracy of measurement results of the impact of interference to other radio communication links, because these are not dependent on the accuracy or reliability of measurement systems. These are dependent on the technique used by the interfered radio communication system, its capability to withstand interference and its capability to recover from interference. In practice the above impact of interference can be estimated for example by error rate measurements and outage measurements of the interfered radio communication system. This can be done, when it is known that the interfering radar has been in operation and what parameters it has been using.

In this work the author has observed that the radar antenna pattern is frequency dependent. This can increase the area of interference caused by radar and so increase the calculated impact of interference significantly. Due to this the accuracy of the whole measurement can deteriorate from the estimated result significantly. The determination of the above radar antenna pattern becomes an important measurement item. Also the dependence of measurement antenna pattern must be known.

When using the measurement setup presented in this work, the relative power level accuracies are estimated to be ±3 dB under field conditions.

7.5 Conclusions and recommendations

Radar measurements done with the measurement system presented in this work show that weather radars operating without filters generate an enormous amount of spurious frequency spectrum components (for example in C-band frequency band 5.250...5.850 GHz). This is because of the fact that cost efficient cross field type components are used. The increasing amount of radar transmitters causes an increase in the amount of interference. This is unavoidably leading to an intolerable situation where other radio communication systems operating in the same frequency bands as radar get interfered. Usable parts of radio spectrum, allocated for other than radar use, so become unusable due to radio smog. It is also possible, that the interfering radar itself gets interfered by other radar stations or other radio communication systems operating in the same frequency band.

The author recommends that the spectrum purity of all high power radars should be checked, especially if these contain cross field type components. The importance of frequency planning increases when one tries to fit together the already existing radar and radio communication systems and new planned systems into the frequency spectrum. Recommendations by the author to improve the situation are as follows:

- International and national frequency harmonization (already in use),
- obeying of the harmonization (seems not to affect all military radar systems),
- coordination of frequencies with neighboring countries,
- anticipating frequency planning (taking into account the above),
- planning and use of interference filters and
- planning of locating of radio communication systems in the field using knowledge of the surrounding terrain.

The author also recommends appropriate teaching of radar techniques to the operating personnel in radar stations. Especially training should be done from the point of view of possible radar interference.

Based on knowledge and measurements the author recommends that all personnel using and maintaining a radar system to familiarize themselves with the signals produced by their radar transmitter. Also familiarizing to other neighboring radio communication systems is recommended.

In cases where a radar system produces higher levels of spurious emissions than the recommended levels these radars must be equipped with appropriate filters. Filters are, however, expensive and their production and installation at a later time is difficult and will cause additional costs. The filter itself and its matching also cause attenuation of the *NF*. This results in a decreasing measurement range of the radar. Additionally, the power loss due to mismatching can be destructive (a 0.1 dB attenuation of a 1 MW pulse power equals a power loss of 22.7 kW). Due to mismatching the matching points voltage *SWR* may increase. This can lead to breakdown in the feed line. Often compromises must be made. In these

cases both the spurious signal suppression and the capabilities of the filter will suffer. The higher the radar output power is the more attention must be paid to filtering of the radar output signal (signal purity).

Based on observations made during start-up inspections and from interviews with operational staff, it has been noted that the complete spectrum transmitted by radar is not well known to the radar operators. Operating staff, however, usually has no suitable or satisfactorily accurate equipment for measuring the radar spectrum. Based on this the author recommends that radar operating staff should be educated not only in handling of the returning echo but also in observing of transmitted signals of the radar and its possible spurious signals with at least one measurement technique, for example the one presented in this work.

The author recommends clarification of the mechanisms that generate radar spurious emissions. Valuable updated information could be at hand when the generation of transmission pulses, the significance of pulse shape and stability are studied. The author's knowledge about radar pulse generation indicates clearly a connection between radar pulse stability and measured spectrum components. Also a connection between radar pulse peak power, pulse length and *PRF* to the generation of spurious emissions has been found. The higher the radar output power is, the higher is the risk of the generation of spurious emissions (long radar pulse + high *PRF* = high risk of interference). By knowing the generation mechanisms of these phenomena it would be possible to limit the amount of spurious emissions and their power levels.

7.6 Further research

For the future it is desirable to further develop the presented measurement system. One item of development would be the increasing of the largest IF measurement bandwidth and reducing of the shortest sweep time (of the SA). These measures would give better possibilities to examine the time domain parameters of a single radar pulse and to analyze more accurately the causal connection between pulses and spurious emissions. Additionally, these would allow faster measurement times or a wider single sweep measurement frequency range.

It is not very well-known how multipath fading in a line-of-sight radio link and scatter loss on a beyond the horizon radio link correlate. In this work it has been assumed that the radar interference level stays constant during multipath fading in the TDRRS. An important topic for further research would therefore be the determination of the statistical distribution of the radar interference level on different distances and especially its dependence of the fading of the disturbed radio communication link.

The adoption of this measurement system to investigate the impact of radar interference to other radio communication systems than TDRRSs should give some new knowledge. A significant role in improvement of the measurement system is to equip the system with a computer and tracking generator. This, however, is not essential because in this work the measurement system is kept as simple as possible and as field capable as possible.

More generally, one future research item would be the measurement and study of different antenna patterns and their dependency of frequency. With a radar antenna it is mandatory to know its own antennas characteristics. The frequency dependency of the measurement antenna pattern was not examined in this work because it was presumed that measurement antenna main lobe measurement results were used. This, however, would be a key future research item.

Radar manufacturers should examine the possibility of adding filters to new radar transmitters or at least make it possible to install filters at a later time, if needed. This kind of filters would be needed in the radar transmitter branch (TX) to attenuate spurious emissions radiated from the antenna. Also the radar receiver branch (RX) might need a filter for attenuation of signals that are generated from other radio communication systems interfering with the echo pulse reception. The production of fine tunable BS filters needed for the measurement system should be started again because they were not commercially available during the time of measurement for this work (the needed filter based on specifications given by the author). Since some radar transmitters regardless of the use of interference filtering will produce spurious emissions to frequency bands allocated for use of other radio communication systems, it should be considered to mark these frequency bands as unusable or limit their future use or at least mark them with the risk of interference due to radar.

According to the latest interference observations the interfering of radar receivers by WLAN, WiMAX and UWB can become more severe in the future. In the newest weather radar systems the radar measuring capabilities have been improved so, that even the drop model of a rain front, the size of drops and their quality (water, snow etc.) can be determined. Based on this it is reasonable to require that the possible interference risk from other radio communication systems to radar frequencies should be taken into account in future investigations. If this is not taken into account interference situations may occur where the improvement of radar sensitivity may be lost. Additionally, the information of a radar echo coming from the same direction as the signal from another radio communication system or the whole returning echo may be lost. This has been reported for instance in [50].

This work has primarily been focused on interference problems between radars and TDRRSs. An own research topic for the future would be the examination of possible interference to other digital radio communication networks (UWB, WLAN etc.) due to spurious emissions by radar.

REFERENCES

[1] ITU-R RECOMMENDATION M.1177-3, Techniques for measurement of unwanted emissions of radar systems, International Telecommunication Union, Geneva, 2003-06, 40 p.

[2] ITU-R RECOMMENDATION M.1314, Radio determination pulsed output device spurious emission characteristics for systems in the 3 and 5 GHz bands, International Telecommunication Union, Geneva, 1997-10, 6 p.

[3] F.H. Sanders, R.L. Hinkle, B.J. Ransey, Analysis of Electromagnetic Compatibility Between Radar Stations and 4 GHz Fixed-Satellite Earth Stations, NTIA Report 94-313, Colorado July 1994, 59 p.

[4] Frank H. Sanders, Robert L. Hinkle, Bradley J. Ramsey, Measurement Procedures for the Radar Spectrum Engineering Criteria (RSEC), NTIA Report TR 05-420, March 2005, 112 p.

[5] RECOMMENDATION ITU-R SM.329-10, Unwanted emissions in the spurious domain, Geneva 2003, 40 p.

[6] ITU-R Recommendation SM.1541-1, Annex 8 Unwanted emissions in the out-of band domain, International Telecommunication Union, Geneva 05-06, 79 p.

[7] Frank Sanders, Comparison of Emission Spectra of Maritime Radiolacation Radars Measured in Multiple Bandwidts in the 2 900-3 100 MHz and 8 500-10 500 MHz, Notes on Informal RCG Discussions, Contribution RCG-27, Southhampton UK, 26.5.2005, 6 p.

[8] Industry Canada Spectrum Management and Telecommunications, Policy Radio Standards Specification RSS-138, Commercial Shipborne Radar in the 2900-3100 MHz, 5470-5650 MHz and 9225-9500 MHz Bands, February 7, 2004, 16 p.

[9] Defence Technical Information Center (DTIC) Goldberg, J. Hinckelmann, O, NEW METHODS FOR MEASURING SPURIOUS EMISSIONS (Rept. no. 1112- 1), Mineola NY, USA, August 1961 (citation update 2002), 73 p.

[10] Science Links Japan, S.Koichi; M.Yoshiyuki; K.Hironori; S.Sadaaki; Y.Yukio, Measurement of unwanted emissions of radar system my ITU-R Method, J-EAST Vol.105 No.369(MW2005 99-111), Japan 2005, p. 7-11, in Japanese

[11] CCIR, Geneva, March 1991, Volume XV-4, Addendum No1, Question 159/9: Effects of unwanted emissions, from Radar systems in the radio determination service on systems in the fixed service

[12] H.U. Eichhorn, Radio interference into high capacity digital radio, Apr 1989 Proc. 2.BCRR, p.187

[13] Recommendation ITU-R F.1190, PROTECTION CRITERIA FOR DIGITAL RADIO-RELAY SYSTEMS TO ENSURE COMPATIBILITY WITH RADAR SYSTEMS IN THE RADIODETERMINATION SERVICE, Geneva 1995

[14] Roger A. Dalke, Frank H. Sander and Brent L. Bedford, "EMC Measurement and Analysis of C-band Radars and Dedicated Short Range Communications Systems", Institute for Telecommunication Sciences, Boulder, Colorado USA.

[15] GFI, GUIDELINES FOR IMPLEMENTATION FIXED WIRELESS SYSTEMS, GFI 0501, 18.5.2005, 17 p.

[16] Bradley J. Ramsey, Frank H. Sander, "Investigations of Radar Interference to Satellite Earth Stations and Terrestrial Microwave Communication Sites.", Institute for Telecommunication Sciences, Boulder, Colorado 80303 USA, IEEE 1998.

[17] Frank H. Sanders, Bandwidth Dependence of Emission Spectra of Selected Pulsed-CW Radars, NTIA Technical Memorandum TM-05-431, August 2005, 19 p

[18] H. Karttunen, K.J. Donner, P. Krögen, H. Oja, M. Puutanen; Principles of astronomy, renewed edition, URSA Astronomical Association, Helsinki 1995, 656 p., in Finnish

[19] J.D. Kraus, Radio Astronomy, 2nd Edition, Cygnus-Quasar Books, Ohio 1986, 368 p.

[20] Distribution Engineering, OY YLEISRADIO AB (Finnish Broadcasting Company), report 1998, 28 p., in Finnish

[21] ETSI TS 151 010-1, V6.5.0 (2005-11), 13.3 Transmitter output power and burst timing, Sophia Antipolis France, 2008, 5117 p.

[22] COUNCIL RECOMMENDATION of 12 July 1999 on the limitation of exposure of the general public to electromagnetic fields (0 Hz...300 GHz) (1999/519/EC), Official Journal of the European Communities L 199/59, Brussels 12 July 1999, p.185.

[23] C. Hülsmeyer, Reichspatent Patent Nr. 165546, 11.11.1904 “the presence of distant metallic objects via radio waves”, Wikipedia (The Free Encyclopedia) 15 April 2008,

[24] International Telecommunication Union, Radio Regulation, Volume 1, Articles 5 Frequency allocations, Geneva, Edition of 2008, 416 p.

[25] Radio Frequency Regulation Ficora 4K/2008 M Annex, Frequency Allocation Table for the 9 kHz...400 GHz frequency band, Ficora Helsinki 19.12.2008, 206 p.

[26] Warren L. Stutzman, Gary A. Thile, Antenna Theory Analysis and Design, Second edition, John Wiley&Sons, New York 1998, 648 p.

[27] A. Lehto, A. Räisänen, Microwave measurement techniques, Otatieto Oy Espoo 1991, 213 p., in Finnish

[28] Hewlett Packard, RF & Microwave, Test Accessories Catalog 1997/98, Adapters, Cables and Connectors, U:S:A: 3/98, 113 p.

[29] Hewlett Packard, Test & Measurement Catalog 1995, Signal Analyzer, Portable HP8564E, U:S:A. 10/94, 704 p.

[30] CEPT/ERC/RECOMMENDATION 74-01E, UNWANTED EMISSION IN THE SPURIOUS DOMAIN, (Siofok 98, Nice 99, Sesimbra 02, Haradec Kralove 05). Edition of October, 2005, p.52.

[31] International Telecommunication Union, Radio Regulation, Volume 1, Articles 5, Frequency Allocations, RR5-89, 5.450B, Geneva, Edition of 2008, p. 125

[32] Antti Räisänen and Arto Lehto, Radio technique 225 p., Otatieto Oy, Espoo 1993, 280 p., in Finnish

[33] Raine Jokinen, Nokia radio history 1965-2000, versio 1.1, 2004, 25.p., in Finnish

[34] EMCEC, Test Report Number TL 990244, Espoo 1999, 2 p.

[35] FINNISH STANDARDS ASSOCIATION SFS, Standard SFS 5626, Quality requirements for digital connections, Finnish Standardizing board 1990, 3 p. in Finnish

[36] ITU-T Recommendation G.801, DIGITAL NETWORKS TRANSMISSION MODELS, International Telecommunication Union, (Extract from the Blue Book), Geneva 1993, 8 p.

[37] FINNISH STANDARDS ASSOCIATION SFS, Standard SFS 5627 Digital fractions, 1990-06-25, 3 p., in Finnish

[38] ITU-T Recommendation G.822, DIGITAL NETWORKS CONTROLLED SLIP RATE OBJECTIVES ON AN INTERNATIONAL DIGITAL CONNECTION International Telecommunication Union, (Extract from the Blue Book), Geneva 1993, 5 p.

[39] FINNISH STANDARDS ASSOCIATION SFS, Standard SFS 5647, General property of public telecommunication networks, National synchronization plan, 1990-10-15, 3.p., in Finnish

[40] ITU-T recommendation G.114, ITU-On-way transmission time, Geneva 05/2003, 20 p.

[41] Recommendation G.106, General Characteristics of International Telephone Connection and Circuits, CCITT Red Book, Fasc. 111.1, Geneva 1985.

[42] Interview of MSc Mr. Erkki Saarinen in 2006.

[43] Peter F. Stenumgaard, A Simple Imulsiveness Correction Factor for Control of Electromagnetic Interference in Dynamic Wireless Applications, IEEE Cummunications letters Vol.10 No.3, March 2006, p. 147-149.

[44] A. Bruce Carlson, Communication Systems, International Student Edition, McGraw-Hill Kogakusha, Ltd, Tokyo, 1968, 462 p.

[45] RECOMMENDATION ITU-R F.699-7, Reference radiation patterns for fixed wireless system antennas for use in coordination studies and interference assessment in the frequency range from 100 MHz to about 70 GHz, Geneva, 2006, 17 p.

[46] ITU-R Recommendation P.530-12, Propagation data and prediction methods required for the design of terrestrial line-of-sight systems, International Telecommunication Union, Geneva 2001, 02-01, 47 p.

[47] ITU-R Recommendation P.1546, Method for point-to-area predictions for terrestrial services in the frequency range 30 MHz to 3 000 MHz Geneva, 2001, 51 p.

[48] K. Siwiak, Radiowave Propagation and Antennas for Personal Communications, Artech House Boston 1998, 418 p.

[49] RECOMMENDATION ITU-R P.617-1, Propagation prediction techniques and data required for the design of trans-horizon radio-relay systems, Geneva, 1992, 9 p.

[50] CEPT, EEC, Project Team FM22(06)43, Radar Spectrum Emission Measurements, Vienna, Report 19-22 September 2006, 6 p.

APPENDIXES

(Appendixes I, II and III by courtesy of the ITU)

Appendix I - ITU measurement recommendation M.1177-4

Block diagram for measurement of radiated unwanted emissions from radars using the automatically controlled direct method

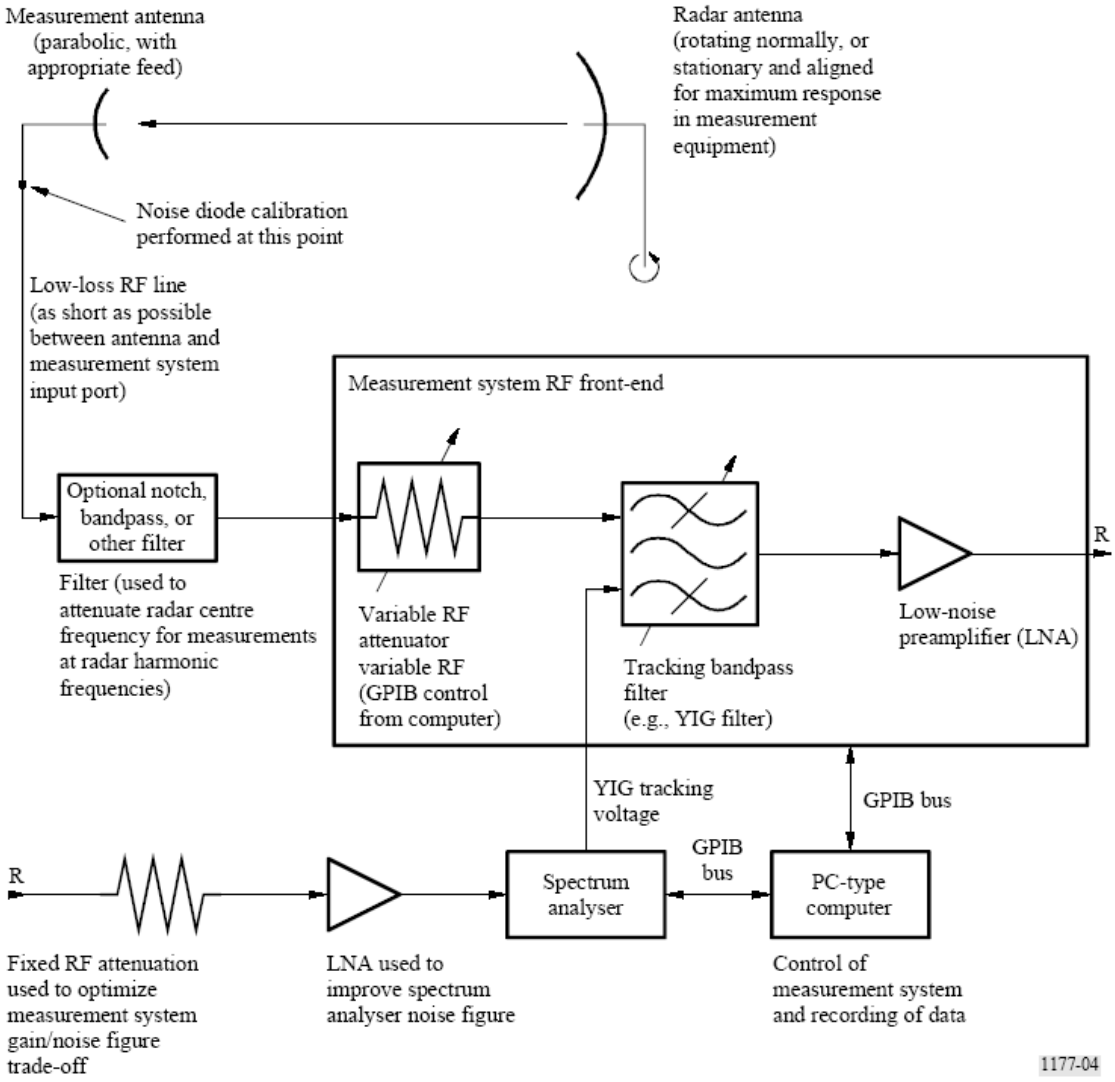

GPIB: general purpose interface bus
YIG: ytrium-iron-garnet

Appendix II - Radio determination pulsed output device spurious emission characteristics for systems in the 3 and 5 GHz bands

TABLE 2

Output device(1)	Spurious emission level			
	Non-harmonic (dBc) in 1 MHz	Harmonic (2), (3) (dBc)		
		2nd	3rd	4th
Crossed-field:				
Crossed-field amplifiers	–35 to –50 (5)	–25	–30	–45
Magnetrons (unlocked) (4)	–65 to –80 (5)	–40	–20	–45
Magnetrons (locked) (4)	–75 to –90 (5)	–40	–20	–45
Coaxial magnetrons (4)	–60 to –75 (5)	–40	–20	–45
Linear beam:	(6)			
Coupled cavity TWT	–105 to –115	–20	–25	–35
Klystron	–110 to –120	–20	–25	–35
Twystron	–105 to –115	–20	–25	–35
Solid state transistors (Parallel-class C modules):				
Si bipolar	–100 to –110	–45	–55	–65
GaAs FET	–100 to –110	–35	–45	–55

(1) Alternative output devices may be more applicable for systems operating above 5 GHz. These options include, but are not limited to, helix/ring bar traveling wave tubes and newer technology magnetrons.

(2) Harmonic spurious emission levels listed are 5 to -10nominal values. The range of harmonic spurious emissions is typically dB of the nominal values.

(3) Harmonic emission levels can be reduced below –100 dBc with a harmonic (low pass) filter.

(4) Older magnetron output devices can have inherent $\pi - 1$ modes which may be only 40 dB below the carrier. These modes are intermittent and of short duration occurring during the start-up of oscillations. New technology magnetrons are designed to suppress these emissions.

(5) Non-harmonic emissions levels in crossed-field devices can be reduced below –100 dBc with a waveguide band pass filter. These filters generally have a few tenths of a dB in insertion loss.

(6) Linear beam output devices may have non-harmonic spurious emissions close to the carrier in the order of –80 to -90 dBc depending on the characteristics of the overall cavity selectivity.

Appendix III - Radar output device characteristics considered in the design of radar systems

Output device	Peak output power range (kW)	Energy efficiency (%)	Instantaneous 1 dB bandwidth (% of carrier frequency)	Pulse-to-pulse coherency	Weight (kg)	Size	Mechanical ruggedness	Relative life expectancy (1)	Relative cost (2)
Crossed-field: (3)									
Crossed-field amplifiers	60-5 000	40-65	5-12 (4)	Yes	25-65	Small	Good	1.0	Low
Magnetrons (unlocked)	20-1 000	35-75	(4)	No	1-25			1.0	
Magnetrons (locked)	20-1 000	35-75	(4)	Yes	1-25			1.0	
Coaxial magnetrons	10-3 000	35-50	(4)	No	2-55			5.4	
Linear beam:									
Coupled cavity travelling wave tube	25-200	20-40	10-15	Yes	10-135	Large	Good	7.4	High
Klystron	20-10 000	30-50	1-12	Yes	25-270			13.5	Medium
Twystron	2 000-5 000	30-40	1-12	Yes	55-65			10.4	High
Solid state transistors (Parallel-class C modules):		(6)							
Si bipolar	10-90	20-30	10-30	Yes	0.5-2.5 per module	Small	Excellent	15	High
GaAs field effect transistor (5)	0.5-5.0	10-25	10-30						

(1) Life expectancy is normalized relative to a 1970s conventional magnetron and does not reflect the longer life expectancy of newer technology conventional magnetrons.

(2) Depends on production volume.

(3) Crossed-field output devices will most likely be phased out in future radar designs; however, their use is expected to continue in maritime radio navigation systems.

(4) Although magnetrons do not have an instantaneous bandwidth capability, tuning frequency ranges up to 10% of the operating frequency can be achieved.

(5) Silicon (Si) bipolar modules are generally used below 3.5 GHz and Gallium Arsenide (GaAs) modules in the 5 GHz band.

(6) Depends on the number of modules combined in the output stage.

Appendix IV - Horn Antenna dimensioning and gain of the measurement antenna

Horn Antenna AU 15/1,7...18 GHz

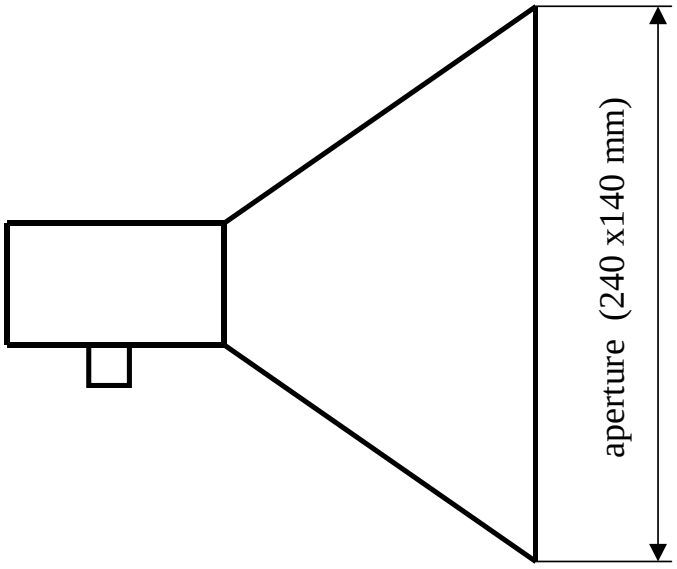

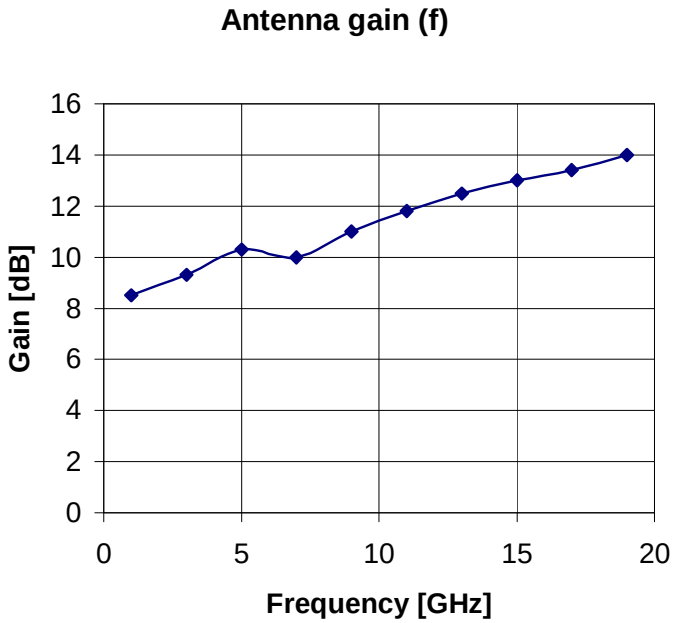

Appendix Va - Measurement procedure for unknown radar systems - flow chart

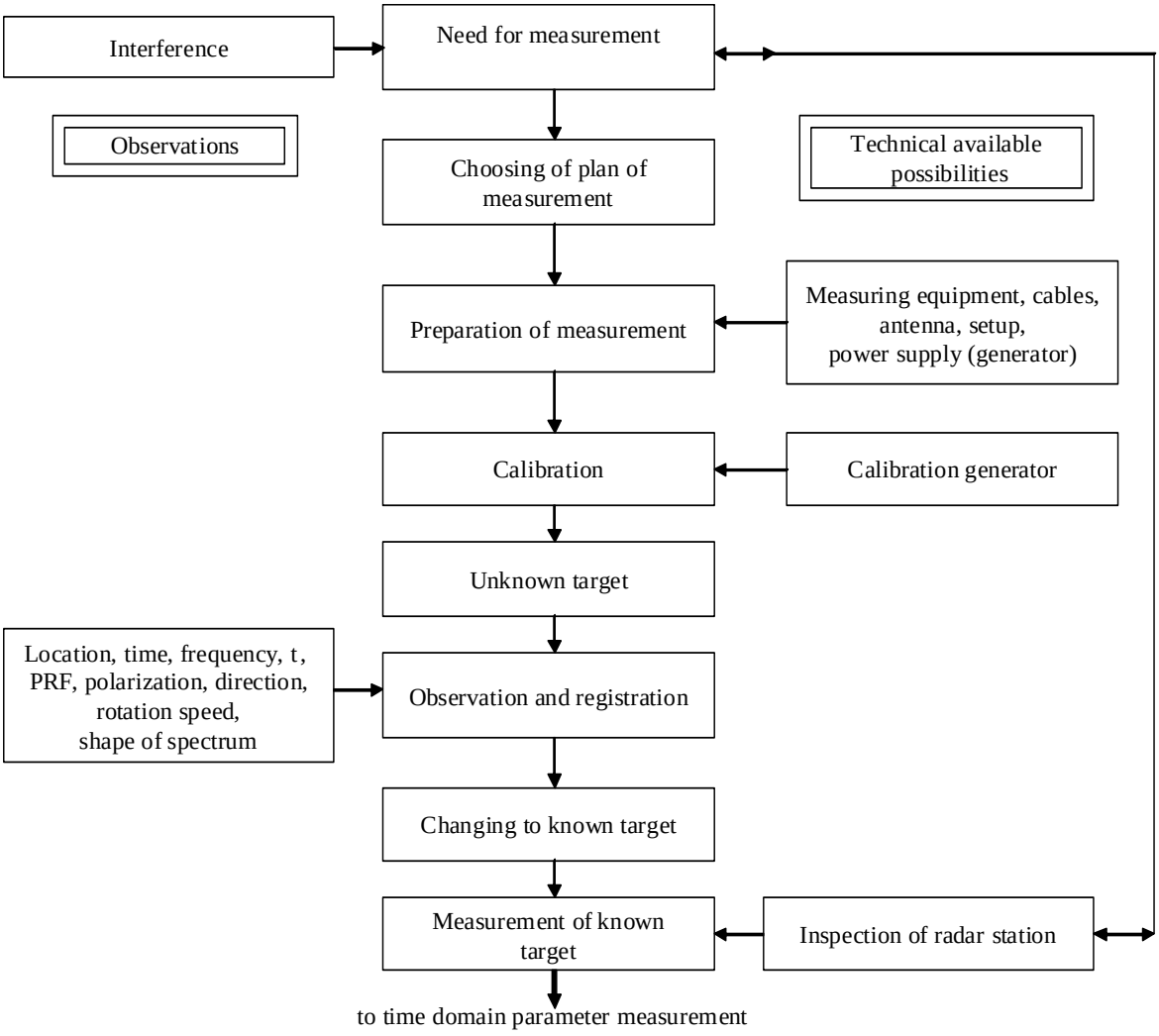

Appendix Vb - Progress of time domain parameter study - flow chart

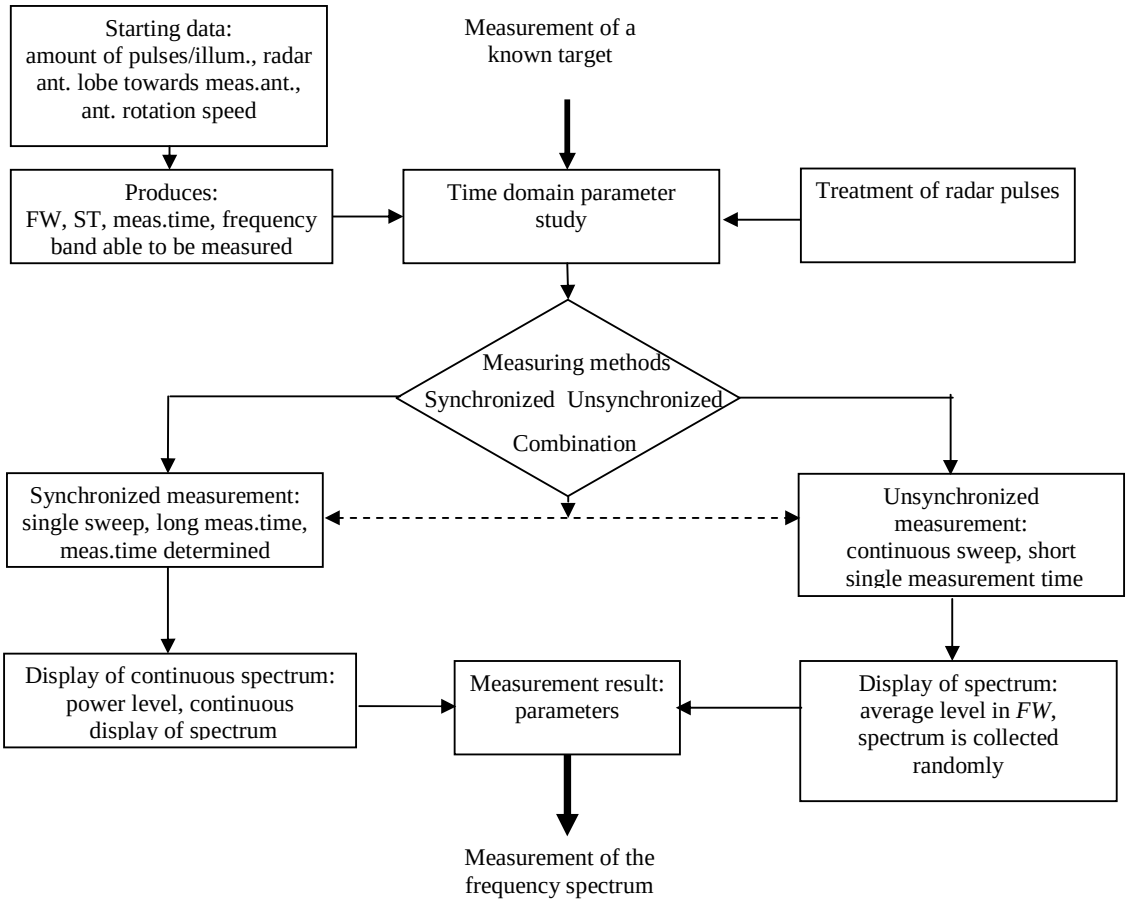

Appendix Vc - Frequency spectrum domain study of impact of antenna - flow chart

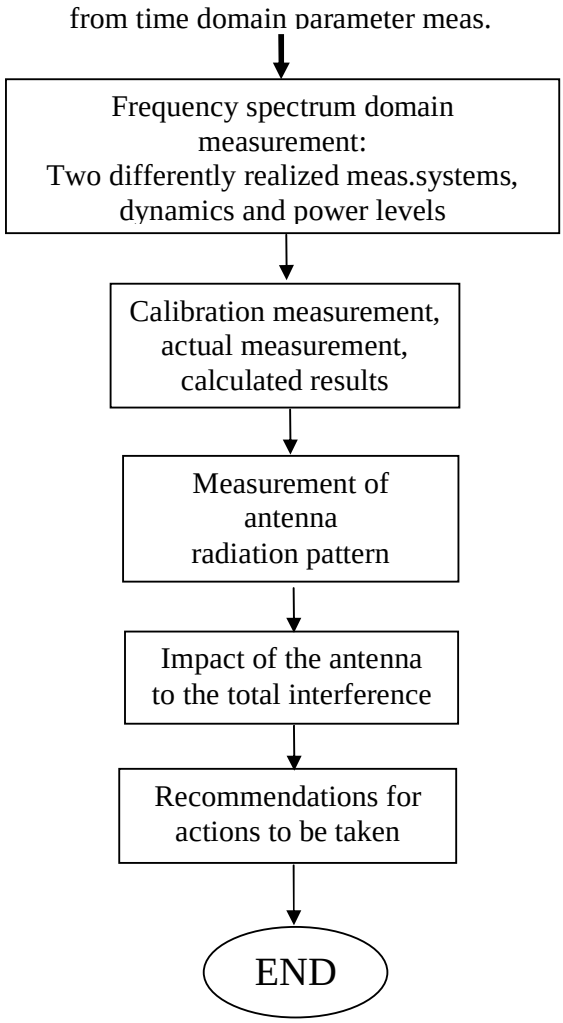

Appendix VIa - Radar protection zones with 4PSK

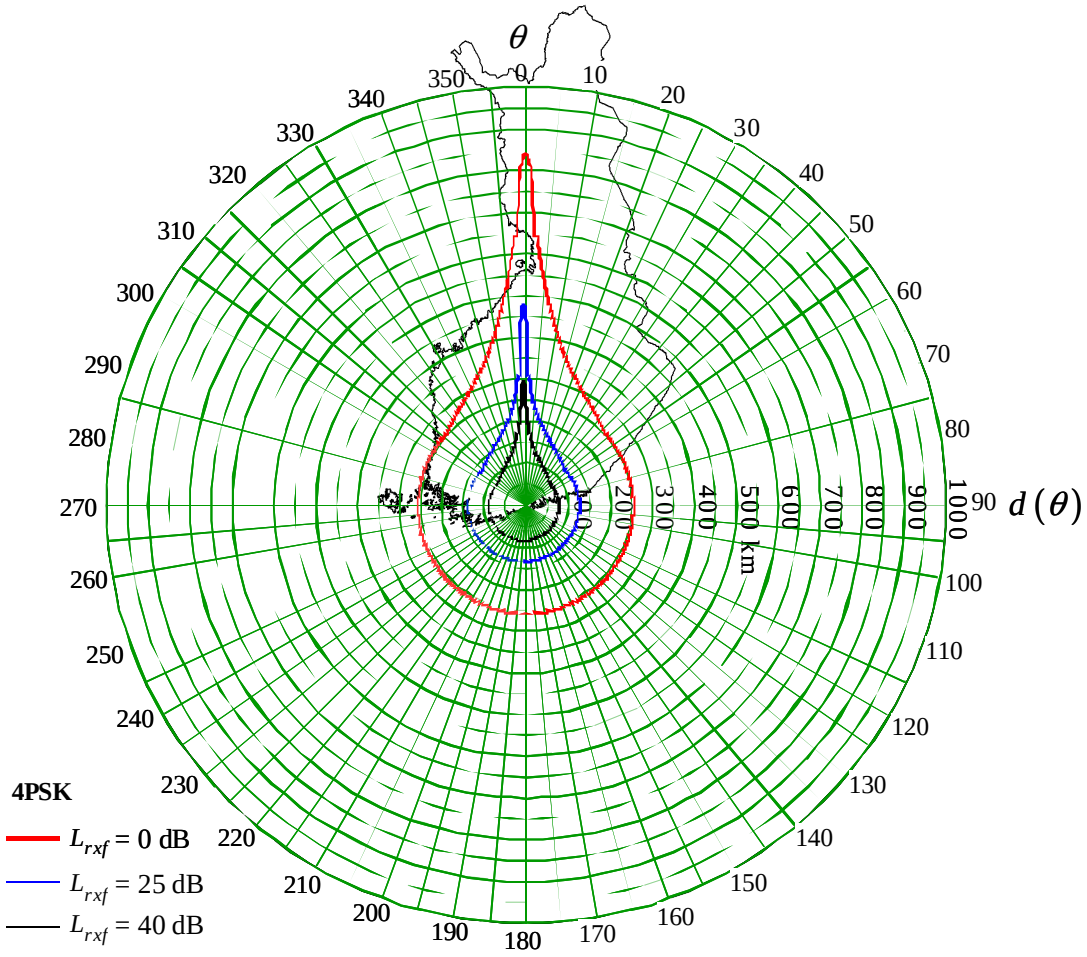

Table 9: Protection zone radii for 4PSK

θ	G(θ)/dBi	L/dB (L_{rxf}=0)	d/km (L_{rxf}=0)	L/dB (L_{rxf}=25)	d/km (L_{rxf}=25)	L/dB (L_{rxf}=40)	d/km (L_{rxf}=40)
0°	40.0	270.0	844	245.0	483	230.0	302
±1°	35.8	265.8	784	240.8	422	225.8	270
±1.5°	30.5	260.4	708	235.4	355	220.4	236
±(1.8°…2.43°)	26.2	256.2	648	231.2	313	216.2	212
±5°	18.4	248.4	532	223.4	254	208.4	172
±10°	10.9	240.9	423	215.9	210	200.9	140
±20°	3.3	233.3	333	208.3	172	193.3	112
±(48°…180°)	–6.1	223.9	257	198.9	132	183.9	83

Appendix VIb - Radar protection zones with 16QAM

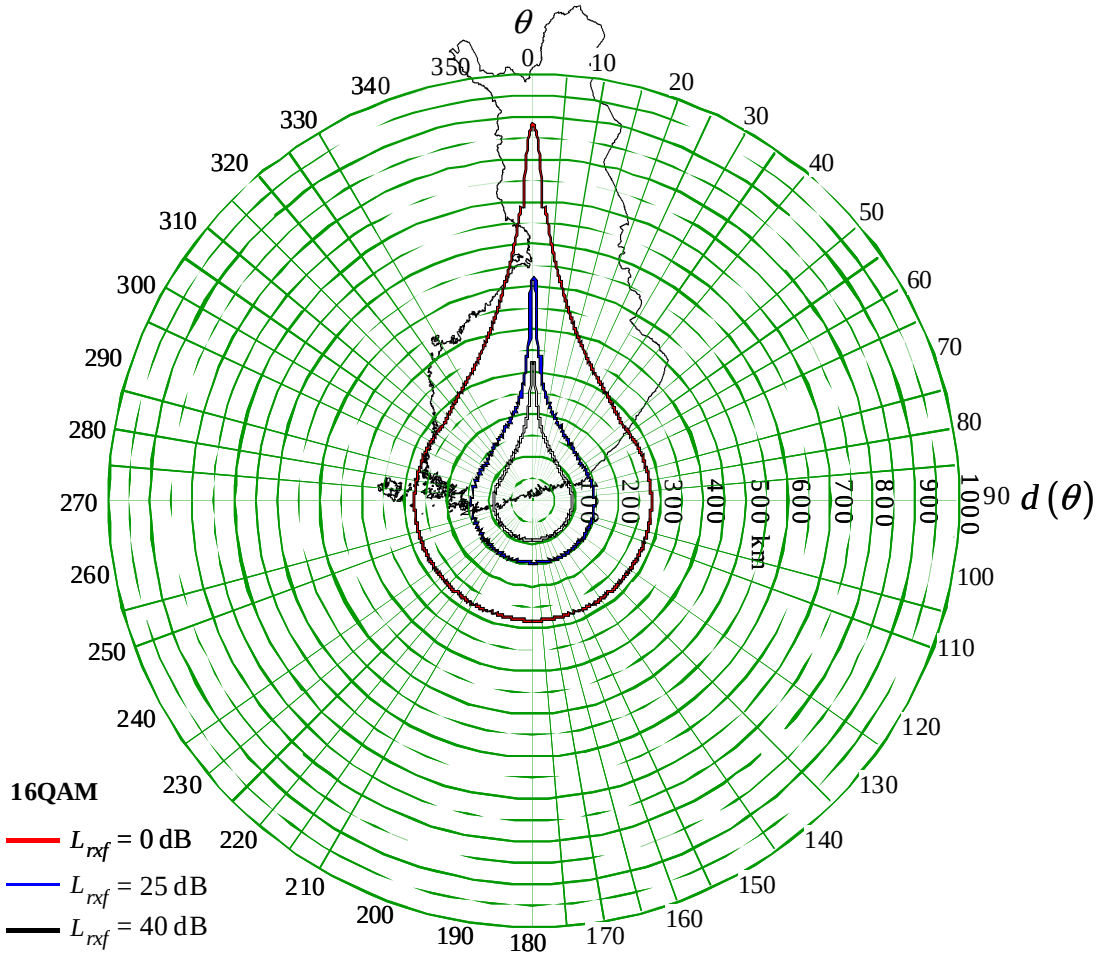

Table 10: Protection zone radii for 16QAM

θ	G(θ)/dBi	L/dB (L_{rxf}=0)	d/km (L_{rxf}=0)	L/dB (L_{rxf}=25)	d/km (L_{rxf}=25)	L/dB (L_{rxf}=40)	d/km (L_{rxf}=40)
0°	40.0	273.0	886	248.0	527	233.0	330
±1°	35.8	268.8	827	243.8	465	228.8	292
±1.5°	30.5	263.4	751	238.4	391	223.4	254
±(1.8°…2.43°)	26.2	259.2	691	234.2	342	219.2	229
±5°	18.4	251.4	577	226.4	274	211.4	189
±10°	10.9	243.9	466	218.9	226	203.9	152
±20°	3.3	236.3	365	211.3	186	196.3	123
±(48°…180°)	–6.1	226.9	278	201.9	144	186.9	92

Appendix VIc - Radar protection zones with 32QAM

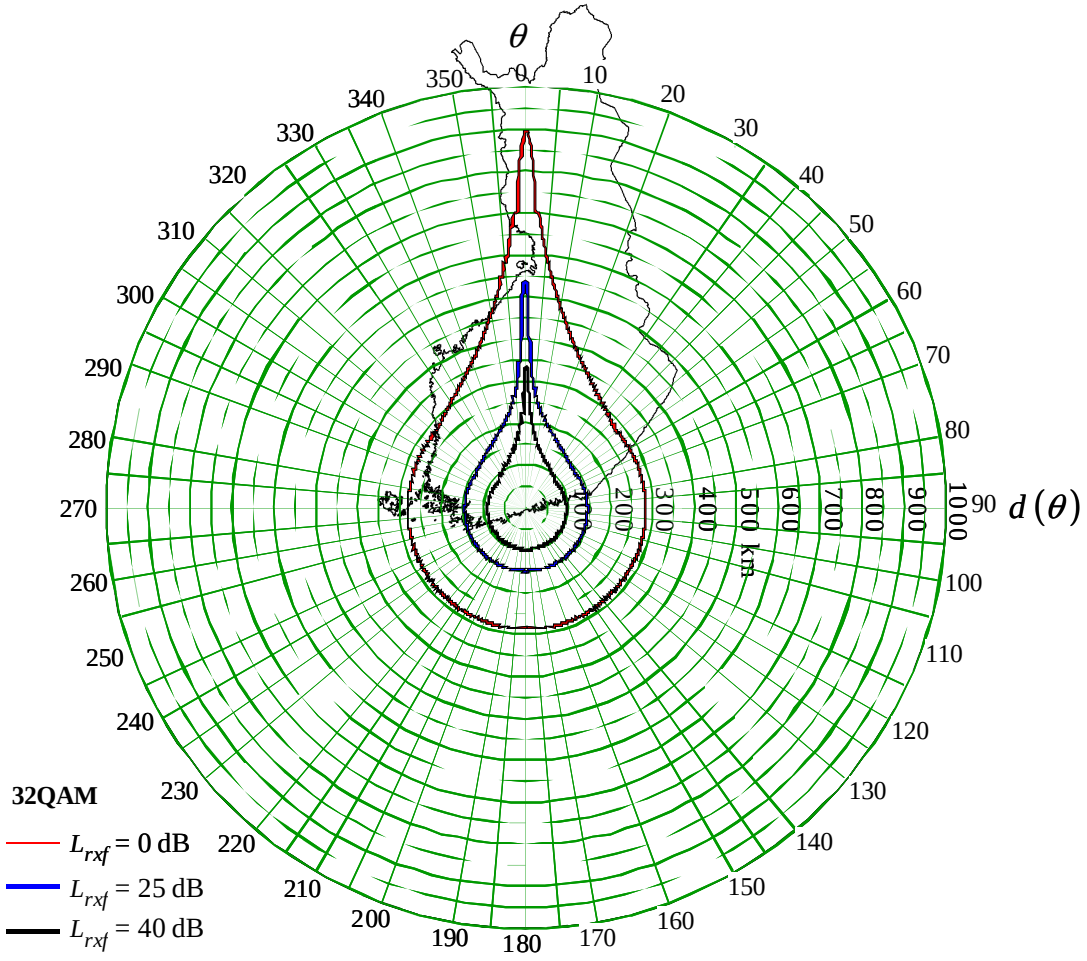

Table 11: Protection zone radii for 32QAM

θ	G(θ)/dBi	L/dB (L_{rxf}=0)	d/km (L_{rxf}=0)	L/dB (L_{rxf}=25)	d/km (L_{rxf}=25)	L/dB (L_{rxf}=40)	d/km (L_{rxf}=40)
0°	40.0	274.0	900	249.0	542	234.0	340
±1°	35.8	269.8	841	244.8	479	229.8	300
±1.5°	30.5	264.4	766	239.4	404	224.4	261
±(1.8°…2.43°)	26.2	260.2	705	235.2	353	220.2	234
±5°	18.4	252.4	591	227.4	282	212.4	192
±10°	10.9	244.9	481	219.9	232	204.9	157
±20°	3.3	237.3	377	212.3	191	197.3	126
±(48°…180°)	–6.1	227.9	285	202.9	148	187.9	95

Appendix VId - Radar protection zones with 128QAM

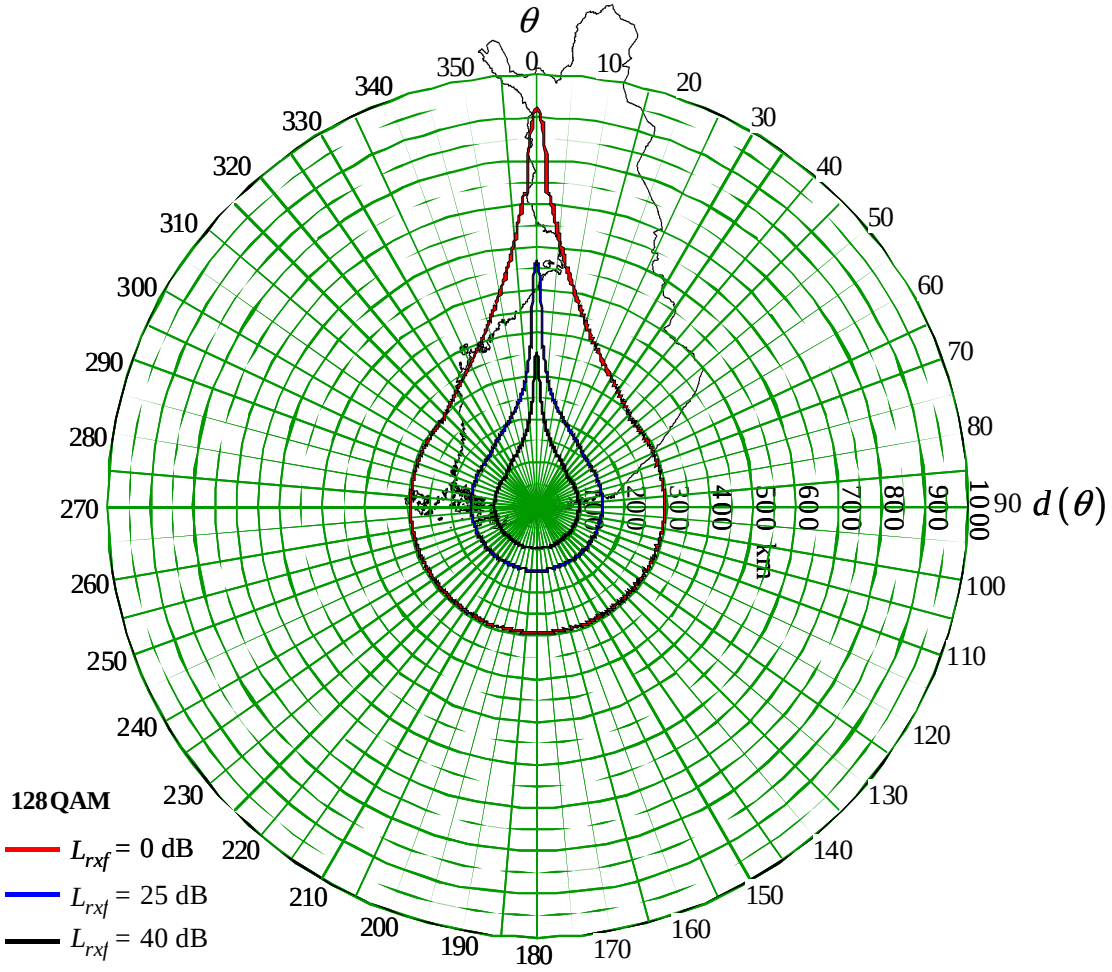

Table 12: Protection zone radii for 128QAM

θ	G(θ)/dBi	L/dB (L_{rxf}=0)	d/km (L_{rxf}=0)	L/dB (L_{rxf}=25)	d/km (L_{rxf}=25)	L/dB (L_{rxf}=40)	d/km (L_{rxf}=40)
0°	40.0	275.4	920	250.4	562	235.4	355
±1°	35.8	271.2	860	246.2	500	231.2	312
±1.5°	30.5	265.8	786	240.8	423	225.8	271
±(1.8°…2.43°)	26.2	261.6	725	236.6	369	221.6	243
±5°	18.4	253.8	612	228.8	292	213.8	199
±10°	10.9	246.3	501	221.3	241	206.3	163
±20°	3.3	238.7	395	213.7	199	198.7	132
±(48°…180°)	–6.1	229.3	296	204.3	154	189.3	99